

Distribution Agreement

In presenting this thesis or dissertation as a partial fulfillment of the requirements for an advanced degree from Emory University, I hereby grant to Emory University and its agents the non-exclusive license to archive, make accessible, and display my thesis or dissertation in whole or in part in all forms of media, now or hereafter known, including display on the world wide web. I understand that I may select some access restrictions as part of the online submission of this thesis or dissertation. I retain all ownership rights to the copyright of the thesis or dissertation. I also retain the right to use in future works (such as articles or books) all or part of this thesis or dissertation.

Signature: A6B03AA4A48F440...

Hannah Mandle
Name

04/15/2024.
Date

Title Pathogen recognition, inflammation, and ovarian cancer

Author Hannah Mandle

Degree Doctor of Philosophy

Program Epidemiology

Approved by the Committee

DocuSigned by:
Joellen M. Schildkraut
ACB8D56CA99C4E5...

Joellen M. Schildkraut
Advisor

DocuSigned by:
Timothy Lash
B0560B9631FB435...

Timothy L. Lash
Advisor

DocuSigned by:
Anke Huels
6FEC7C88FBB3492...

Anke Huels
Committee Member

DocuSigned by:
Veronika Fedirko
643162AF237B465...

Veronika Fedirko
Committee Member

Andrew Berchuck

Andrew Berchuck
Committee Member

Accepted by the Laney Graduate School:

Kimberly Jacob Arriola, Ph.D, MPH
Dean, James T. Laney Graduate School

Date

Pathogen recognition, inflammation, and ovarian cancer

By

Hannah B. Mandle

M.P.H., Emory University, 2018

B.A., University of Massachusetts Lowell, 2012

Chair: Joellen M. Schildkraut, PhD, MPH

Co-Chair: Timothy L. Lash, DSc, MPH

An abstract of a dissertation submitted to the Faculty of the James T. Laney School of Graduate
Studies of Emory University in partial fulfillment of the requirements for the degree of

Doctor of Philosophy in Epidemiology

2024

Abstract

Pathogen recognition, inflammation, and ovarian cancer

By

Hannah B. Mandle

Epithelial ovarian cancer (EOC) accounts for roughly 2.5% of all cancers among natal women and yet EOC has the fifth highest mortality rate among female cancers in the US. Although studies have identified factors associated with EOC risk and survival, the underlying biologic mechanisms of these factors are still largely unknown. The overarching goal of this research is to evaluate genetic variants in pathogen recognition and downstream inflammation processes as they relate to EOC and high-grade serous EOC (HGSOC, the most common histotype) risks and survival among Black and White women.

In Aim 1, we investigate the aggregate association of TLR, NFkB and TNF signaling genes and pathways with ovarian cancer risk among Black and White women separately. Per $P_{raw} < 0.05$, MAPK-related genes, present in all three pathways, were associated with EOC/HGSOC risks among both Black and White women. Among White women *MYD88* and *CCL2* were associated with EOC risk; *PARP1* and *TICAM2* were associated with HGSOC risk. Among Black women, *MAP3K8*, *MAP3K7*, and *PRKCB* were associated with EOC risk *and* indicated to have an interaction with BMI.

In Aim 2, we investigate the association TLR, NFkB and TNF signaling genes and pathways with EOC/HGSOC 5-year overall survival. *AKT3* and *CTSK* genes were associated with EOC/HGSOC 5-year survival in both Black and White women. *LTA* was the only gene observed to possibly have a Black EOC 5-year survival association differential by BMI.

In Aim 3, we investigate differentially expressed genes (DEGs) using RNA-Seq data from Black and White HGSOC tumor tissues. Black and White women were analyzed separately, and we compare DEGs between 5-year survival (yes/no) and FIGO stage (early/late). *CXCL9* was differentially expressed for survival in both Black and White women. *BLNK*, *CEBPB*, *PIK3R1*, *PIK3CD*, *TLR4*, *MMP14*, *JUN*, *ICAM1*, *MAPK10*, and *TRAF6* were also differentially expressed by stage at diagnosis regardless of race.

In this dissertation, we identified genes associated with EOC and/or HGSOC risk and survival that may provide mechanistic insight for ovarian carcinogenesis and progression and possible novel hypothesis generation.

Pathogen recognition, inflammation, and ovarian cancer

By

Hannah B. Mandle

M.P.H., Emory University, 2018

B.A., University of Massachusetts Lowell, 2012

Chair: Joellen M. Schildkraut, PhD, MPH

Co-Chair: Timothy L. Lash

A dissertation submitted to the Faculty of the James T. Laney School of Graduate Studies of Emory University in partial fulfillment of the requirements for the degree of

Doctor of Philosophy in Epidemiology
2024

Table of Contents

List of Tables.	1
List of Figures.	4
Chapter 1: Background and Literature Review	5
Ovarian Cancer	5
<i>Epithelial Ovarian Cancer Epidemiology</i>	5
<i>Biological Hypotheses for Epithelial Ovarian Carcinogenesis</i>	11
Inflammation and Cancer	11
Inflammation and Innate Immunity: The Toll-Like Receptor Pathway	15
<i>TLRs/inflammation and Obesity</i>	17
<i>TLRs, inflammation, and race</i>	18
<i>TLR polymorphisms and Cancer Risk and Survival</i>	19
Summary of Critical Literature Review	19
Chapter 2: Specific Aims	21
Chapter 3: Data Sources and Methods	21
3.1. Data Sources	22
3.1.1 <i>The African American Cancer Epidemiology Study</i>	22
3.1.2 <i>The Ovarian Cancer Association Consortium</i>	22
3.2. Study Populations	22
3.3. Variables	23
3.3.1 <i>Exposures</i>	23
3.3.1a <i>SNP selection, genotype data and quality control</i>	23
3.3.1b <i>RNA Extraction and quantification of gene expression data</i>	24
3.3.2 <i>Outcomes</i>	25
3.3.3 <i>Covariates</i>	25
3.4. Analytic Methods	27
3.4.1 <i>Aim 1</i>	27
3.4.2 <i>Aim 2</i>	28
3.4.3 <i>Aim 3</i>	29
Chapter 4: Aim 1	30
4.1. Abstract	31
4.2 Introduction	33
4.3 Methods	36

4.3.1	<i>Case/control ascertainment and selection</i>	36
4.3.2	<i>SNP Selection, Genotyping, and Quality Control</i>	36
4.3.3	<i>Genes and Pathways</i>	37
4.3.4	<i>Statistical Analysis</i>	37
4.4.	Results	39
4.5.	Discussion	41
4.6.	Tables and Figures	48
Chapter 5: Aim 2.	54
5.1.	Abstract	55
5.2.	Introduction.....	56
5.3.	Methods	58
5.3.1	<i>Case ascertainment and vital status</i>	58
5.3.2	<i>SNP Selection, Genotyping, and Quality Control</i>	59
5.3.3	<i>Genes and Pathways</i>	60
5.3.4	<i>Statistical Analysis</i>	60
5.4.	Results	62
5.5.	Discussion	64
5.6.	Tables and Figures	68
Chapter 6: Aim 3.	72
6.1.	Abstract	73
6.2	Introduction.....	75
6.3.	Methods	77
6.3.1	<i>Study Population</i>	77
6.3.2	<i>RNA Extraction</i>	78
6.3.3	<i>Quantification of gene expression data</i>	79
6.3.4	<i>Germline Genotyping and Quality Control</i>	80
6.3.5	<i>Statistical analysis</i>	80
6.4.	Results	81
6.4.1	<i>Survival</i>	81
6.4.2	<i>Stage</i>	82
6.5.	Discussion	83
6.6.	Tables and Figures	87
Chapter 7: Public Health Implications and Future Directions	97

References	99
Supplementary Tables and Figures	123

List of Tables.

Table 4.1. Select baseline characteristics of the Black and White analytic populations from AACES and OCAC participants. **Table 4.2.** Statistically significant gene associations and lead SNPs within TLR, NFkB, and TNF pathways with invasive EOC and HGSOC risk among Black women in AACES and OCAC.

Table 4.3. Statistically significant BMI interactions and lead SNPs among raw statistically significant genes associated with EOC risk among Black women in AACES and OCAC.

Table 4.4. Statistically significant genes and lead SNPs within TLR, NFkB, and TNF pathways with invasive EOC and HGSOC risk among White women in OCAC.

Table 4.5. Statistically significant BMI interactions and lead SNPs among raw statistically significant genes associated with EOC or HGSOC risk among White women in OCAC.

Table 5.1. Select baseline characteristics of the Black and White invasive epithelial ovarian cancer populations.

Table 5.2. Gene associations and lead SNPs within TLR, NFkB, and TNF pathways with invasive EOC and HGSOC 5-year overall survival among Black women in AACES and OCAC.

Table 5.3. Gene associations and lead SNPs within TLR, NFkB, and TNF pathways with invasive EOC and HGSOC 5-year survival among White women in OCAC.

Table 6.1. Selected demographic and clinical characteristics of the Black and White HGSOC study populations.

Table 6.2. Statistically significant gene expression in association with 5-year invasive HGSOC survival (no vs yes) among Black and White cases.

Table 6.3. Statistically significant associations of high/low gene expression with 5-year survival (no/yes) in TLR, NFkB, and TNF pathway genes among Black and White HGSOC cases.

Table 6.4. Statistically significant gene expression in association with FIGO stage at diagnosis (III/IV vs 0/I/II) among Black and White HGSOC cases.

Table 6.5. Statistically significant associations of high/low gene expression with stage at diagnosis (late/early) in TLR, NFkB, and TNF pathway genes among Black and White HGSOC cases.

Supplementary Table ST1. FIGO Staging for Carcinoma of the Ovary

Supplementary Table ST2. Studies Participating in the Ovarian Cancer Association Consortium.

Supplementary Table ST3. Pathways, genes, and chromosomal coordinates included for analysis

Supplementary Table ST4.1. Gene associations/BMI interactions within TLR, NFkB, and TNF pathways with invasive EOC risk among Black women.

Supplementary Table ST4.2. Gene associations/BMI interactions within TLR, NFkB, and TNF pathways with invasive HGSOC risk among Black women.

Supplementary Table ST4.3. Gene associations/BMI interactions within TLR, NFkB, and TNF pathways with invasive EOC risk among White women.

Supplementary Table ST4.4. Gene associations/BMI interactions within TLR, NFkB, and TNF pathways with invasive HGSOC risk among White women.

Supplementary Table ST5.1. Gene associations/BMI interactions within TLR, NFkB, and TNF pathways with 5-year overall survival among Black women with EOC.

Supplementary Table ST5.2. Gene associations/BMI interactions within TLR, NFkB, and TNF pathways with 5-year overall survival among Black women with HGSOC.

Supplementary Table ST5.3. Gene associations/BMI interactions within TLR, NFkB, and TNF pathways with EOC 5-year survival among White women.

Supplementary Table 5.4. Gene associations/BMI interactions within TLR, NFkB, and TNF pathways with HGSOC 5-year survival among White women.

Supplementary Table ST6.1. RNASeq Metadata.

Supplementary Table ST6.2. DEGs for HGSOc 5- year survival (no vs yes) among Black and White HGSOc cases.

Supplementary Table ST6.3. Cox proportional hazard models to assess high/low RNA expression in association with 5-year Survival (no/yes) in TLR, NFkB, TNF genes among Black and White HGSOc cases.

Supplementary Table ST6.4. DEGs for stage at diagnosis (late vs early) among Black and White HGSOc cases.

Supplementary Table ST6.5. Logistic Regression assessing high/low RNA expression in association with stage at diagnosis (late/early) in TLR, NFkB, and TNF genes among Black and White HGSOc cases.

List of Figures.

Figure 1.1. Stage distribution (%) for invasive ovarian cancer, 2014-2018.

Figure 1.2. 5-year relative survival for invasive ovarian cancer by stage, 2011-2017.

Figure 1.3. Mapped locations for invasive ovarian cancer histotype cells-of-origin and pathologic presentations.

Figure 1.4. Distribution of the stage at diagnosis for ovarian cancer by race, 2014-2018.

Figure 1.5. Five-year relative survival by stage at diagnosis and race, 2011-2017.

Figure 1.6. Types of inflammation in tumorigenesis and cancer.

Figure 1.7. A simplified schematic of TLR4 sensing and signaling processes.

Figure 6.1. Volcano plot of DEGs for HGSOC survival among Black women.

Figure 6.2. Volcano plot of DEGs for HGSOC survival among White women.

Figure 6.3. Volcano plot of DEGs for stage at diagnosis among Black women.

Figure 6.4. Volcano plot of DEGs for stage at diagnosis among White women.

Supplementary Figure SF1. Genome-wide association QxQ plot assessing inflation due to population admixture among Black women.

Supplementary Figure SF2. Genome-wide association QxQ plot assessing inflation due to population admixture among White women.

Supplementary Figure SF6.1.

Supplementary Figure SF6.2.

Supplementary Figure SF6.3.

Chapter 1: Background and Literature Review

Ovarian Cancer

Ovarian cancer occurs when gynecological tissues grow out of control and form a malignant tumor.¹ Within these gynecologic tissues, three types of cells can develop into different malignancies: epithelial, germ cell, and stromal. The majority of ovarian tumors arise from the epithelium (~90%); germ cell and stromal tumors are rare.² The forthcoming discussion of ovarian cancer encompasses a group of malignancies involving the ovary, fallopian tube, and peritoneum that arise from epithelial cells collectively referred to as epithelial ovarian cancer (EOC).

Epithelial Ovarian Cancer Epidemiology

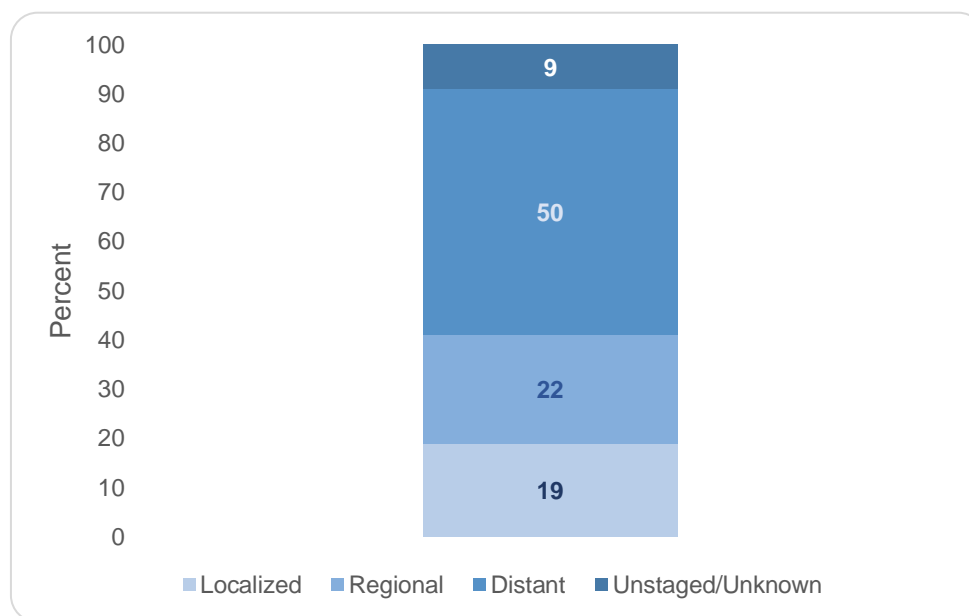
EOC accounts for roughly 2.5% of all cancers among natal women and has a lifetime risk occurrence of about 1 out of every 78 women.^{3,4} Two systems for the classification of tumor staging are used for EOC: 1) the International Federation of Gynecology and Obstetrics (FIGO) classifications,⁵ which are presented in **Table 1.1** along with the corresponding summary staging;⁶ 2) the American Joint Committee on Cancer (AJCC) TNM staging system which provides more details about the size of the tumor (T), lymph node involvement (N), and metastasis (M) to further determine stage grouping.⁵ A detailed list of all stages and stage groupings are presented in **Supplementary Table 1**. Only 19% of all EOCs are diagnosed at the localized stage (stage I), followed by 22% at regional (stage II) and 50% at distant (stage III+; **Figure 1.1**).⁷

Table 1.1. FIGO and summary staging for EOC.

FIGO Stage	Summary Stage	Description
I	Localized	Tumor limited to the ovaries (one or both)
II	Regionalized	The cancer is in one or both ovaries or fallopian tubes and has spread to other organs within the pelvis or there is primary peritoneal cancer. It has not spread to nearby lymph nodes or to distant sites.

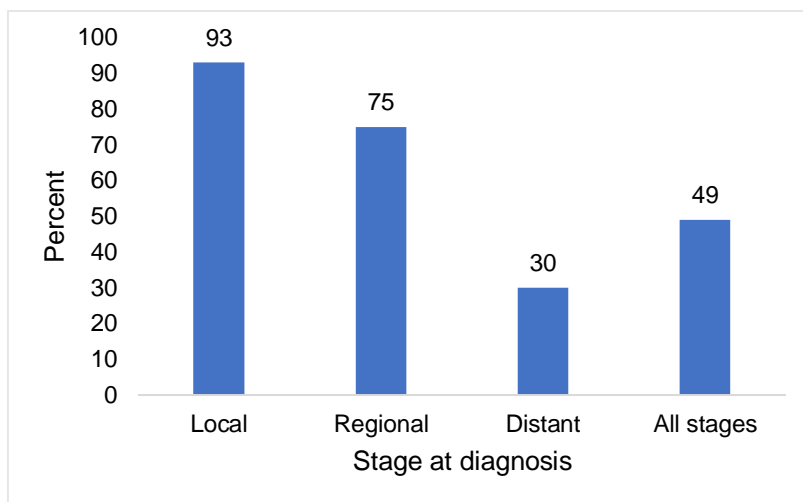
III	Distant	Tumor involves one or both ovaries with microscopically confirmed peritoneal metastasis outside the pelvis and/or retroperitoneal lymph node involvement
IV		Distant metastasis, excluding peritoneal metastases

Figure 1.1: Stage distribution (%) for invasive ovarian cancer, 2014-2018.⁷



Despite a low incidence, EOC is the fifth leading cause of cancer deaths among natal women in the US, the highest fatality rate of all gynecologic cancers.⁷ One-half of all women diagnosed with EOC will not survive after the first five years.⁷ One of the greatest contributing factors to poor EOC survival is the stage at diagnosis. Although women diagnosed with EOC during the localized stage have a high chance of survival (~93%), only one in five women will be diagnosed at this stage (**Figure 1.1**). Women who are diagnosed during the distant stage, half of all EOC cases, only have an estimated 30% likelihood of survival in the first five years. The 5-year survival rates for each stage are presented in **Figure 1.2** below.

Figure 1.2: 5-year relative survival for invasive ovarian cancer by stage, 2011-2017⁷



Development of an effective screening program has failed in multiple trials.^{8,9} Cancer antigen 125 (CA125), a mucinous glycoprotein found on the surface of ovarian cancer cells, appeared to be a promising tumor biomarker for EOC but lacked sensitivity in early stages of disease. In addition, increased CA125 is also observed during menstruation, pregnancy, endometriosis and inflammatory diseases of the peritoneum.^{10,11}

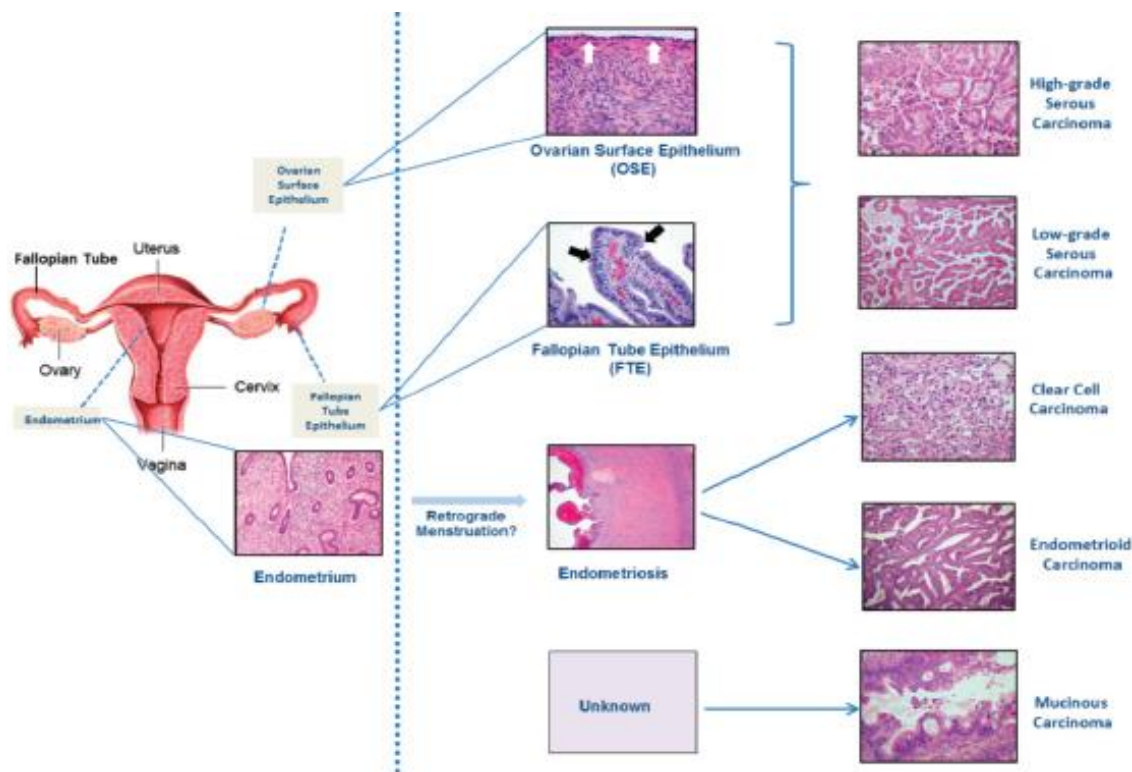
Numerous risk factors have been identified for EOC incidence. Parous vs nulliparous, any oral contraceptive pill use, age at menarche 15 years or greater, and tubal ligation are all associated with a decrease in risk.^{12,13} An increase in EOC risk is associated with older age, use of body powder, BRCA1/2 germline mutations, first-degree family history of ovarian or breast cancer, age at menopause greater than 55 years (relative to ages 50-55), endometriosis, elevated body mass index (BMI), circulating C-reactive protein levels >10mg/L compared to <1mg/L, and use of postmenopausal hormone replacement therapy.¹²⁻¹⁵ Factors associated with poor EOC prognosis include a BMI category of obese measured 1-5 years before diagnosis, smoking (worse for current smokers), Black race, lower SES, and older age.¹⁶⁻¹⁹ Interestingly, despite an association with an

increased risk of EOC, menopausal hormone therapy of greater than 5 years before diagnosis is associated with a better EOC survival.²⁰

Epithelial Ovarian Cancer Subtypes

First, tumors are classified as benign, borderline, or malignant (carcinomas) according to tumor behavior. Borderline tumors exhibit epithelial proliferation that is higher than benign tumors and have variable nuclear atypia, yet they do not destroy and invade nearby stroma.²¹ Prognosis of a borderline tumor is also much better than a malignant tumor.²¹ Second, EOC consists of five major histotypes that have different cells of origin, morphology, molecular features, epidemiologic risk factors, clinical characteristics and survival. The most common histotype is high grade serous (HGSOC), which accounts for roughly 63% of all EOCs followed by endometrioid (~10%), clear cell (~10%), mucinous (~9%), and low grade serous (~3%) cancers.²² High- and low-grade serous carcinomas arise from fallopian tube and ovarian surface epithelial cells (though via separate mechanisms) while endometrioid and clear cell carcinomas arise from the endometrium and are associated with endometriosis, possibly due to endometriotic cysts.²³ The origin of mucinous carcinomas is unclear, but are theorized to evolve from transitional cells at the fallopian tube-peritoneal junction.²³ A schematic of where the cells-of-origin are in the female reproductive tract and pathological presentations of each histotype is shown in **Figure 1.3**.

Figure 1.3. Mapped locations for invasive ovarian cancer histotype cells-of-origin and pathologic presentations²⁴



EOC histotypes have been observed to have different.^{12,25–27} At the genomic level, HGSOC is associated with *TP53* mutations resulting in somatic chromosome instability and DNA repair copy number changes.²⁸ Roughly half of all HGSOC cases are characterized by homologous recombination DNA repair pathway mutations, namely *BRCA1* and *BRCA2*. Risk factors for EOC differentially associated with risk by histotype include first-degree family history of breast cancer (HGSOC), smoking per 20 pack-years (mucinous ovarian cancers), BMI (non-serous), and endometriosis (endometrioid and clear cell ovarian cancers).^{12,27}

Epithelial Ovarian Cancer Disparities

Despite a having lower incidence and a similar distribution of stage at diagnosis (**Figure 1.4**),⁷ Black women experience markedly worse outcomes²⁹ and have a five-year relative survival

approximately 10% lower than for White women (**Figure 1.5**).⁷ Recently, the Ovarian Cancer in Women of African Ancestry (OCWAA) consortium reported that risk factors, including BMI, oral contraceptive use, parity, tubal ligation, first-degree family history of ovarian cancer, first-degree family history of breast cancer, aspirin use, use of body powder applied to genital areas, education, and history of endometriosis accounted for slightly more risk among Black women than White women when considered together.^{30 30}

Figure 1.4: Distribution of the stage at diagnosis for ovarian cancer by race, 2014-2018.⁷

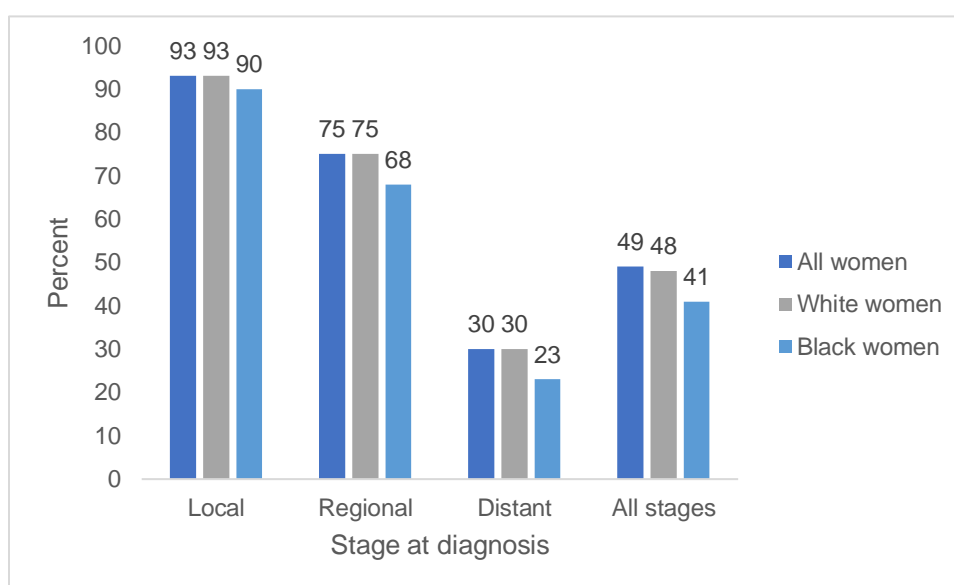
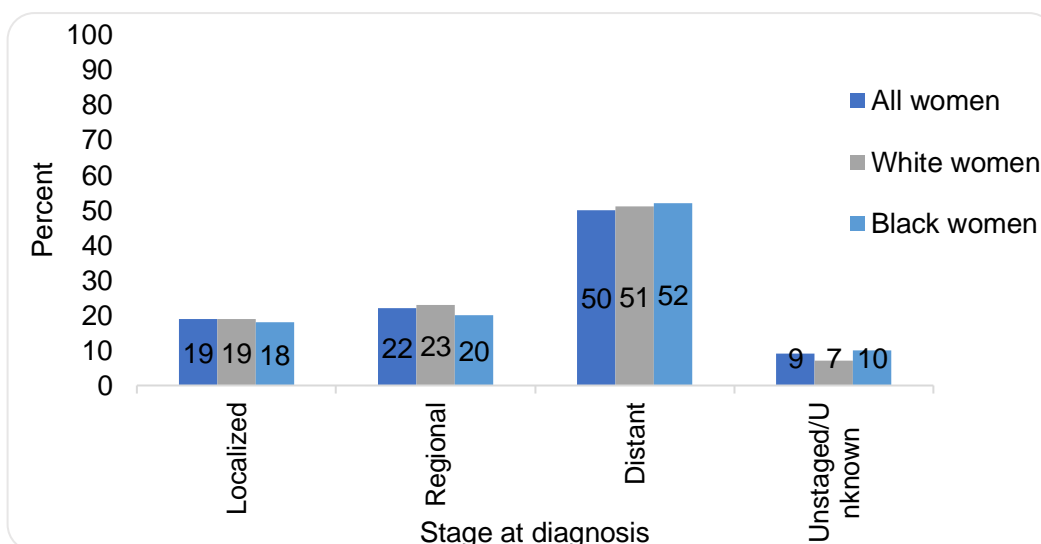


Figure 1.5: Five-year relative survival by stage at diagnosis and race, 2011-2017.⁷



Until there are effective, non-invasive screening programs for ovarian cancer, the best way to reduce EOC burden and cancer-specific deaths is through prevention. While there is no chemopreventive agent for EOC established via clinical trials, oral contraceptive (OC) use is associated with a significantly lower incidence in a meta-analysis of 55 studies.³¹ Longer duration of OC use was associated with decreasing incidence of EOC,³¹ but the benefits are not without risks. In the same meta-analysis, OC users were observed to have slight, yet significant, risks of breast cancer and vascular events.³¹ Further understanding of EOC etiology is a critical step in identifying chemopreventive agents, high-risk groups, gene treatment targets, and modifiable factors associated with risk and survival. This is particularly crucial among Black women as there are limited studies and small sample sizes inhibiting thorough investigations of biological mechanisms contributing to EOC and possible differences compared to other racial groups.

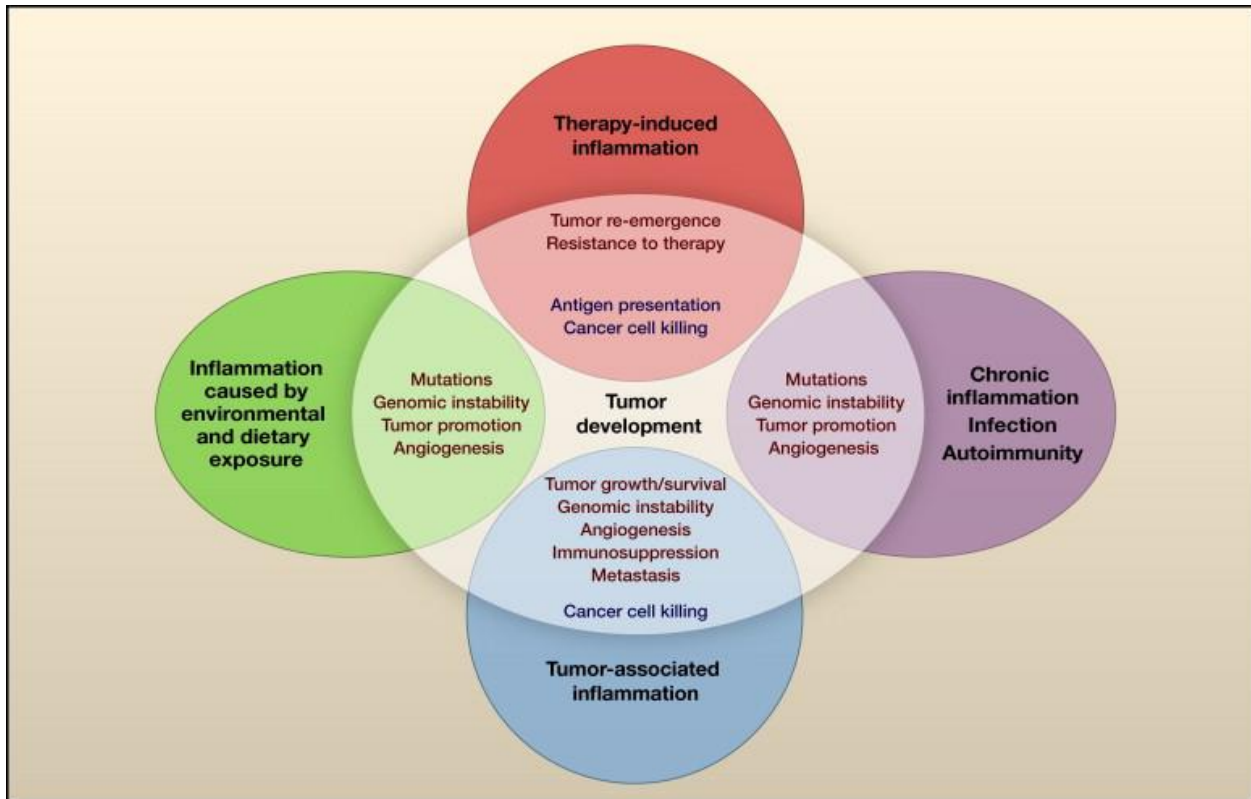
Biological Hypotheses for Epithelial Ovarian Carcinogenesis

Risk factors for EOC identified early on, such as parity, contraceptive use, ages of menarche and menopause, led researchers to propose incessant ovulation³² and gonadotropin hormone levels³³ were the two major mechanisms by which ovarian carcinogenesis occurred. However, there has been accumulating epidemiologic evidence of risk factors associated with EOC that do not directly affect ovulation or hormones levels. These risk factors include use of body powder use, obesity, endometriosis, and tubal ligation, all of which are associated with local inflammation, leading Ness and Cottreau to propose the hypothesis of inflammation as a pathophysiologic contributor to EOC etiology.³⁴ In fact, there are several cyclical processes necessary for ovulation that share commonalities with inflammatory responses such as the production of chemokines and cytokines, an influx of leukocytes to the microenvironment and rapid angiogenesis.³⁵

Inflammation and Cancer

Inflammation is one of the hallmarks of cancer,³⁶ and generally considered to be one of the most important environmental factors for tumorigenesis and tumor progression.³⁷ There are multiple mechanisms by which inflammation can promote cancer, illustrated in Figure 1.6 created by Grivennikov et al.³⁸

Figure 1.6: Types of inflammation in tumorigenesis and cancer



Inflammation caused by environmental exposures is demonstrated by established lifestyle factors associated with cancer, e.g. smoking. There is a plethora of evidence to support smoking as a Class 1 carcinogen³⁹ and smoking can lead to oxidative stress which can elicit inflammatory responses and alter the epigenome.^{40,41} This process can lead to additional oxidative damage thus creating a cycle of inflammation and tumor promotion.

Chronic inflammation from autoimmune and infectious diseases, such as Crohn's disease and *Helicobacter pylori*, respectively, can also lead to a tumor-promoting environment. Coussens

and Werb³⁷ have reported numerous cancers that are associated with pathologic inflammatory conditions (**Table 1.2**).

Table 1.2. Inflammatory conditions associated with neoplasms.^a		
Neoplasm(s)	Pathologic condition	Condition Type
Mesothelioma, lung carcinoma	Asbestosis, silicosis	Chronic
Lung carcinoma	Bronchitis	Chronic
Bladder carcinoma	Cystitis, bladder inflammation	Chronic
Oral squamous cell carcinoma	Gingivitis, lichen planus	Chronic
Colorectal carcinoma	Inflammatory bowel disease, Crohn's disease, chronic ulcerative colitis	Chronic
Vulvar squamous cell carcinoma	Lichen sclerosus	Chronic
Pancreatic carcinoma	Chronic and hereditary pancreatitis	Chronic
Oesophageal carcinoma	Reflux and Barrett's oesophagitis	Chronic
Salivary gland carcinoma	Sialadenitis	Chronic
MALT lymphoma	Sjögren syndrome, Hashimoto's thyroiditis	Chronic
Melanoma	Skin inflammation	Chronic
Cholangiosarcoma, colon carcinoma	<i>Opisthorchis</i> , <i>Cholangitis</i>	Infectious
Gall bladder cancer	Chronic cholecystitis	Infectious
Gastric adenocarcinoma, MALT	Gastritis/ulcers (<i>Helicobacter pylori</i>)	Infectious
B-cell non-Hodgkin's lymphoma, Burkitt's lymphoma	Mononucleosis (Epstein-Barr Virus)	Infectious
Non-Hodgkin's lymphoma, squamous cell carcinomas, Kaposi's sarcoma	AIDS	Infectious
Skin carcinoma in draining sinuses	Osteomyelitis	Infectious
Ovarian Cancer	Pelvic inflammatory disease, chronic cervicitis (Gonorrhoea, chlamydia, human papillomavirus)	Infectious
Bladder, liver, rectal carcinoma, follicular lymphoma of the spleen	Chronic cystitis	Infectious

^aModified from Coussens and Werb³⁷

Many of the established inflammatory conditions associated with tumorigenesis presented above are a result of infectious agents. Once a tumor has developed, further exposure and response to

pathogenic microbes may promote metastasis and impact survival by sustaining a chronic inflammatory state, activating leukocytes and fibroblasts within the tumor microenvironment.⁴²

Therapy-induced inflammation is duplicitous by nature. Chemotherapeutic agents and radiation induce signaling events that eliminate and control tumor cells *and* trigger an inflammatory stress response⁴³ termed cellular senescence.⁴⁴ In primary murine and human cells, researchers found several chemotherapy drugs induced a senescence response which promotes local and systemic inflammation⁴⁴ and tumor progression.⁴⁵

Tumor-associated inflammation occurring in the tumor microenvironment is an established driver of proliferation, progression, metastasis, and chemoresistance.³⁷ The tumor microenvironment milieu contains both inflammatory and immunosuppressive components that are coopted by the malignant and infiltrating immune cells.⁴⁶ Tumor-associated macrophages, for example, are often functionally transformed into M2-like phenotype which favor tumor growth and promote tumor microenvironment remodeling by producing growth and immunosuppressive factors.⁴⁷

As previously stated, EOC risk has established associations with numerous inflammatory factors (smoking, elevated BMI, body powder, endometriosis). Among EOC cases, pre-diagnosis exposure to inflammation-related lifestyle factors and chronic diseases exposures have been associated with poorer survival. In one study, 12 exposures (alcohol use; aspirin use; other nonsteroidal anti-inflammatory drug use; body mass index; environmental tobacco smoke exposure; history of pelvic inflammatory disease, polycystic ovarian syndrome, and endometriosis; menopausal hormone therapy use; physical inactivity; smoking status; and talc use) were used to create a weighted inflammation-related risk score (IRRS) among mostly White women with EOC. Per each increasing quartile of the IRRS there was an associated increase in risk of death (HR = 1.09; 95% CI: 1.03, 1.14).⁴⁸ Additionally, women in the upper quartile of the IRRS had a 31% higher death

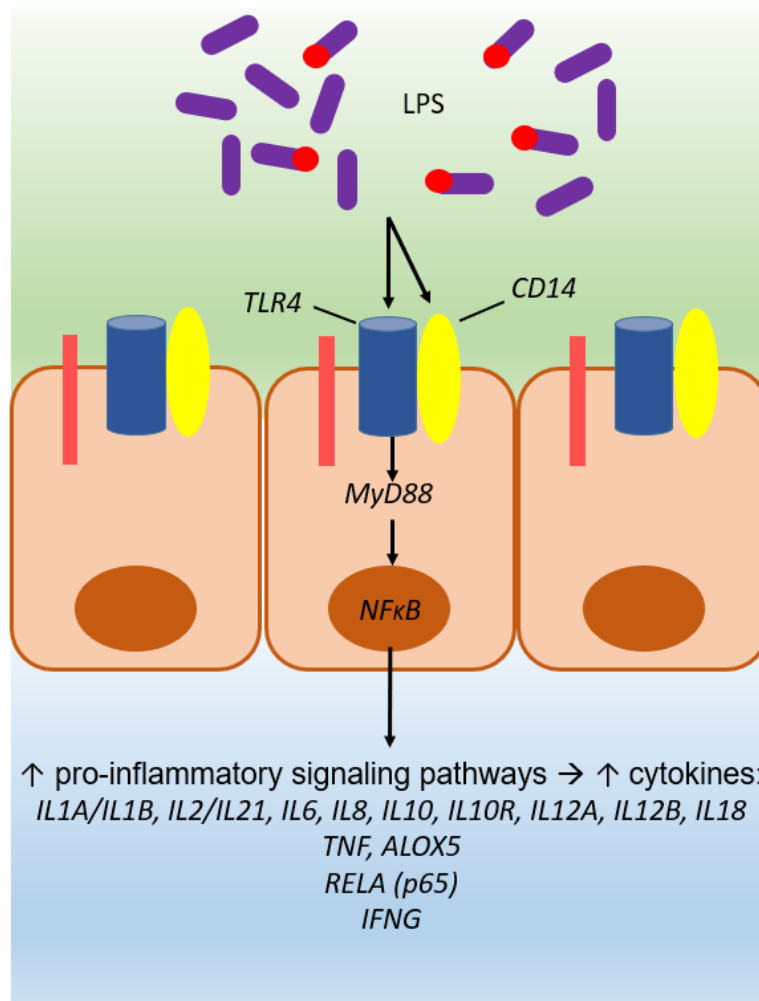
rate compared with the lowest quartile (95% CI: 1.11, 1.54).⁴⁸ Johnson et al. sought to replicate this study in a cohort of 592 Black women with EOC and similarly observed a higher IRRS was associated with worse overall survival (per quartile HR: 1.11; 95% CI: 1.01, 1.22). The authors also evaluated the energy-adjusted Dietary Inflammatory Index (E-DII). Adding the E-DII attenuated the association of the IRRS with survival and the greater E-DII, i.e. a more pro-inflammatory diet, was associated with shorter survival (per quartile HR: 1.12; 95% CI: 1.02, 1.24).⁴⁹

Inflammation and Innate Immunity: The Toll-Like Receptor Pathway

Toll-like receptors (TLRs) are type 1 transmembrane proteins that play a key role in immunity and subsequent inflammatory responses by recognizing small, conserved microbial motifs, known as pathogen-associated (exogenous) and danger-associated (endogenous) molecular patterns, expressed by microorganisms.^{50,51} One example of a pathogen-associated molecular pattern (PAMP) is lipopolysaccharide (LPS), the major component of the outer membrane of Gram-negative bacteria,⁵² and one example of a danger-associated molecular pattern (DAMP) is heat shock protein 60.^{53,54} To date, there have been 13 mammalian TLRs discovered, with TLRs 1-10 present in humans.⁵¹ TLRs 1, 2, 4, 5, and 6 primarily recognize bacterial and fungal components and are located on the cell surface.⁵⁵ TLRs 3, 7, 8, and 9 are localized to intracellular membranes and primarily recognize viral and microbial nucleic acids.⁵⁵ TLR10 is the only “orphan” TLR with no discovered ligand and unknown biological function,⁵⁶ however, it has been associated with anti-inflammatory effects.⁵⁷ TLR ligation triggers an intricate signaling cascade, beginning first with recruiting and binding to adapter proteins from inside the intracellular domain. The adapter proteins include the Myeloid differentiation primary response (MyD88), Toll–interleukin-1 receptor (TIR)-domain-containing adaptor protein inducing beta interferon (TRIF), TIR-domain-containing adaptor protein (TIRAP), and TIR-domain-containing adaptor molecule (TRAM). MyD88-dependent signaling is

perhaps the most common pathway as it can bind with TLRs 1, 2, 4, 5, 6, 7, 8, and 9. To illustrate TLR signaling, a simplified schematic of the TLR4 signaling pathway is shown in **Figure 1.7**.

Figure 1.7: A simplified schematic of TLR4 sensing and signaling processes.



However, TLRs expressed in tumor tissues can promote proliferation and anti-apoptosis through the activation of proinflammatory processes.⁵⁸⁻⁶⁰ In a small study by Zhou et al., healthy ovarian tissue samples were collected from patients undergoing routine gynecologic procedures and EOC tumor tissue samples were collected among stage III/IV patients.⁶¹ TLR2, TLR3, TLR4, and TLR5 were strongly expressed on the surface epithelium of healthy tissues, TLR6 and TLR8 expression was inconsistent among samples, and TLR1, TLR7, and TLR9 were either weak or

absent.⁶¹ Similar to normal tissues, tumor tissues expressed TLR2, TLR3, TLR4, and TLR5, but other TLRs had inconsistent results. Of note, epithelial cells from tumors had strong TLR staining regardless of tumor stage.⁶¹ EOC tumor tissue expression has also been studied specifically for TLR4 and its adapter protein, MyD88, but many studies have conflicting results,⁶¹⁻⁶⁵ and are comprised of over 90% white women. Li et al found that immunohistochemical expression of both TLR4 and MyD88 was associated with serous histology and poorer survival. and⁶⁵ TLR4 activation, additionally, has been observed to lead to chemoresistance through ligation with paclitaxel in EOC cell lines when signaling through a MyD88-dependent pathway.^{60,66}

Activation of nuclear factor kappa B (NFkB) signaling was observed to contribute to colon cancer development and progression via transcriptional upregulation of cell proliferation and angiogenesis, inhibition of apoptosis, and overexpression of cyclooxygenase-2 (COX-2), which additionally promotes inflammation and cell proliferation.⁶⁷ Worse overall survival in EOC is observed to be associated with elevated expressions of NFkB pathway subunits, activating I κ B kinases (IKKs).⁴⁶ In the previously mentioned study by Li et al, tumors with elevated TLR4 and MyD88 expression were significantly correlated with the expression of NFkB pathway proteins.⁶⁵

TLRs/inflammation and Obesity

Being obese has previously been found to be associated with higher plasma concentrations of LPS, which is recognized by TLR4, and higher circulating concentrations of pro-inflammatory markers such as IL-6 and TNF- α . In one small study, mRNA and immunohistochemistry expression of TLR2, TLR4, and MyD88 in both adipose tissues and peripheral blood mononuclear cells were significantly higher in obese and overweight individuals compared to lean individuals.⁶⁸ Furthermore, TLR and adapter protein expression (IRAK1 and MyD88) was strongly correlated with TNF- α and IL-6 expression, possibly indicating a greater inflammatory immune response in obese individuals.⁶⁸

TLR2 and 4 stimulation in adipocytes from human adipose tissue via abdominal subcutaneous fat increased NFkB mRNA expression and activated NFkB p65 at the protein level.⁶⁹ In one study by Nikpay et al., SNPs in an inflammatory gene-set, based off of a genetic investigation of systemic inflammation and innate immunity⁷⁰ (though which genes were selected is not stated by the authors), accounted for roughly 28% of obesity heritability.⁷¹

Within EOC, obesity has a disparate prevalence between Black and White (women as well as different strengths of association with EOC risk.³⁰ A high BMI (≥ 35 vs. 20 to < 25 kg/m²) is also associated with increased risks for all complications in primary ovarian cancer surgery⁷² and an increased risk of highly aggressive (death in ≤ 1 year) disease.⁷³ Whether there is a gene*environment interaction between TLR/inflammation genes and pathways and obesity in relation to EOC risk and survival has not yet been investigated.

TLRs, inflammation, and race

In a study among healthy controls selected from the African American Breast Cancer Etiology and Risk Consortium, the Women's Circle of Health Study, and the Carolina Breast Cancer Study, roughly half of the 14 cytokines studied were found to be differential between Black and White women.⁷⁴ Black women were observed to have higher levels of TNF α and lower levels of IL4 and IL10 relative to White women.⁷⁴ White women were observed to have higher levels of chemokines CCL2 and CCL11 but lower levels of type I interferon $\alpha 2$ relative to Black women.⁷⁴ In an aggregated mRNA expression analysis from a total of 7,142 samples, Singh et al. investigated gene expression differences between Black and White individuals.⁷⁵ Regardless of diseased or non-diseased state, the chemokine CCL3L3 was upregulated in Blacks relative to Whites.⁷⁵ Another study comparing variation in *TLRs* among Black and White women with pelvic inflammatory disease found that SNPs in *TLR1*, *TLR2*, *TLR6*, and *TIRAP* (the gene to encode the TIRAP adapter protein) significantly differed

between the two races.⁷⁶ Furthermore, healthy men and women from the Genetics of Evoked Responses to Niacin and Endotoxemia (GENE) study observed Black participants exposed to low-dose endotoxemia via LPS were found to have a lower cytokine response compared to White women, yet they had higher baseline levels.^{74,77}

TLR polymorphisms and Cancer Risk and Survival

To date, no individual SNP in the 224 genes selected for this project has been found to be associated with EOC risk or survival and previous candidate gene analyses have not focused on many of the genes in the TLR pathway. Most importantly, previous studies have only selected a few genes from a functional pathway. This study takes a broader approach to studying pathogen recognition and downstream inflammation with EOC by investigating associations at the gene *and* functional pathway level. Furthermore, investigation of these genes and pathways are conducted separately among Black and White women. Last, as genetic differences are rarely the entire causal mechanism for carcinogenesis, investigating possible gene*environment interaction may yield more actionable results. In this study, we assess whether obesity, a state of chronic inflammation and associated with *TLR* genetic variants and race, has a possible interaction with the included genes and pathways.

Summary of Critical Literature Review

EOC is the most fatal of all gynecologic malignancies and has known racial disparities for both risk and survival.^{4,30,78} Although studies have identified factors associated with EOC risk and survival, the underlying biologic mechanisms of these factors are still largely unknown. Furthermore, there has been little study of whether potential biological mechanisms leading to ovarian tumorigenesis differ between racial groups. Evidence supports the idea that immunological responses to bacterial and viral products, which induce inflammatory processes, can mediate

tumorigenesis.³⁷ After tumor development, further exposure and response to pathogenic microbes may impact survival by creating a chronic inflammatory state within the tumor microenvironment.⁴² Toll-like receptors (TLRs) are transmembrane proteins that play a key role in immunity by recognizing pathogen- and danger-associated molecular patterns expressed by microorganisms.⁷⁹ TLR ligation triggers an intricate signaling cascade that activates downstream pro-inflammatory pathways.

Chapter 2: Specific Aims

Overarching research question: The overarching goal of this research is to evaluate genetic variants in pathogen recognition and downstream inflammation processes as they relate to ovarian cancer risk and survival among Black and White women. We aim to investigate whether there may be differences in these processes among Black and White women. The following specific aims are proposed:

AIM 1: To investigate the association of Toll-like receptor signaling genes and pathway with ovarian cancer risk among Black and White women separately.

1a. Investigate the association with downstream inflammatory processes and ovarian cancer risk.

1b. Investigate gene*environment effect modification by body mass index (BMI), which is associated with inflammation.

1c. Compare results among White and Black women.

AIM 2: To investigate the association of Toll-like receptor signaling genes and pathway with ovarian cancer survival among Black and White women separately.

2a. Investigate the association with downstream inflammatory processes and ovarian cancer survival.

2b. Investigate gene*environment effect modification by body mass index (BMI).

2c. Compare results among White and Black women.

AIM 3. To evaluate differentially expressed TLR, NFkB, and TNF pathway genes in high-grade serous ovarian cancer (HGSOC) tumor tissues among Black and White women.

3a. Investigate differentially expressed genes (DEGs) for HGSOC 5-year survival.

3b. Investigate DEGs for HGSOC stage at diagnosis.

Chapter 3: Data Sources and Methods

3.1. Data Sources

3.1.1 *The African American Cancer Epidemiology Study*

The African American Cancer Epidemiology Study (AACES)⁸⁰ is a population-based case-control study of ovarian cancer in Black women in 11 geographic locations. The sites were selected for geographic regions with a relatively high density of Black residents in the population and that had the ability to rapidly identify newly diagnosed cases of EOC. Eligible cases included women who self-identified as African American/Black aged 20 to 79 years with a newly diagnosed, histologically confirmed invasive EOC starting December 1, 2010, via population-based and hospital registries. Controls were frequency-matched based on age and geographic location. Controls were identified via an outside contractor (Kreider Research and Consulting) using list-assisted, random-digit dialing to select control women who self-identify as AA race. Controls were matched to cases by state of residence and 5-year age category. Eligible controls could not have had a previous diagnosis of EOC or bilateral oophorectomy. Contact of eligible cases for AACES stopped in 2016 and the last date of diagnosis was 12/31/2015.

3.1.2. *The Ovarian Cancer Association Consortium*

The Ovarian Cancer Association Consortium (OCAC)⁸¹ was formed in 2005 to allow for high-throughput and greater powered genetic association investigations, replication analyses for previously reported associations, and the identification of possible rare variants and novel genes that may promote EOC. To date, OCAC consists of more than 80 participating groups from four continents: North America, Europe, Asia, and Australia. Eligible case-control and cohort studies provided germline DNA for genotyping, managed by the University of Cambridge, and epidemiologic data, which was centrally harmonized at the OCAC data-coordination center at Duke University. A list of all participating OCAC studies is presented in **Supplementary Table ST2**.

3.2. Study Populations

The study population for Aim 1 will be comprised of all non-Hispanic Black cases and controls in AACES and OCAC ($N_{\text{cases}} = 720$; $N_{\text{controls}} = 1,201$) and non-Hispanic White cases and

controls in OCAC ($N_{\text{cases}} = 13,747$; $N_{\text{controls}} = 19,174$). Aim 2 will be a subset of the Aim 1 study population consisting of cases only. Specific Aim 3 will be a subset of Black AACES and North Carolina Ovarian Cancer Study (NCO; a participating OCAC study) and White NCO HGSOC cases who agreed to provide tumor tissue samples ($N_{\text{Black}} = 214$; $N_{\text{White}} = 255$).

3.3. Variables

3.3.1. Exposures

The 224 candidate genes included for analysis were selected from the Kyoto Encyclopedia of Genes and Genomes (KEGG)⁸² TLR, NFkB and TNF pathways. In situations where a gene appears in multiple pathways, we assigned the gene to only one pathway based off function (for example, lipopolysaccharide binding protein [*LBP*] is in both and NFkB and TLR pathways but analyzed only in the TLR pathway). In total, 95, 74, and 55 genes were in the TLR, NFkB, and TNF pathways, respectively. SNPs within each candidate gene were selected based on the chromosomal coordinates of the start and end positions (Ensembl GRCh37/hg19 for the Black dataset and GRCh38/hg38 for the White)^{83,84} $\pm 10,000$ base pairs to capture promoter and regulatory regions. All included genes and the chromosomal coordinates are shown per pathway in **Supplementary Table ST3**. For Aims 1 and 2, we investigate germline expression of these genes and pathways with EOC/HGSOC risk and outcomes. The exposure in Aim 3 is mRNA expression of genes in the TLR, NFkB, and TNF pathways within HGSOC tumor tissues among Black and White women.

3.3.1a. SNP selection, genotype data and quality control

Genotyping was performed at five centers: University of Cambridge, Center for Inherited Disease Research (CIDR), National Cancer Institute (NCI), Genome Quebec and Mayo Clinic using an Illumina Infinium iSelect BeadChip. Genotype data quality control (QC) was previously carried out according to the OncoArray QC guidelines.⁸¹ A small number of subjects that were not genetically female (XX) or those who had ambiguous sex, or were duplicates were omitted from the dataset.^{26,85}

Only those SNPs that passed QC for all consortia were used for imputation. White OCAC genotyped samples were imputed using the Michigan Imputation Server to the Trans-Omics for Precision Medicine (TOPMed) imputation with 97,256 samples (Version R2 on GRCh38/hg38).⁸⁶ Phasing was performed with Eagle2⁸⁷ and imputation with Minimac3.⁸⁸ In the Black genomic data, SNPs that were not directly genotyped were imputed according to the 1,000 Genomes Phase 3 v5 reference set (GRCh37/hg19) using Minimac3.⁸⁸ SNP level post-imputation QC included filtering on call rate >95%, Hardy–Weinberg Equilibrium $p > 1 \times 10^{-5}$, and a minor allele frequency (MAF) ≥ 0.01 using PLINK 2.0.^{89,90}

3.3.1b. RNA Extraction and quantification of gene expression data

RNA was extracted from FFPE tumor tissue and stored at -80°C . An initial quality control (QC) evaluation revealed substantial RNA degradation, so a repurification step consisting of DNAase treatment and purification on a Zymo research spin column was completed before library preparation to reduce the bulk of degraded RNA product (i.e., <200 nucleotides in length). Following repurification, RNA libraries were prepared from total RNA samples (5-100 ng) using reagents from the Illumina Stranded mRNA Prep (cat# 20020189) and TruSeq RNA UD Indexes (20040534) for reverse transcription, adapter ligation, and PCR amplification. Amplified libraries were hybridized to biotin-labeled probes from the Illumina Exome Panel (cat# 20020183) using the Illumina RNA Fast Hyb Enrichment kit (20040540) to generate strand-specific libraries enriched for coding regions of the transcriptome. Exon-enriched libraries were qualified on an Agilent Technologies 2200 TapeStation using a D1000 ScreenTape assay (cat# 5067-5582 and 5067-5583). The molarity of adapter-modified molecules was defined by quantitative PCR using the Kapa Biosystems Kapa Library Quant Kit (cat#KK4824). Individual libraries were normalized to 0.95 nM in preparation for Illumina sequence analysis. Sequencing libraries were chemically denatured and applied to an Illumina NovaSeq flow cell using the NovaSeq XP workflow (20043131). Following the

transfer of the flow cell to an Illumina NovaSeq 6000 instrument, a 150 x 150 cycle paired-end sequence run was performed using a NovaSeq 6000 S4 reagent Kit v1.5 (20028312).

Adapters were trimmed and read quality was filtered using fastp.⁹¹ Filtering was set to reads with a PHRED score of at least 15 and at least 20 base pairs long. Pair-end reads were quantified with salmon (version 1.4.0)⁹² using GRCh38 release 95. We used the seqBias and gcBias flags to correct for sequence-specific biases. The recommended rangeFactorizationBins parameter value was set to 4, which improves quantification accuracy on difficult-to-quantify transcripts. Then, low-expression genes were filtered out by excluding 10,608 genes with a median expression across all samples of 0. Samples were library-size normalized using 85th quantile normalization.

3.3.2. Outcomes

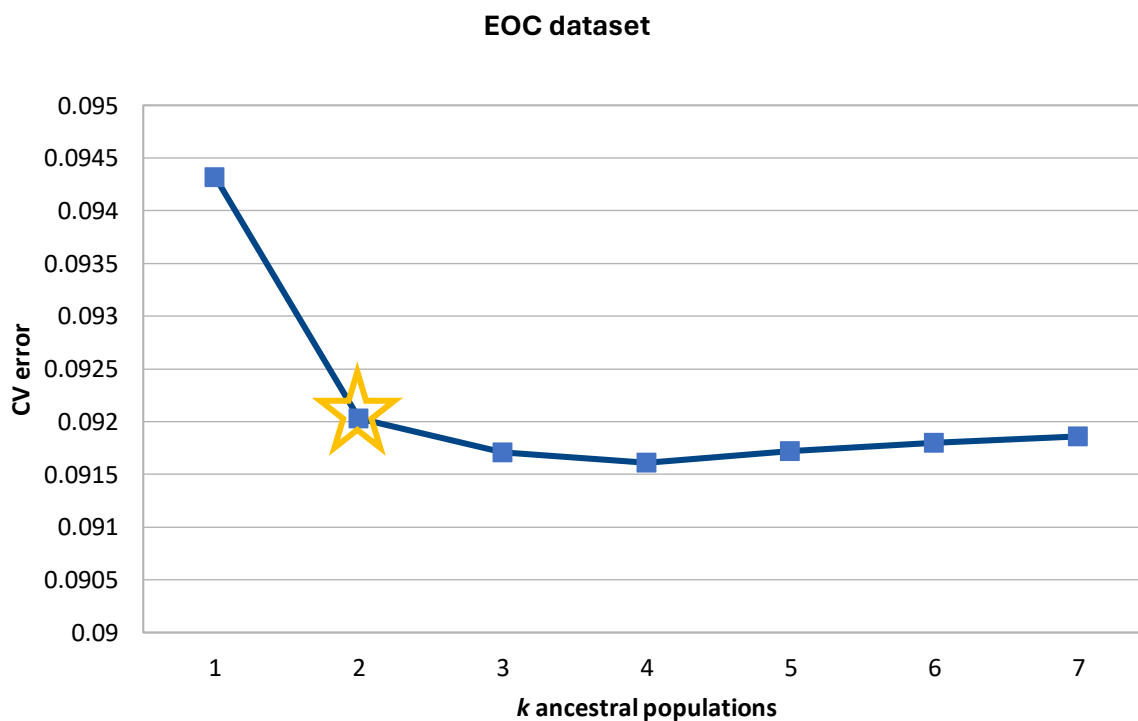
The outcome assessed in Aim 1 is the association with overall EOC and HGSOc-only risks among Black and White women. In Aim 2, we assess 5-year overall survival (yes/no) for both EOC and HGSOc cases. Aim 3 is a preliminary investigation of differentially expressed genes (DEGs) via mRNA expression in associated with two HGSOc clinical outcomes: overall 5-year survival and FIGO stage at diagnosis.⁹³ We further investigate possible associations and overall HGSOc survival and stage at diagnosis.

3.3.3. Covariates

For Aims 1 and 2, due to population stratification and possible differences in minor allele frequencies, all outcomes and analyses were stratified by self-reported race. We analyzed the five major EOC histotype together as well as restricted to high-grade serous only. In best practice, investigations should always stratify by histotype, but this can often present a challenge regarding power within certain histotypes, especially for minority groups and survival analyses. Risk estimates were controlled for age (continuous) and ancestry. Ancestry was controlled using principal

components (PCs). Ancestry was calculated for the OCAC and AACES using the software package FastPop, developed specifically for the OncoArray.^{26,85} To confirm the correct number of PCs to use for Black women, we used the Admixture program which estimates ancestry in a model-based manner from large autosomal SNP genotype datasets.⁹⁴ Using the cross-validation procedure, selection of the ideal number of ancestral populations was chosen based on a low cross-validation error estimates (**Figure 3.1**). To assess adequate control for admixture or possible inflation, QxQ plots and λ values were generated from the results of a genome-wide association analysis assuming an additive logistic regression model controlling for age and the first two PCs. We observed adequate control per the calculated λ values ($\lambda_{\text{Black}} = 1.02$, $\lambda_{\text{White}} = 1.10$) and QxQ plots (shown in **Supplementary Figures SF1 and SF2**).

Figure 2.1: Ancestral population (k) determination for principal components in Black



The analyses for Aim 3 control for ancestry using the previously derived PCs. For the exploratory Cox PH investigation of select gene mRNA expressions and survival. We control for two PC age at diagnosis and FIGO stage. Tumor cellularity is accounted for *post hoc* from the expression data via Cibersort to estimate cell fractions.⁹⁵ All analyses controlled for age at diagnosis, tumor purity, and two principal components. The survival analyses were additionally adjusted for FIGO stage at diagnosis.

3.4. Analytic Methods

We provide descriptive statistics (mean, median, and proportion) to describe selected demographic, tumor, and survival characteristics. All data and analyses presented are stratified by race and conducted for all EOC and HGSOC-only outcomes.

3.4.1. Aim 1

Additive, unconditional logistic regression models are used to calculate the genome-wide association of individual SNPs with EOC/HGSOC risks and 5-year overall survival (yes/no). Risk models adjust for age (continuous) and two PCs (continuous). The survival models additionally control for FIGO stage at diagnosis and histotype (for EOC models only). To conduct sub-analyses assessing interaction by BMI (continuous), we use the same additive risk and survival models with a SNP*BMI interaction term and assess significance via a Wald χ^2 test statistic *P*-value.

To examine the associations between genes (a combination of SNPs) and pathways (a combination of genes) and EOC/HGSOC risk, we use the Multi-marker Analysis of GenoMic Annotation (MAGMA) tool for gene and generalized gene-set analyses of GWAS data.⁵⁸ In brief, MAGMA accounts for local linkage disequilibrium and aggregates multiple logistic regression model-derived *P*-values for SNPs within the same gene body. We applied the same additive genetic model used in the genome-wide association analyses adjusting for age (continuous), and two ancestry PCs (continuous). To examine the associations between pathways and risk, each gene *P*-value computed

in the previous model is converted to a Z-value and normalized to yield a distribution that reflects the strength of the association for each gene with EOC/HGSOC risk. The competitive gene-set analysis is implemented as a linear regression model on this gene-level data matrix where the resulting *P*-value tests whether the mean association with EOC/HGSOC risk varies among genes in a specified gene-set (in this case, a pathway) relative to the genes not in the gene-set. MAGMA adjusts for gene size, gene density, the inverse of the mean MAC in the gene and the log value of each. To evaluate a possible interaction among genes and pathways with body mass index (BMI, kg/m², continuous), we use an extension of the MAGMA tool by adding a SNP by covariate interaction to the gene-level model. To correct for multiple testing, we adjust the raw gene-level *P*-values by the number of genes tested using the Benjamini-Hochberg false-discovery rate (FDR). We present both raw and FDR-corrected results. To better understand what may be driving a gene-level association with EOC/HGSOC risk, we report the lead SNP for gene and gene*BMI interactions. The measure of association and *P*-value for each lead SNP in a gene is extracted from the post-QC genome-wide analysis used to generate the QxQ plots and λ values. For statistically significant unadjusted gene*BMI interaction, we use the same genome-wide additive logistic regression model with a SNP*BMI interaction term. We report the SNP rsID, odds ratio (OR), 95% confidence interval (CI) and raw *P*-value for the most statistically significant gene-specific SNP.

As these data are the largest collection of genomic ovarian cancer case/control data and, therefore, cannot be validated in external data sources, we randomly split our White analytic dataset into a 67% test set and 33% internal validation set.

3.4.2. Aim 2

Analyses for Aim 2 follow the same procedures as in Aim 1 but the outcome is 5-year overall survival (yes/no) for EOC/HGSOC. We use MAGMA to estimate the association of genes and pathways with overall EOC and HGSOC survival. Interaction with BMI will also be implemented the

same as in Aim 1. Multivariable odds ratios and 95% confidence intervals for each SNP are calculated using logistic regression models adjusting for two PCs, age (continuous), FIGO stage, and histotype (EOC model only) assuming a log-additive model.

3.4.3. Aim 3

We investigate mRNA gene expression in HGSOC tumor tissues among Black and White women. Differentially expressed genes (DEGs) within the TLR, NFkB, and TNF pathways for HGSOC 5-year survival and stage at diagnosis are presented. Furthermore, binary variables for each gene are calculated as 'low': expression levels less than or equal to the gene-specific median and 'high': expression greater than the median. We perform exploratory analyses for dichotomized expression and survival and stage at diagnosis. Cox proportional hazard models are used to estimate hazard ratios (HRs) and 95% confidence intervals (CIs) for association of high vs low gene expression and survival adjusting for age, stage at diagnosis, and two ancestry principal components (PCs). Unconditional logistic regression models are used to estimate odds ratios (ORs) and corresponding 95% CIs for the association with FIGO stage at diagnosis adjusted for age and two ancestry PCs.

Chapter 4: Aim 1.

Pathogen-recognition and Inflammatory Genes and Pathways Associated with Epithelial Ovarian Cancer Risk

4.1. Abstract

Background: Epithelial ovarian cancer (EOC) has the highest mortality rate among all gynecologic cancers and is the fifth deadliest malignancy among women in the US. EOC mortality is largely attributable to the late stage of diagnosis as symptoms are often vague and non-specific. Due to these limitations, reducing EOC-specific mortality may best be accomplished by identifying groups at high risk of disease and factors that promote tumorigenesis. The goal of this study is to investigate whether genetic variation in genes belonging to toll-like receptor (TLR), nuclear factor kappa B (NFkB), and tumor necrosis factor (TNF) signaling pathways is associated with EOC risk at the gene or pathway level among Black and White women.

Methods: Eligible cases and controls were self-reported, non-Hispanic Black and White women genotype data from the African American Cancer Epidemiology Study (AACES) and the Ovarian Cancer Association Consortium (OCAC). Single-nucleotide polymorphisms (SNPs) were mapped to 224 genes in the Kyoto Encyclopedia of Genes and Genomes TLR, NFkB, and TNF pathways based on chromosomal location $\pm 10,000$ base pairs to capture promoter and regulatory regions. Due to differences in minor allele frequencies and population stratification, all analyses were stratified by race (Black and White women). To test and internally validate our results, we further randomized the White population into a 67% test cohort or a 33% validation cohort. We examine the associations of genes (a combination of SNPs) and pathways (a combination of genes or 'gene-set') and EOC risk, we use the Multi-marker Analysis of GenoMic Annotation (MAGMA) tool for gene and generalized gene-set analyses of GWAS data. We assumed an additive genetic model to assess the association with EOC or high-grade serous EOC (HGSOC) risk (yes vs no) adjusting for age and ancestry principal components. In addition, we investigated a possible gene x environment (GxE) interaction between observed statistically significant genes/pathways and body mass index

(BMI), which is disparately associated with EOC *and* race and is considered a chronic state of inflammation.

Results: Our study consisted of 720 Black invasive EOC cases and 1,201 Black controls (those with $\geq 50\%$ African ancestry) and 13,747 and 19,174 White cases and controls, respectively. Genes in White women had noticeably fewer SNPs mapped within the chromosomal locations. No pathway was statistically significant for any group in relation to EOC or HGSOC risk nor was any gene after correcting for multiple testing. Per raw P-values < 0.05 , MAPK-related genes, which trigger the transcription of genes involved in the regulation of cellular processes present in all three pathways, were associated with EOC and/or HGSOC risks among both Black and White women. Among White women specifically, four genes were associated with EOC/HGSOC risks in both the test and validation dataset. These genes included *MYD88* and *CCL2* associated with EOC risk and *PARP1* and *TICAM2* associated with HGSOC risk ($P_{\text{raw}} < 0.05$). Among Black women, *MAP3K8*, *MAP3K7*, and *PRKCB* were indicated to have an interaction with BMI for EOC but not HGSOC risk.

Conclusion: Although we had no statistically significant gene results after multiple testing correction, this study observed genes associated ($P_{\text{raw}} < 0.05$) with EOC and HGSOC risk among Black and White women that are biologically consistent with previously published literature among EOC and/or other cancer sites. These results may provide insight or generate new hypotheses regarding EOC carcinogenesis.

4.2 Introduction

Despite accounting for only ~3% of all cancers diagnosed among women, ovarian cancer ranks fifth among female cancer-specific fatality rates in the US.⁴ The most fatal gynecologic cancer,⁴ poor survival is largely attributable to the fact that most cases are diagnosed at stage III or later (65-75%), for which survival is only 30%² (vs 70-90% survival for stages I or II).⁴ The majority of ovarian tumors arise from the epithelium (~90%); germ cell and stromal tumors are rare.² Thus, forthcoming discussion of ovarian cancer is collectively referred to as epithelial ovarian cancer (EOC), which encompasses a group of malignancies involving the ovary, fallopian tube, and peritoneum that arise from epithelial cells.

EOC is a heterogeneous disease that consists of five major histotypes that have differing cells of origin, morphology, molecular features, methylation patterns, gene and RNA expression signatures, epidemiologic risk factors, and clinical characteristics.^{13,25-27} The incidence of EOC is also disparate among racial groups where Black women have an estimated 25% lower age-standardized incidence of ovarian cancer relative to White women.⁷⁸ In addition, modifiable risk factors such as BMI, oral contraceptive use, aspirin and body powder have been observed to account for more of the risk in Black women relative to White women.³⁰

Symptoms of EOC are vague and non-specific and may not be present during the earliest stages.⁹⁶ Development of an effective screening program has failed in multiple trials with low sensitivity and specificity,^{8,9} which may be, in part, due to a relatively short interval between the presence of detectable disease and dissemination of the tumor throughout the peritoneal cavity.⁹⁷ Because the effectiveness of screening and early intervention is inherently limited by the natural history of the disease, identifying high-risk groups and factors associated with tumorigenesis may be the best way to reduce EOC burden and reduce cancer-specific mortality.

A hallmark of cancer, inflammation is generally considered to be one of the most important environmental factors for tumorigenesis. Pathologic inflammatory conditions resulting from autoimmune diseases or exposure to infectious agents have been associated with tumor development for numerous cancer sites.³⁷ In EOC, pelvic inflammatory disease and chronic cervicitis following gonorrhea, chlamydia, or human papillomavirus infections are hypothesized risk factors.⁹⁸ There is growing evidence to support the idea that immunological responses to bacterial and viral products, and subsequently induced inflammatory processes, can mediate tumorigenesis.³⁷ Toll-like receptors (TLRs) are pattern recognition receptors that play a key role in immunity and downstream inflammatory responses by recognizing small, conserved microbial motifs expressed by microorganisms.^{50,51} TLRs expressed in non-neoplastic tissues can stimulate adaptive immune responses and activate immune cells that dynamically combat tumors.^{58,99} However, TLR expression in neoplastic cells can promote chronic inflammation and are anti-apoptotic in the tumor microenvironment. In a few small studies, TLR expression has been observed in both normal ovary and tumor tissues, and in EOC cell lines.⁶¹ TLR ligation and binding with adapter proteins activates an immune response and inflammatory signaling pathways such as nuclear factor kappa-light-chain-enhancer of activated B cells (NFκB)^{100,101} and tumor necrosis factor α (TNFα). NFκB is hypothesized to be a major link between chronic inflammation and cancer as it functions in all cell types present within the tumor microenvironment and modulates further inflammation and metastasis.¹⁰²

Despite experimental evidence of the involvement of TLRs and downstream inflammatory processes in association with EOC, and the polymorphic nature of these genes, few studies have comprehensively investigated the respective signaling pathways in relation to EOC risk. Many studies have investigated *TLR* polymorphisms with overall and site-specific cancer risks, the majority of which are now summarized in numerous meta-analyses.¹⁰³⁻¹¹⁷ There are a number

publications that show *TLR2*, *TLR4*, and *TLR9* polymorphisms, especially among cancers that occur in sites exposed to microbiota such as the stomach, colon, and cervix,^{105,106,109,113,117-119} are associated with cancer risks. However, among statistically significant SNPs, many are in opposing directions, underpowered, or only show an association when all cancer sites are analyzed together, which may not be the best approach given the heterogeneity among different sites. Given the modest to null associations observed, it is unlikely that a single SNP in *TLRs* and inflammatory pathway-associated genes could be a causal mechanism of carcinogenesis. In addition, most studies chose candidate SNPs based on previous literature, therefore only a select and small number of SNPs are evaluated. Last, the populations and cell lines that comprise these studies are almost entirely of White ancestry despite evidence of Black-White differences in genetic associations, gene expression and molecular biomarkers related to inflammatory processes.^{75,120,121} TLR genetic variants known to increase inflammation have been found to differ between the two racial groups as well.⁷⁶

In this study, we investigate whether genetic variation at the gene and/or pathway level for TLR, NFκB, and TNF signaling is associated with EOC risk. Additionally, we investigate whether there is a possible interaction with a chronic inflammatory state, characterized by body mass index (BMI), and risk of EOC. To account for population stratification and to evaluate any gene or pathway differences between Black and White women, all outcomes and analyses are stratified by race. Because EOC is a heterogeneous disease and histotypes have different risk factors¹² and gene expression profiles,²⁵ we also conduct all analyses restricting to high-grade serous ovarian cancer (HGSOC) cases, the most common histotype,⁴ relative to controls.

4.3 Methods

4.3.1 Case/control ascertainment and selection

The African American Cancer Epidemiology Study (AACES) is a population-based case-control study of Black women with invasive EOC and controls residing in 11 geographic locations in the U.S. enrolled between December 2010 and August 2016.⁸⁰ Cases were identified through cancer registries and hospitals and were eligible for the study if they were 1) aged 20–79 years, 2) self-reported Black race, and 3) resided in one of the included geographic regions. Controls were identified via an outside contractor using list-assisted, random-digit dialing to select control women who self-identify as Black. Controls were frequency-matched to cases by state of residence and 5-year age category. Eligible controls could not have had a previous diagnosis of EOC or bilateral oophorectomy. Institutional review board approval was obtained from all participating institutions. Methods have been described in further detail previously.⁸⁰

The Ovarian Cancer Association Consortium (OCAC)⁸¹ consists of more than 80 participating groups from four continents: North America, Europe, Asia, and Australia. Eligible case-control and cohort studies provided germline DNA for genotyping and epidemiologic data, which was centrally harmonized by members of OCAC at the data-coordination center. A list of all participating OCAC studies is presented in **Supplementary Table ST2**.

All invasive EOC cases and controls from OCAC who self-identified as non-Hispanic White women were eligible for inclusion in the White analytic dataset. The Black cases and controls from AACES and OCAC were previously subset to include women with >50% African ancestry, calculated using the software package FastPop.^{85,122}

4.3.2. SNP Selection, Genotyping, and Quality Control

Genotyping was performed at five centers: University of Cambridge, Center for Inherited Disease Research (CIDR), National Cancer Institute (NCI), Genome Quebec and Mayo Clinic using an Illumina Infinium iSelect BeadChip. Genotype data quality control (QC) was previously carried

out according to the OncoArray QC guidelines. A small number of subjects that were not genetically female (XX) or those who had ambiguous sex, or were duplicates were omitted from the dataset.^{26,85} White OCAC genotyped samples were imputed using the Michigan Imputation Server to the Trans-Omics for Precision Medicine (TOPMed) imputation with 97,256 samples (Version R2 on GRCh38/hg38).⁸⁶ Phasing was performed with Eagle2⁸⁷ and imputation with Minimac3.⁵¹ In the Black genomic data, SNPs that were not directly genotyped were imputed according to the 1,000 Genomes Phase 3 v5 reference set (GRCh37/hg19) using Minimac3.⁸⁸ SNP level post-imputation QC included filtering on call rate >95%, Hardy–Weinberg Equilibrium $p > 1 \times 10^{-5}$, and a minor allele frequency (MAF) ≥ 0.01 using PLINK 2.0.^{89,90}

4.3.3. Genes and Pathways

The 224 candidate genes included for analysis were selected from the Kyoto Encyclopedia of Genes and Genomes (KEGG)⁸² TLR, NFkB and TNF pathways. In situations where a gene appears in multiple pathways, we assigned the gene to only one pathway based off function (for example, lipopolysaccharide binding protein [*LBP*] is in both and NFkB and TLR pathways but analyzed only in the TLR pathway). In total, 95, 74, and 55 genes were in the TLR, NFkB, and TNF pathways, respectively. SNPs within each candidate gene were selected based on the chromosomal coordinates of the start and end positions (Ensembl GRCh37/hg19 for the Black dataset and GRCh38/hg38 for the White)^{83,84} $\pm 10,000$ base pairs to capture promoter and regulatory regions. All included genes and the chromosomal coordinates are shown per pathway in **Supplementary Table ST3**.

4.3.4. Statistical Analysis

To control for population admixture we use ancestry principal components (PCs). PCs were previously, separately calculated for the Black and White datasets using the software package FastPop, developed specifically for the OncoArray.^{26,85} To confirm the correct number of PCs to use,

we used the Admixture program, which estimates ancestry in a model-based manner from large autosomal SNP genotype datasets, on the raw Black genomic data.⁹⁴ Using the cross-validation procedure, selection of two PCs was indicated as the the ideal number of ancestral populations based on a low cross-validation error estimate (**Figure 3.1**). We applied the same number of PCs to our White population and assessed adequate control for possible inflation via QxQ plots and λ values generated from the P -values of all genome-wide SNPs assuming an additive logistic regression model controlling for age and the first two PCs. While using two PCs, we observed adequate control per the calculated λ values ($\lambda_{\text{Black}} = 1.02$, $\lambda_{\text{White}} = 1.10$) and QxQ plots (shown in **Supplementary Figures SF1-SF2**).

To examine the associations between genes (a combination of SNPs) and pathways (a combination of genes) and EOC/HGSOC risk, we use the Multi-marker Analysis of GenoMic Annotation (MAGMA) tool for gene and generalized gene-set analyses of GWAS data.¹²³ In brief, MAGMA accounts for local linkage disequilibrium and aggregates multiple logistic regression model-derived P -values for SNPs within the same gene body. We applied the same additive genetic model used in the genome-wide association analyses adjusting for age (continuous), and two ancestry PCs (continuous). To examine the associations between pathways and risk, each gene P -value computed in the previous model is converted to a Z-value and normalized to yield a distribution that reflects the strength of the association for each gene with EOC/HGSOC risk. The competitive gene-set analysis is implemented as a linear regression model on this gene-level data matrix where the resulting P -value tests whether the mean association with EOC/HGSOC risk varies among genes in a specified gene-set (in this case, a pathway) relative to the genes not in the gene-set. MAGMA adjusts for gene size, gene density, the inverse of the mean MAC in the gene and the log value of each. To evaluate a possible interaction among genes and pathways with body mass index (BMI, kg/m², continuous), we use an extension of the MAGMA tool by adding a SNP by covariate interaction to the gene-level

model. To correct for multiple testing, we adjust the raw gene-level P -values by the number of genes tested using the Benjamini-Hochberg false-discovery rate (FDR).¹²⁴ We present both raw and FDR-corrected results. To better understand what may be driving a gene-level association with EOC/HGSOC risk, we report the lead SNP for gene and gene*BMI interactions. The measure of association and P -value for each lead SNP in a gene is extracted from the post-QC genome-wide analysis used to generate the QxQ plots and λ values. For statistically significant unadjusted gene*BMI interaction, we use the same genome-wide additive logistic regression model with a SNP*BMI interaction term. We report the SNP rsID, odds ratio (OR), 95% confidence interval (CI) and raw P -value for the most statistically significant gene-specific SNP.

As these data are the largest collection of genomic ovarian cancer case/control data ($N_{\text{Black}} = 1,921$; $N_{\text{White}} = 32,921$) and, therefore, cannot be validated in external data sources, we randomly split our White analytic dataset into a 67% test set and 33% internal validation set. We compared selected baseline characters between the two sets and determined successful randomization (**Table 4.1**). Although this remains the largest genomic dataset for Black women with EOC as well, we unfortunately lack power the conduct internal validation in this group.

4.4. Results

In total, the final Black analytic dataset (AACES + OCAC) included 720 invasive EOC cases and 1,201 controls. The final White (OCAC) analytic test dataset included 9,181 and 12,876 cases and controls, respectively, while the White analytic validation dataset included 4,566 cases and 6,298 controls. Selected baseline characteristics for each study population are presented in **Table 4.1**. Cases had an average age of 57 years while controls were roughly 54 years old for all groups. Although mean BMI did not meaningfully differ between cases and controls within each group, the BMI among Black women was noticeably higher compared to White women.

All aggregate associations of SNPs at the gene and pathway levels for TLR, NFkB, and TNF signalling with EOC and HGSOC risk among Black and White women are shown in **Supplementary Tables ST4.1-ST4.4**. No pathway-level or FDR-corrected gene-level association was statistically significant for either racial group.

In **Table 4.2**, we present the genes ($P_{raw} < 0.05$) associated with EOC and/or HGSOC risk among Black women. In total, 19 genes were associated with Black EOC risk and 11 with Black HGSOC risk. Seven genes: *PRKCB* and *RELB* in the NFkB pathway, *PIK3CA*, *MAPK14*, *IRAK4*, and *MAPK8* in the TLR pathway, and *CREB3L4* in the TNF pathway, were associated with both EOC and HGSOC risk.

Mitogen activated protein kinases (MAPKs) related genes: *MAPK8*, *MAPK14*, *MAP2K2*, *MAP3K5*, *MAP3K7* and *MAP3K8* were associated with EOC at the gene level (all $P_{raw} < 0.04$. *MAPK8* and *MAPK14* were also associated with Black HGSOC risk. In addition, *MAP3K7* and *MAP3K8* were observed to have raw, statistically significant interactions with BMI for EOC risk ($P = 0.039$; **Table 4.3**). *PRKCB* also had an interaction with BMI for EOC risk and the lead SNP for all three genes was associated with an increase in risk per a one-unit increase in BMI. No gene associated with HGSOC risk was observed to have an interaction with BMI. It is possible we lack the power to detect an association for this group as the Black HGSOC*BMI analytic population was the smallest in the study (403 cases, 760 controls).

Genes in White women had noticeably fewer SNPs mapped within the chromosomal locations. This may be due to differences in minor allele and haplotype frequencies between the two groups, particularly for the TOPMed White genomic data where 96% of SNPs had a MAF < 0.01 . Six genes had no SNPs mapped after post-imputation and MAGMA internal QC filters while two genes (*MAPK11* and *MAPK12*) had chromosomal coordinates that were not included in the OCAC data

(**Supplementary Tables ST4.3-ST4.4**). In **Table 4.4** we present the genes observed to be associated ($P_{raw} < 0.05$) with EOC and/or HGSOC risks among the 67% test cohort of White women. Two genes were statistically significantly associated with EOC risk in both the White test and validation cohorts: *MYD88* and *CCL2*. Two different genes, *PARP1* and *TICAM2*, were associated with HGSOC in the test and validation sets. We observed 20 genes with raw, statistically significant associations with White EOC risk and 24 genes for HGSOC risk. Four genes were associated with both outcomes: *CSNK2A1* (NFkB) and *IL12B*, *TLR1* and *MYD88* (TLR). Several genes related to encoding members of the caspase family (*CASP8*, *CASP10*, *CFLAR*, *CARD10*, *CARD11*) and the TNF receptor superfamily (*TNFSF11*, *TNFRSF1A*, *TNFRSF1B*, *TRAF6*, *TNFAIP3*) were associated with White EOC and/or HGSOC risk. While we found two MAPK-related genes also associated with risk among White women (*MAP3K14*, *MAP3K8*), only *MAP3K8* was also observed in Black women. Also consistent with our results for HGSOC risk among Black women, *LY96* and *TNFAIP3* were associated with HGSOC risk in White women.

Among the statistically significant genes in the White women, only two were observed to differ by BMI (**Table 4.5**). We found *EDN1* indicated to be differentially associated with EOC risk while *CARD11* was observed to interact with BMI regarding HGSOC risk. Unlike our results in Black women, both lead SNPs were associated with a reduced risk of cancer per a one-unit increase in BMI. It should be noted that the lead SNP for *EDN1* was not statistically significant ($P_{raw} = 0.09$)

4.5. Discussion

In this analysis of genetic variation, we investigated whether TLR, NFkB, and TNF genes and/or pathways were associated with Black and White EOC or HGSOC risk. Despite null results after FDR correction, a discussion of the genes associated with our outcomes within and between the two groups before correction could possibly provide mechanistic insight or hypothesis

generation. Thus, the following discussion will present possible biological mechanisms consistent with our results.

We observed multiple MAPK genes associated with EOC and HGSOC risks for both Black and White women. MAPK mutations have been observed in numerous cancers including ovarian, breast, colon, melanoma, pancreas, lung, and thyroid.¹²⁵⁻¹³⁰ MAPKs in innate immune cells are activated downstream of pattern recognition receptors, such as TLRs, alongside NFkB. Activated by a wide range of intra- and extra-cellular stimuli, the MAPK cascade triggers the transcription of genes involved in the regulation of cellular processes including proliferation, differentiation, inflammation, and apoptosis.¹³¹ Ras proteins and downstream Raf kinases act as ‘molecular switches’ of the three-tiered cascade where an activated MAP3K (aka MEKK, MKKK) phosphorylates a MAP2K (MEK, MKK) which, in turn, phosphorylates MAPK.^{131,132} *Ras* is perhaps the most well studied and frequently mutated oncogene in human cancer, while *Raf* somatic mutations have been observed in multiple malignancies including serous EOC.¹³³⁻¹³⁵

MAP3K8 was associated with EOC risk for both Black and White women. Also known as the oncogene tumor progression locus 2 (*Tpl2*), *MAP3K8* encodes a protein that can induce NFkB and promote the production of TNF α and IL-2.¹³⁶ Dysregulation of *MAP3K8* expression has been observed in multiple malignancies and is associated with increased inflammation, malignant transformation, and angiogenesis.¹³⁷⁻¹³⁹ If genetic variations in *MAP3K8* lead to aberrant inflammatory processes, an increase in cancer risk seems plausible. Supporting this theory, the lead SNPs for *MAP3K8* in both groups had an OR > 1.

Black women additionally were observed to have interactions between *MAP3K8* and *MAP3K7* and BMI. Being obese has previously been found to be associated with higher plasma concentrations of LPS, which is recognized by TLR4, and higher circulating concentrations of pro-

inflammatory markers such as IL-6 and TNF- α . Within EOC, obesity has a disparate prevalence between Black and White (women as well as different strengths of association with EOC risk).¹⁴⁰ Similarly in our two populations, BMI was higher among Black women relative to White women, regardless of case or control status. MAP3K8 is expressed in human subcutaneous adipose tissues and mRNA expression is increased in obese and morbidly obese subjects relative to lean ones.¹⁴⁰ Within adipocytes, MAP3K8 is implicated to play a role in COX-2 expression¹⁴¹ and cross talk with macrophages to produce inflammatory cytokines in LPS-induced adipose tissue inflammation. In turn, MAP3K8 is activated by some of these inflammatory cytokines (such as TNF α) thus creating a pro-inflammatory signaling loop.^{142,143} In mice, MAP3K8 knockout attenuates immune cell infiltration and inflammation in adipose tissues.¹⁴² Slattery et al. found several SNPs in *MAPK* genes to have statistically significant interactions with dietary and lifestyle factors, such as BMI, with risks for colorectal or breast cancer risk.^{143,144}

MAPK8 and *MAPK14* were associated with both EOC and HGSOC risks among Black women only. MAPKs signal through one of two pathways: Jun N-terminal kinases (JNKs) and p38 MAPKs. *MAPK8* encodes JNK1 while *MAPK14* encodes p38 α .¹⁴⁵ Previous investigations regarding these genes and the proteins they encode are scarce in relation to EOC. In ovarian cancer cells, the JNK1 pathway was implicated to play a role in resistance to cisplatin, a platinum combination chemotherapy agent.¹⁴⁶ Pharmacological blockade of p38 α in 3 major EOC cell lines lead to a reduction of cell growth and viability¹⁴⁷ and immunohistochemical expression of p38 α was higher in FFPE EOC tumor tissues (N=120) relative to normal fallopian tube tissues (N=35).¹⁴⁸

MAP3K14 was associated with HGSOC risk among White women. Commonly known as NF κ B-inducing kinase (NIK), MAP3K14 plays a major role in regulating non-canonical NF κ B activation¹⁴⁹ which has been observed in EOC cell lines.¹⁵⁰ In EOC cell lines xenografted in mice,

depletion of NIK was observed to slow tumor growth.¹⁵⁰ In the same study, researchers also silenced NIK in cells via RNA interference and observed a reduction in NFkB2 DNA binding activity.¹⁵⁰

Although we observed other MAPK-related genes to be associated with EOC/HGSOC between Black vs White women, there is scant literature on observed racial differences in *MAPK* genetic variation (outside of upstream *Ras* and *Raf*).¹⁵¹⁻¹⁵³ One review reports key signaling proteins associated with the ERK1/2 signaling pathway, another major MAPK subfamily, to have racially disparate expression in Black relative to White cancer patients.¹⁵⁴ A study of early-stage breast cancer cases observed Black patients with *ERBB2* (previously *HER2*) positive tumors were significantly more likely to have MAPK pathway alterations (comprised of *EGFR*, *NF1*, *KRAS*, *BRAF*, and *MAP2K*) than White patients via tumor next-generation sequencing.¹⁵⁵ In colorectal cancer, Black cases had more *MAP2K1* mutations relative to White cases.¹⁵³

Upstream of MAPK signaling activation, TLR ligation induces IL-1R-associated kinases (IRAKs), genetic variations in which have been previously associated with cancer and inflammatory conditions.¹⁵⁶ *IRAK1* was associated with EOC risk among Black women in our study while *IRAK4* was associated with both outcomes. *IRAK4*, which recruits and phosphorylates *IRAK1*, plays an essential role in innate immune responses via the IL-1 signaling cascade, especially regarding cytokine signaling.¹⁵⁷ Overexpression of *IRAK4* can activate MAPK and NFkB pathways.^{157,158}

We observed *CREB3L4* associated with both EOC and HGSOC risks in Black women. In prostate cancer cell lines, *CREB3L4* is essential for proliferation and is modulated by and interacts with androgens and androgen receptors.¹⁵⁹ *CREB3L4* expression was observed to be upregulated in breast cancer tissues, which frequently express androgen receptors,¹⁶⁰ and knockdown of the gene in breast cancer cell lines inhibited proliferation and promoted apoptosis.^{161,162} Androgens and androgen receptors have been hypothesized to play a role in EOC¹⁶³⁻¹⁶⁶ as well as polycystic ovarian

syndrome,^{167,168} a known risk factor for EOC.^{169,170} Genetic variation of follistatin (*FST*), an encoding gene for a gonadal protein that inhibits follicle-stimulating hormone release, has been connected to PCOS and was associated with HGSOC risk in the previously conducted GWAS of the Black AACES and OCAC study population.⁸⁵

Among White women, *MYD88*, was associated with both EOC and HGSOC risks. A TLR adapter protein. MyD88 (often along with TLR4) is one of the more commonly studied genes in the TLR pathway. Yet, previous investigations of MYD88 expression in EOC tumor tissues have conflicting results^{61,62} or are focused on outcomes related to treatment or survival.^{64,65}

For White HGSOC risk only, five associated genes belong to the TNF receptor superfamily: *TRAF6*, *TNFSF11*, *TNFRSF1A*, *TNFRSF1B*, and *TNFAIP3*. In a study analyzing genetic variation in *TRAFs* from The Cancer Genome Atlas (TCGA) and the Catalog of Somatic Mutations in Cancer (COSMIC) datasets, Zhu et al found eight cancers with a greater proportion of *TRAF6* variation, including EOC (5.1%).¹⁷¹ The consistency between the TCGA/COSMIC-wide results and our findings among White women only may be due to the high number (or larger sample size) of White cases in the datasets.¹⁷² The tumor necrosis factor receptor-associated factor (TRAF) family consists of adapter proteins that regulate signaling pathways including TLR, NFkB, and TNF and therefore play a role in downstream cellular processes such as proliferation and differentiation.^{173,174} Binding of the TNFRSF1A protein with TNF induces activation of NFkB^{175,176} and *TNFRSF1A* SNP rs767455 is associated with an increased risk of breast cancer.¹⁷⁷

The major strength of our study is the largest sample size of high quality, EOC genotype data that has been previously QCed and pathologically confirmed. To our knowledge this is the first comprehensive analysis of TLR, NFkB, and TNF genes and pathways for EOC risk. By studying genes and pathways, we sought to ameliorate the challenges of interpreting a meaningful change in a single

SNP associated with an outcome. The gene level allows us to assess a singular function while the pathway level considers cellular processes at large with other genes that share biological functions up or downstream. In addition, our selection of pathways and genes was hypothesis driven.

Although we have discussed biologically plausible support for our results regardless of the lack of statistical significance after FDR correction, that is not to say the data are without limitations that should be critically considered. First and foremost, cancer is a stochastic disease and genetics account for very few causal mechanisms at any cancer site. Furthermore, race is a social construct and racial disparities in health are rarely a direct result of genetic differences. However, if genes are differentially associated with risk, it may provide insight to the etiology/ biological processes that are associated with ovarian carcinogenesis and/or EOC disparities.

Although this is the largest genetic dataset for women with EOC, we were still hindered by small sample sizes in subgroups such as histotype, which are known to be differentially associated with race and genetic markers. To reduce histotype variability, we also restricted our analyses to HGSOC cases vs controls and observed genes that were associated with EOC remained. Still these genes may not be generalizable to other histotypes such as low-grade serous and mucinous.

The validity of the White OCAC data may also be a major limitation in our analyses. More than 96% of all SNPs imputed had MAFs less than or equal to 0.01 and far fewer passed MAGMA QC filtering relative to the Black imputed data. We explored multiple datasets and QC thresholds but could not map SNPs to every selected gene among the White datasets. Nor could we replicate previously published OCAC GWAS SNP totals, λ or QxQ plot. Upon our request for scripts to reproduce these results, we were informed the findings were generated using an in-house logit program. Furthermore, some of the raw genomic data was truncated resulting in missing data for entire genes. These reasons could be why we observed very few internally validated results between

our 67/33% randomly split cohorts. Another possibility for the lack of validation could be an extreme sensitivity to sample size in the MAGMA program. Considering the 33% cohort is still larger than our total Black population, those results could potentially be invalid as well. While the simple answer to this question would be to analyze the same data using another gene/gene-set analysis program, there are no programs (to our knowledge) that are currently maintained which suit all our analytic needs (raw GWAS data, interaction assessment, gene, and gene-set analyses) for comparison.

In conclusion, this study has presented possible genetic variations in TLR and downstream NFkB and TNF inflammatory genes/pathways associated with EOC risk among Black and White women that are biologically consistent with previously published literature among EOC and/or other cancer sites. This study also highlights the necessity for documenting and facilitating methods of reproducibility and validity for both data sets and analytic programs. Further investigations of these genes and biological processes in relation to EOC risk may be more fruitful when investigating somatic expression within the tumor microenvironment rather than germline expression.

4.6. Tables and Figures

Table 4.1. Select baseline characteristics of the Black and White analytic populations from AACES and OCAC participants.

	Black Women		White Women			
			Test (67%)		Validation (33%)	
	Controls	Cases	Controls	Cases	Controls	Cases
N	1,201	720	12,876	9,181	6,298	4,566
Age, mean (sd)	54.6 (11.8)	57.1 (11.2)	54.6 (12.1)	58.8 (11.4)	54.6 (12.1)	58.8 (11.6)
BMI (kg/m ²), mean (sd)	32 (8.4)	32.8 (8.3)	27.2 (6.3)	27.1 (6.1)	27.3 (6.6)	27.6 (6.8)
missing, N (%)	431 (35.9)	166 (23.1)	10,524 (81.7)	7,055 (76.8)	5,133 (81.5)	3,537 (77.5)
Year of diagnosis, N (%)						
1990-1999		11 (1.5)		74 (0.8)		41 (0.9)
2000-2009		119 (16.5)		1,212 (13.2)		1,386 (30.4)
2010-2019		423 (58.8)		2,884 (31.4)		647 (14.2)
missing		167 (23.2)		5,010 (54.6)		2,492 (54.6)
Stage, N (%)						
localized		128 (17.8)		1,082 (11.8)		545 (11.9)
regional		66 (9.2)		1,395 (15.2)		695 (15.2)
distant		400 (55.6)		4,414 (48.1)		2,315 (50.7)
unstaged/missing		126 (17.5)		2,290 (24.9)		1,191 (26.1)
Histotype, N (%)						
high-grade serous		423 (58.8)		5,612 (61.1)		2,774 (60.8)
low-grade serous		20 (2.8)		310 (3.4)		167 (3.7)
endometrioid		64 (8.9)		612 (6.7)		292 (6.4)
clear cell		26 (3.6)		528 (5.6)		281 (6.2)
mucinous		34 (4.7)		514 (5.6)		274 (6)
other EOC		153 (21.3)		1,605 (17.5)		754 (16.5)

Abbreviations: AACES = African American Cancer Epidemiology Study, OCAC = Ovarian Cancer Association Consortium, N = number, BMI = body mass index, EOC = epithelial ovarian cancer.

Table 4.2. Statistically significant gene associations and lead SNPs within TLR, NFkB, and TNF pathways with invasive EOC and HGSOC risk among Black women in AACES and OCAC.^a

Pathway	Gene	# SNPs	<i>P</i> ^b	<i>P</i> _{FDR} ^c	Lead SNP	Ref. allele	Alt. allele	OR (95% CI) ^d	<i>P</i> _{SNP}
EOC									
NFkB	<i>PRKCB</i>	2,384	0.003	0.351	rs148451701	G	A	2.65 (1.70-4.15)	<0.001
	<i>GADD45G</i>	7	0.006	0.351	rs3138505	G	A	0.48 (0.33-0.70)	<0.001
	<i>LTB</i>	4	0.009	0.351	rs3093556	A	G	0.46 (0.26-0.80)	0.007
	<i>PIDD1</i>	82	0.010	0.351	rs1865782162	CT	C	1.42 (1.17-1.72)	<0.001
	<i>PLCG2</i>	1,937	0.018	0.375	rs9938253	G	A	0.67 (0.54-0.81)	<0.001
	<i>RELB</i>	193	0.046	0.556	rs74394107	T	C	1.97 (1.22-3.19)	0.006
TLR	<i>PIK3CA</i>	326	0.007	0.351	rs116367233	C	T	1.86 (1.35-2.55)	<0.001
	<i>MAPK14</i>	400	0.012	0.351	rs138487031	A	G	2.03 (1.26-3.27)	0.004
	<i>IRAK4</i>	144	0.012	0.351	rs9849	C	T	1.26 (1.10-1.43)	0.001
	<i>MAP2K2</i>	176	0.012	0.351	rs6630	G	T	1.25 (1.09-1.42)	0.001
	<i>MAP3K8</i>	144	0.017	0.375	rs303437	G	A	1.36 (1.16-1.59)	<0.001
	<i>IRAK1</i>	25	0.029	0.474	rs5987026	T	C	1.13 (0.98-1.67)	0.095
	<i>MAPK8</i>	598	0.033	0.474	rs73296755	A	C	0.28 (0.13-0.63)	0.002
	<i>MAP3K7</i>	318	0.035	0.474	rs34087194	T	A	0.36 (0.17-0.75)	0.006
TNF	<i>CREB3L4</i>	11	0.015	0.375	rs4845586	G	T	0.83 (0.73-0.96)	0.009
	<i>CXCL5</i>	5	0.023	0.446	rs352047	G	C	0.85 (0.74-0.96)	0.013
	<i>TRAF2</i>	253	0.034	0.474	rs17250483	G	A	0.67 (0.53-0.85)	0.001
	<i>MAP3K5</i>	1,047	0.035	0.474	rs1022690	T	C	0.77 (0.67-0.89)	<0.001
	<i>CREB5</i>	3,041	0.045	0.556	rs56271133	C	T	2.04 (1.37-3.06)	<0.001
HGSOC									
NFkB	<i>PRKCB</i>	2,384	0.007	0.559	rs74560827	G	T	2.25 (1.47-3.44)	<0.001
	<i>RELB</i>	193	0.006	0.559	rs34491117	G	T	1.94 (1.30-2.89)	0.001
	<i>IKBKE</i>	163	0.012	0.674	rs41295982	A	G	1.96 (1.44-2.66)	<0.001
	<i>LY96</i>	221	0.020	0.761	rs143496381	A	C	3.10 (1.55-6.19)	0.001
TLR	<i>PIK3CA</i>	326	0.023	0.761	rs115920312	C	A	0.68 (0.51-0.92)	0.012
	<i>CTSK</i>	22	0.030	0.803	rs1811698	T	C	1.24 (1.06-1.45)	0.007
	<i>MAPK14</i>	400	0.045	0.803	rs7750653	T	G	1.37 (1.07-1.75)	0.014
	<i>MAPK8</i>	598	0.045	0.803	rs140396817	A	G	2.62 (1.37-5.01)	0.003
	<i>IRAK4</i>	144	0.045	0.803	rs3794262	A	T	1.23 (1.05-1.44)	0.011
TNF	<i>CREB3L4</i>	11	0.007	0.559	rs4845586	G	T	0.82 (0.69-0.97)	0.021
	<i>TNFAIP3</i>	48	0.023	0.761	rs74880481	T	TA	0.79 (0.65-0.97)	0.023

Abbreviations: TLR = toll-like receptor; NFkB = nuclear factor kappa B; TNF = tumor necrosis factor; EOC = epithelial ovarian cancer; HGSOC = high grade serous ovarian cancer; AACES = African American Cancer Epidemiology Study; OCAC = Ovarian Cancer Association Consortium; SNP = single nucleotide polymorphism; FDR = false discovery rate; Ref = referent; Alt = alternate; OR = odds ratio; CI = confidence interval.

^aWith unadjusted P-value < 0.05.

^bAggregate P-value of MAGMA model results. Each model controls for age and the first two ancestry principal components.

^cCorrected for multiple testing by the number of genes tested using the Benjamini-Hochberg false discovery rate (FDR).

^dAdditive model adjusted for age and two ancestry principal components

Table 4.3. Statistically significant BMI interactions and lead SNPs among raw statistically significant genes associated with EOC risk among Black women in AACES and OCAC.^a

Pathway	Gene	# SNPs	P_{BMI}^b	$P_{BMI\ FDR}^c$	Lead SNP	Ref. allele	Alt. allele	OR _{SNPxBMI} (95% CI) ^d	$P_{SNPxBMI}$
NfκB	<i>PRKCB</i>	2384	0.044	0.748	rs198200	C	G	1.07 (1.03-1.11)	<0.001
TLR	<i>MAP3K8</i>	144	0.004	0.748	rs7910678	A	T	1.09 (1.04-1.13)	<0.001
	<i>MAP3K7</i>	318	0.039	0.748	rs9362755	T	C	1.03 (1.01-1.06)	0.006

Abbreviations: BMI = body mass index; EOC = epithelial ovarian cancer; AACES = African American Cancer Epidemiology Study; OCAC = Ovarian Cancer Association Consortium; SNP = single nucleotide polymorphism; FDR = false discovery rate; Ref = referent; Alt = alternate; OR = odds ratio; CI = confidence interval; TLR = toll-like receptor; NFκB = nuclear factor kappa B.

^aWith unadjusted P-value < 0.05.

^bAggregate P-value of MAGMA model results for gene*BMI interaction. Each model controls for age, BMI, and the first two ancestry principal components.

^cCorrected for multiple testing by the number of genes tested using the Benjamini-Hochberg false discovery rate (FDR).

^dOR for SNP*BMI interaction term in an additive model adjusted for age, BMI and two ancestry principal components.

Table 4.4. Statistically significant genes and lead SNPs within TLR, NFkB, and TNF pathways with invasive EOC and HGSOC risk among White women in OCAC.^a

Pathway	Gene	# SNPs	Test 67% (N _{EOC} = 9,181, N _{HGSOC} = 5,612, N _{controls} = 12,876)		Validation 33% (N _{EOC} = 4,566, N _{HGSOC} = 2,774, N _{controls} = 6,298)		Lead SNP	Ref. allele	Alt. allele	OR (95% CI) ^d	P _{SNP}
			P ^b	P _{FDR} ^c	P ^b	P _{FDR} ^c					
EOC											
NfκB	<i>CSNK2A1</i>	166	0.008	0.297	0.084	0.565	rs80001974	C	T	0.81 (0.73-0.90)	<0.001
	<i>BLNK</i>	253	0.011	0.297	0.784	1.000	rs117791247	G	A	1.21 (1.08-1.35)	0.001
	<i>RIPK1</i>	119	0.012	0.297	0.318	0.825	rs183512622	G	A	1.47 (1.17-1.85)	0.001
	<i>EDA2R</i>	56	0.016	0.334	0.792	1.000	rs146182380	T	G	0.83 (0.72-0.97)	0.020
	<i>ERC1</i>	1,966	0.016	0.334	0.927	1.000	rs77087493	T	A	0.79 (0.71-0.89)	<0.001
	<i>TAB3</i>	67	0.033	0.477	0.402	0.868	rs17283005	A	G	0.92 (0.86-0.99)	0.028
	<i>CARD10</i>	155	0.042	0.522	0.386	0.868	rs4080481	C	A	1.04 (1.01-1.08)	0.016
TLR	<i>CFLAR</i>	200	< 0.001	0.052	0.167	0.745	rs137937873	C	T	1.22 (1.08-1.38)	0.001
	<i>CASP8</i>	221	< 0.001	0.052	0.211	0.825	rs3769821	T	C	1.06 (1.03-1.10)	<0.001
	<i>IL12B</i>	73	0.005	0.267	0.706	1.000	rs2546892	G	A	0.93 (0.89-0.96)	<0.001
	<i>MAP3K8</i>	42	0.006	0.267	0.910	1.000	rs3824589	T	A	1.08 (1.02-1.14)	0.009
	<i>CD86</i>	206	0.020	0.340	0.281	0.825	rs2681416	G	A	0.96 (0.93-0.99)	0.014
	<i>TLR1</i>	161	0.020	0.340	0.727	1.000	rs5743594	G	A	0.94 (0.90-0.98)	0.003
	<i>MYD88</i>	35	0.021	0.340	0.028	0.385	rs6853	A	G	1.09 (1.04-1.14)	0.001
	<i>IFNAR1</i>	157	0.039	0.522	0.668	0.976	rs13046940	G	A	1.15 (1.07-1.25)	<0.001
	<i>AKT3</i>	546	0.044	0.522	0.258	0.825	rs145558771	T	C	0.79 (0.67-0.94)	0.007
TNF	<i>CASP10</i>	131	0.002	0.141	0.280	0.825	rs115407041	C	A	1.18 (1.05-1.32)	0.004
	<i>EDN1</i>	118	0.010	0.297	0.069	0.506	rs9349158	A	C	0.94 (0.90-0.99)	0.010
	<i>CCL2</i>	59	0.023	0.345	0.039	0.393	rs4586	T	C	1.05 (1.02-1.09)	0.002
	<i>PGAM5</i>	117	0.046	0.522	0.848	1.000	rs1409015057	TGGG	T	0.89 (0.82-0.96)	0.003
HGSOC											

NfκB	<i>GADD45B</i>	31	<0.001	0.069	0.693	1.000	rs2024144	C	T	1.05 (0.99-1.10)	0.087
	<i>MAP3K14</i>	166	0.005	0.223	0.276	0.937	rs1352312	T	G	1.11 (1.07-1.16)	<0.001
	<i>IL1R1</i>	417	0.006	0.229	0.272	0.937	rs115860741	G	A	1.28 (1.10-1.5)	0.002
	<i>CARD11</i>	447	0.011	0.349	0.955	1.000	rs2527506	G	A	1.08 (1.04-1.13)	<0.001
	<i>TRAF6</i>	95	0.019	0.404	0.617	1.000	rs200798752	T	TAGA	0.76 (0.64-0.90)	0.001
	<i>CSNK2A1</i>	159	0.019	0.404	0.193	0.935	rs80001974	C	T	0.77 (0.68-0.87)	<0.001
	<i>TNFSF11</i>	215	0.024	0.413	0.605	1.000	rs78205134	C	G	0.76 (0.64-0.90)	0.002
	<i>CXCL2</i>	31	0.025	0.413	0.055	0.745	rs11574449	C	G	0.82 (0.67-0.99)	0.037
	<i>BCL2L1</i>	123	0.031	0.421	0.161	0.900	rs117957706	A	T	0.79 (0.67-0.94)	0.009
	<i>PARP1</i>	217	0.035	0.421	0.016	0.448	rs78797064	T	G	0.80 (0.69-0.91)	0.001
TLR	<i>LY96</i>	172	0.001	0.077	0.541	0.970	rs142442787	T	C	0.77 (0.66-0.89)	0.001
	<i>TLR1</i>	161	0.012	0.349	0.149	0.900	rs3924113	G	T	1.06 (1.02-1.11)	0.009
	<i>TLR6</i>	163	0.019	0.404	0.480	0.959	rs79025411	G	A	0.78 (0.68-0.90)	0.001
	<i>PIK3CB</i>	292	0.030	0.421	0.570	0.983	rs869187727	TAA	T	1.07 (1.03-1.12)	0.001
	<i>IL12B</i>	73	0.033	0.421	0.228	0.937	rs2569253	C	T	1.06 (1.03-1.10)	0.001
	<i>MYD88</i>	35	0.035	0.421	0.715	1.000	rs6853	A	G	1.09 (1.04-1.16)	0.001
	<i>TICAM2</i>	90	0.043	0.445	0.046	0.745	rs256945	T	A	0.93 (0.89-0.96)	<0.001
	<i>PIK3R1</i>	301	0.045	0.445	0.456	0.957	rs831229	G	A	0.94 (0.90-0.97)	0.001
TNF	<i>CREB5</i>	1,712	0.003	0.196	0.098	0.900	rs12671650	C	T	1.10 (1.06-1.14)	<0.001
	<i>CREB3</i>	33	0.003	0.196	0.203	0.937	rs10814274	C	T	1.06 (1.02-1.10)	0.002
	<i>TNFRSF1A</i>	39	0.022	0.413	0.787	1.000	rs4149587	C	G	1.05 (1.01-1.09)	0.012
	<i>TNFRSF1B</i>	103	0.043	0.445	0.529	0.970	rs5745961	C	T	0.78 (0.65-0.95)	0.015
	<i>TNFAIP3</i>	77	0.045	0.445	0.748	1.000	rs79608867	G	C	0.84 (0.70-1.00)	0.051
	<i>RPS6KA4</i>	85	0.047	0.445	0.840	1.000	rs117514762	C	T	0.83 (0.73-0.95)	0.006

Abbreviations: TLR = toll-like receptor; NfκB = nuclear factor kappa B; TNF = tumor necrosis factor; EOC = epithelial ovarian cancer; HGSOC = high grade serous ovarian cancer; AACES = African American Cancer Epidemiology Study; OCAC = Ovarian Cancer Association Consortium; SNP = single nucleotide polymorphism; FDR = false discovery rate; Ref = referent; Alt = alternate; OR = odds ratio; CI = confidence interval.

^aWith unadjusted P-value < 0.05.

^bAggregate P-value of MAGMA linreg, snp-wise=mean and snp-wise=top model results. Each model controls for age and the first two ancestry principal components.

^cCorrected for multiple testing by the number of genes tested using the Benjamini-Hochberg false discovery rate (FDR).

^dAdditive model adjusted for age and two ancestry principal components

Table 4.5. Statistically significant BMI interactions and lead SNPs among raw statistically significant genes associated with EOC or HGSOC risk among White women in OCAC. ^a										
Pathway	Gene	Test 67%		Validation 33%		Lead SNP	Ref. allele	Alt. allele	OR _{SNPxBMI} ^d (95% CI)	<i>P</i> _{SNPxBMI}
		<i>P</i> _{BMI} ^b	<i>P</i> _{BMI FDR} ^c	<i>P</i> _{BMI} ^b	<i>P</i> _{BMI FDR} ^c					
EOC										
TNF	<i>EDN1</i>	0.016	0.392	0.868	1.000	rs9296344	T	C	0.98 (0.96-1.00)	0.088
HGSOC										
NfκB	<i>CARD11</i>	0.027	0.517	0.123	1.000	rs144144335	C	T	0.90 (0.85-0.95)	<0.001

Abbreviations: BMI = body mass index; EOC = epithelial ovarian cancer; HGSOC = high grade serous ovarian cancer; OCAC = Ovarian Cancer Association Consortium; SNP = single nucleotide polymorphism; FDR = false discovery rate; Ref = referent; Alt = alternate; OR = odds ratio; CI = confidence interval; TNF = tumor necrosis factor.

^aWith unadjusted P-value < 0.05.

^bAggregate P-value of MAGMA model results for gene*BMI interaction. Each model controls for age, BMI, and the first two ancestry principal components.

^cCorrected for multiple testing by the number of genes tested using the Benjamini-Hochberg false discovery rate (FDR).

^dOR for SNP*BMI interaction term in an additive model adjusted for age, BMI and two ancestry principal components.

Chapter 5: Aim 2.

Pathogen-recognition and Inflammatory Genes and Pathways Associated with Epithelial Ovarian
Cancer Survival

5.1. Abstract

Background: Despite being a rare cancer, epithelial ovarian cancer (EOC) is the most lethal gynecologic malignancy in the US. EOC survival is further complicated by the heterogeneity of histologic subtypes and racial disparities in clinical outcomes. Inflammation in the tumor microenvironment is an established driver of cancer progression and may represent targetable processes for treatment. In this study we investigate whether genetic variation in the toll-like receptor (TLR) and downstream pro-inflammatory NF κ B- and TNF-signaling pathways is associated with EOC survival at the gene or pathway level among Black and White women.

Methods: Eligible EOC cases were self-reported, non-Hispanic Black and White women with OncoArray genotype data from the African American Cancer Epidemiology Study (AACES) and the Ovarian Cancer Association Consortium (OCAC). Single-nucleotide polymorphisms (SNPs) were mapped to 224 genes in the Kyoto Encyclopedia of Genes and Genomes TLR, NF κ B, and TNF pathways based on chromosomal location \pm 10,000 base pairs to capture promoter and regulatory regions. Due to differences in minor allele frequencies and population stratification, all analyses were stratified by race (Black and White women). To test and internally validate our results, we further randomized the White population into a 67% test cohort or a 33% validation cohort. To examine the associations of genes (a combination of SNPs) and pathways (a combination of genes or 'gene-set') with EOC survival, we used the Multi-marker Analysis of GenoMic Annotation (MAGMA) tool for gene and generalized gene-set analyses of GWAS data. We assumed an additive genetic model to assess the associations with EOC or high-grade serous EOC (HGSOC) 5-year survival (yes vs. no) adjusting for age, FIGO stage, tumor histotype (EOC model only) and ancestry principal components. In addition, we investigated a possible gene x environment interaction with

the genes/pathways with body mass index (BMI), which is disparately associated with EOC and race and is considered a chronic state of inflammation.

Results: Our study consisted of 720 Black and 13,747 invasive EOC cases. Genes in White women had noticeably fewer SNPs mapped within the chromosomal locations. No pathway was statistically significant for any group in relation to EOC or HGSOC 5-year survival nor was any gene after correcting for multiple testing. Per raw P -values < 0.05 , *AKT3* and *CTSK* genes were associated with EOC and/or HGSOC 5-year survival in both Black and White women. *LTA* was the only gene observed to possibly have a Black EOC 5-year survival association differential by BMI. No interactions with BMI were observed for White women.

Conclusion: No gene results were statistically significant after multiple testing correction. We observed genes associated ($P_{\text{raw}} < 0.05$) with EOC and HGSOC 5-year survival among Black and White women that are biologically plausible and consistent with previously published literature among EOC and/or other cancer sites. These results may provide insight or generate new hypotheses regarding processes contributing to EOC survival.

5.2. Introduction

The most fatal of all gynecologic malignancies, ovarian cancer-specific mortality ranks fifth highest among female cancers in the US, despite being a rare cancer.⁴ Although Black women have a lower risk of developing epithelial ovarian cancer (EOC), they experience markedly worse outcomes relative to White women²⁹ and have a five-year relative survival approximately 10% lower.¹⁷⁸

Tumor-associated inflammation in the tumor microenvironment (TME) is an established driver of proliferation, progression, metastasis, chemoresistance, and genomic instability.^{37,179} The tumor microenvironment milieu contains both inflammatory and immunosuppressive components

that are coopted by malignant and infiltrating immune cells.⁴⁶ Tumor-associated macrophages, for example, are often functionally transformed into the M2-like phenotype which favor tumor growth and promote TME remodeling by producing growth and immunosuppressive factors.⁴⁷

Toll-like receptors (TLRs) are pattern recognition receptors that play a key role in immunity and downstream inflammatory responses by recognizing small, conserved microbial motifs expressed by microorganisms.^{50,51} TLRs expressed in cancer cells can promote proliferation, anti-apoptosis, and chemoresistance of EOC through the activation of multiple proinflammatory cytokines.^{42,58} Select TLRs also recognize endogenous ligands released as part of cellular debris following cell death.⁵¹ Cellular debris released during primary debulking surgery or chemotherapy can be recognized by TLRs and may initiate tumor repair processes leading to recurrence. Downstream of TLR ligation and binding with adapter proteins, an intricate signaling cascade is triggered that activates immune response and inflammatory signaling pathways such as nuclear factor kappa-light-chain-enhancer of activated B cells (NFkB)¹⁰⁰ and tumor necrosis factor α (TNF α).¹⁰¹ NFkB is hypothesized to be a major link between chronic inflammation and cancer as it functions in all cell types present within the tumor microenvironment and modulates further inflammation and metastasis.¹⁰² In EOC, a meta-analysis of 9 retrospective studies showed that a systemic immune inflammation index (calculated *via* pre-treatment neutrophil, platelet, and lymphocyte counts) was associated with lymph-node metastasis and progression-free and disease-free survival.¹⁸⁰

EOC is a heterogeneous disease that consists of five major histotypes (a combination of histology and grade) that have differing cells of origin, morphology, molecular features, methylation patterns, gene and RNA expression signatures, epidemiologic risk factors, clinical characteristics, and survival rates.^{12,13,25-27} The most common histotype, high grade serous ovarian cancer (HGSOC) tumors were observed to have a greater endogenous immune response (indicated by tumor

infiltrating lymphocytes) relative to other histotypes.¹⁸¹ In a study of inflammatory serum biomarkers (glycoproteins A, B, and C) among HGSOC cases, researchers observed significantly higher levels in HGSOC and was associated with tumor progression.¹⁸²

Black-White differences in genetic associations, gene expression and molecular biomarkers related to inflammatory processes have been observed in previous GWAS and candidate SNP studies^{74,75,121} and TLR genetic variants known to increase inflammation have been found to differ between the two racial groups.⁷⁶ Immune and inflammatory responses have been observed to differ between Black and White individuals in numerous cancers including ovarian, breast, colon, prostate, and lung.^{183,184} Despite these findings and the polymorphic nature of these genes, no study has thoroughly investigated racial differences in genetic variation of pathogen recognition and inflammatory pathways among Black and White women with EOC. Therefore, in this study we investigate whether genetic variation at the gene and/or pathway level of TLR, NFkB, and TNF is associated with EOC 5-year overall survival (OS). Additionally, we assess whether there is a possible gene x environment interaction with a chronic inflammatory state, characterized by body mass index (BMI), and OS. To account for population stratification and to elucidate if there are any gene or pathway differences between Black and White women, all outcomes and analyses are stratified by genetic ancestry (European, referred to in this paper as 'White' or >50% African, referred to as 'Black'). We additionally restrict our analyses to HGSOC cases to limit possible confounding due to histotype heterogeneity.

5.3. Methods

5.3.1. Case ascertainment and vital status

The African American Cancer Epidemiology Study (AACES) is a population-based case-control study of Black women with invasive EOC and controls residing in 11 geographic locations in the U.S. enrolled between December 2010 and August 2016.⁸⁰ Cases were identified through cancer

registries and hospitals and were eligible for the study if they were 1) aged 20–79 years, 2) self-reported Black race, and 3) resided in one of the included geographic regions.⁸⁰ Annual follow-up interviews were attempted to collect information regarding vital status and length of overall survival (OS). The goal for time between baseline interview and follow-up was one year. When follow-up interviews were not possible, thorough searches withing Lexus Nexus, obituaries, and the National Death Index were implemented to obtain date and cause of death where applicable.⁸⁰

The Ovarian Cancer Association Consortium (OCAC)⁸¹ consists of more than 80 participating groups from four continents: North America, Europe, Asia, and Australia. Eligible case-control and cohort studies provided germline DNA for genotyping, epidemiologic data, and vital status information, which was centrally harmonized at the OCAC data-coordination center. A list of all participating OCAC studies is presented in **Supplementary table ST2**.

All White invasive EOC cases from OCAC genotype data who self-identified as non-Hispanic were eligible for analysis in this project. The Black cases from AACES and OCAC were previously subset to include women with >50% African genetic ancestry, calculated using the software package FastPop.^{85,122}

5.3.2. SNP Selection, Genotyping, and Quality Control

Genotyping was performed at five centers: University of Cambridge, Center for Inherited Disease Research (CIDR), National Cancer Institute (NCI), Genome Quebec and Mayo Clinic using an Illumina Infinium iSelect BeadChip. Genotype data quality control (QC) was previously carried out according to the OncoArray QC guidelines. A small number of subjects that were not genetically female (XX) or those who had ambiguous sex, or were duplicates were omitted from the dataset.^{26,85} White OCAC genotyped samples were imputed using the Michigan Imputation Server to the Trans-Omics for Precision Medicine (TOPMed) imputation with 97,256 samples (Version R2 on GRCh38/hg38).⁸⁶ Phasing was performed with Eagle2⁸⁷ and imputation with Minimac3.⁵¹ In the Black

genomic data, SNPs that were not directly genotyped were imputed according to the 1,000 Genomes Phase 3 v5 reference set (GRCh37/hg19) using Minimac3.⁸⁸ SNP level post-imputation QC included filtering on call rate >95%, Hardy–Weinberg Equilibrium $p > 1 \times 10^{-5}$, and a minor allele frequency (MAF) ≥ 0.01 using PLINK 2.0.^{89,90}

5.3.3. Genes and Pathways

The 224 candidate genes included for analysis were selected from the Kyoto Encyclopedia of Genes and Genomes (KEGG)⁹² TLR, NFkB and TNF pathways. In situations where a gene appears in multiple pathways, we assigned the gene to only one pathway based off function (for example, lipopolysaccharide binding protein [*LBP*] is in both and NFkB and TLR pathways but analyzed only in the TLR pathway). In total, 95, 74, and 55 genes were in the TLR, NFkB, and TNF pathways, respectively. SNPs within each candidate gene were selected based on the chromosomal coordinates of the start and end positions (Ensembl GRCh37/hg19 for the Black dataset and GRCh38/hg38 for the White)^{83,84} $\pm 10,000$ base pairs to capture promoter and regulatory regions. All included genes and the chromosomal coordinates are shown per pathway in **Supplementary Table ST3**.

5.3.4. Statistical Analysis

To control for population admixture we use ancestry principal components (PCs). PCs were previously, separately calculated for the Black and White datasets using the software package FastPop, developed specifically for the OncoArray.^{26,85} To confirm the correct number of PCs to use, we used the Admixture program, which estimates ancestry in a model-based manner from large autosomal SNP genotype datasets, on the raw Black genomic data.⁹⁴ Using the cross-validation procedure, selection of two PCs was indicated as the the ideal number of ancestral populations based on a low cross-validation error estimate (**Figure 3.1**). We applied the same number of PCs to our White population and assessed adequate control for possible inflation via QxQ plots and λ values

generated from the P -values of all genome-wide SNPs assuming an additive logistic regression model controlling for age and the first two PCs. While using two PCs, we observed adequate control per the calculated λ values ($\lambda_{\text{Black}} = 1.02$, $\lambda_{\text{White}} = 1.10$) and QxQ plots (shown in **Supplementary Figures SF1-SF2**).

To examine the associations between genes (a combination of SNPs) and pathways (a combination of genes) and EOC 5-year survival, we use the Multi-marker Analysis of GenoMic Annotation (MAGMA) tool for gene and generalized gene-set analyses of GWAS data.¹²³ In brief, MAGMA accounts for local linkage disequilibrium and aggregates multiple logistic regression model-derived P -values for SNPs within the same gene. We applied the additive genetic model to assess the association with EOC or HGSOC 5-year overall survival (OS; yes vs no) adjusting for age (continuous), FIGO stage, histotype (EOC model only), and two ancestry PCs (continuous). To examine the associations between pathways (a combination of genes) and OS, each gene P -value computed in the previous model is converted to a Z-value to yield a roughly normal distribution that reflects the strength of the association for each gene with 5-year survival. The competitive gene-set analysis is implemented as a linear regression model on this gene-level data matrix where the resulting P -value tests whether the mean association with EOC/HGSOC survival varies among genes in a specified gene-set (in this case, a pathway) relative to the genes not in the gene-set. MAGMA adjusts for gene size, gene density, the inverse of the mean MAC in the gene and the log value of each. To evaluate a possible interaction among genes and pathways with pre-diagnosis body mass index (BMI, kg/m^2 , continuous), we used an extension of the MAGMA tool by adding a SNP by covariate interaction to the gene-level model. To correct for multiple testing, we adjust the raw gene-level P -values by the number of genes tested using the Benjamini-Hochberg false-discovery rate (FDR).¹²⁴ We present both raw and FDR-corrected results.

To better understand what may be driving a gene-level association with EOC/HGSOC 5-year survival, we report the lead SNP for gene and gene*BMI interactions that are statistically significant at $P_{\text{raw}} < 0.05$. The measure of association and P -value for each lead SNP in a gene are calculated via a genome-wide association analysis for EOC/HGSOC 5-year OS via logistic regression controlling for age, FIGO stage, histotype (EOC model only), and two ancestry PCS. For statistically significant unadjusted gene*BMI interaction, we use the same genome-wide additive logistic regression model with a SNP*BMI interaction term. We report the SNP rsID, odds ratio (OR), 95% confidence interval (CI) and raw P -value for the most statistically significant gene-specific SNP.

As these data are the largest collection of genomic invasive EOC data and, therefore, cannot be validated in external data sources, we randomly split our White analytic dataset into a 67% test set and 33% internal validation set. We compared selected baseline characters between the two sets and determined successful randomization (**Table 5.1**). Although this the remains the largest genomic dataset for Black women with EOC as well, we unfortunately lack the sample size to conduct internal validation in this group.

5.4. Results

In total, the Black dataset (AACES + OCAC) included 720 cases and the White test and validation datasets included 9,181 and 4,566 cases, respectively. Selected baseline characteristics per study population are presented in **Table 5.1**. Black cases had an average of 5 years follow-up time while White women had an average of 6 years. About one quarter of the White cases, regardless of test/validation group were missing information regarding FIGO stage compared to only 17.5% of Black cases.

All aggregate associations of SNPs at the gene and pathway levels for TLR, NFkB, and TNF signalling with EOC and HGSOC 5-year survival among Black and White women are shown in

Supplementary Tables ST5.1- ST5.4. No pathway-level or FDR-correct gene-level association was statistically significant for either racial group.

We present genes associated with EOC/HGSOC 5-year survival among Black women with a raw P -value of < 0.05 in **Table 5.2**. Results for BMI interactions are presented alongside each raw, statistically significant gene. In total, 11 genes were associated with Black EOC survival and six with HGSOC survival. Although no genes in the TNF pathway were associated with either outcome among Black women, several TNF superfamily genes that are part of processes in the TLR and NF κ B pathways were observed. *TNFRSF11A* and *CTSK* were associated with both EOC and HGSOC survival. *LTA* was the only gene among Black women to have an interaction with BMI for EOC survival. No HGSOC survival-associated genes were observed to have an interaction ($P_{\text{BMI}} = 0.03$; $P_{\text{BMI FDR}} = 0.60$), however, the lead SNP joint interaction was not statistically significant [rs3093544; OR = 1.10 (95% CI: 0.99-1.23)].

The P_{raw} statistically significantly associated genes for EOC/HGSOC 5-year OS among White women are presented in **Table 5.3**. Genes in White women had noticeably fewer SNPs mapped within the chromosomal locations. This may be due to differences in minor allele and haplotype frequencies between the two groups, particularly for the TOPMed White genomic data where 96% of SNPs had a MAF < 0.01 .⁵⁹ Six genes had no SNPs mapped after post-imputation and MAGMA internal QC filters, such as MAF, MAC, and differential missingness. Two genes (*MAPK11* and *MAPK12*) had chromosomal coordinates that were not included in the OCAC data (**Supplementary Tables ST5.3-ST5.4**). *CTSK* was also associated with EOC survival among White women but unlike in the Black women, no associated was observed for HGSOC 5-year OS. *AKT3*, however, was associated with HGSOC survival in both groups. In total, six genes were associated with EOC and HGSOC 5-year survival among White women: *PTSG2*, *GADD45B*, *VCAM1*, *TAB1*, *TLR9*, *TLR8*, and *PIK3CA*. Although we did observe associated genes in the TNF pathway for survival among White women, in contrast

to Black women, no genes overlapped between the two outcomes. Furthermore, no gene among White women had a raw, statistically significant interaction with BMI for EOC or HGSOC. Only three genes were associated with White EOC/HGSOC 5-year survival among both the test and validation cohorts: *VCAM1* (HGSOC survival only), *TLR9* and *IL6* (both EOC only).

5.5. Discussion

In this analysis of genetic variation, we investigated whether TLR, NFkB, and TNF genes and/or pathways were associated with Black and White EOC or HGSOC 5-year OS. Although our results were null after FDR correction, we did observe genes that were associated with EOC/HGSOC 5-year OS in both groups when considering the P_{raw} threshold of < 0.05 . While these results do not indicate an irrefutable association with these genes and ovarian cancer survival, discussion of these genes may elucidate possible biological mechanisms or generate new hypotheses that could contribute to our understanding of what drives the fatality of this disease.

CTSK was associated with both EOC and HGSOC 5-year survival among Black women and EOC 5-year survival among White women. Cathepsin K (CTSK) is part of the cathepsin superfamily, members of which are highly expressed in various cancers and mediate metastasis.¹⁸⁵ *CTSK* in EOC is differentially expressed in peritoneal metastatic ovarian (N=57) relative to primary ovarian tumor tissues (N=153) and validated in 30 pairs of matched fresh tissues.¹⁸⁶ In another small study, immunohistochemistry expression of *CTSK* in EOC tumor and paired, adjacent normal tissues was observed to be upregulated in EOC tissues and was also associated with metastasis and poorer survival.¹⁸⁷

AKT3 was associated with HGSOC 5-year survival among both Black and White women as well. AKT protein isoforms are part of the PI3K/AKT signalling pathway that promotes cell survival, growth, migration, and progression.^{188,189} Dysfunction of this pathway is a known driver of cancer progression and treatment resistance.^{188,190} *AKT3* is not as well studied as its first two isoforms. By

way of EOC, results are conflicting. One study observed knockdown of AKT3 in EOC cell lines was associated with increased tumor size relative to controls¹⁹¹ while another found knockdown led to a decrease in ovarian cancer cell proliferation.¹⁹² The authors of the former study did note that they observed decreased proliferation in two EOC cell lines, which were the two lines exhibiting the highest levels of AKT3 at baseline.¹⁹¹ Perhaps this is why we only observed AKT3 associated with HGSOC in our study. mRNA *AKT3* expression via laser capture micro-dissected ovarian tissues was observed to be differential in HGSOC tumors relative to benign tumors or normal epithelium.¹⁹³ Whether there would be differential expression between HGSOC and other EOC histotypes, however, is unknown. Mutations in a PI3K subunit gene, *PIK3CA*, which was also associated with White EOC and HGSOC 5-year survival in our study, have been shown to stimulate downstream AKT signalling and increase cell invasion and metastasis.¹⁸⁹

In Black women, TNF superfamily member 11 encoding gene (*TNFSF11*) was associated with EOC survival and the gene that encodes its receptor, *TNFRSF11A*, was associated with both EOC and HGSOC survival. Binding of TNFSF11 induces NFκB and MAPK8 activation. Also known as receptor activator NFκB ligand (RANKL; RANK for TNFRSF11A), high protein expression has been observed in cancers such as colorectal, cervical, and breast.¹⁹⁴ RANKL is implicated in tumorigenesis at every step from epithelial-mesenchymal transition to distant metastasis.^{194,195}

LTA was also associated with Black EOC 5-year survival and was the only gene in our analysis indicated to possibly differ by BMI. Previously referred to as TNF-beta, lymphotoxins alpha (LTA) is a cytotoxic protein in the TNF superfamily. Polymorphisms in *LTA* have been observed in association with cancer risks such as breast and lung.¹⁹⁶⁻²⁰¹ Lymphotoxins and their possible role in cancer survival is less well understood. In colorectal cancer cells, LTA was associated with increased cell migration, proliferation, pro-inflammatory signalling and chemoresistance.^{202,203} Cancer cell-derived lymphotoxin was found to induce chemokine expression in fibroblasts via NFκB signalling in EOC

cells.²⁰⁴ There is epidemiologic evidence that polymorphisms in *LTA*, some of which overlap with our analyses, are associated with metabolic diseases (highly prevalent in Black women),²⁰⁵ including BMI, although none of the study populations included Black participants.^{206–210}

The greatest strength of our study is the largest sample of high quality, EOC genotype data and pathologist-confirmed clinical outcomes. In addition, to our knowledge, this is the first comprehensive analysis of TLR, NFkB, and TNF genes and pathways for EOC and HGSOC 5-year survival. Our selection of pathways and genes was hypothesis-driven and the aggregate analysis of SNPs at the gene level facilitates investigation of a singular function while the pathway level considers cellular processes at large.

Ovarian cancer is a rare disease and Black women are ubiquitously under-represented in large-scale cancer studies.²¹¹ Although this is the largest genetic dataset for Black and White women with EOC, we were still hindered by small sample sizes in subgroups such as histotype, which are known to be differentially associated with race, genetic markers, and clinical outcomes. To reduce histotype variability, we restricted our analyses to HGSOC cases *only* and observed genes that were associated with EOC remained statistically significant. Still, these genes may not be generalizable to other histotypes such as low-grade serous and mucinous. We must also acknowledge the inherent limitations of genetic studies between racial groups and cautiously interpret results as race is a social construct and disparities in health are rarely a direct result of genetic differences. Furthermore, cancer is a stochastic disease and genetics account for very few *causal* mechanisms at any cancer site. However, genes associated with survival may provide insight for novel therapies and prognostic markers.

The validity of the White OCAC data may also be a major limitation in our analyses. The vast majority of SNPs imputed had MAFs less than or equal to 0.01 and far fewer passed QC filtering

relative to the Black imputed data. We explored multiple datasets and QC thresholds but could not map SNPs to every selected gene among the White datasets. Nor could we replicate previously published OCAC GWAS SNP totals, λ or QxQ plot. Upon our request for scripts to reproduce these results, we were informed the findings were generated using an in-house logit program. Furthermore, some of the raw genomic data was truncated resulting in missing data for entire genes. These reasons could be why we observed very few internally validated results between our 67/33% randomly split cohorts. Another possibility for the lack of validation could be an extreme sensitivity to sample size in the MAGMA program. Considering the 33% cohort is still larger than our total Black population, concerns regarding the validity of those results should be acknowledged. Unfortunately, very few programs outside of MAGMA can incorporate gene*environment interactions or input raw GWAS data. There are no publicly available summary statistics for EOC survival.

In conclusion, there are genetic variations in pathogen recognition and downstream inflammatory pathways that are associated ($P_{raw} < 0.05$) with EOC and/or HGSOC 5-year survival which are biologically consistent and plausible with cell mechanisms and cancer progression. These results, along with EOC disparities studies overall, require larger minority populations for replication and subgroup analyses.

5.6. Tables and Figures

Table 5.1. Select baseline characteristics of the Black and White invasive epithelial ovarian cancer populations.			
	Black cases	White cases 67% Validation	White cases 33% Test
N	720	9,181	4,566
Age, mean (sd)	57.1 (11.2)	58.8 (11.4)	58.8 (11.6)
BMI, mean (sd)	32.8 (8.3)	27.1 (6.1)	27.6 (6.8)
missing, N (%)	166 (23.1)	7,055 (76.8)	3,537 (77.5)
Year of diagnosis, N (%)			
1990-1999	11 (1.5)	74 (0.8)	41 (0.9)
2000-2009	119 (16.5)	1,212 (13.2)	1,386 (30.4)
2010-2019	423 (58.8)	2,884 (31.4)	647 (14.2)
missing	167 (23.2)	5,010 (54.6)	2,492 (54.6)
Stage, N (%)			
localized	128 (17.8)	1,082 (11.8)	545 (11.9)
regional	66 (9.2)	1,395 (15.2)	695 (15.2)
distant	400 (55.6)	4,414 (48.1)	2,315 (50.7)
unstaged/missing	126 (17.5)	2,290 (24.9)	1,191 (26.1)
Histotype, N (%)			
high-grade serous	423 (58.8)	5,612 (61.1)	2,774 (60.8)
low-grade serous	20 (2.8)	310 (3.4)	167 (3.7)
endometrioid	64 (8.9)	612 (6.7)	292 (6.4)
clear cell	26 (3.6)	528 (5.6)	281 (6.2)
mucinous	34 (4.7)	514 (5.6)	274 (6)
other EOC	153 (21.3)	1,605 (17.5)	754 (16.5)
Years of follow-up, mean (sd)	5.3 (3.9)	6.2 (4.7)	6.2 (4.8)
missing, N (%)	92 (12.8)		
5-year survival, N (%)			
yes	313 (43.5)	3,150 (34.3)	1,557 (34.1)
no	296 (41.1)	3,201 (34.9)	1,573 (34.5)
missing	111 (15.4)	2,830 (30.8)	1,436 (31.4)

Abbreviations: BMI = body mass index; N = number; sd = standard deviation; EOC = epithelial ovarian cancer.

Table 5.2. Gene associations and lead SNPs within TLR, NFkB, and TNF pathways with invasive EOC and HGSOC 5-year overall survival among Black women in AACES and OCAC.^a

Path way	Gene	# SNPs	P^b	P_{FDR}^c	Lead SNP	Ref. allele	Alt. allele	OR (95% CI) ^d	P_{SNP}
EOC									
NFkB									
	<i>LTA</i>	11	0.026	0.916	rs4647195	T	C	0.18 (0.05-0.61)	0.006
	<i>BCL2L1</i>	155	0.030	0.916	rs6058431	T	C	1.51 (1.14-1.99)	0.004
	<i>TNFRSF11A</i>	355	0.032	0.916	rs11152342	G	C	1.71 (1.30-2.25)	<0.001
	<i>LCK</i>	125	0.044	0.916	rs79979643	G	A	0.29 (0.13-0.66)	0.003
	<i>ZAP70</i>	120	0.046	0.916	rs57831860	C	T	0.66 (0.52-0.84)	0.001
TLR									
	<i>FOS</i>	11	0.009	0.916	rs2239615	A	T	0.64 (0.45-0.91)	0.013
	<i>STAT1</i>	195	0.020	0.916	rs144222846 9	TG	T	1.5 (1.17-1.93)	0.002
	<i>MAP2K4</i>	382	0.032	0.916	rs115783238	T	C	0.36 (0.18-0.71)	0.003
	<i>TAB2</i>	548	0.035	0.916	rs144021633 7	TA	T	0.67 (0.50-0.88)	0.005
	<i>CTSK</i>	22	0.035	0.916	rs929955171	CA	C	2.98 (1.46-6.09)	0.003
	<i>IKBKE</i>	163	0.037	0.916	rs12093831	C	T	1.36 (1.07-1.73)	0.013
HGSOC									
NFkB									
	<i>TNFSF11</i>	216	0.004	0.764	rs633137	T	C	2.13 (1.41-3.22)	<0.001
	<i>TNFRSF11A</i>	355	0.007	0.764	rs12454677	C	T	4.12 (2.06-8.25)	<0.001
	<i>BCL2</i>	961	0.021	0.971	rs4987856	C	T	9.9 (2.24-43.8)	0.003
TLR									
	<i>CTSK</i>	22	0.010	0.775	rs16841797	C	T	1.77 (1.22-2.58)	0.003
	<i>AKT3</i>	1176	0.027	0.971	rs116556988	T	G	2.27 (1.16-4.44)	0.017
	<i>TICAM2</i>	194	0.039	0.971	5:114920059	ACTT	A	2.72 (1.27-5.85)	0.010

Abbreviations: TLR = toll-like receptor; NFkB = nuclear factor kappa B; TNF = tumor necrosis factor; EOC = epithelial ovarian cancer; HGSOC = high grade serous ovarian cancer; AACES = African American Cancer Epidemiology Study; OCAC = Ovarian Cancer Association Consortium; SNP = single nucleotide polymorphism; FDR = false discovery rate; Ref = referent; Alt = alternate; OR = odds ratio; CI = confidence interval.

^aWith unadjusted P-value < 0.05.

^bAggregate P-value of MAGMA model results. Each model controls for age, two ancestry principal components stage at diagnosis, and histotype (EOC model only).

^cCorrected for multiple testing by the number of genes tested using the Benjamini-Hochberg false discovery rate (FDR).

^dAdditive model adjusted for age, two ancestry principal components, stage at diagnosis, and histotype (EOC model only).

Table 5.3. Gene associations and lead SNPs within TLR, NFkB, and TNF pathways with invasive EOC and HGSOC 5-year survival among White women in OCAC. ^a											
Pathway	Gene	# SNPs	Test set		Validation Set		lead SNP	Ref. allele	Alt. allele	OR (95% CI) ^d	<i>P</i> _{SNP}
			<i>P</i> ^b	<i>P</i> _{FDR} ^c	<i>P</i> ^b	<i>P</i> _{FDR} ^c					
EOC											
NFkB											
	<i>PTGS2</i>	115	0.002	0.434	0.827	0.979	rs4648284	T	C	0.79 (0.65-0.96)	0.019
	<i>CXCL12</i>	158	0.017	0.628	0.753	0.956	rs71494727	G	A	0.86 (0.75-0.98)	0.027
	<i>TAB3</i>	66	0.020	0.535	0.975	0.993	rs62590400	G	C	0.80 (0.67-0.95)	0.012
	<i>GADD45B</i>	30	0.029	0.628	0.100	0.817	rs2024144	C	T	1.05 (0.97-1.14)	0.222
	<i>SYK</i>	512	0.030	0.628	0.128	0.817	rs7852876	T	A	1.10 (1.03-1.16)	0.002
	<i>VCAM1</i>	30	0.041	0.628	0.270	0.826	rs3176862	C	G	1.21 (0.97-1.49)	0.087
TLR											
	<i>CTSK</i>	52	0.010	0.628	0.662	0.956	rs111905669	T	C	0.92 (0.87-0.98)	0.007
	<i>TAB1</i>	94	0.011	0.628	0.769	0.959	rs3830119	T	C	1.13 (1.05-1.22)	0.001
	<i>TLR9</i>	37	0.024	0.628	0.023	0.817	rs352139	C	T	1.12 (1.06-1.19)	<0.001
	<i>IL6</i>	94	0.029	0.628	0.013	0.801	rs1548216	G	C	0.77 (0.64-0.93)	0.008
	<i>PIK3CA</i>	335	0.030	0.628	0.576	0.910	rs79786599	A	G	0.80 (0.69-0.92)	0.002
	<i>TLR8</i>	33	0.039	0.535	0.197	0.787	rs143598634	C	T	0.78 (0.67-0.92)	0.003
	<i>IFNAR2</i>	164	0.045	0.628	0.375	0.844	rs189110596	A	G	0.72 (0.59-0.89)	0.003
	<i>IRAK4</i>	123	0.045	0.628	0.086	0.817	rs4251520	T	C	0.92 (0.84-1.01)	0.068
TNF											
	<i>CREB3L4</i>	30	0.011	0.628	0.625	0.948	rs35138279	C	T	1.05 (0.96-1.15)	0.255
	<i>CSF1</i>	240	0.036	0.628	0.346	0.829	rs183849981	C	G	0.72 (0.52-0.99)	0.045
	<i>SELE</i>	88	0.045	0.628	0.660	0.956	rs3917438	G	A	0.88 (0.75-1.02)	0.095
	<i>TNFRSF1B</i>	76	0.046	0.628	0.130	0.817	rs547731360	TTTTGTTG	T	1.47 (1.04-2.09)	0.029
HGSOC											
NFkB											
	<i>PTGS2</i>	115	0.016	0.872	0.555	0.956	rs4648298	T	C	0.80 (0.62-1.03)	0.087
	<i>VCAM1</i>	29	0.025	0.872	0.012	0.628	rs3176862	C	G	1.28 (0.98-1.69)	0.075

	<i>PLCG2</i>	1052	0.026	0.872	0.197	0.916	rs11648625	T	C	0.60 (0.45-0.79)	<0.001
	<i>GADD45B</i>	30	0.038	0.872	0.164	0.852	rs2024144	C	T	1.05 (0.95-1.16)	0.348
TLR											
	<i>TAB1</i>	86	0.018	0.872	0.501	0.956	rs3830119	T	C	1.14 (1.04-1.26)	0.007
	<i>TLR9</i>	37	0.026	0.872	0.491	0.956	rs352139	C	T	1.12 (1.04-1.21)	0.003
	<i>PIK3CA</i>	335	0.028	0.872	0.362	0.956	rs576007456	G	A	0.58 (0.39-0.88)	0.009
	<i>TLR8</i>	33	0.036	0.755	0.532	0.956	rs143598634	C	T	0.76 (0.62-0.92)	0.006
	<i>AKT3</i>	541	0.038	0.872	0.474	0.956	rs76075275	A	G	2.33 (1.33-4.09)	0.003
TNF											
	<i>MMP3</i>	88	0.003	0.801	0.622	0.956	rs679620	T	C	1.08 (1.01-1.16)	0.034
	<i>CX3CL1</i>	104	0.033	0.872	0.228	0.951	rs4151117	G	T	1.11 (1.01-1.21)	0.031
	<i>CREB3L1</i>	100	0.047	0.964	0.277	0.951	rs191404853	T	G	0.55 (0.39-0.79)	0.001

Abbreviations: TLR = toll-like receptor; NFkB = nuclear factor kappa B; TNF = tumor necrosis factor; EOC = epithelial ovarian cancer; HGSOC = high grade serous ovarian cancer; OCAC = Ovarian Cancer Association Consortium; SNP = single nucleotide polymorphism; FDR = false discovery rate; Ref = referent; Alt = alternate; OR = odds ratio; CI = confidence interval.

^aWith unadjusted P-value < 0.05.

^bAggregate P-value of MAGMA model results. Each model controls for age, two ancestry principal components stage at diagnosis, and histotype (EOC model only).

^cCorrected for multiple testing by the number of genes tested using the Benjamini-Hochberg FDR.

^dAdditive model adjusted for age, two ancestry principal components, stage at diagnosis, and histotype (EOC model only).

Chapter 6: Aim 3.

Expression of pathogen-recognition and inflammatory pathway genes associated with high grade serous ovarian cancer survival among Black and White women.

6.1. Abstract

Background: Tumor-associated inflammation in the tumor microenvironment is an established driver of proliferation, progression, metastasis, chemoresistance, and genomic instability. Epithelial ovarian cancer (EOC) is the fifth most lethal cancer among Women in the U.S. High grade serous ovarian cancer (HGSOC) is the most common EOC histotype diagnosed (~60-70%) and has the lowest survival relative to other common histotypes, regardless of stage at diagnosis. Furthermore, prior studies indicate Black women have poorer overall EOC survival and poorer three-year and six-year HGSOC survival when compared to White women. In this study, we leverage RNA-sequencing (RNA-seq) data from tumor tissues to investigate differential expression of TLR, NFkB, and TNF pathway genes in HGSOC tumors from both Black and White women in association with 5-year survival and stage at diagnosis.

Methods: We included newly generated RNA-Seq data from 214 Black and 255 White individuals from the African American Cancer Epidemiology Study (AACES) and the North Carolina Ovarian Cancer Study (NCOCS). Differentially expressed genes (DEGs) were analyzed via the Bioconductor package DESeq2 in R separately for Black and White HGSOC cases in association with 5-year overall survival (no vs yes) and stage at diagnosis (late vs early). We also performed exploratory analyses to investigate possible associations between the level of gene expression and survival or stage. A binary variable for each gene was calculated as expression levels less than or equal to the gene-specific median expression (“low”) and greater than the median (“high”). Cox proportional hazard (PH) models were used to estimate hazard ratios (HRs) and 95% confidence intervals (CIs) for association of high vs low gene expression and mortality. Logistic regression models were used to estimate odds ratios (ORs) and corresponding 95% CIs for the association with FIGO stage.

Results: We observed several statistically significant genes that are differentially expressed by 5-year overall survival among Black (*CCL13*, *CREB5*) and White (*CXCL1*, *CXCL6*, *CSF2*, *BLNK*, *LTB*, *TLR8*) HGSOC tumor tissues. In the exploratory analyses, although we were limited in power due to sample size, *CREB5* among Black women and *BLNK* and *CXCL6* among White women were also associated with survival via Cox PH models. Among Black women, statistically significant DEGs included *BLNK*, *TLR4*, *JUN*, and *MAPK10*. Fifteen unique genes were differentially expressed for late vs early stage at diagnosis among Black women. Nine of these genes, *BLNK*, *CEBPB*, *PIK3R1*, *PIK3CD*, *TLR4*, *MMP14*, *JUN*, and *ICAM1* were also statistically significant DEGs among White women. No statistically significant DEG was present in White women but not Black.

Conclusions: Several genes in TLR, NFkB, and TNF pathways were observed to be differentially expressed in association with HGSOC survival and stage at diagnosis among Black and/or White women. These findings provide a platform for further investigation and validation of tumor-specific markers that may serve prognostic value or targetable mechanisms for treatment.

6.2 Introduction

Epithelial ovarian cancer (EOC) is a group of malignancies involving the ovary, fallopian tube, and peritoneum that arise from epithelial cells. A highly fatal disease, EOC is the fifth most lethal cancer among women in the US. Comprised of multiple histotypes (a combination of histology and grade) EOC has heterogeneous cells of origin, morphology, molecular features, methylation patterns, gene and RNA expression signatures, epidemiologic risk factors, clinical characteristics, and survival rates.^{12,13,25-27} At the genomic level, high grade serous ovarian cancer (HGSOC), the most common histotype, is associated with *TP53* mutations resulting in somatic chromosome instability and DNA repair copy number changes.²⁸ Just under half of all HGSOC cases are characterized by homologous recombination DNA repair pathway mutations, namely *BRCA1* and *BRCA2*.²⁸ HGSOC has the lowest survival relative to other common histotypes, regardless of FIGO stage at diagnosis.²² Furthermore, prior studies have found Black women have poorer overall EOC survival⁷ and poorer three-year and six-year HGSOC survival when compared to White women.^{212,213}

Pre-diagnosis exposure to inflammation-related lifestyle factors and chronic diseases have also been associated with poorer survival. In one study, 12 exposures (alcohol use; aspirin use; other nonsteroidal anti-inflammatory drug use; body mass index; environmental tobacco smoke exposure; history of pelvic inflammatory disease, polycystic ovarian syndrome, and endometriosis; menopausal hormone therapy use; physical inactivity; smoking status; and talc use) were used to create a weighted inflammation-related risk score (IRRS) among mostly White women with EOC. Per each increasing quartile of the IRRS there was an associated increase in risk of death (HR = 1.09; 95% CI: 1.03, 1.14).⁴⁸ Additionally, women in the upper quartile of the IRRS had a 31% higher death rate compared with the lowest quartile (95% CI: 1.11, 1.54).⁴⁸ Johnson et al. sought to replicate this study in a cohort of 592 Black women with EOC and similarly observed a higher IRRS was associated with worse overall survival (per quartile HR: 1.11; 95% CI: 1.01, 1.22). The authors also evaluated the

energy-adjusted Dietary Inflammatory Index (E-DII). Adding the E-DII attenuated the association of the IRRS with survival and the greater E-DII, i.e. a more pro-inflammatory diet, was associated with shorter survival (per quartile HR: 1.12; 95% CI: 1.02, 1.24).^{49,102} A meta-analysis investigating a systemic immune inflammation index (calculated via pre-treatment neutrophil, platelet, and lymphocyte counts) was associated with lymph-node metastasis and progression-free and disease-free survival in EOC.¹⁸⁰

Tumor-associated inflammation in the tumor microenvironment (TME) is an established driver of proliferation, progression, metastasis, chemoresistance, and genomic instability.^{37,179} The tumor microenvironment milieu contains both inflammatory and immunosuppressive components that are coopted by the malignant and infiltrating immune cells.⁴⁶ Toll-like receptors (TLRs) are transmembrane proteins that play a key role in immunity by recognizing pathogen- and danger-associated molecular patterns expressed by microorganisms. TLR ligation triggers an intricate signaling cascade that activates downstream pro-inflammatory pathways such as NFκB and TNF. TLRs expressed in tumor tissues can promote proliferation and anti-apoptosis through the activation of proinflammatory processes.⁵⁸⁻⁶⁰ TLR4 in particular has been observed to confer chemoresistance through ligation with paclitaxel in EOC cell lines.^{60,66}

EOC tumor tissue expression has also been studied specifically for TLR4 and its adapter protein, MyD88, but many studies have conflicting results,⁶¹⁻⁶⁵ likely due to differences in analytic histotype stratifications and expression classification (high/low, none/weak/moderate/strong, or weak/moderate/strong) and results include studies that are comprised of over 90% white women. However, Block et al., Kim et al., and Li et al. all observed differential gene expression levels and associations with EOC survival between histotypes. In HGSOE, specifically, strong immunohistochemical expression of both TLR4 and MyD88 was associated with serous histology and poorer survival.^{62,65}

By way of downstream inflammation, worse overall survival in EOC has been observed to be associated with elevated expressions of NFkB pathway subunits, activating Ikb kinases (IKKs).⁴⁶ In the previously mentioned study by Li et al., tumors with elevated TLR4 and MyD88 expression were significantly correlated with the expression of NFkB pathway proteins.⁶⁵ TNF is an established mediator of inflammation-associated cancers.²¹⁴ Ligation of TNF at its receptors triggers various signalling transduction pathways, such as NFkB and MAPK, leading to different cellular responses: 1) cell death, 2) transcription of pro-inflammatory genes and 3) proliferation and cell survival.^{214,215} In malignant epithelial cells, TNF is synthesized and secreted into the tumor microenvironment creating an inflammatory feedback loop promoting cell migration, invasion, and infiltration of macrophages.²¹⁵⁻²¹⁸ In the validated ProTYPE assay, a robust and 55-gene classifier based on NanoString gene-expression platform to identify HGSOC molecular subtypes, three of the finalized 55 genes overlap with our analyses (*CCL5*, *CXCL9*, and *CXCL11*).²¹⁹

In this study, we leverage RNA-sequencing (RNA-seq) data from tumor tissues to investigate differential expression of TLR, NFkB, and TNF pathway genes in HGSOC tumors from both Black and White women in association with 5-year survival and stage at diagnosis.

6.3. Methods

6.3.1. Study Population

The study population consisted of epithelial HGSOC cases enrolled in one of two population-based case-control studies, the North Carolina Ovarian Cancer Study (NCOCS, diagnosis dates 1999-2005), and the African American Cancer Epidemiology Study (AACES, diagnosis dates 2010-2015).^{80,220} Both studies enrolled epithelial ovarian cancer cases covering a range of histotypes, grades, and stages, though some of the most aggressive cases were missed because they were feeling very ill or were already deceased by the time they were invited to participate in research.²²⁰ Written informed consent was obtained for NCOCS participants, while

AACES participants provided signed consent for blood draw, medical record and pathology release forms to allow for access to tumor tissue. All cases were confirmed via centralized pathology review. Both the NCOCS and AACES studies were approved by the Duke Medical Center Institutional Review Board (IRB) and the IRBs of participating enrollment sites. Detailed methodologies for both studies have been previously published.^{80,212,220} Diagnosis dates for enrollment in AACES were between 2010-2015 and between 1999-2005 for NCOCS. In total, AACES and NCOCS included 720 Black ovarian cancer cases, 423 of which were HGOSC. Of these, 325 provided consent to participate in biospecimen-based research and had adequate tissue available to pursue RNA extraction (**Supplementary Figure 6.1A**).²²¹ Fifty-three of these cases were excluded from gene expression analyses due to a history of neoadjuvant chemotherapy, which can influence observed gene expression (**Supplementary Figure 6.1B**). We further excluded any HGSOC cases that did not have germline DNA data to calculate ancestry principal components (PCs) or had missing outcome or covariate data. In total, our analytic population of Black HGSOC tumor tissues was 214. The NCOCS study included 1,014 White cases, 484 of which were HGSC. Of these, 316 provided consent to participate in biospecimen-based research and had sufficient tissue available to pursue RNA extraction (**Supplementary Figure 6.2A**). After excluding cases without germline DNA, outcome, or covariate data, 255 White HGSOC cases remained. None of these cases had neoadjuvant chemotherapy prior to tissue collection.

6.3.2. RNA Extraction

RNA was extracted from FFPE tumor tissue and stored at -80°C. An initial quality control (QC) evaluation revealed substantial RNA degradation, so a repurification step consisting of

DNAase treatment and purification on a Zymo research spin column was completed before library preparation to reduce the bulk of degraded RNA product (i.e., <200 nucleotides in length). Following repurification, RNA libraries were prepared from total RNA samples (5-100 ng) using reagents from the Illumina Stranded mRNA Prep (cat# 20020189) and TruSeq RNA UD Indexes (20040534) for reverse transcription, adapter ligation, and PCR amplification. Amplified libraries were hybridized to biotin-labeled probes from the Illumina Exome Panel (cat# 20020183) using the Illumina RNA Fast Hyb Enrichment kit (20040540) to generate strand-specific libraries enriched for coding regions of the transcriptome. Exon-enriched libraries were qualified on an Agilent Technologies 2200 TapeStation using a D1000 ScreenTape assay (cat# 5067-5582 and 5067-5583). The molarity of adapter-modified molecules was defined by quantitative PCR using the Kapa Biosystems Kapa Library Quant Kit (cat#KK4824). Individual libraries were normalized to 0.95 nM in preparation for Illumina sequence analysis. Sequencing libraries were chemically denatured and applied to an Illumina NovaSeq flow cell using the NovaSeq XP workflow (20043131). Following the transfer of the flow cell to an Illumina NovaSeq 6000 instrument, a 150 x 150 cycle paired-end sequence run was performed using a NovaSeq 6000 S4 reagent Kit v1.5 (20028312).

6.3.3. *Quantification of gene expression data*

We trimmed adapters and filtered read quality using fastp.⁹¹ and filtered to reads with a PHRED score of at least 15 and a length of at least 20 base pairs. While a minimum PHRED score of 15 may include some reads with low quality, we found that most bases across all samples in the Black and White populations had a quality score greater than 30 (**Supplementary Figure 6.3**). We quantified paired-end reads with Salmon (version 1.4.0)⁹² using GRCh38 release 95. We used the seqBias and gcBias flags to correct for sequence-specific biases. We also used the recommended rangeFactorizationBins parameter value 4, which improves quantification accuracy on difficult-to-quantify transcripts. We then filtered out low-expression genes by excluding genes with a median

expression of 0 within a dataset (Black: 10,620 genes removed, White: 10,410 genes removed). We library-size normalized samples using upper quantile normalization. This normalization matches the 85th percentile across samples to correct for library size differences across samples.

6.3.4. Germline Genotyping and Quality Control

Genotyping was performed at five centers: University of Cambridge, Center for Inherited Disease Research (CIDR), National Cancer Institute (NCI), Genome Quebec and Mayo Clinic using an Illumina Infinium iSelect BeadChip. Genotype data quality control (QC) was previously carried out according to the OncoArray QC guidelines. A small number of subjects that were not genetically female (XX) or those who had ambiguous sex, or were duplicates were omitted from the dataset.^{26,85} SNPs that were not directly genotyped were imputed according to the 1,000 Genomes Phase 3 v5 reference set using Minimac3.⁸⁵ SNP level QC included filtering on call rate >95%, Hardy–Weinberg Equilibrium $p > 1 \times 10^{-5}$, and a minor allele frequency (MAF) >0.05 using PLINK 2.0.^{89,90}

6.3.5. Statistical analysis

The candidate genes for analysis were selected from the Kyoto Encyclopedia of Genes and Genomes⁸² (KEGG) TLR, NFkB and TNF pathways. In situations where a gene appears in multiple pathways, we assigned the gene to only one pathway based off function (for example, lipopolysaccharide binding protein [*LBP*] is in both and NFkB and TLR pathways but analyzed only in the TLR pathway). To account for population admixture, we excluded subjects who did not have ancestral principal components (PCs) available from our analyses. Principal components (PCs; continuous) were calculated for OCAC using the software package FastPop, developed specifically for the OncoArray.^{26,85} To assess adequate control for admixture or possible inflation, λ values were calculated ($\lambda_{\text{Black}} = 1.02$, $\lambda_{\text{White}} = 0.95$) and QxQ plots were assessed (**Supplementary Figures SF1-SF2**). To reduce inherent variation in RNA-seq data we also controlled for tumor purity (continuous) which is the proportion of cancer cells in a given tissue sample.

The two outcomes of interest in this project are dichotomized FIGO stage ('early:' 0/I/II vs 'late:' II/IV) and 5-year survival (yes vs no). Differentially expressed genes (DEGs) were analyzed via the Bioconductor package DESeq2 in R separately in Black and White HGSOC cases for both outcomes. *P*-values for DEGs were adjusted for multiple comparisons by the number of genes tested using the Benjamini-Hochberg false-discovery rate (FDR); a $P_{adj} < 0.05$ is considered statistically significant. Visualization of DEGs among all genes included for analysis are presented in volcano plots generated via DESeq2. We also performed exploratory analyses to investigate possible associations between the level of gene expression and survival or stage. A binary variable for each gene was calculated as expression levels less than or equal to the gene-specific median expression ("low") and greater than the median ("high"). Cox proportional hazard models were used to estimate hazard ratios (HRs) and 95% confidence intervals (CIs) for association of high vs low gene expression and mortality. Logistic regression models were used to estimate odds ratios (ORs) and corresponding 95% CIs for the association with FIGO stage. All analyses controlled for age at diagnosis, tumor purity, and two principal components. The survival analyses (DEGs and HRs) were additionally adjusted for stage. The purpose of modeling gene expression with HGSOC outcomes is exploratory and for hypothesis-generation and all genes were chosen *a priori*, therefore we present and discuss the raw *P*-values generated by the models.

6.4. Results

In total, our analytic population is comprised of 211 and 231 Black and White HGSOC cases, respectively (**Table 6.1**). The majority of cases in both groups were diagnosed with FIGO stage III and the average follow up was 5.5 years among Black cases and 6.3 years in White cases.

6.4.1. Survival

Results for the estimated differential expression of each gene in the TLR, NFkB, and TNF KEGG pathways are presented in Supplementary Table 1. We observed two statistically significant

genes associated with 5-year survival among Black HGSOC cases: *CCL13* was under-expressed [log fold change (LFC) = -1.8 (95% CI: -2.2, -1.3)] while *CREB5* was overexpressed [LFC = 0.6 (0.4, 0.7)] in cases who did not survive the first 5 years after diagnosis compared to cases who did (**Figure 6.1** and **Table 6.2**). Among White HGSOC cases, six genes, *CXCL1*, *CXCL6*, *CSF2*, *BLNK*, *LTB*, and *TLR8* were statistically significant after FDR correction, all of which were under-expressed (**Figure 6.2** and **Table 6.2**).

Statistically significant results for our exploratory analysis of high vs low gene expression in association with survival are presented in **Table 6.3** (all results in **Supplementary Table ST6.4**). *CXCL9* high expression was associated with a decrease in mortality among both groups of HGSOC cases [HR_{Black} : 0.67 (95% CI: 0.48, 0.93); HR_{White} : 0.68 (95% CI: 0.51, 0.90)]. The only statistically significant gene that was overexpressed in the DEG analysis, *CREB5* was also associated with an increased risk of mortality among Black HGSOC cases (HR = 1.89, 95%CI: 1.36, 2.61). In White cases, *BLNK* and *CXCL6* Cox model results were consistent with the under-expression observed in our DEG analysis. Relative to low, high expression of *BLNK* or *CXCL6* was associated with a lower risk of mortality after HGSOC diagnosis.

6.4.2. Stage

We observed 15 genes that are differentially expressed by stage (late vs early) in Black and/or White HGSOC cases included in our study (**Figures 6.3** and **6.4**). All statistically significant DEGs for stage are shown in **Table 6.4** (all genes in **Supplementary Table ST6.5**). Relative to cases who were diagnosed at stages II or earlier, late-stage diagnosis was associated with differential expression of *BLNK*, *CEBPB*, *PIK3R1*, *PIK3CD*, *TLR4*, *MMP14*, *JUN*, and *ICAM1* regardless of race. *JUN*, *ICAM1*, and *CEBPB* were overexpressed in late-stage Black and White HGSOC. All statistically significant White

DEGs for stage were observed in Black cases as well. In Black cases, *SOCS3* and *CARD14* were additionally overexpressed while *FAS*, *XIAP*, and *CFLAR* were under-expressed.

Fifty-one unique genes were observed to be associated with stage between Black and White HGSOC cases (**Table 6.5 and Supplementary Table ST6.6**). Within both groups, high expression of *JUN* or *MMP14* was associated with a late stage at diagnosis. These genes were also differentially expressed for both groups but we observed under-expression in late stage relative to early cases. *MAP2K7* was also associated with stage in both populations, however the direction of the associations differed [$OR_{\text{Black}} = 1.99$ (95% CI: 1.02, 3.86); $OR_{\text{White}} = 0.41$ (95%CI: 0.18, 0.94)].

6.5. Discussion

This is the first study of differentially expressed genes among Black HGSOC cases and the first study to evaluate RNA expression from candidate genes with the TLR, NFkB, and TNF pathways in ovarian cancer tissues. We observed several genes differentially expressed for survival as well as stage at diagnosis. In our exploratory analyses, although we were limited in power due to sample size, we did observe several estimated associations for RNA expression levels with survival, which were consistent with genes that were differentially expressed.

CREB5 was overexpressed in 5-year HGSOC mortality among Black women in our study. This was the only gene we observed to be overexpressed in mortality regardless of race and remained associated with an increased risk of mortality for Black HGSOC in the Cox PH model. The cAMP responsive element binding protein 5 is an encoding gene that produces a cAMP response element (CRE)-binding protein family member. In a small study utilizing both EOC cell lines and fresh tumor tissues, He et al. similarly observed *CREB5* mRNA and protein levels overexpressed in EOC cell lines and tissues.²²² Furthermore, patients with higher *CREB5* expression had shorter overall survival and relapse-free times.²²² Immunohistochemistry (IHC) expression also positively correlated with

disease progression and FIGO stage at diagnosis.²²² *CREB5* expression has also been observed to play a role in metastasis of colorectal cancer,^{223–225} androgen receptor treatment resistance in prostate cancer,²²⁶ and poor prognosis in hepatocellular carcinoma.²²⁷ *CREB5* was the only gene we observed to be associated with both survival and stage among Black women.

CCL13 was under-expressed in HGSOC mortality among Black women but was not statistically significant in the exploratory survival model. A chemoattractant cytokine subfamily member, also known as monocyte chemoattractant protein 4 (MCP-4), *CCL13*, and the CCL family, have been indicated to play essential roles in the recruitment of immune cells. In a study among individuals with rheumatoid arthritis, *CCL13* expression in synovial tissues was positively regulated by TNF and inhibited apoptosis.²²⁸ In a RNAseq analysis in lung cancer, *CCL13* low expression was similarly associated with worse survival.²²⁹

Among white women, all statistically significant DEGs were under-expressed for 5-year mortality relative to survival. We observed two chemokine ligand encoding genes, *CXCL1* and *CXCL6*, differentially expressed; *CXCL6* high expression was also associated with better survival [HR = 0.70 (95% CI: 0.53-0.92)] via the Cox PH model. Although counterintuitive to these findings, previous experimental and population-based gastric, liver, lung, and cervical cancer studies have observed positive correlations with these ligand-encoding genes and proliferation, invasion, and metastasis.^{230–235}

BLNK was statistically significantly differentially expressed for stage at diagnosis regardless of race. Among White HGSOC cases, under-expression of *BLNK* and high vs low expression was also associated with a lower risk of mortality. In both populations, *BLNK* expression was lower in late-stage cases while high *BLNK* expression was associated with a lower risk of late-stage diagnoses via logistic regression in Black HGSOC cases but not White ($P = 0.168$). The B-cell linker gene encodes

an adapter protein vital for B-cell receptor signaling and has observed tumor-suppressive properties via mouse models of hematologic cancers.²³⁶⁻²³⁸ In colorectal cancer, high *BLNK* expression in IHC staining of tumor tissues was associated with perineural invasion, lymph node metastasis, lower 5-year recurrence-free survival.²³⁹ RNA expression of *BLNK* is also lower in colorectal cancer tissues relative to adjacent normal tissues²⁴⁰ and positively correlated with relapse-free survival in ErbB2-positive breast cancer.²⁴¹

In both Black and White HGSOC cases, *JUN* was overexpressed in later stages relative to early, and high expression was associated with over a 2-fold increased likelihood of late-stage diagnosis. Commonly referred to as the Jun Proto-Oncogene or AP-1 transcription factor subunit, the protein encoded by *JUN* binds to AP-1 promoter sites and plays a role in activation-induced T cell death. In a previous study of ovarian tumors and cell lines, Jun family proteins (pc-Jun, Jun B, Jun D) were observed to have higher expression in primary, metastatic and borderline tumors relative to benign tissues via Western blot analysis.²⁴² A similar Western blot analysis also found pc-Jun expression associated with shorter overall and progression-free survival and high Jun D expression was associated with worse survival relative to moderate expression.²⁴³

TLR4 was under-expressed in late-stage cases among both Black and White women. TLRs expressed in non-neoplastic tissues can stimulate adaptive immune responses and activate immune cells that dynamically combat tumors.^{58,99} The activation of TLR4 signalling by binding with LPS via LBP and CD14 can stimulate antibody production through the modification of B cell responses²⁴ and induces pro-inflammatory cytokine production.²⁴⁴ Although this could be problematic in the tumor microenvironment, this process is an integral part of innate immunology. It is plausible that under-expression of *TLR4*, and thereby impaired immune response, could lead to an abundance of pathogenic gram-negative bacteria and perhaps promote more aggressive tumors.

Exposure to pathogenic bacteria can result in endotoxemia and systemic inflammation,^{245,246} which, in turn, can promote tumorigenesis via upregulation of cell proliferation, resistance to apoptosis, increased angiogenesis, and other mechanisms.²⁴⁷

The major strength of this study is the novelty of the data and results that will hopefully facilitate and inspire further investigation of tumor-based gene expression in ovarian cancer to identify targetable mechanisms for improved survival. This is also one of few studies prioritizing tissue-specific investigations of ovarian cancer survival in Black women and the largest collection of tissue samples in this population to date. Although we did not have specific cause of death, due to the unfortunate trends in EOC survival, there likely are not enough instances of EOC-independent deaths to dramatically alter our results. Additionally, while our results are only generalizable to HGSOC cases, this histotype represents roughly 60-70% of all EOC and is associated with the worst survival. Considering the rarity of EOC overall and that the remaining 4 histotypes comprise less than half of all cases, analyses in these subgroups are not currently adequately powered.

In conclusion, we identified, for the first time, several genes in TLR, NFkB, and TNF pathways to be differentially expressed in association with HGSOC survival and stage at diagnosis. These findings provide a platform for further investigation and validation of tumor-specific markers that may serve prognostic value or targetable mechanisms for treatment.

6.6. Tables and Figures

Table 6.1. Selected demographic and clinical characteristics of the Black and White HGSOc study populations.		
	Black (N = 214)	White (N= 255)
Age at diagnosis (SD)	58.0 (9.6)	58.5 (9.5)
Follow-up time, years (SD)	5.5 (3.5)	6.4 (5.3)
FIGO stage, N (%)		
0	3 (1.4)	3 (1.2)
I	23 (10.7)	16 (6.3)
II	22 (10.3)	10 (3.9)
III	157 (73.4)	217 (85.1)
IV	9 (4.2)	9 (3.5)
Primary debulking status, N (%)		
optimal	91 (42.5)	72 (28.2)
suboptimal	45 (21.0)	9 (3.5)
missing	78 (36.4)	174 (68.2)
5-year survival, N (%)		
no	115 (53.7)	152 (59.6)
yes	99 (46.3)	103 (40.4)

Abbreviations: HGSOc = high grade serous ovarian cancer; FIGO = International Federation of Gynecology and Obstetrics (Fédération Internationale de Gynécologie et d'Obstétrique).

Table 6.2. Statistically significant gene expression in association with 5-year invasive HGSOC survival (no vs yes) among Black and White cases.

Gene	Mean	Log fold change (95% CI)	<i>P</i>	<i>P</i> _{adj} ^a
Black women				
<i>CCL13</i>	16	-1.8 (-2.2, -1.3)	0.00002	0.006
<i>CREB5</i>	1113	0.6 (0.4, 0.7)	0.00016	0.019
White women				
<i>CXCL1</i>	362	-1.1 (-1.4, -0.9)	0.00003	0.003
<i>CSF2</i>	3	-2.2 (-2.7, -1.7)	0.00002	0.003
<i>CXCL6</i>	29	-1.3 (-1.6, -1.0)	0.00011	0.006
<i>BLNK</i>	395	-0.5 (-0.7, -0.4)	0.00012	0.006
<i>LTB</i>	32	-1.3 (-1.7, -1.0)	0.00021	0.009
<i>TLR8</i>	98	-0.5 (-0.7, -0.4)	0.00044	0.016

Abbreviations: HGSOC = high grade serous ovarian carcinoma; CI = confidence interval; adj = adjusted *P*-value.

Table 6.3. Statistically significant associations of high/low gene expression with 5-year survival (no/yes) in TLR, NFkB, and TNF pathway genes among Black and White HGSOC cases.^a

	Gene	HR (95% CI) ^b	P
Black women			
	<i>CREB5</i>	1.89 (1.36, 2.62)	0.0001
	<i>CXCL8</i>	0.57 (0.41, 0.79)	0.0007
	<i>PLAU</i>	1.49 (1.08, 2.06)	0.015
	<i>BCL10</i>	0.66 (0.48, 0.93)	0.016
	<i>CXCL9</i>	0.67 (0.48, 0.93)	0.017
	<i>CXCL11</i>	0.67 (0.49, 0.93)	0.017
	<i>CARD14</i>	1.49 (1.06, 2.08)	0.021
	<i>RELB</i>	1.46 (1.05, 2.04)	0.026
	<i>TNFRSF11A</i>	1.44 (1.04, 2.01)	0.029
	<i>CXCL3</i>	0.70 (0.51, 0.97)	0.033
	<i>UBE2I</i>	1.42 (1.03, 1.97)	0.033
White women			
	<i>BLNK</i>	0.63 (0.48, 0.83)	0.001
	<i>CD80</i>	0.64 (0.48, 0.84)	0.001
	<i>MLKL</i>	0.64 (0.49, 0.84)	0.002
	<i>NOD2</i>	0.69 (0.52, 0.90)	0.007
	<i>CXCL9</i>	0.68 (0.51, 0.90)	0.007
	<i>TICAM1</i>	0.70 (0.53, 0.92)	0.010
	<i>CXCL6</i>	0.70 (0.53, 0.92)	0.012
	<i>CX3CL1</i>	0.71 (0.54, 0.93)	0.014
	<i>MAPK13</i>	0.72 (0.55, 0.94)	0.018
	<i>FADD</i>	0.72 (0.54, 0.95)	0.018
	<i>PIK3R2</i>	1.37 (1.04, 1.80)	0.024
	<i>MAP3K7</i>	1.32 (1.01, 1.73)	0.043
	<i>LYN</i>	0.75 (0.57, 0.99)	0.044

Abbreviations: TLR = toll-like receptor; NFkB = nuclear factor kappa B; TNF = tumor necrosis factor; HGSOC = high grade serous ovarian cancer; HR = hazard ratio; CI = confidence interval.

^aWith unadjusted P-value < 0.05.

^bAdjusted for age, stage at diagnosis, and two principal components.

Table 6.4. Statistically significant gene expression in association with FIGO stage at diagnosis (III/IV vs 0/I/II) among Black and White HGSOC cases.

Gene	Log fold change	<i>P</i>	<i>P_{adj}</i>
Black women			
<i>BLNK</i>	-1.0 (-1.2, -0.9)	0.0000000004	0.000000008
<i>TLR4</i>	-0.5 (-0.7, -0.4)	0.00005	0.002
<i>JUN</i>	0.5 (0.4, 0.6)	0.0005	0.015
<i>MAPK10</i>	-0.7 (-0.9, -0.5)	0.0007	0.016
White women			
<i>TLR4</i>	-0.5 (-0.6, -0.4)	0.0003	0.012
<i>JUN</i>	0.5 (0.4, 0.7)	0.001	0.029
<i>MAPK10</i>	-0.7 (-0.9, -0.5)	0.001	0.029
<i>BLNK</i>	-1.3 (-1.6, -1.1)	0.000002	0.0005

Abbreviations: HGSOC = high grade serous ovarian carcinoma; Abbreviations: HGSOC = high grade serous ovarian carcinoma; adj = adjusted *P*-value.

Table 6.5. Statistically significant associations of high/low gene expression with stage at diagnosis (late/early) in TLR, NfκB, and TNF pathway genes among Black and White HGSOC cases.^a

Gene	OR (95% CI)	P
Black cases		
<i>DAB2IP</i>	3.65 (1.78, 7.49)	0.000
<i>ATF4</i>	0.28 (0.14, 0.57)	0.000
<i>PIK3R2</i>	3.52 (1.73, 7.16)	0.001
<i>TRAF6</i>	0.29 (0.14, 0.59)	0.001
<i>BCL2L1</i>	3.26 (1.61, 6.6)	0.001
<i>CEBPB</i>	3.10 (1.55, 6.22)	0.001
<i>PARP1</i>	2.74 (1.38, 5.46)	0.004
<i>ATM</i>	0.37 (0.18, 0.73)	0.004
<i>TNFSF14</i>	2.68 (1.34, 5.37)	0.005
<i>NFKBIA</i>	2.65 (1.33, 5.3)	0.006
<i>SOCS3</i>	2.56 (1.29, 5.07)	0.007
<i>MAPK3</i>	2.56 (1.28, 5.11)	0.008
<i>IRAK1</i>	2.54 (1.28, 5.04)	0.008
<i>BLNK</i>	0.41 (0.21, 0.81)	0.010
<i>LYN</i>	0.41 (0.21, 0.83)	0.013
<i>EDARADD</i>	2.36 (1.2, 4.65)	0.013
<i>JUN</i>	2.36 (1.19, 4.65)	0.014
<i>ITCH</i>	0.42 (0.21, 0.85)	0.015
<i>MAP2K4</i>	0.43 (0.22, 0.85)	0.016
<i>XIAP</i>	0.46 (0.24, 0.9)	0.024
<i>TBK1</i>	0.47 (0.24, 0.91)	0.025
<i>TOLLIP</i>	2.13 (1.1, 4.16)	0.026
<i>TLR6</i>	0.47 (0.24, 0.91)	0.026
<i>MMP14</i>	2.12 (1.09, 4.13)	0.027
<i>CCL2</i>	0.48 (0.24, 0.93)	0.030
<i>RELB</i>	2.08 (1.06, 4.1)	0.033
<i>CSF1</i>	2.04 (1.05, 3.99)	0.036
<i>MAPK10</i>	0.49 (0.25, 0.96)	0.039
<i>MAP2K7</i>	1.99 (1.02, 3.86)	0.043
White cases		
<i>CTSK</i>	4.52 (1.76, 11.6)	0.002
<i>MMP14</i>	4.07 (1.63, 10.16)	0.003
<i>CD40LG</i>	0.27 (0.11, 0.67)	0.004
<i>CD40</i>	0.27 (0.11, 0.67)	0.004
<i>IL6</i>	3.58 (1.47, 8.73)	0.005
<i>CCL13</i>	0.28 (0.11, 0.69)	0.005
<i>BCL2</i>	0.28 (0.12, 0.69)	0.006
<i>CASP8</i>	0.31 (0.13, 0.73)	0.008
<i>MLKL</i>	0.33 (0.14, 0.79)	0.012
<i>TLR8</i>	0.34 (0.14, 0.80)	0.013
<i>TNFSF11</i>	2.93 (1.24, 6.92)	0.014
<i>PIK3R1</i>	2.93 (1.24, 6.92)	0.014
<i>ZAP70</i>	0.34 (0.14, 0.81)	0.015
<i>BIRC3</i>	0.37 (0.16, 0.86)	0.021
<i>TLR3</i>	0.38 (0.16, 0.87)	0.023
<i>CXCL10</i>	0.39 (0.17, 0.91)	0.029

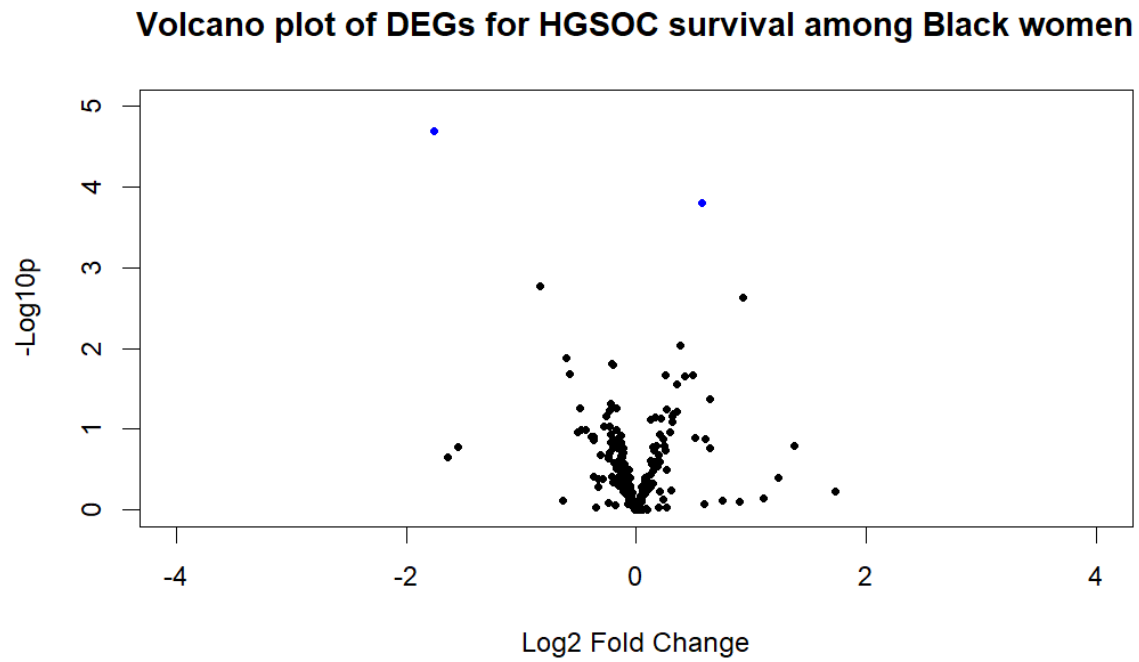
<i>TLR4</i>	0.40 (0.17, 0.92)	0.030
<i>JUN</i>	2.51 (1.09, 5.81)	0.031
<i>GADD45G</i>	0.40 (0.17, 0.93)	0.032
<i>FOS</i>	2.48 (1.08, 5.72)	0.033
<i>MAP2K7</i>	0.41 (0.18, 0.94)	0.034
<i>SYK</i>	2.45 (1.06, 5.65)	0.035
<i>GADD45A</i>	2.40 (1.04, 5.52)	0.039
<i>PRKCB</i>	0.41 (0.18, 0.96)	0.040
<i>PLCG2</i>	0.42 (0.18, 0.97)	0.042

Abbreviations: TLR = toll-like receptor; NFkB = nuclear factor kappa B; TNF = tumor necrosis factor; HGSOC = high grade serous ovarian cancer; OR = odds ratio; CI = confidence interval.

^aWith unadjusted P-value < 0.05.

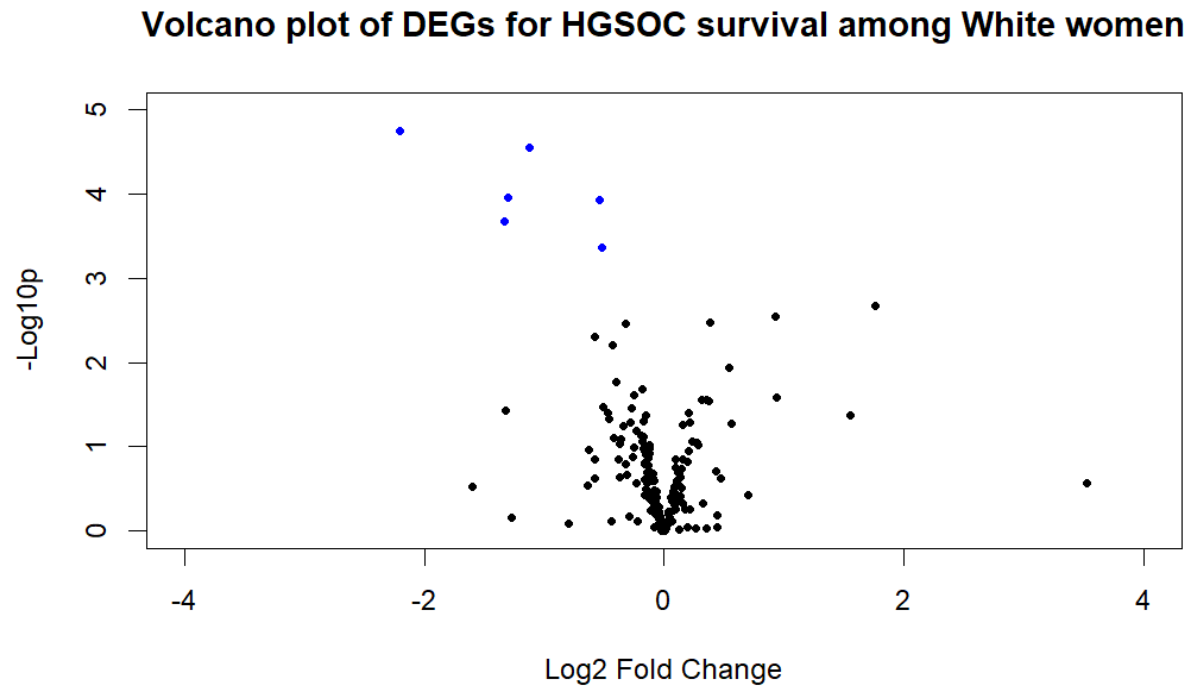
^bAdjusted for age and two principal components.

Figure 6.1.



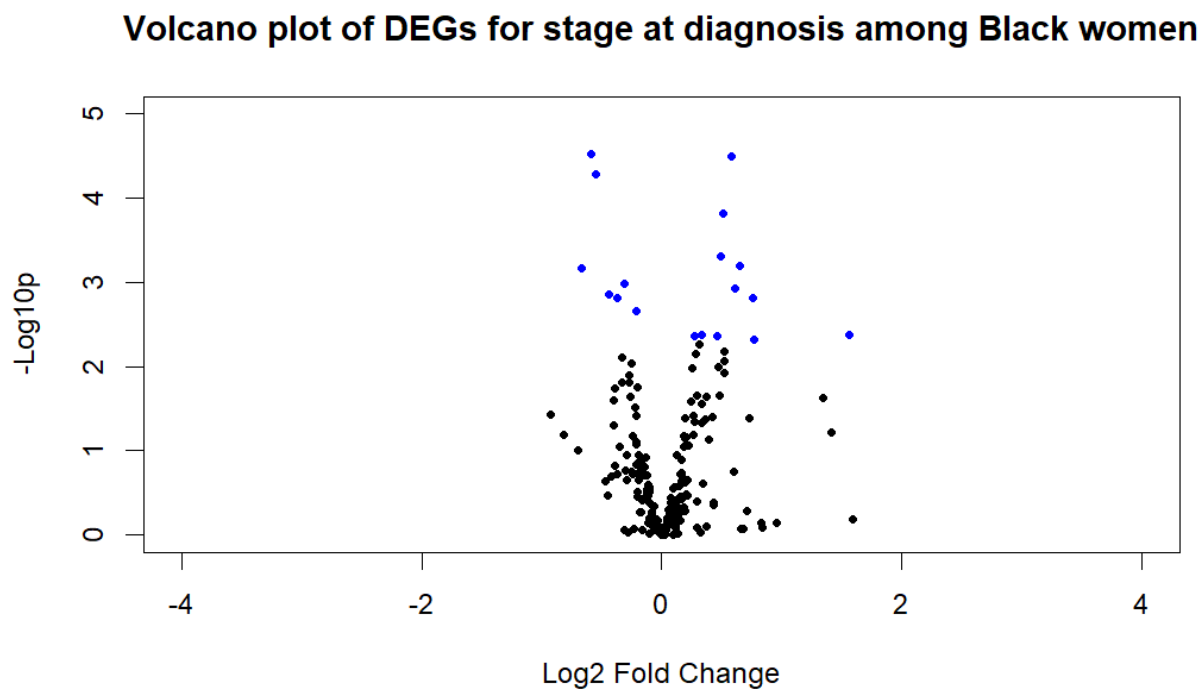
Differential expression of genes in the TLR, NFkB, and TNF pathways by 5-year overall survival status (no vs yes). Blue = $P_{\text{adj}} < 0.05$. Abbreviations: DEGs = differentially expressed genes; HGSOC = high grade serous ovarian carcinoma; adj = adjusted P-value.

Figure 6.2



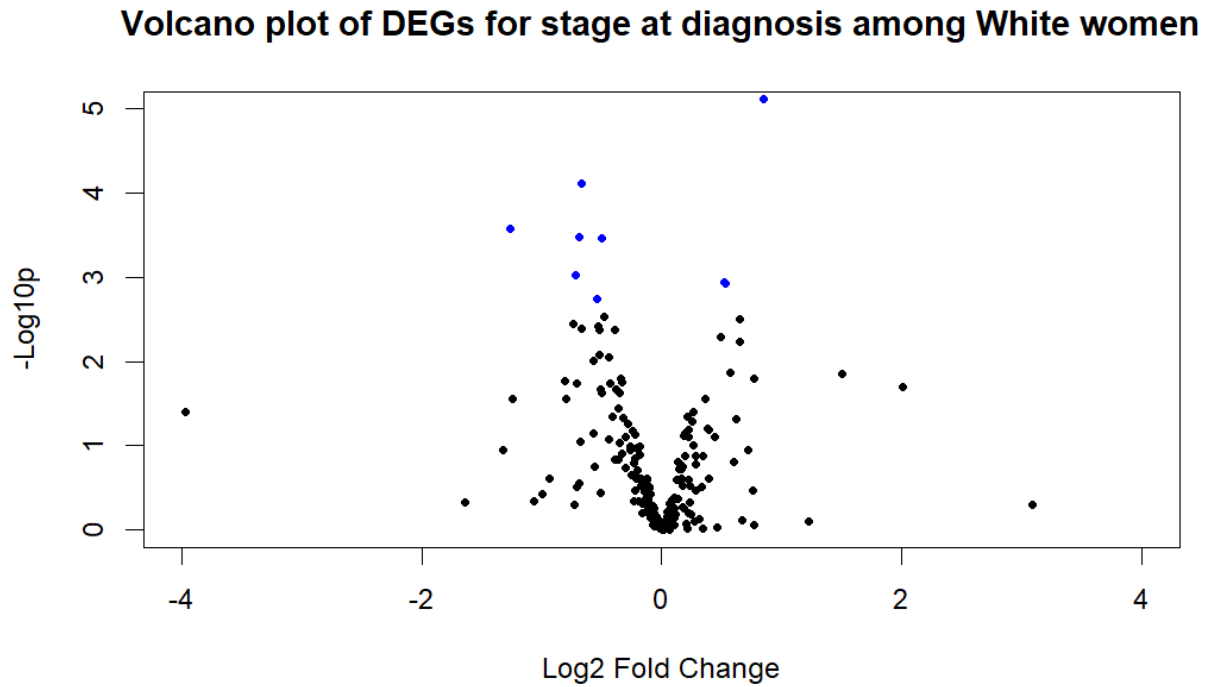
Differential expression of genes in the TLR, NFkB, and TNF pathways by 5-year overall survival status (no vs yes). Blue = $P_{\text{adj}} < 0.05$. Abbreviations: DEGs = differentially expressed genes; HGSOC = high grade serous ovarian carcinoma; adj = adjusted P-value.

Figure 6.3.



Differential expression of genes in the TLR, NFkB, and TNF pathways by stage at diagnosis (late vs early). Blue = $P_{\text{adj}} < 0.05$. Abbreviations: DEGs = differentially expressed genes; HGSOC = high grade serous ovarian carcinoma; adj = adjusted P-value.

Figure 6.4.



Differential expression of genes in the TLR, NFkB, and TNF pathways by by stage at diagnosis (late vs early). Blue = $P_{\text{adj}} < 0.05$. Abbreviations: DEGs = differentially expressed genes; HGSOC = high grade serous ovarian carcinoma; adj = adjusted P-value.

Chapter 7: Future Directions

Although this is the largest genetic dataset for Black and White women with EOC, we were still hindered by small sample sizes in subgroups such as histotype, which are known to be differentially associated with race, genetic markers, and clinical outcomes. We must also acknowledge the inherent limitations of genetic studies between racial groups and cautiously interpret results as race is a social construct and disparities in health are rarely a direct result of genetic differences. In addition, the validity of the White OCAC data and the sensitivity of MAGMA results to sample size necessitate replication studies to confirm our results. Unfortunately, very few programs outside of MAGMA can incorporate gene*environment interactions or input raw GWAS data.

Our investigations of the TLR, NFkB, and TNF gene expressions within the tumor microenvironment in relation to HGSOC survival resulted in some consistent findings between both Black and White women but no DEG identified as statistically significant in HGSOC survival was consistent with our findings in Aim 2. Despite our null results, we cannot rule out the involvement of these genes in EOC carcinogenesis and/or progression. It is my belief that studying the somatic expression of genes, especially within the tumor microenvironment, may prove more fruitful than germline expression for targetable interventions for EOC development and survival. Several barriers, however, exist for EOC (and all other sites) tumor expression investigations. Perhaps the most important are the time and costs of preparation, staining, processing, and quantification of tissue-based expression data. Furthermore, some genes are only available to measure using single-plex stains, therefore poorly suited for complex quantitative analyses and the simultaneous evaluation of multiple biomarkers. Ovarian tumors are also rare and often small, leading to availability issues and exhausted tissue inventories from using single-plex stains. Therefore, investigators must be

frugal and deliberate in the biomarkers they select to measure thus limiting exploration and hypothesis generation. An emerging area in cancer research is digital pathology, which provides automated image analysis algorithms for quantitative measurements and computer aided diagnosis.^{248,249} As part of this field, many advances have been made in digital staining.²⁵⁰ Continued research and advances in the digital preparation and measurement of biomarkers in cancer tissues could drastically improve the economy and efficiency (and thereby, hopefully, equity) of molecular cancer epidemiology endeavors. I am greatly looking forward to learning and contributing in this field to continue to investigate pathogen recognition and inflammation-related processes and cancer.

References

1. Kurman, R. J. & Shih, I.-M. The Origin and Pathogenesis of Epithelial Ovarian Cancer- a Proposed Unifying Theory. *Am. J. Surg. Pathol.* **34**, 433–443 (2010).
2. Torre, L. A. *et al.* Ovarian cancer statistics, 2018. *CA. Cancer J. Clin.* **68**, 284–296 (2018).
3. American Cancer Society. Cancer Facts & Figures 2019.
4. Siegel, R. L., Miller, K. D., Fuchs, H. E. & Jemal, A. Cancer Statistics, 2021. *CA. Cancer J. Clin.* **71**, 7–33 (2021).
5. Ovarian Cancer Stages | Staging for Ovarian Cancer.
<https://www.cancer.org/cancer/types/ovarian-cancer/detection-diagnosis-staging/staging.html>.
6. Summary Staging | SEER Training.
<https://training.seer.cancer.gov/staging/systems/summary/>.
7. Siegel, R. L., Miller, K. D., Fuchs, H. E. & Jemal, A. Cancer statistics, 2022. *CA. Cancer J. Clin.* **72**, 7–33 (2022).
8. Menon, U. *et al.* Ovarian cancer population screening and mortality after long-term follow-up in the UK Collaborative Trial of Ovarian Cancer Screening (UKCTOCS): a randomised controlled trial. *The Lancet* **397**, 2182–2193 (2021).
9. Buys, S. S. *et al.* Effect of screening on ovarian cancer mortality: the Prostate, Lung, Colorectal and Ovarian (PLCO) Cancer Screening Randomized Controlled Trial. *JAMA* **305**, 2295–2303 (2011).
10. Dochez, V. *et al.* Biomarkers and algorithms for diagnosis of ovarian cancer: CA125, HE4, RMI and ROMA, a review. *J. Ovarian Res.* **12**, 28 (2019).
11. Charkhchi, P. *et al.* CA125 and Ovarian Cancer: A Comprehensive Review. *Cancers* **12**, 3730 (2020).

12. Wentzensen, N. *et al.* Ovarian Cancer Risk Factors by Histologic Subtype: An Analysis From the Ovarian Cancer Cohort Consortium. *J. Clin. Oncol.* **34**, 2888 (2016).
13. Fortner, R. T. *et al.* Ovarian cancer risk factor associations by primary anatomic site: the Ovarian Cancer Cohort Consortium. *Cancer Epidemiol. Biomark. Prev. Publ. Am. Assoc. Cancer Res. Cosponsored Am. Soc. Prev. Oncol.* **29**, 2010 (2020).
14. Peres, L. C. *et al.* High levels of C-reactive protein are associated with an increased risk of ovarian cancer: Results from the Ovarian Cancer Cohort Consortium. *Cancer Res.* **79**, 5442 (2019).
15. Ovarian Cancer and Body Size: Individual Participant Meta-Analysis Including 25,157 Women with Ovarian Cancer from 47 Epidemiological Studies. *PLoS Med.* **9**, e1001200 (2012).
16. Nagle, C. M. *et al.* Obesity and survival among women with ovarian cancer: results from the Ovarian Cancer Association Consortium. *Br. J. Cancer* **113**, 817 (2015).
17. Poole, E. M., Konstantinopoulos, P. A. & Terry, K. L. Prognostic implications of reproductive and lifestyle factors in ovarian cancer. *Gynecol. Oncol.* **142**, 574–587 (2016).
18. Minlikeeva, A. N. *et al.* Joint exposure to smoking, excessive weight, and physical inactivity and survival of ovarian cancer patients, evidence from the Ovarian Cancer Association Consortium. *Cancer Causes Control CCC* **30**, 537 (2019).
19. Præstegaard, C. *et al.* Cigarette smoking is associated with adverse survival among women with ovarian cancer: Results from a pooled analysis of 19 studies. *Int. J. Cancer* **140**, 2422 (2017).
20. Brieger, K. K. *et al.* Menopausal hormone therapy prior to the diagnosis of ovarian cancer is associated with improved survival. *Gynecol. Oncol.* **158**, 702 (2020).
21. Prat, J. Pathology of borderline and invasive cancers. *Best Pract. Res. Clin. Obstet. Gynaecol.* **41**, 15–30 (2017).

22. Peres, L. C. *et al.* Invasive Epithelial Ovarian Cancer Survival by Histotype and Disease Stage. *JNCI J. Natl. Cancer Inst.* **111**, 60 (2019).
23. Reid, B. M., Permuth, J. B. & Sellers, T. A. Epidemiology of ovarian cancer: a review. *Cancer Biol. Med.* **14**, 9 (2017).
24. Ovarian cancers: Evolving paradigms in research and care. *Ovarian Cancers Evol. Paradig. Res. Care* 1–396 (2016) doi:10.17226/21841.
25. Zorn, K. K. *et al.* Gene Expression Profiles of Serous, Endometrioid, and Clear Cell Subtypes of Ovarian and Endometrial Cancer. *Clin. Cancer Res.* **11**, 6422–6430 (2005).
26. Phelan, C. M. *et al.* Identification of 12 new susceptibility loci for different histotypes of epithelial ovarian cancer. *Nat. Genet.* **49**, 680–691 (2017).
27. Gates, M. A., Rosner, B. A., Hecht, J. L. & Tworoger, S. S. Risk factors for epithelial ovarian cancer by histologic subtype. *Am. J. Epidemiol.* **171**, 45–53 (2010).
28. Hollis, R. L. & Gourley, C. Genetic and molecular changes in ovarian cancer. *Cancer Biol. Med.* **13**, 236–247 (2016).
29. DeSantis, C., Naishadham, D. & Jemal, A. Cancer statistics for African Americans, 2013. *CA. Cancer J. Clin.* **63**, 151–166 (2013).
30. Peres, L. C. *et al.* Racial Differences in Population Attributable Risk for Epithelial Ovarian Cancer in the OCWAA Consortium. *JNCI J. Natl. Cancer Inst.* (2020) doi:10.1093/jnci/djaa188.
31. Havrilesky, L. J. *et al.* Oral contraceptive use for the primary prevention of ovarian cancer. *Evid. ReportTechnology Assess.* 1–514 (2013).
32. Fathalla, M. F. INCESSANT OVULATION-A FACTOR IN OVARIAN NEOPLASIA ? *The Lancet* vol. 298 163 Preprint at [https://doi.org/10.1016/S0140-6736\(71\)92335-X](https://doi.org/10.1016/S0140-6736(71)92335-X) (1971).
33. Cramer, D. W., Welch, W. R., DW Cramer & Welch, W. R. Determinants of ovarian cancer risk. II. Inferences regarding pathogenesis. *J Natl Cancer Inst* **71**, 717–21 (1983).

34. Ness, R. B. & Cottreau, C. Possible Role of Ovarian Epithelial Inflammation in Ovarian Cancer. *JNCI J. Natl. Cancer Inst.* **91**, 1459–1467 (1999).
35. Duffy, D. M., Ko, C., Jo, M., Brannstrom, M. & Curry, T. E. Ovulation: Parallels With Inflammatory Processes. *Endocr. Rev.* **40**, 369–416 (2019).
36. Hanahan, D. & Weinberg, R. A. The Hallmarks of Cancer. *Cell* **100**, 57–70 (2000).
37. Coussens, L. M. & Werb, Z. Inflammation and cancer. *Nature* **420**, 860 (2002).
38. Grivennikov, S. I., Greten, F. R. & Karin, M. Immunity, Inflammation, and Cancer. *Cell* **140**, 883–899 (2010).
39. List of Classifications – IARC Monographs on the Identification of Carcinogenic Hazards to Humans. <https://monographs.iarc.who.int/list-of-classifications>.
40. Caliri, A. W., Tommasi, S. & Besaratinia, A. Relationships among smoking, oxidative stress, inflammation, macromolecular damage, and cancer. *Mutat. Res. Mutat. Res.* **787**, 108365 (2021).
41. Ziech, D., Franco, R., Pappa, A. & Panayiotidis, M. I. Reactive Oxygen Species (ROS)—Induced genetic and epigenetic alterations in human carcinogenesis. *Mutat. Res. Mol. Mech. Mutagen.* **711**, 167–173 (2011).
42. Chen, R., Alvero, A. B., Silasi, D.-A. & Mor, G. Inflammation, Cancer and Chemoresistance: Taking Advantage of the Toll-Like Receptor Signaling Pathway. *Am. J. Reprod. Immunol.* **57**, 93–107 (2007).
43. Zong, W.-X. & Thompson, C. B. Necrotic death as a cell fate. *Genes Dev.* **20**, 1–15 (2006).
44. Demaria, M. *et al.* Cellular Senescence Promotes Adverse Effects of Chemotherapy and Cancer Relapse. *Cancer Discov.* **7**, 165–176 (2017).
45. Salam, R. *et al.* Cellular senescence in malignant cells promotes tumor progression in mouse and patient Glioblastoma. *Nat. Commun.* **14**, 441 (2023).

46. Harrington, B. S. & Annunziata, C. M. NF- κ B Signaling in Ovarian Cancer. *Cancers* **11**, 1182 (2019).
47. He, Z. & Zhang, S. Tumor-Associated Macrophages and Their Functional Transformation in the Hypoxic Tumor Microenvironment. *Front. Immunol.* **12**, 741305 (2021).
48. Brieger, K. K. *et al.* High pre-diagnosis inflammation-related risk score associated with decreased ovarian cancer survival. *Cancer Epidemiol. Biomark. Prev. Publ. Am. Assoc. Cancer Res. Cosponsored Am. Soc. Prev. Oncol.* **31**, 443–452 (2022).
49. Johnson, C. E. *et al.* Association of inflammation-related exposures and ovarian cancer survival in a multi-site cohort study of Black women. *Br. J. Cancer* (2023) doi:10.1038/s41416-023-02385-w.
50. Moresco, E. M. Y., LaVine, D. & Beutler, B. Toll-like receptors. *Curr. Biol.* **21**, R488–R493 (2011).
51. Takeda, K. & Akira, S. Toll-Like Receptors. *Curr. Protoc. Immunol.* **109**, 14.12.1-14.12.10 (2015).
52. Raetz, C. R. H. & Whitfield, C. Lipopolysaccharide Endotoxins. *Annu. Rev. Biochem.* **71**, 635–700 (2002).
53. Kolb, K., Ohashi, V., Burkart, S. & Flohé, H. Receptor-4 Complex Putative Endogenous Ligand of the Toll-Like Cutting Edge: Heat Shock Protein 60 Is a. *J Immunol Ref.* **164**, 558–561 (2021).
54. McCarthy, C. G. *et al.* Pathophysiology of Hypertension: Toll-like receptors and damage-associated molecular patterns: novel links between inflammation and hypertension. *Am. J. Physiol. - Heart Circ. Physiol.* **306**, H184 (2014).
55. Hennessy, E. J., Parker, A. E. & O'Neill, L. A. J. Targeting Toll-like receptors: emerging therapeutics? *Nat. Rev. Drug Discov.* **9**, 293–307 (2010).

56. Henrick, B. M. *et al.* TLR10 Senses HIV-1 Proteins and Significantly Enhances HIV-1 Infection. *Front. Immunol.* **10**, (2019).
57. Oosting, M. *et al.* Human TLR10 is an anti-inflammatory pattern-recognition receptor. *Proc. Natl. Acad. Sci. U. S. A.* **111**, E4478–E4484 (2014).
58. Huang, B., Zhao, J., Unkeless, J. C., Feng, Z. H. & Xiong, H. TLR signaling by tumor and immune cells: A double-edged sword. *Oncogene* vol. 27 218–224 Preprint at <https://doi.org/10.1038/sj.onc.1210904> (2008).
59. Muccioli, M. & Benencia, F. Toll-like Receptors in Ovarian Cancer as Targets for Immunotherapies. *Front Immunol* **5**, 341 (2014).
60. Kelly, M. G. *et al.* TLR-4 signaling promotes tumor growth and paclitaxel chemoresistance in ovarian cancer. *Cancer Res.* **66**, 3859–3868 (2006).
61. Zhou, M. *et al.* Toll-like receptor expression in normal ovary and ovarian tumors. *Cancer Immunol. Immunother.* **58**, 1375–1385 (2009).
62. Block, M. S. *et al.* MyD88 and TLR4 Expression in Epithelial Ovarian Cancer. *Mayo Clin. Proc.* **93**, 307–320 (2018).
63. Bates, M. *et al.* The role of the MAD2-TLR4-MyD88 axis in paclitaxel resistance in ovarian cancer. **15**, e0243715 (2020).
64. Kim, K. H. *et al.* Expression and Significance of the TLR4/MyD88 Signaling Pathway in Ovarian Epithelial Cancers. (2012) doi:10.1186/1477-7819-10-193.
65. Li, Z. *et al.* The inflammatory microenvironment in epithelial ovarian cancer: a role for TLR4 and MyD88 and related proteins. *Tumor Biol.* **37**, 13279–13286 (2016).
66. Szajnik, M. *et al.* TLR4 signaling induced by lipopolysaccharide or paclitaxel regulates tumor survival and chemoresistance in ovarian cancer. *Oncogene* **28**, 4353–4363 (2009).

67. Patel, M., Horgan, P. G., McMillan, D. C. & Edwards, J. NF- κ B pathways in the development and progression of colorectal cancer. *Transl. Res. J. Lab. Clin. Med.* **197**, 43–56 (2018).
68. Ahmad, R. *et al.* Elevated expression of the toll like receptors 2 and 4 in obese individuals: its significance for obesity-induced inflammation. *J. Inflamm.* **2012** *91* **9**, 1–11 (2012).
69. Vitseva, O. I. *et al.* Inducible Toll-like Receptor and NF- κ B Regulatory Pathway Expression in Human Adipose Tissue. *Obesity* **16**, 932–937 (2008).
70. Calvano, S. E. *et al.* A network-based analysis of systemic inflammation in humans. *Nat.* **2005** *437* **7061** **437**, 1032–1037 (2005).
71. Nikpay, M., Turner, A. W. & McPherson, R. Partitioning the Pleiotropy Between Coronary Artery Disease and Body Mass Index Reveals the Importance of Low Frequency Variants and Central Nervous System–Specific Functional Elements. *Circ. Genomic Precis. Med.* **11**, e002050 (2018).
72. Cai, B., Li, K. & Li, G. Impact of Obesity on Major Surgical Outcomes in Ovarian Cancer: A Meta-Analysis. *Front. Oncol.* **12**, 841306 (2022).
73. Fortner, R. T. *et al.* Ovarian cancer risk factors by tumor aggressiveness: an analysis from the Ovarian Cancer Cohort Consortium. *Int. J. Cancer* **145**, 58–69 (2019).
74. Yao, S. *et al.* Genetic ancestry and population differences in levels of inflammatory cytokines in women: Role for evolutionary selection and environmental factors. *PLOS Genet.* **14**, e1007368 (2018).
75. Singh, U., Hernandez, K. M., Aronow, B. J. & Wurtele, E. S. African Americans and European Americans exhibit distinct gene expression patterns across tissues and tumors associated with immunologic functions and environmental exposures. *Sci. Rep.* **11**, 9905 (2021).

76. Taylor, B. D., Darville, T., Ferrell, R. E., Ness, R. B. & Haggerty, C. L. Racial Variation in Toll-like Receptor Variants Among Women With Pelvic Inflammatory Disease. *J. Infect. Dis.* **207**, 940–946 (2013).
77. Ferguson, J. F. *et al.* Race and gender variation in response to evoked inflammation. *J. Transl. Med.* **2013 111** **11**, 1–9 (2013).
78. Song, H. *et al.* American Cancer Society. Cancer Facts & Figures for African Americans 2019–2021. *Cancer Res.* **459**, 996–1000 (2013).
79. Mogensen, T. H. Pathogen recognition and inflammatory signaling in innate immune defenses. *Clin Microbiol Rev* **22**, 240–73, Table of Contents (2009).
80. Schildkraut, J. M. *et al.* A multi-center population-based case-control study of ovarian cancer in African-American women: the African American Cancer Epidemiology Study (AACES). *BMC Cancer* **14**, 688 (2014).
81. Berchuck, A., Schildkraut, J. M., Pearce, C. L., Chenevix-Trench, G. & Pharoah, P. D. Role of genetic polymorphisms in ovarian cancer susceptibility: development of an international ovarian cancer association consortium. *Adv Exp Med Biol* **622**, 53–67 (2008).
82. Kanehisa, M. & Goto, S. KEGG: kyoto encyclopedia of genes and genomes. *Nucleic Acids Res* **28**, 27–30 (2000).
83. Homo sapiens genome assembly GRCh38. *NCBI* https://www.ncbi.nlm.nih.gov/data-hub/assembly/GCF_000001405.26/.
84. Howe, K. L. *et al.* Ensembl 2021. *Nucleic Acids Res.* **49**, D884–D891 (2021).
85. Manichaikul, A. *et al.* Identification of novel epithelial ovarian cancer loci in women of African ancestry. *Int. J. Cancer* **146**, 2987 (2020).
86. Taliun, D. *et al.* Sequencing of 53,831 diverse genomes from the NHLBI TOPMed Program. 563866 Preprint at <https://doi.org/10.1101/563866> (2019).

87. Loh, P.-R. *et al.* Reference-based phasing using the Haplotype Reference Consortium panel. *Nat. Genet.* **48**, 1443–1448 (2016).
88. Das, S. *et al.* Next-generation genotype imputation service and methods. *Nat. Genet.* **48**, 1284–1287 (2016).
89. Chang, C. C. *et al.* Second-generation PLINK: rising to the challenge of larger and richer datasets. *GigaScience* **4**, s13742-015-0047-8 (2015).
90. Chang, C. C. & Purcell, S. M. PLINK v2.00a5.
91. Chen, S., Zhou, Y., Chen, Y. & Gu, J. fastp: an ultra-fast all-in-one FASTQ preprocessor. *Bioinforma. Oxf. Engl.* **34**, i884–i890 (2018).
92. Patro, R., Duggal, G., Love, M. I., Irizarry, R. A. & Kingsford, C. Salmon provides fast and bias-aware quantification of transcript expression. *Nat. Methods* **14**, 417–419 (2017).
93. Bandera, E. V *et al.* Impact of body mass index on ovarian cancer survival varies by stage. *Br. J. Cancer* **117**, 282 (2017).
94. Alexander, D. H., Novembre, J. & Lange, K. Fast model-based estimation of ancestry in unrelated individuals. *Genome Res.* **19**, 1655–1664 (2009).
95. Chen, B., Khodadoust, M. S., Liu, C. L., Newman, A. M. & Alizadeh, A. A. Profiling tumor infiltrating immune cells with CIBERSORT. *Methods Mol. Biol. Clifton NJ* **1711**, 243 (2018).
96. Goff, B. A. *et al.* Development of an ovarian cancer symptom index: possibilities for earlier detection. *Cancer* **109**, 221–227 (2007).
97. Havrilesky, L. J., Sanders, G. D., Kulasingam, S. & Myers, E. R. Reducing ovarian cancer mortality through screening: Is it possible, and can we afford it? *Gynecol. Oncol.* **111**, 179–187 (2008).
98. Ingerslev, K. *et al.* The potential role of infectious agents and pelvic inflammatory disease in ovarian carcinogenesis. *Infect. Agent. Cancer* **12**, 25 (2017).

99. Akira, S., Uematsu, S. & Takeuchi, O. Pathogen recognition and innate immunity. *Cell* vol. 124 783–801 Preprint at <https://doi.org/10.1016/j.cell.2006.02.015> (2006).
100. McCall, K. D., Muccioli, M. & Benencia, F. Toll-Like Receptors Signaling in the Tumor Microenvironment. *Adv. Exp. Med. Biol.* **1223**, 81–97 (2020).
101. Takeda, K. & Akira, S. TLR signaling pathways. *Semin. Immunol.* **16**, 3–9 (2004).
102. Taniguchi, K. & Karin, M. NF- κ B, inflammation, immunity and cancer: coming of age. *Nat. Rev. Immunol.* *2018* **18**, 309–324 (2018).
103. Zhang, K., Zhou, B., Wang, Y., Rao, L. & Zhang, L. The TLR4 gene polymorphisms and susceptibility to cancer: a systematic review and meta-analysis. *Eur. J. Cancer Oxf. Engl.* *1990* **49**, 946–954 (2013).
104. Zhu, L. *et al.* Association of TLR2 and TLR4 polymorphisms with risk of cancer: a meta-analysis. *PloS One* **8**, e82858 (2013).
105. Castaño-Rodríguez, N., Kaakoush, N. O., Goh, K.-L., Fock, K. M. & Mitchell, H. M. The role of TLR2, TLR4 and CD14 genetic polymorphisms in gastric carcinogenesis: a case-control study and meta-analysis. *PloS One* **8**, e60327 (2013).
106. Chen, J. *et al.* Associations between the four toll-like receptor polymorphisms and the risk of gastric cancer: a meta-analysis. *Cancer Biother. Radiopharm.* **28**, 674–681 (2013).
107. Wang, X.-Q., Liu, L., Liu, Y. & Zhang, K. TLR-2 gene polymorphisms and susceptibility to cancer: evidence from meta-analysis. *Genet. Test. Mol. Biomark.* **17**, 864–872 (2013).
108. El-Omar, E. M., Ng, M. T. & Hold, G. L. Polymorphisms in Toll-like receptor genes and risk of cancer. *Oncogene* **27**, 244–252 (2008).
109. Boraska Jelavić, T. *et al.* Microsatellite GT polymorphism in the toll-like receptor 2 is associated with colorectal cancer. *Clin. Genet.* **70**, 156–160 (2006).

110. Cheng, I., Plummer, S. J., Casey, G. & Witte, J. S. Toll-like receptor 4 genetic variation and advanced prostate cancer risk. *Cancer Epidemiol. Biomark. Prev. Publ. Am. Assoc. Cancer Res. Cosponsored Am. Soc. Prev. Oncol.* **16**, 352–355 (2007).
111. Shui, I. M. *et al.* Genetic variation in the toll-like receptor 4 and prostate cancer incidence and mortality. *The Prostate* **72**, 209–216 (2012).
112. Etokebe, G. E. *et al.* Single-nucleotide polymorphisms in genes encoding toll-like receptor -2, -3, -4, and -9 in case-control study with breast cancer. *Genet. Test. Mol. Biomark.* **13**, 729–734 (2009).
113. Chen, X. *et al.* A genetic variant in the promoter region of Toll-like receptor 9 and cervical cancer susceptibility. *DNA Cell Biol.* **31**, 766–771 (2012).
114. Kutikhin, A. G., Yuzhalin, A. E., Volkov, A. N., Zhivotovskiy, A. S. & Brusina, E. B. Correlation between genetic polymorphisms within IL-1B and TLR4 genes and cancer risk in a Russian population: a case-control study. *Tumour Biol. J. Int. Soc. Oncodevelopmental Biol. Med.* **35**, 4821–4830 (2014).
115. Kutikhin, A. G. Association of polymorphisms in TLR genes and in genes of the Toll-like receptor signaling pathway with cancer risk. *Hum. Immunol.* **72**, 1095–1116 (2011).
116. Kutikhin, A. G. Impact of Toll-like receptor 4 polymorphisms on risk of cancer. *Hum. Immunol.* **72**, 193–206 (2011).
117. Zhang, L., Qin, H., Guan, X., Zhang, K. & Liu, Z. The TLR9 gene polymorphisms and the risk of cancer: evidence from a meta-analysis. *PloS One* **8**, e71785 (2013).
118. Meng, S. *et al.* Effect of TLR2 on the proliferation of inflammation-related colorectal cancer and sporadic colorectal cancer. *Cancer Cell Int.* **20**, 95 (2020).
119. Semlali, A. *et al.* Expression and Polymorphism of Toll-Like Receptor 4 and Effect on NF- κ B Mediated Inflammation in Colon Cancer Patients. *PloS One* **11**, e0146333 (2016).

120. Yao, S. *et al.* Genetic ancestry and population differences in levels of inflammatory cytokines in women: Role for evolutionary selection and environmental factors. *PLoS Genet.* **14**, e1007368 (2018).
121. Nédélec, Y. *et al.* Genetic Ancestry and Natural Selection Drive Population Differences in Immune Responses to Pathogens. *Cell* **167**, 657-669.e21 (2016).
122. FastPop. *SourceForge* <https://sourceforge.net/projects/fastpop/> (2015).
123. Leeuw, C. A. de, Mooij, J. M., Heskes, T. & Posthuma, D. MAGMA: Generalized Gene-Set Analysis of GWAS Data. *PLOS Comput. Biol.* **11**, e1004219 (2015).
124. Benjamini, Y. & Hochberg, Y. Controlling the False Discovery Rate: A Practical and Powerful Approach to Multiple Testing. *J. R. Stat. Soc. Ser. B Methodol.* **57**, 289–300 (1995).
125. De Luca, A., Maiello, M. R., D'Alessio, A., Pergameno, M. & Normanno, N. The RAS/RAF/MEK/ERK and the PI3K/AKT signalling pathways: role in cancer pathogenesis and implications for therapeutic approaches. *Expert Opin. Ther. Targets* **16**, S17–S27 (2012).
126. Burotto, M., Chiou, V. L., Lee, J.-M. & Kohn, E. C. The MAPK pathway across different malignancies: A new perspective. *Cancer* **120**, 3446–3456 (2014).
127. Gonzalez-Hormazabal, P. *et al.* Polymorphisms in RAS/RAF/MEK/ERK Pathway Are Associated with Gastric Cancer. *Genes* **10**, 20 (2019).
128. Slattery, M. L., Lundgreen, A. & Wolff, R. K. MAP kinase genes and colon and rectal cancer. *Carcinogenesis* **33**, 2398–2408 (2012).
129. Zheng, Q., Ye, J., Wu, H., Yu, Q. & Cao, J. Association between Mitogen-Activated Protein Kinase Kinase Kinase 1 Polymorphisms and Breast Cancer Susceptibility: A Meta-Analysis of 20 Case-Control Studies. *PLOS ONE* **9**, e90771 (2014).
130. Liu, H. *et al.* Association between functional polymorphisms in genes involved in the MAPK signaling pathways and cutaneous melanoma risk. *Carcinogenesis* **34**, 885–892 (2013).

131. Dong, C., Davis, R. J. & Flavell, R. A. MAP kinases in the immune response. *Annu. Rev. Immunol.* **20**, 55–72 (2002).
132. Simanshu, D. K., Nissley, D. V. & McCormick, F. RAS Proteins and Their Regulators in Human Disease. *Cell* **170**, 17–33 (2017).
133. Hsu, C.-Y. *et al.* Characterization of Active Mitogen-Activated Protein Kinase in Ovarian Serous Carcinomas. *Clin. Cancer Res.* **10**, 6432–6436 (2004).
134. Davies, H. *et al.* Mutations of the BRAF gene in human cancer. *Nature* **417**, 949–954 (2002).
135. Prior, I. A., Lewis, P. D. & Mattos, C. A comprehensive survey of Ras mutations in cancer. *Cancer Res.* **72**, 2457–2467 (2012).
136. Vougioukalaki, M., Kanellis, D. C., Gkouskou, K. & Eliopoulos, A. G. Tpl2 kinase signal transduction in inflammation and cancer. *Cancer Lett.* **304**, 80–89 (2011).
137. Tunca, B. *et al.* Overexpression of CK20, MAP3K8 and EIF5A correlates with poor prognosis in early-onset colorectal cancer patients. *J. Cancer Res. Clin. Oncol.* **139**, 691–702 (2013).
138. Lehmann, B. D. *et al.* Identification of Targetable Recurrent MAP3K8 Rearrangements in Melanomas Lacking Known Driver Mutations. *Mol. Cancer Res. MCR* **17**, 1842–1853 (2019).
139. Njunge, L. W., Estania, A. P., Guo, Y., Liu, W. & Yang, L. Tumor progression locus 2 (TPL2) in tumor-promoting Inflammation, Tumorigenesis and Tumor Immunity. *Theranostics* **10**, 8343–8364 (2020).
140. Jager, J. *et al.* Tpl2 Kinase Is Upregulated in Adipose Tissue in Obesity and May Mediate Interleukin-1 β and Tumor Necrosis Factor- α Effects on Extracellular Signal-Regulated Kinase Activation and Lipolysis. *Diabetes* **59**, 61–70 (2010).
141. Berthou, F. *et al.* The Tpl2 Kinase Regulates the COX-2/Prostaglandin E2 Axis in Adipocytes in Inflammatory Conditions. *Mol. Endocrinol.* **29**, 1025–1036 (2015).

142. Ballak, D. B. *et al.* MAP3K8 (TPL2/COT) affects obesity-induced adipose tissue inflammation without systemic effects in humans and in mice. *PLoS One* **9**, e89615 (2014).
143. Slattery, M. L., Lundgreen, A. & Wolff, R. K. Dietary Influence on MAPK-Signaling Pathways and Risk of Colon and Rectal Cancer. *Nutr. Cancer* **65**, 729–738 (2013).
144. Slattery, M. L. *et al.* MAPK Genes Interact with Diet and Lifestyle Factors to Alter Risk of Breast Cancer: The Breast Cancer Health Disparities Study. *Nutr. Cancer* **67**, 292–304 (2015).
145. Wagner, E. F. & Nebreda, Á. R. Signal integration by JNK and p38 MAPK pathways in cancer development. *Nat. Rev. Cancer* **9**, 537–549 (2009).
146. Echevarría-Vargas, I. M., Valiyeva, F. & Vivas-Mejía, P. E. Upregulation of miR-21 in cisplatin resistant ovarian cancer via JNK-1/c-Jun pathway. *PLoS One* **9**, e97094 (2014).
147. Matrone, A. *et al.* p38alpha is required for ovarian cancer cell metabolism and survival. *Int. J. Gynecol. Cancer Off. J. Int. Gynecol. Cancer Soc.* **20**, 203–211 (2010).
148. Song, W.-J., Dong, Y., Luo, C. & Chen, Y.-Y. p38MAPK family isoform p38 α and activating transcription factor 2 are associated with the malignant phenotypes and poor prognosis of patients with ovarian adenocarcinoma. *Pathol. - Res. Pract.* **213**, 1282–1288 (2017).
149. Pflug, K. M. & Sitcheran, R. Targeting NF- κ B-Inducing Kinase (NIK) in Immunity, Inflammation, and Cancer. *Int. J. Mol. Sci.* **21**, 8470 (2020).
150. Uno, M. *et al.* NF- κ B Inducing Kinase, a Central Signaling Component of the Non-Canonical Pathway of NF- κ B, Contributes to Ovarian Cancer Progression. *PLoS ONE* **9**, e88347 (2014).
151. Yoon, H. H. *et al.* Racial Differences in BRAF/KRAS Mutation Rates and Survival in Stage III Colon Cancer Patients. *JNCI J. Natl. Cancer Inst.* **107**, djv186 (2015).
152. Watanabe, M., Shiraishi, T., Yatani, R., Nomura, A. M. Y. & Stemmermann, G. N. International comparison on ras gene mutations in latent prostate carcinoma. *Int. J. Cancer* **58**, 174–178 (1994).

153. Heath, E. I. *et al.* Racial Disparities in the Molecular Landscape of Cancer. *Anticancer Res.* **38**, 2235–2240 (2018).
154. Mishra, S. *et al.* Racially Disparate Expression of mTOR/ERK-1/2 Allied Proteins in Cancer. *Front. Cell Dev. Biol.* **9**, (2021).
155. Zhao, F. *et al.* Racial Disparities in Pathological Complete Response Among Patients Receiving Neoadjuvant Chemotherapy for Early-Stage Breast Cancer. *JAMA Netw. Open* **6**, e233329 (2023).
156. Rhyasen, G. W. & Starczynowski, D. T. IRAK signalling in cancer. *Br. J. Cancer* **112**, 232–237 (2015).
157. Li, S., Strelow, A., Fontana, E. J. & Wesche, H. IRAK-4: a novel member of the IRAK family with the properties of an IRAK-kinase. *Proc. Natl. Acad. Sci. U. S. A.* **99**, 5567–5572 (2002).
158. Ringwood, L. & Li, L. The involvement of the interleukin-1 receptor-associated kinases (IRAKs) in cellular signaling networks controlling inflammation. *Cytokine* **42**, 1–7 (2008).
159. Kim, T.-H., Park, J.-M., Kim, M.-Y. & Ahn, Y.-H. The role of CREB3L4 in the proliferation of prostate cancer cells. *Sci. Rep.* **7**, 45300 (2017).
160. Michmerhuizen, A. R., Spratt, D. E., Pierce, L. J. & Speers, C. W. ARE we there yet? Understanding androgen receptor signaling in breast cancer. *Npj Breast Cancer* **6**, 1–19 (2020).
161. Pu, Q. *et al.* The Novel Transcription Factor CREB3L4 Contributes to the Progression of Human Breast Carcinoma. *J. Mammary Gland Biol. Neoplasia* **25**, 37–50 (2020).
162. Hong, C.-C. *et al.* Genetic Variants in Immune-Related Pathways and Breast Cancer Risk in African American Women in the AMBER Consortium. *Cancer Epidemiol. Biomark. Prev. Publ. Am. Assoc. Cancer Res. Cosponsored Am. Soc. Prev. Oncol.* **27**, 321–330 (2018).

163. Chung, W.-M. *et al.* Androgen/Androgen Receptor Signaling in Ovarian Cancer: Molecular Regulation and Therapeutic Potentials. *Int. J. Mol. Sci.* **22**, 7748 (2021).
164. Ose, J. *et al.* Androgens Are Differentially Associated with Ovarian Cancer Subtypes in the Ovarian Cancer Cohort Consortium. *Cancer Res.* **77**, 3951–3960 (2017).
165. Mizushima, T. & Miyamoto, H. The Role of Androgen Receptor Signaling in Ovarian Cancer. *Cells* **8**, 176 (2019).
166. Schildkraut, J. M. *et al.* Trinucleotide Repeat Polymorphisms in the Androgen Receptor Gene and Risk of Ovarian Cancer. *Cancer Epidemiol. Biomarkers Prev.* **16**, 473–480 (2007).
167. Ye, W., Xie, T., Song, Y. & Zhou, L. The role of androgen and its related signals in PCOS. *J. Cell. Mol. Med.* **25**, 1825–1837 (2021).
168. Kanbour, S. A. & Dobs, A. S. Hyperandrogenism in Women with Polycystic Ovarian Syndrome: Pathophysiology and Controversies. *Androg. Clin. Res. Ther.* **3**, 22–30 (2022).
169. Schildkraut, J. M., Schwingl, P. J., Bastos, E., Evanoff, A. & Hughes, C. Epithelial ovarian cancer risk among women with polycystic ovary syndrome. *Obstet. Gynecol.* **88**, 554–559 (1996).
170. Yin, W., Falconer, H., Yin, L., Xu, L. & Ye, W. Association Between Polycystic Ovary Syndrome and Cancer Risk. *JAMA Oncol.* **5**, 106–107 (2019).
171. Zhu, S. *et al.* Genetic Alterations of TRAF Proteins in Human Cancers. *Front. Immunol.* **9**, (2018).
172. Wang, X. *et al.* Characteristics of The Cancer Genome Atlas cases relative to U.S. general population cancer cases. *Br. J. Cancer* **119**, 885 (2018).
173. Sun, G., Zheng, C., Deng, Z., Huang, C. & Huang, J. TRAF5 promotes the occurrence and development of colon cancer via the activation of PI3K/AKT/NF- κ B signaling pathways. *J. Biol. Regul. Homeost. Agents* **34**, 1257–1268 (2020).

174. Inoue, J., Gohda, J., Akiyama, T. & Semba, K. NF- κ B activation in development and progression of cancer. *Cancer Sci.* **98**, 268–274 (2007).
175. Egusquiaguirre, S. P., Yeh, J. E., Walker, S. R., Liu, S. & Frank, D. A. The STAT3 Target Gene TNFRSF1A Modulates the NF- κ B Pathway in Breast Cancer Cells. *Neoplasia N. Y. N* **20**, 489–498 (2018).
176. PubChem. TNFRSF1A - TNF receptor superfamily member 1A (human).
<https://pubchem.ncbi.nlm.nih.gov/gene/TNFRSF1A/human>.
177. Madeleine, M. M. *et al.* Genetic variation in proinflammatory cytokines IL6, IL6R, TNF-region, and TNFRSF1A and risk of breast cancer. *Breast Cancer Res. Treat.* **129**, 887–899 (2011).
178. Siegel, R. L., Miller, K. D. & Jemal, A. Cancer statistics, 2018. *CA. Cancer J. Clin.* **68**, 7–30 (2018).
179. Mantovani, A., Garlanda, C. & Allavena, P. Molecular pathways and targets in cancer-related inflammation. *Ann. Med.* **42**, 161–170 (2010).
180. Ji, Y. & Wang, H. Prognostic prediction of systemic immune-inflammation index for patients with gynecological and breast cancers: a meta-analysis. *World J. Surg. Oncol.* **18**, 197 (2020).
181. Goode, E. L. *et al.* Dose-Response Relationship of CD8+ Tumor Infiltrating Lymphocytes and Survival Time in High-Grade Serous Ovarian Cancer. *JAMA Oncol.* **3**, e173290 (2017).
182. Bae, G. *et al.* Stratification of ovarian cancer borderline from high-grade serous carcinoma patients by quantitative serum NMR spectroscopy of metabolites, lipoproteins, and inflammatory markers. *Front. Mol. Biosci.* **10**, (2023).
183. Kiely, M., Lord, B. & Ambs, S. Immune response and inflammation in cancer health disparities. *Trends Cancer* **8**, 316–327 (2022).

184. Peres, L. C. *et al.* Racial Differences in the Tumor Immune Landscape and Survival of Women with High-Grade Serous Ovarian Carcinoma. *Cancer Epidemiol. Biomark. Prev. Publ. Am. Assoc. Cancer Res. Cosponsored Am. Soc. Prev. Oncol.* **31**, 1006–1016 (2022).
185. Tan, G.-J., Peng, Z.-K., Lu, J.-P. & Tang, F.-Q. Cathepsins mediate tumor metastasis. *World J. Biol. Chem.* **4**, 91–101 (2013).
186. Xu, H. *et al.* Identification of Cathepsin K in the Peritoneal Metastasis of Ovarian Carcinoma Using In-silico, Gene Expression Analysis. *J. Cancer* **7**, 722–729 (2016).
187. Fan, X. *et al.* Elevated Cathepsin K potentiates metastasis of epithelial ovarian cancer. *Histol. Histopathol.* **33**, 673–680 (2018).
188. Manning, B. D. & Cantley, L. C. AKT/PKB signaling: navigating downstream. *Cell* **129**, 1261–1274 (2007).
189. Ligresti, G. *et al.* PIK3CA mutations in human solid tumors. *Cell Cycle* **8**, 1352–1358 (2009).
190. Glaviano, A. *et al.* PI3K/AKT/mTOR signaling transduction pathway and targeted therapies in cancer. *Mol. Cancer* **22**, 138 (2023).
191. Linnerth-Petrik, N. M. *et al.* Akt isoform specific effects in ovarian cancer progression. *Oncotarget* **7**, 74820–74833 (2016).
192. Cristiano, B. E. *et al.* A specific role for AKT3 in the genesis of ovarian cancer through modulation of G(2)-M phase transition. *Cancer Res.* **66**, 11718–11725 (2006).
193. Yeganeh, P. N., Richardson, C., Bahrani-Mostafavi, Z., Tait, D. L. & Mostafavi, M. T. Dysregulation of AKT3 along with a small panel of mRNAs stratifies high-grade serous ovarian cancer from both normal epithelia and benign tumor tissues. *Genes Cancer* **8**, 784–798 (2017).
194. Renema, N., Navet, B., Heymann, M.-F., Lezot, F. & Heymann, D. RANK–RANKL signalling in cancer. *Biosci. Rep.* **36**, e00366 (2016).

195. de Groot, A. F., Appelman-Dijkstra, N. M., van der Burg, S. H. & Kroep, J. R. The anti-tumor effect of RANKL inhibition in malignant solid tumors – A systematic review. *Cancer Treat. Rev.* **62**, 18–28 (2018).
196. Seifart, C. *et al.* TNF-alpha, TNF-beta, IL-6, and IL-10 polymorphisms in patients with lung cancer. *Dis. Markers* **21**, 157–165 (2005).
197. Lee, K.-M. *et al.* Genetic polymorphisms of TGF-beta1 & TNF-beta and breast cancer risk. *Breast Cancer Res. Treat.* **90**, 149–155 (2005).
198. Gaudet, M. M. *et al.* Genetic variation in tumor necrosis factor and lymphotoxin-alpha (TNF-LTA) and breast cancer risk. *Hum. Genet.* **121**, 483–490 (2007).
199. Li, J., Wang, Y., Chang, X. & Han, Z. The effect of LTA gene polymorphisms on cancer risk: an updated systematic review and meta-analysis. *Biosci. Rep.* **40**, BSR20192320 (2020).
200. Jongeneel, C. V. *et al.* Extensive genetic polymorphism in the human tumor necrosis factor region and relation to extended HLA haplotypes. *Proc. Natl. Acad. Sci. U. S. A.* **88**, 9717–9721 (1991).
201. Huang, Y. *et al.* Four genetic polymorphisms of lymphotoxin-alpha gene and cancer risk: a systematic review and meta-analysis. *PloS One* **8**, e82519 (2013).
202. Buhrmann, C. *et al.* Evidence that TNF- β induces proliferation in colorectal cancer cells and resveratrol can down-modulate it. *Exp. Biol. Med. Maywood NJ* **244**, 1–12 (2019).
203. Buhrmann, C. *et al.* Resveratrol Chemosensitizes TNF- β -Induced Survival of 5-FU-Treated Colorectal Cancer Cells. *Nutrients* **10**, 888 (2018).
204. Lau, T.-S. *et al.* Cancer cell-derived lymphotoxin mediates reciprocal tumour-stromal interactions in human ovarian cancer by inducing CXCL11 in fibroblasts. *J. Pathol.* **232**, 43–56 (2014).

205. Moore, J. X., Chaudhary, N. & Akinyemiju, T. Metabolic Syndrome Prevalence by Race/Ethnicity and Sex in the United States, National Health and Nutrition Examination Survey, 1988–2012. *Prev. Chronic. Dis.* **14**, E24 (2017).
206. Upadhyay, V. & Fu, Y.-X. Linking the microbiota and metabolic disease with lymphotoxin. *Int. Immunol.* **25**, 397–403 (2013).
207. Hamid, Y. H. *et al.* The common T60N polymorphism of the lymphotoxin-alpha gene is associated with type 2 diabetes and other phenotypes of the metabolic syndrome. *Diabetologia* **48**, 445–451 (2005).
208. Ozaki, K. *et al.* Functional SNPs in the lymphotoxin-alpha gene that are associated with susceptibility to myocardial infarction. *Nat. Genet.* **32**, 650–654 (2002).
209. Norman, R. A., Bogardus, C. & Ravussin, E. Linkage between obesity and a marker near the tumor necrosis factor-alpha locus in Pima Indians. *J. Clin. Invest.* **96**, 158–162 (1995).
210. Mahajan, A. *et al.* Obesity-dependent association of TNF-LTA locus with type 2 diabetes in North Indians. *J. Mol. Med. Berl. Ger.* **88**, 515–522 (2010).
211. Hamel, L. M. *et al.* Barriers to Clinical Trial Enrollment in Racial and Ethnic Minority Patients With Cancer. *Cancer Control J. Moffitt Cancer Cent.* **23**, 327–337 (2016).
212. Schildkraut, J. M. *et al.* Survival of epithelial ovarian cancer in Black women: a society to cell approach in the African American cancer epidemiology study (AACES). *Cancer Causes Control CCC* **34**, 251–265 (2023).
213. Peres, L. C. *et al.* Predictors of survival trajectories among women with epithelial ovarian cancer. *Gynecol. Oncol.* **156**, 459–466 (2020).
214. Balkwill, F. Tumour necrosis factor and cancer. *Nat. Rev. Cancer* **9**, 361–371 (2009).
215. Waters, J. P., Pober, J. S. & Bradley, J. R. Tumour necrosis factor and cancer. *J. Pathol.* **230**, 241–248 (2013).

216. Schmiegel, W., Roeder, C., Schmielau, J., Rodeck, U. & Kalthoff, H. Tumor necrosis factor alpha induces the expression of transforming growth factor alpha and the epidermal growth factor receptor in human pancreatic cancer cells. *Proc. Natl. Acad. Sci. U. S. A.* **90**, 863–867 (1993).
217. Al-Lamki, R. S. *et al.* Tumor necrosis factor receptor expression and signaling in renal cell carcinoma. *Am. J. Pathol.* **177**, 943–954 (2010).
218. Kalthoff, H., Roeder, C., Brockhaus, M., Thiele, H. G. & Schmiegel, W. Tumor necrosis factor (TNF) up-regulates the expression of p75 but not p55 TNF receptors, and both receptors mediate, independently of each other, up-regulation of transforming growth factor alpha and epidermal growth factor receptor mRNA. *J. Biol. Chem.* **268**, 2762–2766 (1993).
219. Talhouk, A. *et al.* Development and validation of the gene-expression Predictor of high-grade-serous Ovarian carcinoma molecular subTYPE (PrOTYPE). *Clin. Cancer Res. Off. J. Am. Assoc. Cancer Res.* **26**, 5411–5423 (2020).
220. Moorman, P. G. *et al.* Ovulation and ovarian cancer: a comparison of two methods for calculating lifetime ovulatory cycles (United States). *Cancer Causes Control* **13**, 807–811 (2002).
221. Davidson, N. R. *et al.* Molecular subtypes of high-grade serous ovarian cancer across racial groups and gene expression platforms. *bioRxiv* 2023.11.01.565179 (2023)
doi:10.1101/2023.11.01.565179.
222. He, S. *et al.* CREB5 promotes tumor cell invasion and correlates with poor prognosis in epithelial ovarian cancer. *Oncol. Lett.* **14**, 8156–8161 (2017).
223. Dai, W. *et al.* The ATF2/miR-3913-5p/CREB5 axis is involved in the cell proliferation and metastasis of colorectal cancer. *Commun. Biol.* **6**, 1026 (2023).

224. Qi, L. & Ding, Y. Involvement of the CREB5 regulatory network in colorectal cancer metastasis. *Yi Chuan Hered.* **36**, 679–684 (2014).
225. Wang, S. *et al.* CREB5 promotes invasiveness and metastasis in colorectal cancer by directly activating MET. *J. Exp. Clin. Cancer Res. CR* **39**, 168 (2020).
226. Hwang, J. H. *et al.* CREB5 Promotes Resistance to Androgen-Receptor Antagonists and Androgen Deprivation in Prostate Cancer. *Cell Rep.* **29**, 2355-2370.e6 (2019).
227. Wu, J., Wang, S.-T., Zhang, Z.-J., Zhou, Q. & Peng, B.-G. CREB5 promotes cell proliferation and correlates with poor prognosis in hepatocellular carcinoma. *Int. J. Clin. Exp. Pathol.* **11**, 4908–4916 (2018).
228. Yamaguchi, A. *et al.* CC motif chemokine ligand 13 is associated with rheumatoid arthritis pathogenesis. *Mod. Rheumatol.* **23**, 856–863 (2013).
229. Zhao, W. *et al.* Clinical Implications of Inter- and Intratumor Heterogeneity of Immune Cell Markers in Lung Cancer. *JNCI J. Natl. Cancer Inst.* **114**, 280–289 (2022).
230. Li, Z. *et al.* CXCL6 promotes human hepatocyte proliferation through the CXCR1-NFκB pathway and inhibits collagen I secretion by hepatic stellate cells. *Biochem. Cell Biol. Biochim. Biol. Cell.* **94**, 229–235 (2016).
231. Junnila, S. *et al.* Gene expression analysis identifies over-expression of CXCL1, SPARC, SPP1, and SULF1 in gastric cancer. *Genes. Chromosomes Cancer* **49**, 28–39 (2010).
232. Li, J. *et al.* CXCL6 promotes non-small cell lung cancer cell survival and metastasis via down-regulation of miR-515-5p. *Biomed. Pharmacother. Biomedecine Pharmacother.* **97**, 1182–1188 (2018).
233. Yamamoto, Y. *et al.* The Clinicopathological Significance of the CXCR2 Ligands, CXCL1, CXCL2, CXCL3, CXCL5, CXCL6, CXCL7, and CXCL8 in Gastric Cancer. *Anticancer Res.* **39**, 6645–6652 (2019).

234. Gao, Q. *et al.* CXCR6 Upregulation Contributes to a Proinflammatory Tumor Microenvironment That Drives Metastasis and Poor Patient Outcomes in Hepatocellular Carcinoma. *Cancer Res.* **72**, 3546–3556 (2012).
235. Fernandez-Avila, L. *et al.* The Value of CXCL1, CXCL2, CXCL3, and CXCL8 as Potential Prognosis Markers in Cervical Cancer: Evidence of E6/E7 from HPV16 and 18 in Chemokines Regulation. *Biomedicines* **11**, 2655 (2023).
236. Nakayama, J. *et al.* BLNK suppresses pre-B-cell leukemogenesis through inhibition of JAK3. *Blood* **113**, 1483–1492 (2009).
237. Flemming, A., Brummer, T., Reth, M. & Jumaa, H. The adaptor protein SLP-65 acts as a tumor suppressor that limits pre-B cell expansion. *Nat. Immunol.* **4**, 38–43 (2003).
238. Jumaa, H. *et al.* Deficiency of the adaptor SLP-65 in pre-B-cell acute lymphoblastic leukaemia. *Nature* **423**, 452–456 (2003).
239. Lee, J. H., Lee, J.-H., Ahn, B. K., Paik, S. S. & Lee, K. H. Prognostic value of B-cell linker protein in colorectal cancer. *Pathol. - Res. Pract.* **216**, 152821 (2020).
240. Holubekova, V. *et al.* Differential gene expression of immunity and inflammation genes in colorectal cancer using targeted RNA sequencing. *Front. Oncol.* **13**, 1206482 (2023).
241. Liu, X. *et al.* ErbB2/Her2-dependent downregulation of a cell death-promoting protein BLNK in breast cancer cells is required for 3D breast tumor growth. *Cell Death Dis.* **13**, 687 (2022).
242. Hein, S. *et al.* Expression of Jun and Fos proteins in ovarian tumors of different malignant potential and in ovarian cancer cell lines. *Oncol. Rep.* **22**, 177–183 (2009).
243. Eckhoff, K. *et al.* The prognostic significance of Jun transcription factors in ovarian cancer. *J. Cancer Res. Clin. Oncol.* **139**, 1673–1680 (2013).
244. Lu, Y.-C., Yeh, W.-C. & Ohashi, P. S. LPS/TLR4 signal transduction pathway. *Cytokine* **42**, 145–151 (2008).

245. Mohammad, S. & Thiemermann, C. Role of Metabolic Endotoxemia in Systemic Inflammation and Potential Interventions. *Front. Immunol.* **11**, 594150 (2021).
246. Newton, K. & Dixit, V. M. Signaling in innate immunity and inflammation. *Cold Spring Harb. Perspect. Biol.* **4**, a006049 (2012).
247. Singh, N. *et al.* Inflammation and cancer. *Ann. Afr. Med.* **18**, 121–126 (2019).
248. Kiran, N. *et al.* Digital Pathology: Transforming Diagnosis in the Digital Age. *Cureus* **15**, e44620.
249. Baxi, V., Edwards, R., Montalto, M. & Saha, S. Digital pathology and artificial intelligence in translational medicine and clinical practice. *Mod. Pathol.* **35**, 23–32 (2022).
250. Bouyssoux, A., Jarnouen, K., Lallement, L., Fezzani, R. & Olivo-Marin, J.-C. Automated staining analysis in digital cytopathology and applications. *Cytom. Part J. Int. Soc. Anal. Cytol.* **101**, 1068–1083 (2022).

Supplementary Tables and Figures

Supplementary Table ST1. FIGO Staging for Carcinoma of the Ovary.	
Stage	Description
I	Tumor confined to the ovary.
IA	Tumor limited to one ovary (capsule intact); no tumor on surface of the ovary; no malignant cells in the ascites or peritoneal washings.
IB	Tumor limited to both ovaries (capsules intact); no tumor on surface of the ovary; no malignant cells in the ascites or peritoneal washings.
IC	Tumor limited to one or both ovaries, with any of the following:
IC1	Surgical spill.
IC2	Capsule ruptured before surgery or tumor on the surface of the ovary.
IC3	Malignant cells in the ascites or peritoneal washings.
II	Tumor involves one or both ovaries with pelvic extension (below pelvic brim) or primary peritoneal cancer.
IIA	Extension and/or implants on uterus and/or fallopian tubes.
IIB	Extension to other pelvic intraperitoneal tissues.
III	Tumor involves one or both ovaries or primary peritoneal cancer, with cytologically or histologically confirmed spread to the peritoneum outside the pelvis and/or metastasis to the retroperitoneal lymph nodes.
IIIA1	Positive retroperitoneal lymph nodes only (cytologically or histologically proven):
IIIA1(i)	Lymph nodes ≤10 mm in greatest dimension.
IIIA1(ii)	Lymph nodes >10 mm in greatest dimension.
IIIA2	Microscopic extrapelvic (above the pelvic brim) peritoneal involvement with or without positive retroperitoneal lymph nodes.
IIIB	Macroscopic peritoneal metastasis beyond the pelvis ≤2 cm in greatest dimension, with or without metastasis to the retroperitoneal lymph nodes

IIIC	Macroscopic peritoneal metastasis beyond the pelvis >2 cm in greatest dimension, with or without metastasis to the retroperitoneal lymph nodes (includes extension of tumor to capsule of liver and spleen without parenchymal involvement of either organ).
IV	Distant metastasis excluding peritoneal metastases.
IVA	Pleural effusion with positive cytology.
IVB	Parenchymal metastases and metastases to extra-abdominal organs (including inguinal lymph nodes and lymph nodes outside of the abdominal cavity).

Supplementary Table ST2. Studies Participating in the Ovarian Cancer Association Consortium.

Study Acronym	Study Name	Country
AAS	African American Cancer Epidemiology Study	USA
AOV	Alberta Ovarian Tumor Types study	Canada
AUS	Australia Ovarian Cancer Study & Australia Cancer Study (Ovarian Cancer)	Australia
BAV	Bavarian Ovarian Cancer Cases and Controls	Germany
BEL	Belgium Ovarian Cancer Study	Belgium
BGS	Breakthrough Generations Study	UK
BRZ	Brazil Gynecologic Tumor Bank Study	Brazil
BVU	The BioVU DNA Repository	USA
CAM	Cancer Research UK, Cambridge Research Institute	UK
CHA	Tianjin China Ovarian Cancer Study	China
CHN	Hebei Medical University	China
CNI	CNIO Ovarian Cancer Study	Spain
COE	Gynecologic Cancer Center of Excellence	USA
CON	Connecticut Ovary Study	USA
CWR	Case Western Reserve University	USA
CZE	CZEch CAncer PaNel for Clinical Analysis	Czech Republic
DKE	Duke University Clinic	USA
DOV	Diseases of the Ovary and their Evaluation	USA
EMC	Rotterdam Ovarian Cancer Study	Netherlands
EPC	European Prospective Investigation into Nutrition and Cancer	Europe
GER	Germany Ovarian Cancer Study	Germany
GRC	Demokritos	Greece
GRR	Familial Ovarian Cancer Registry	Global
HAW	Hawaii Ovarian Cancer Study	USA
HJO	Hannover-Jena Ovarian Cancer Study	Germany
HMO	Hannover-Minsk Ovarian Cancer Study	Germany
HOP	Hormones and Ovarian Cancer Prediction	USA
HSK	Dr. Horst Schmidt Kliniken	Germany
HUO	Hannover-Ufa Ovarian Cancer Study	Germany
ITL	University of Milan-Bicocca/ASST Monza Ovarian Cancer Study	Italy
JGO	Japanese Gynecologic Oncology Study	Japan
JPN	Hospital-based Epidemiologic Research Program at Aichi Cancer Center	Japan
KRA	Korean Epithelial Ovarian Cancer Study	Korea
LAX	Women's Cancer Program at the Samuel Oschin Comprehensive Cancer Institute	USA
LUN	Departments of Cancer Epidemiology and Oncology, University Hospital, Lund	Sweden
MAC	Mayo Clinic Case-Only Ovarian Cancer Study	USA
MAL	Danish Malignant Ovarian Tumor Study	Denmark
MAS	Malaysia Ovarian Cancer Genetic Study	Malaysia
MAY	Mayo Clinic Ovarian Cancer Case Control Study	USA
MCC	Melbourne Collaborative Cohort Study	Australia
MDA	MD Anderson Ovarian Cancer Study	USA
MEC	Multiethnic Cohort Study	USA
MOF	Moffitt Cancer Center Ovarian Cancer Study	USA
MSK	Memorial Sloan Kettering Cancer Center	USA

NCO	North Carolina Ovarian Cancer Study	USA
NEC	New England Case-Control Study	USA
NHS	Nurses' Health Study I and II	USA
NJO	New Jersey Ovarian Cancer Study	USA
NOR	University of Bergen, Haukeland University Hospital, Norway	Norway
NTH	Nijmegen Ovarian Cancer Study	Netherlands
OPL	Ovarian Cancer Prognosis and Lifestyle Study	Australia
ORE	Oregon Ovarian Cancer Registry	USA
OVA	Ovarian Cancer in Alberta and British Columbia	Canada
PLC	The Prostate, Lung, Colorectal and Ovarian Cancer Screening Trial	USA
POC	Polish Ovarian Cancer Study	Poland
POL	Polish Ovarian cancer Case Control Study (NCI)	Poland
PVQ	PREvention of OVarian cancer in Quebec	Canada
RBH	Royal Brisbane Hospital	Australia
RMH	Royal Marsden Hospital Ovarian Cancer Study	UK
RPC	Roswell Park Cancer Institute Ovarian Cancer Cohort	USA
SEA	UK Studies of Epidemiology and Risk Factors in Cancer Heredity (SEARCH) Ovarian Cancer Study	UK
SIS	The Sister Study	USA
SMC	Swedish Mammography Cohort	Sweden
SOC	Southampton Ovarian Cancer Study	UK
SON	Southern Ontario Ovarian Cancer Study	Canada
SRO	Scottish Randomised Trial in Ovarian Cancer	UK
STA	Family Registry for Ovarian Cancer AND Genetic Epidemiology of Ovarian Cancer	USA
SWE	Sweden Western Region Ovarian Cancer Study	Sweden
SWH	Shanghai Women's Health Study	China
TBO	Tampa Bay Ovarian Cancer Study	USA
TOR	Familial Ovarian Tumor Study	Canada
TWH	Tuebingen University Women's Hospital Study	Germany
UCI	UC Irvine Ovarian Cancer Study	USA
UHN	Princess Margaret Cancer Centre	Canada
UKO	UK Ovarian Cancer Population Study	UK
UKR	UK Familial Ovarian Cancer Registry	UK
USC	Los Angeles County Case-Control Studies of Ovarian Cancer	USA
VAN	OVCARE Gynecologic Tissue Bank and Outcomes Unit	Canada
VTL	VITamins And Lifestyle Cohort Study	USA
WMH	Westmead Institute for Cancer Research – Westmead Hospital	Australia
WOC	Warsaw Ovarian Cancer Study	Poland

Supplementary Table ST3. Pathways, genes, and chromosomal coordinates included for analysis							
Pathway	Gene #	Gene Name	Chromosome	GRCh37/hg19		GRCh38/hg38	
				Start	Stop	Start	Stop
NfκB	5743	<i>PTGS2</i>	1	186640944	186649559	186671812	186680427
	7535	<i>ZAP70</i>	2	98330031	98356990	97713568	97744327
	3554	<i>IL1R1</i>	2	102686836	102796334	102069638	102179874
	8809	<i>IL18R1</i>	2	102979093	103015230	102356283	102398777
	1386	<i>ATF2</i>	2	175936978	176032934	175072250	175168206
	6772	<i>STAT1</i>	2	191833762	191878976	190969036	191014250
	1385	<i>CREB1</i>	2	208394616	208470284	207529892	207605560
	7096	<i>TLR1</i>	4	38797876	38806814	38787555	38805800
	3600	<i>IL15</i>	4	142557749	142655140	141636596	141733987
	7424	<i>VEGFC</i>	4	177604689	177713899	176683534	176792745
	929	<i>CD14</i>	5	140011313	140013286	140631728	140633701
	5601	<i>MAPK9</i>	5	179660594	179719071	180233594	180292071
	5603	<i>MAPK13</i>	6	36098261	36112301	36130484	36144524
	7128	<i>TNFAIP3</i>	6	138188325	138204451	137866317	137883314
	9586	<i>CREB5</i>	7	28338940	28865511	28299321	28825894
	3663	<i>IRF5</i>	7	128577976	128590089	128937737	128950042
	64764	<i>CREB3L2</i>	7	137559725	137686847	137874979	138002101
	9530	<i>BAG4</i>	8	38034106	38070819	38176588	38213301
	3551	<i>IKBKB</i>	8	42128820	42190171	42271302	42332653
	4067	<i>LYN</i>	8	56792386	56925006	55878463	56012447
	3456	<i>IFNB1</i>	9	21077104	21077943	21077105	21077944
	10488	<i>CREB3</i>	9	35732317	35737005	35732320	35737008
	7099	<i>TLR4</i>	9	120466453	120479769	117704175	117717491
	5588	<i>PRKCQ</i>	10	6435558	6622254	6393595	6580646
	5599	<i>MAPK8</i>	10	49514682	49647403	48306639	48439360
	5328	<i>PLAU</i>	10	75670862	75677259	73909182	73917501
	355	<i>FAS</i>	10	90750288	90775542	88969801	89017059
	4791	<i>NFKB2</i>	10	104153867	104162286	102394110	102402529
	840	<i>CASP7</i>	10	115438921	115490668	113679162	113730909

55367	<i>PIDD1</i>	11	799179	809872	799179	809501
54472	<i>TOLLIP</i>	11	1295598	1330892	1274368	1309662
90993	<i>CREB3L1</i>	11	46299189	46342972	46277638	46321422
329	<i>BIRC2</i>	11	102217913	102249401	102347182	102378670
472	<i>ATM</i>	11	108093559	108239829	108222500	108369102
7132	<i>TNFRSF1A</i>	12	6437923	6451283	6328757	6342117
10059	<i>DNM1L</i>	12	32832134	32898584	32679200	32745650
51135	<i>IRAK4</i>	12	44152747	44183346	43758944	43789543
29110	<i>TBK1</i>	12	64845840	64895899	64452060	64502119
192111	<i>PGAM5</i>	12	133287393	133299323	132710807	132722737
4323	<i>MMP14</i>	14	23305742	23316809	22836533	22847600
9252	<i>RPS6KA5</i>	14	91335086	91526993	90868122	91060649
7187	<i>TRAF3</i>	14	103243816	103377837	102777475	102911500
5604	<i>MAP2K1</i>	15	66679182	66783882	66386873	66491544
597	<i>BCL2A1</i>	15	80253232	80263643	79960890	79971301
27040	<i>LAT</i>	16	28996147	29002104	28984826	28990783
5595	<i>MAPK3</i>	16	30125426	30134630	30114105	30123309
64127	<i>NOD2</i>	16	50727507	50766990	50693581	50733081
1540	<i>CYLD</i>	16	50775961	50835847	50742050	50801936
1459	<i>CSNK2A2</i>	16	58191811	58231782	58157907	58197878
197259	<i>MLKL</i>	16	74705753	74734789	74671855	74701148
6347	<i>CCL2</i>	17	32582296	32584222	34255277	34257203
9020	<i>MAP3K14</i>	17	43340488	43394414	45263119	45317064
5608	<i>MAP2K6</i>	17	67410838	67538470	69414697	69542329
9021	<i>SOCS3</i>	17	76352858	76356160	78356777	78360079
10892	<i>MALT1</i>	18	56338618	56417371	58671386	58750139
8792	<i>TNFRSF11A</i>	18	59992520	60054943	62325287	62387710
596	<i>BCL2</i>	18	60790579	60987011	63123346	63319778
4616	<i>GADD45B</i>	19	2476123	2478257	2476125	2478259
84699	<i>CREB3L3</i>	19	4153598	4173051	4153601	4173054
148022	<i>TICAM1</i>	19	4815936	4831754	4815924	4831742
3383	<i>ICAM1</i>	19	10380707	10397291	10270841	10286615

	3726	<i>JUNB</i>	19	12902310	12904125	12791496	12793311
	602	<i>BCL3</i>	19	45246070	45263301	44748045	44760044
	4318	<i>MMP9</i>	20	44637547	44645200	46008908	46016561
	958	<i>CD40</i>	20	44746899	44758384	46118250	46129745
	3454	<i>IFNAR1</i>	21	34696748	34732129	33324443	33359823
	10454	<i>TAB1</i>	22	39795759	39833132	39399754	39437127
	468	<i>ATF4</i>	22	39916569	39918691	39520559	39522686
	6300	<i>MAPK12</i>	22	50691331	50700248	50252902	50261759
	257397	<i>TAB3</i>	23	30845559	30907511	30827442	30889394
	60401	<i>EDA2R</i>	23	65815479	65859140	66594384	66639298
	1896	<i>EDA</i>	23	68835911	69259322	69616067	70039472
	331	<i>XIAP</i>	23	122993662	123047829	123859812	123913979
	959	<i>CD40LG</i>	23	135730281	135742549	136648177	136660390
TLR	7133	<i>TNFRSF1B</i>	1	12227044	12269279	12166949	12209222
	1647	<i>GADD45A</i>	1	68150860	68154021	67685177	67688338
	8915	<i>BCL10</i>	1	85731459	85742604	85265776	85276904
	7412	<i>VCAM1</i>	1	101185196	101204601	100719640	100739045
	1435	<i>CSF1</i>	1	110453233	110473616	109910611	109930994
	1513	<i>CTSK</i>	1	150768684	150780917	150796208	150808441
	9641	<i>IKBKE</i>	1	206643586	206670223	206470243	206496890
	7100	<i>TLR5</i>	1	223282748	223316624	223109404	223143282
	128178	<i>EDARADD</i>	1	236557680	236648008	236394380	236484708
	10000	<i>AKT3</i>	1	243651535	244014381	243488233	243851079
	10913	<i>EDAR</i>	2	109510927	109605828	108894471	108989372
	3553	<i>IL1B</i>	2	113587337	113594356	112829751	112836779
	8837	<i>CFLAR</i>	2	201980877	202037411	201116154	201172688
	841	<i>CASP8</i>	2	202098166	202152434	201233443	201287711
	4615	<i>MYD88</i>	3	38179969	38184513	38138478	38143022
	54106	<i>TLR9</i>	3	52255096	52260179	52221080	52226163
	941	<i>CD80</i>	3	119243140	119278481	119523948	119559634
	942	<i>CD86</i>	3	121774209	121839990	122055362	122121143
	5291	<i>PIK3CB</i>	3	138371540	138553780	138652698	138834938

3592	<i>IL12A</i>	3	159706623	159713806	159988836	159996019
5290	<i>PIK3CA</i>	3	178866311	178952500	179148114	179240084
10333	<i>TLR6</i>	4	38825325	38858438	38823704	38857711
2919	<i>CXCL1</i>	4	74735109	74737019	73869392	73871302
6374	<i>CXCL5</i>	4	74861359	74864446	73995642	73998729
2921	<i>CXCL3</i>	4	74902306	74904490	74036589	74038773
2920	<i>CXCL2</i>	4	74962752	74964997	74097035	74099280
5602	<i>MAPK10</i>	4	86933452	87374283	86012299	86594110
6696	<i>SPP1</i>	4	88896802	88904563	87975650	87983411
4790	<i>NFKB1</i>	4	103422486	103538459	102501329	102617302
7097	<i>TLR2</i>	4	154605404	154627243	153684256	153706091
7098	<i>TLR3</i>	4	186990309	187006252	186069155	186085098
5295	<i>PIK3R1</i>	5	67511584	67597649	68215756	68301821
353376	<i>TICAM2</i>	5	114914339	114952142	115578496	115602479
1437	<i>CSF2</i>	5	131409485	131411863	132073792	132076170
3659	<i>IRF1</i>	5	131817301	131826465	132481609	132490777
1460	<i>CSNK2B</i>	6	31632995	31637844	31665880	31670070
1388	<i>ATF6B</i>	6	32083045	32096017	32115268	32128240
1432	<i>MAPK14</i>	6	35995412	36079013	36027635	36111236
4217	<i>MAP3K5</i>	6	136878184	137113656	136557046	136793051
23118	<i>TAB2</i>	6	149639436	149732747	149217924	149411613
84433	<i>CARD11</i>	7	2945709	3083579	2906075	3043945
3569	<i>IL6</i>	7	22766766	22771621	22725442	22732002
23643	<i>LY96</i>	8	74903564	74941314	73991329	74032562
3452	<i>IFNA21</i>	9	21165636	21166659	21165637	21166660
3441	<i>IFNA4</i>	9	21186617	21187598	21186618	21187599
3446	<i>IFNA10</i>	9	21206180	21207142	21206181	21207143
3449	<i>IFNA16</i>	9	21216372	21217310	21216373	21217311
3451	<i>IFNA17</i>	9	21227242	21228221	21227243	21228222
3448	<i>IFNA14</i>	9	21239201	21239978	21239202	21239979
3442	<i>IFNA5</i>	9	21304613	21305312	21304614	21305313
3447	<i>IFNA13</i>	9	21367371	21368075	21367372	21368076

3440	<i>IFNA2</i>	9	21384254	21385396	21384255	21385397
3439	<i>IFNA1</i>	9	21440453	21441315	21440454	21441316
6363	<i>CCL19</i>	9	34689567	34691274	34689570	34691277
6366	<i>CCL21</i>	9	34709002	34710164	34709005	34710167
10912	<i>GADD45G</i>	9	92219913	92221470	89605012	89606555
6850	<i>SYK</i>	9	93564012	93660842	90801680	90898560
153090	<i>DAB2IP</i>	9	124329162	124547809	121566883	121785530
6387	<i>CXCL12</i>	10	44865601	44880545	44370153	44385097
1147	<i>CHUK</i>	10	101948123	101989367	100186113	100229610
283106	<i>CSNK2A3</i>	11	11373489	11374904	11351942	11353357
7189	<i>TRAF6</i>	11	36505317	36531863	36483767	36510313
5970	<i>RELA</i>	11	65421067	65430443	65653596	65662972
330	<i>BIRC3</i>	11	102188181	102210134	102317373	102339403
4314	<i>MMP3</i>	11	102706528	102714342	102835797	102843611
8600	<i>TNFSF11</i>	13	43136872	43182149	42562736	42608013
10673	<i>TNFSF13B</i>	13	108921875	108960832	108269420	108308484
11035	<i>RIPK3</i>	14	24805227	24809242	24336021	24340036
5579	<i>PRKCB</i>	16	23847300	24231932	23835979	24220611
6376	<i>CX3CL1</i>	16	57406414	57418956	57372461	57385048
5336	<i>PLCG2</i>	16	81812899	81996290	81779258	81962693
5606	<i>MAP2K3</i>	17	21187968	21218552	21284656	21315240
6357	<i>CCL13</i>	17	32683471	32685629	34356452	34358610
6348	<i>CCL3</i>	17	34415602	34417506	36088256	36090160
6351	<i>CCL4</i>	17	34431220	34433014	36103827	36105621
414062	<i>CCL3L3</i>	17	34522268	34524147	36194869	36196748
9560	<i>CCL4L2</i>	17	34538468	34540275	36211063	36212878
7706	<i>TRIM25</i>	17	54965270	54991409	56887909	56914048
79092	<i>CARD14</i>	17	78143791	78183130	80169992	80209331
51588	<i>PIAS4</i>	19	4007749	4038067	4007598	4039386
5605	<i>MAP2K2</i>	19	4090319	4124126	4090321	4124184
8740	<i>TNFSF14</i>	19	6661264	6670599	6658135	6670588
208	<i>AKT2</i>	19	40736224	40791443	40230317	40285531

	5971	<i>RELB</i>	19	45504707	45541456	45001449	45038198
	3661	<i>IRF3</i>	19	50162826	50169132	49659569	49665875
	1457	<i>CSNK2A1</i>	20	463338	524482	472969	543838
	182	<i>JAG1</i>	20	10618332	10654694	10637684	10674046
	598	<i>BCL2L1</i>	20	30252261	30311752	31664452	31723964
	3455	<i>IFNAR2</i>	21	34602231	34636831	33229895	33264513
	29775	<i>CARD10</i>	22	37886400	37915543	37490362	37519203
	115650	<i>TNFRSF13C</i>	22	42321036	42322821	41925032	41926817
	51284	<i>TLR7</i>	23	12885202	12908480	12867083	12890361
	51311	<i>TLR8</i>	23	12924739	12941288	12906620	12923169
	695	<i>BTK</i>	23	100604435	100641212	101349447	101390796
	8517	<i>IKBKG</i>	23	153769419	153796804	154541204	154568573
TNF	5293	<i>PIK3CD</i>	1	9711789	9789172	9629889	9729114
	3932	<i>LCK</i>	1	32716840	32751766	32251239	32286170
	8503	<i>PIK3R3</i>	1	46505812	46642167	46040140	46176495
	3725	<i>JUN</i>	1	59246463	59249785	58780791	58784113
	148327	<i>CREB3L4</i>	1	153940315	153946840	153967839	153974364
	6401	<i>SELE</i>	1	169691781	169703220	169722640	169734079
	7188	<i>TRAF5</i>	1	211499849	211548403	211326579	211374946
	142	<i>PARP1</i>	1	226548392	226595801	226360691	226408100
	843	<i>CASP10</i>	2	202047621	202094129	201182898	201229406
	6364	<i>CCL20</i>	2	228678558	228682280	227813842	227817564
	3576	<i>CXCL8</i>	4	74606223	74609433	73740506	73743716
	6372	<i>CXCL6</i>	4	74702273	74704477	73836556	73838760
	4283	<i>CXCL9</i>	4	76922623	76928641	76001342	76007523
	3627	<i>CXCL10</i>	4	76942269	76944689	76021116	76023536
	6373	<i>CXCL11</i>	4	76954835	76957350	76033682	76036197
	836	<i>CASP3</i>	4	185548850	185570629	184627696	184649475
	3593	<i>IL12B</i>	5	158741791	158757481	159314783	159330473
	8737	<i>RIPK1</i>	6	3064201	3115421	3063967	3115187
	1906	<i>EDN1</i>	6	12290529	12297427	12261214	12297194
	4049	<i>LTA</i>	6	31539876	31542101	31560550	31574324

7124	<i>TNF</i>	6	31543344	31546113	31575567	31578336
4050	<i>LTB</i>	6	31548335	31550202	31580558	31582425
6885	<i>MAP3K7</i>	6	91223292	91297020	90513573	90587301
5879	<i>RAC1</i>	7	6414126	6443598	6374495	6403967
3444	<i>IFNA7</i>	9	21201468	21202204	21201469	21202205
3443	<i>IFNA6</i>	9	21350317	21350886	21350318	21350887
3445	<i>IFNA8</i>	9	21409146	21410184	21409147	21410185
7185	<i>TRAF1</i>	9	123664671	123691451	120902393	120929173
7186	<i>TRAF2</i>	9	139776341	139821853	136881933	136926621
1326	<i>MAP3K8</i>	10	30722950	30750762	30434003	30461833
29760	<i>BLNK</i>	10	97951455	98031333	96191699	96271576
3665	<i>IRF7</i>	11	612555	615999	612553	615999
8986	<i>RPS6KA4</i>	11	64126625	64139687	64359153	64372215
8772	<i>FADD</i>	11	70049269	70053508	70203163	70207402
114609	<i>TIRAP</i>	11	126152800	126164828	126281893	126294933
23085	<i>ERC1</i>	12	1100404	1605099	991208	1495933
4055	<i>LTBR</i>	12	6484534	6500737	6375368	6391571
4792	<i>NFKBIA</i>	14	35870716	35873960	35401510	35404754
2353	<i>FOS</i>	14	75745477	75748937	75278778	75282234
207	<i>AKT1</i>	14	105235686	105262080	104769349	104795743
3492	<i>IGH</i>	14	106032614	107288051	105566277	106879844
7329	<i>UBE2I</i>	16	1357420	1377019	1309153	1327018
8717	<i>TRADD</i>	16	67188088	67193812	67154185	67159909
6416	<i>MAP2K4</i>	17	11924135	12047148	12020818	12143831
6352	<i>CCL5</i>	17	34198495	34207377	35871491	35880373
5609	<i>MAP2K7</i>	19	7968665	7979363	7903780	7914483
5296	<i>PIK3R2</i>	19	18263988	18281343	18153178	18170533
83737	<i>ITCH</i>	20	32951041	33099198	34363235	34511393
3929	<i>LBP</i>	20	36974814	37005653	38346411	38377011
5335	<i>PLCG1</i>	20	39766159	39804359	41137519	41175721
1051	<i>CEBPB</i>	20	48807120	48809227	50190583	50192690
5594	<i>MAPK1</i>	22	22113946	22221970	21759657	21867680

3976	<i>LIF</i>	22	30636436	30642840	30240447	30257923
5600	<i>MAPK11</i>	22	50702142	50708779	50263713	50270393
3654	<i>IRAK1</i>	23	153275957	153285342	154010506	154024584

Supplementary Table ST4.1. Gene associations/BMI interactions within TLR, NFkB, and TNF pathways with invasive EOC risk among Black women.

Pathway	Gene	# SNPs	P_{raw}	P_{BH}	$P_{BMI\ raw}$	$P_{BMI\ FDR}$
NFkB			0.099		0.165	
	<i>PRKCB</i>	2384	0.003	0.351	0.044	0.748
	<i>GADD45G</i>	7	0.006	0.351	0.188	0.886
	<i>LTB</i>	4	0.009	0.351	0.875	1.000
	<i>PIDD1</i>	82	0.010	0.351	0.307	0.886
	<i>PLCG2</i>	1937	0.018	0.375	0.521	0.943
	<i>RELB</i>	193	0.046	0.556	0.196	0.886
	<i>ZAP70</i>	120	0.060	0.571	0.391	0.886
	<i>LYN</i>	857	0.065	0.571	0.696	0.961
	<i>CARD14</i>	271	0.072	0.571	0.397	0.886
	<i>TRAF6</i>	108	0.088	0.608	0.289	0.886
	<i>TRADD</i>	14	0.094	0.614	0.837	1.000
	<i>CXCL12</i>	104	0.117	0.702	0.135	0.886
	<i>CARD11</i>	1090	0.137	0.767	0.058	0.748
	<i>VCAM1</i>	80	0.144	0.782	0.265	0.886
	<i>MAP3K14</i>	208	0.156	0.794	0.429	0.901
	<i>TNFSF13B</i>	158	0.167	0.817	0.357	0.886
	<i>CSNK2A3</i>	12	0.168	0.817	0.033	0.748
	<i>RIPK1</i>	368	0.196	0.856	0.159	0.886
	<i>SYK</i>	662	0.197	0.856	0.277	0.886
	<i>RELA</i>	41	0.201	0.856	0.125	0.886
	<i>CSNK2A2</i>	166	0.202	0.856	0.997	1.000
	<i>IGH</i>	2142	0.209	0.856	0.744	0.961
	<i>TNFSF11</i>	216	0.217	0.857	0.009	0.748
	<i>CXCL1</i>	16	0.223	0.867	0.238	0.886
	<i>XIAP</i>	254	0.256	0.902	0.031	0.748
	<i>CD40LG</i>	34	0.276	0.903	0.395	0.886
	<i>EDARADD</i>	710	0.301	0.903	0.012	0.748
	<i>PLCG1</i>	87	0.321	0.903	0.613	0.951
	<i>CCL19</i>	7	0.334	0.903	0.457	0.901
	<i>TNFRSF11A</i>	355	0.339	0.903	0.071	0.748
	<i>PLAU</i>	22	0.350	0.903	0.981	1.000
	<i>BIRC3</i>	65	0.375	0.913	0.399	0.886
	<i>PARP1</i>	240	0.421	0.915	0.331	0.886
	<i>TRIM25</i>	80	0.426	0.915	0.116	0.886
	<i>CCL21</i>	5	0.430	0.915	0.729	0.961
	<i>NFKB2</i>	26	0.431	0.915	0.168	0.886
	<i>CARD10</i>	197	0.441	0.916	0.889	1.000
	<i>GADD45B</i>	9	0.451	0.916	0.159	0.886
	<i>ERC1</i>	3618	0.452	0.916	0.877	1.000

<i>CXCL3</i>	6	0.470	0.929	0.482	0.919
<i>GADD45A</i>	16	0.486	0.942	0.025	0.748
<i>NFKBIA</i>	18	0.526	0.948	0.417	0.901
<i>NFKB1</i>	441	0.548	0.950	0.131	0.886
<i>MALT1</i>	389	0.570	0.951	0.211	0.886
<i>LCK</i>	125	0.586	0.951	0.515	0.943
<i>BCL2A1</i>	48	0.594	0.951	0.535	0.945
<i>PIAS4</i>	214	0.606	0.951	0.460	0.901
<i>BCL2</i>	961	0.613	0.951	0.172	0.886
<i>ATM</i>	671	0.632	0.951	0.900	1.000
<i>CSNK2B</i>	16	0.637	0.951	0.905	1.000
<i>EDA</i>	1492	0.648	0.951	0.412	0.901
<i>ICAM1</i>	75	0.668	0.951	0.679	0.961
<i>BCL10</i>	59	0.681	0.951	0.445	0.901
<i>CSNK2A1</i>	249	0.681	0.951	0.124	0.886
<i>TNFSF14</i>	47	0.700	0.962	0.206	0.886
<i>CCL13</i>	7	0.702	0.962	0.465	0.903
<i>BLNK</i>	487	0.737	0.976	0.259	0.886
<i>LTA</i>	11	0.771	0.987	0.203	0.886
<i>CHUK</i>	192	0.790	0.990	0.082	0.814
<i>EDAR</i>	500	0.814	0.990	0.088	0.837
<i>BCL2L1</i>	155	0.815	0.990	0.772	0.970
<i>TAB3</i>	180	0.824	0.990	0.792	0.974
<i>BTK</i>	152	0.833	0.990	0.366	0.886
<i>LAT</i>	16	0.838	0.990	0.795	0.974
<i>CXCL2</i>	4	0.841	0.990	0.537	0.945
<i>BIRC2</i>	99	0.877	0.990	0.615	0.951
<i>IL1R1</i>	679	0.879	0.990	0.950	1.000
<i>PTGS2</i>	34	0.885	0.990	0.603	0.951
<i>TNFRSF13C</i>	9	0.902	0.990	0.318	0.886
<i>PRKCQ</i>	1222	0.906	0.990	0.730	0.961
<i>UBE2I</i>	198	0.914	0.990	0.934	1.000
<i>CYLD</i>	242	0.937	0.990	0.479	0.919
<i>EDA2R</i>	82	0.941	0.990	0.715	0.961
<i>LTBR</i>	87	0.962	0.997	0.230	0.886
TLR		0.118		0.481	
<i>PIK3CA</i>	326	0.007	0.351	0.586	0.951
<i>MAPK14</i>	400	0.012	0.351	0.946	1.000
<i>IRAK4</i>	144	0.012	0.351	0.171	0.886
<i>MAP2K2</i>	176	0.012	0.351	0.521	0.943
<i>MAP3K8</i>	144	0.017	0.375	0.004	0.748
<i>IRAK1</i>	25	0.029	0.474	0.675	0.961
<i>MAPK8</i>	598	0.033	0.474	0.548	0.950
<i>MAP3K7</i>	318	0.035	0.474	0.039	0.748

LY96	221	0.056	0.571	0.115	0.886
IFNA5	3	0.057	0.571	0.097	0.855
MAPK11	28	0.058	0.571	0.674	0.961
IRF5	62	0.067	0.571	0.739	0.961
MAPK12	58	0.072	0.571	0.164	0.886
IKBKE	163	0.081	0.594	0.581	0.951
CCL5	23	0.083	0.594	0.210	0.886
TLR9	6	0.083	0.594	0.216	0.886
CTSK	22	0.124	0.729	0.959	1.000
IFNA6	3	0.132	0.753	0.722	0.961
TAB1	122	0.156	0.794	0.740	0.961
CFLAR	228	0.171	0.817	0.219	0.886
MAPK9	313	0.189	0.856	0.240	0.886
CD14	6	0.208	0.856	0.894	1.000
CCL3L3	1	0.214	0.857	0.425	0.901
IFNAR1	193	0.257	0.902	0.457	0.901
MYD88	6	0.260	0.902	0.319	0.886
IFNA16	12	0.273	0.903	0.791	0.974
IFNA8	4	0.282	0.903	0.927	1.000
IL1B	30	0.287	0.903	0.455	0.901
TICAM1	109	0.290	0.903	0.282	0.886
IFNA21	6	0.300	0.903	0.291	0.886
MAP2K4	382	0.309	0.903	0.757	0.961
IFNA2	7	0.318	0.903	0.365	0.886
FADD	13	0.319	0.903	0.203	0.886
IFNA13	1	0.329	0.903	0.954	1.000
TIRAP	61	0.331	0.903	0.661	0.961
PIK3R3	454	0.337	0.903	0.531	0.945
IFNA7	2	0.351	0.903	0.922	1.000
CXCL10	15	0.369	0.913	0.370	0.886
IRF7	25	0.371	0.913	0.971	1.000
TLR2	122	0.400	0.915	0.183	0.886
MAPK10	2512	0.403	0.915	0.061	0.748
CCL4L1	2	0.410	0.915	0.286	0.886
PIK3R2	73	0.414	0.915	0.759	0.961
IL12A	36	0.418	0.915	0.043	0.748
MAP2K6	609	0.423	0.915	0.046	0.748
MAP2K7	61	0.426	0.915	0.392	0.886
PIK3R1	380	0.431	0.915	0.563	0.950
CD86	226	0.432	0.915	0.270	0.886
TICAM2	194	0.466	0.928	0.025	0.748
TAB2	548	0.478	0.936	0.058	0.748
TLR4	60	0.493	0.942	0.973	1.000
IKBKB	243	0.497	0.942	0.859	1.000

<i>TLR7</i>	103	0.502	0.942	0.895	1.000
<i>STAT1</i>	195	0.506	0.942	0.737	0.961
<i>CXCL11</i>	24	0.513	0.948	0.291	0.886
<i>CXCL8</i>	9	0.525	0.948	0.070	0.748
<i>IFNA1</i>	8	0.539	0.950	0.217	0.886
<i>CCL4</i>	23	0.551	0.950	0.582	0.951
<i>AKT2</i>	154	0.552	0.950	0.787	0.974
<i>TLR3</i>	98	0.570	0.951	0.357	0.886
<i>IFNA4</i>	6	0.585	0.951	0.632	0.961
<i>PIK3CD</i>	323	0.587	0.951	0.512	0.943
<i>MAPK13</i>	46	0.597	0.951	0.970	1.000
<i>IFNAR2</i>	178	0.626	0.951	0.635	0.961
<i>IFNA10</i>	14	0.652	0.951	0.912	1.000
<i>MAP2K1</i>	542	0.652	0.951	0.910	1.000
<i>AKT3</i>	1176	0.657	0.951	0.703	0.961
<i>TLR1</i>	69	0.661	0.951	0.695	0.961
<i>PIK3CB</i>	702	0.671	0.951	0.523	0.943
<i>IFNB1</i>	5	0.676	0.951	0.562	0.950
<i>IL12B</i>	72	0.681	0.951	0.899	1.000
<i>IL6</i>	29	0.701	0.962	0.398	0.886
<i>CXCL9</i>	18	0.709	0.963	0.263	0.886
<i>CCL3</i>	16	0.717	0.963	0.743	0.961
<i>AKT1</i>	167	0.719	0.963	0.678	0.961
<i>MAP2K3</i>	185	0.728	0.969	0.048	0.748
<i>TLR5</i>	175	0.752	0.985	0.336	0.886
<i>JUN</i>	15	0.754	0.985	0.599	0.951
<i>MAPK1</i>	513	0.757	0.985	0.385	0.886
<i>IFNA17</i>	10	0.770	0.987	0.735	0.961
<i>MAPK3</i>	24	0.828	0.990	0.206	0.886
<i>TLR6</i>	346	0.850	0.990	0.775	0.970
<i>LBP</i>	265	0.884	0.990	0.700	0.961
<i>IRF3</i>	23	0.886	0.990	0.251	0.886
<i>SPP1</i>	42	0.888	0.990	0.120	0.886
<i>TOLLIP</i>	158	0.908	0.990	0.039	0.748
<i>TBK1</i>	177	0.909	0.990	0.701	0.961
<i>CD40</i>	48	0.924	0.990	0.700	0.961
<i>CD80</i>	217	0.926	0.990	0.522	0.943
<i>IKBKG</i>	25	0.928	0.990	0.803	0.978
<i>CASP8</i>	240	0.938	0.990	0.199	0.886
<i>FOS</i>	11	0.943	0.990	0.245	0.886
<i>RAC1</i>	241	0.958	0.997	0.851	1.000
<i>TLR8</i>	83	0.971	1.000	0.066	0.748
<i>IFNA14</i>					
<i>CCL3L1</i>					

CCL4L2					
TNF		0.762		0.882	
CREB3L4	11	0.015	0.375	0.398	0.886
CXCL5	5	0.023	0.446	0.391	0.886
TRAF2	253	0.034	0.474	0.818	0.991
MAP3K5	1047	0.035	0.474	0.170	0.886
CREB5	3041	0.045	0.556	0.898	1.000
SELE	81	0.055	0.571	0.436	0.901
TNFAIP3	48	0.069	0.571	0.457	0.901
DAB2IP	1151	0.091	0.614	0.097	0.855
CASP7	276	0.110	0.697	0.759	0.961
BAG4	115	0.116	0.702	0.647	0.961
BCL3	72	0.147	0.785	0.246	0.886
DNM1L	494	0.190	0.856	0.583	0.951
JAG1	173	0.233	0.889	0.013	0.748
VEGFC	572	0.240	0.902	0.564	0.950
JUNB	3	0.244	0.902	0.072	0.748
CREB3L1	191	0.257	0.902	0.180	0.886
MMP3	46	0.270	0.903	0.068	0.748
EDN1	30	0.275	0.903	0.961	1.000
PGAM5	108	0.308	0.903	0.555	0.950
TNF	10	0.342	0.903	0.856	1.000
SOCS3	8	0.349	0.903	0.391	0.886
IRF1	60	0.362	0.913	0.487	0.922
CREB3L3	105	0.374	0.913	0.978	1.000
CX3CL1	76	0.420	0.915	0.993	1.000
CASP3	117	0.439	0.916	0.391	0.886
CREB3	14	0.448	0.916	0.607	0.951
CREB1	227	0.465	0.928	0.564	0.950
TNFRSF1B	211	0.498	0.942	0.871	1.000
CCL2	7	0.520	0.948	0.360	0.886
CCL20	20	0.546	0.950	0.324	0.886
LIF	29	0.549	0.950	0.437	0.901
MLKL	147	0.560	0.951	0.393	0.886
ATF2	435	0.573	0.951	0.354	0.886
CSF2	12	0.622	0.951	0.459	0.901
CASP10	190	0.639	0.951	0.240	0.886
TNFRSF1A	42	0.646	0.951	0.945	1.000
NOD2	165	0.656	0.951	0.193	0.886
ATF6B	34	0.664	0.951	0.917	1.000
CSF1	74	0.678	0.951	0.737	0.961
RPS6KA5	968	0.719	0.963	0.333	0.886
CXCL6	7	0.766	0.987	0.362	0.886
ATF4	19	0.778	0.990	0.725	0.961

<i>ITCH</i>	458	0.791	0.990	0.370	0.886
<i>CEBPB</i>	2	0.834	0.990	0.941	1.000
<i>RIPK3</i>	19	0.836	0.990	0.682	0.961
<i>MMP9</i>	41	0.838	0.990	0.673	0.961
<i>IL18R1</i>	202	0.842	0.990	0.447	0.901
<i>RPS6KA4</i>	65	0.857	0.990	0.585	0.951
<i>CREB3L2</i>	728	0.860	0.990	0.755	0.961
<i>TRAF3</i>	541	0.903	0.990	0.717	0.961
<i>IL15</i>	372	0.907	0.990	0.601	0.951
<i>TRAF5</i>	162	0.911	0.990	0.300	0.886
<i>TRAF1</i>	145	0.937	0.990	0.608	0.951
<i>FAS</i>	154	0.952	0.995	0.284	0.886
<i>MMP14</i>	73	0.974	1.000	0.234	0.886

Abbreviations: TLR = toll-like receptor; NFkB = nuclear factor kappa B; TNF = tumor necrosis factor; EOC = epithelial ovarian cancer; HGSOC = high grade serous ovarian cancer; AACES = African American Cancer Epidemiology Study; OCAC = Ovarian Cancer Association Consortium;

^aAggregate P-value of MAGMA model results. Each model controls for age, and two ancestry principal components.

^bCorrected for multiple testing by the number of genes tested using the Benjamini-Hochberg false discovery rate (FDR).

Supplementary Table ST4.2. Gene associations/BMI interactions within TLR, NFkB, and TNF pathways with invasive HGSOc risk among Black women.

Pathway	Gene	# SNPs	P^a	P_{FDR}^b	P_{BMI}^a	$P_{BMI,FDR}^b$
NFkB						
	<i>RELB</i>	193	0.006	0.559	0.110	0.888
	<i>PRKCB</i>	2384	0.007	0.559	0.133	0.888
	<i>ZAP70</i>	120	0.055	0.803	0.838	0.996
	<i>CXCL12</i>	104	0.060	0.803	0.552	0.966
	<i>TRAF6</i>	108	0.070	0.803	0.643	0.988
	<i>CSNK2A3</i>	12	0.107	0.859	0.167	0.919
	<i>PLCG2</i>	1937	0.108	0.859	0.482	0.964
	<i>GADD45G</i>	7	0.116	0.859	0.276	0.963
	<i>CARD14</i>	271	0.160	0.981	0.135	0.888
	<i>TNFSF13B</i>	158	0.166	0.981	0.269	0.963
	<i>LTB</i>	4	0.178	0.981	0.873	0.996
	<i>RELA</i>	41	0.232	1.000	0.129	0.888
	<i>CSNK2A2</i>	166	0.243	1.000	0.677	0.988
	<i>CD40LG</i>	34	0.255	1.000	0.574	0.974
	<i>GADD45B</i>	9	0.276	1.000	0.035	0.888
	<i>CCL19</i>	7	0.288	1.000	0.459	0.964
	<i>CARD11</i>	1090	0.307	1.000	0.141	0.888
	<i>EDAR</i>	500	0.312	1.000	0.164	0.919
	<i>MAP3K14</i>	208	0.313	1.000	0.133	0.888
	<i>TRADD</i>	14	0.320	1.000	0.936	1.000
	<i>PIDD1</i>	82	0.322	1.000	0.245	0.963
	<i>LCK</i>	125	0.330	1.000	0.397	0.964
	<i>ATM</i>	671	0.333	1.000	0.758	0.988
	<i>TNFSF11</i>	216	0.377	1.000	0.036	0.888
	<i>VCAM1</i>	80	0.379	1.000	0.233	0.963
	<i>IGH</i>	2142	0.389	1.000	0.758	0.988
	<i>EDARADD</i>	710	0.425	1.000	0.051	0.888
	<i>TRIM25</i>	80	0.426	1.000	0.259	0.963
	<i>CCL13</i>	7	0.428	1.000	0.348	0.963
	<i>SYK</i>	662	0.448	1.000	0.108	0.888
	<i>CCL21</i>	5	0.458	1.000	0.506	0.964
	<i>IL1R1</i>	679	0.487	1.000	0.807	0.996
	<i>ICAM1</i>	75	0.494	1.000	0.828	0.996
	<i>TNFRSF11A</i>	355	0.495	1.000	0.039	0.888
	<i>CXCL3</i>	6	0.548	1.000	0.867	0.996
	<i>BTK</i>	152	0.571	1.000	0.426	0.964
	<i>XIAP</i>	254	0.574	1.000	0.021	0.888
	<i>PLCG1</i>	87	0.586	1.000	0.654	0.988

<i>GADD45A</i>	16	0.613	1.000	0.006	0.648
<i>EDA</i>	1492	0.622	1.000	0.142	0.888
<i>BCL2L1</i>	155	0.623	1.000	0.476	0.964
<i>TNFSF14</i>	47	0.652	1.000	0.401	0.964
<i>CYLD</i>	242	0.679	1.000	0.509	0.964
<i>BIRC3</i>	65	0.693	1.000	0.580	0.976
<i>BCL2A1</i>	48	0.698	1.000	0.487	0.964
<i>CXCL1</i>	16	0.708	1.000	0.680	0.988
<i>CARD10</i>	197	0.716	1.000	0.891	0.998
<i>PTGS2</i>	34	0.727	1.000	0.783	0.988
<i>BCL10</i>	59	0.727	1.000	0.094	0.888
<i>BLNK</i>	487	0.743	1.000	0.345	0.963
<i>ERC1</i>	3618	0.746	1.000	0.693	0.988
<i>EDA2R</i>	82	0.748	1.000	0.520	0.964
<i>CHUK</i>	192	0.749	1.000	0.093	0.888
<i>NFKB1</i>	441	0.760	1.000	0.204	0.963
<i>PIAS4</i>	214	0.805	1.000	0.773	0.988
<i>PLAU</i>	22	0.815	1.000	0.989	1.000
<i>MALT1</i>	389	0.852	1.000	0.117	0.888
<i>PARP1</i>	240	0.862	1.000	0.878	0.996
<i>RIPK1</i>	368	0.873	1.000	0.346	0.963
<i>LYN</i>	857	0.877	1.000	0.465	0.964
<i>NFKBIA</i>	18	0.880	1.000	0.349	0.963
<i>CXCL2</i>	4	0.881	1.000	0.400	0.964
<i>CSNK2B</i>	16	0.883	1.000	0.935	1.000
<i>LTA</i>	11	0.891	1.000	0.172	0.919
<i>PRKCQ</i>	1222	0.895	1.000	0.411	0.964
<i>BCL2</i>	961	0.896	1.000	0.134	0.888
<i>LAT</i>	16	0.916	1.000	0.977	1.000
<i>TNFRSF13C</i>	9	0.936	1.000	0.238	0.963
<i>TAB3</i>	180	0.940	1.000	0.823	0.996
<i>CSNK2A1</i>	249	0.940	1.000	0.266	0.963
<i>NFKB2</i>	26	0.958	1.000	0.241	0.963
<i>BIRC2</i>	99	0.966	1.000	0.543	0.964
<i>UBE2I</i>	198	0.994	1.000	0.454	0.964
<i>LTBR</i>	87	0.997	1.000	0.234	0.963
TLR					
<i>IKBKE</i>	163	0.012	0.674	0.689	0.988
<i>LY96</i>	221	0.020	0.761	0.210	0.963
<i>PIK3CA</i>	326	0.023	0.761	0.324	0.963
<i>CTSK</i>	22	0.030	0.803	0.782	0.988
<i>MAPK14</i>	400	0.045	0.803	0.964	1.000
<i>MAPK8</i>	598	0.045	0.803	0.418	0.964
<i>IRAK4</i>	144	0.045	0.803	0.369	0.964

MAP2K2	176	0.051	0.803	0.045	0.888
IRF5	62	0.053	0.803	0.745	0.988
MAP3K8	144	0.064	0.803	0.060	0.888
MAPK12	58	0.068	0.803	0.128	0.888
TIRAP	61	0.093	0.859	0.714	0.988
IL1B	30	0.095	0.859	0.805	0.996
IFNA5	3	0.102	0.859	0.318	0.963
FADD	13	0.119	0.859	0.235	0.963
IFNA21	6	0.120	0.859	0.503	0.964
TAB1	122	0.144	0.981	0.785	0.988
IFNA16	12	0.165	0.981	0.311	0.963
TAB2	548	0.167	0.981	0.078	0.888
MAP2K6	609	0.175	0.981	0.282	0.963
MAP3K7	318	0.178	0.981	0.383	0.964
PIK3CB	702	0.180	0.981	0.680	0.988
IFNA6	3	0.201	1.000	0.622	0.988
CCL5	23	0.223	1.000	0.152	0.909
MAP2K4	382	0.238	1.000	0.338	0.963
IFNA4	6	0.238	1.000	0.438	0.964
MAPK11	28	0.266	1.000	0.541	0.964
PIK3R1	380	0.289	1.000	0.551	0.966
IRAK1	25	0.291	1.000	0.271	0.963
IFNA8	4	0.301	1.000	0.644	0.988
IFNA1	8	0.314	1.000	0.405	0.964
IL12A	36	0.322	1.000	0.005	0.648
MAPK9	313	0.328	1.000	0.218	0.963
CD14	6	0.339	1.000	0.725	0.988
TLR9	6	0.374	1.000	0.355	0.964
MYD88	6	0.389	1.000	0.155	0.909
CCL4	23	0.402	1.000	0.783	0.988
TLR3	98	0.406	1.000	0.046	0.888
TICAM2	194	0.423	1.000	0.037	0.888
AKT3	1176	0.439	1.000	0.629	0.988
IRF7	25	0.441	1.000	0.947	1.000
IFNA7	2	0.441	1.000	0.999	1.000
IKBKG	25	0.447	1.000	0.874	0.996
CCL4L1	2	0.467	1.000	0.333	0.963
IFNAR1	193	0.477	1.000	0.526	0.964
CD86	226	0.483	1.000	0.099	0.888
IFNA13	1	0.501	1.000	0.930	1.000
IFNA2	7	0.512	1.000	0.358	0.964
PIK3R2	73	0.515	1.000	0.765	0.988
IFNA10	14	0.515	1.000	0.846	0.996
CFLAR	228	0.536	1.000	0.487	0.964

TICAM1	109	0.551	1.000	0.122	0.888
MAP2K1	542	0.558	1.000	0.865	0.996
CXCL8	9	0.583	1.000	0.225	0.963
PIK3R3	454	0.603	1.000	0.702	0.988
FOS	11	0.617	1.000	0.421	0.964
STAT1	195	0.621	1.000	0.573	0.974
TLR5	175	0.631	1.000	0.282	0.963
IL12B	72	0.642	1.000	0.900	0.998
PIK3CD	323	0.643	1.000	0.344	0.963
TOLLIP	158	0.647	1.000	0.043	0.888
MAPK10	2512	0.648	1.000	0.234	0.963
TLR1	69	0.654	1.000	0.427	0.964
MAP2K7	61	0.658	1.000	0.343	0.963
RAC1	241	0.673	1.000	0.515	0.964
IFNB1	5	0.674	1.000	0.705	0.988
IKBKB	243	0.680	1.000	0.849	0.996
IFNA17	10	0.714	1.000	0.840	0.996
CCL3L3	1	0.717	1.000	0.860	0.996
LBP	265	0.731	1.000	0.710	0.988
AKT1	167	0.737	1.000	0.598	0.988
MAP2K3	185	0.743	1.000	0.127	0.888
CCL3	16	0.752	1.000	0.923	1.000
MAPK1	513	0.777	1.000	0.310	0.963
SPP1	42	0.782	1.000	0.570	0.974
TLR7	103	0.807	1.000	0.656	0.988
TLR4	60	0.810	1.000	0.999	1.000
MAPK13	46	0.815	1.000	0.832	0.996
MAPK3	24	0.816	1.000	0.133	0.888
AKT2	154	0.836	1.000	0.783	0.988
IRF3	23	0.853	1.000	0.336	0.963
CASP8	240	0.885	1.000	0.789	0.988
TLR6	346	0.886	1.000	0.874	0.996
CD40	48	0.893	1.000	0.643	0.988
TLR2	122	0.904	1.000	0.209	0.963
CXCL9	18	0.920	1.000	0.641	0.988
IL6	29	0.924	1.000	0.216	0.963
TBK1	177	0.927	1.000	0.403	0.964
CXCL11	24	0.928	1.000	0.779	0.988
JUN	15	0.939	1.000	0.904	0.998
IFNAR2	178	0.965	1.000	0.617	0.988
TLR8	83	0.983	1.000	0.064	0.888
CD80	217	0.984	1.000	0.366	0.964
CXCL10	15	0.988	1.000	0.907	0.998
IFNA14					

CCL3L1					
CCL4L2					
TNF					
<i>CREB3L4</i>	11	0.007	0.559	0.292	0.963
<i>TNFAIP3</i>	48	0.023	0.761	0.395	0.964
<i>JUNB</i>	3	0.051	0.803	0.083	0.888
<i>MAP3K5</i>	1047	0.067	0.803	0.143	0.888
<i>CREB5</i>	3041	0.089	0.859	0.889	0.998
<i>MMP3</i>	46	0.092	0.859	0.076	0.888
<i>TRAF2</i>	253	0.102	0.859	0.682	0.988
<i>VEGFC</i>	572	0.114	0.859	0.761	0.988
<i>CXCL5</i>	5	0.146	0.981	0.172	0.919
<i>MMP9</i>	41	0.207	1.000	0.866	0.996
<i>BCL3</i>	72	0.208	1.000	0.433	0.964
<i>JAG1</i>	173	0.252	1.000	0.111	0.888
<i>CREB3L3</i>	105	0.265	1.000	0.696	0.988
<i>PGAM5</i>	108	0.295	1.000	0.700	0.988
<i>DNM1L</i>	494	0.300	1.000	0.538	0.964
<i>ATF2</i>	435	0.320	1.000	0.111	0.888
<i>EDN1</i>	30	0.342	1.000	0.950	1.000
<i>NOD2</i>	165	0.352	1.000	0.111	0.888
<i>CREB1</i>	227	0.359	1.000	0.906	0.998
<i>CEBPB</i>	2	0.365	1.000	0.665	0.988
<i>ATF4</i>	19	0.376	1.000	0.428	0.964
<i>CASP7</i>	276	0.438	1.000	0.473	0.964
<i>CREB3</i>	14	0.439	1.000	0.598	0.988
<i>SOCS3</i>	8	0.458	1.000	0.846	0.996
<i>IRF1</i>	60	0.469	1.000	0.373	0.964
<i>SELE</i>	81	0.480	1.000	0.609	0.988
<i>CX3CL1</i>	76	0.513	1.000	0.976	1.000
<i>TNFRSF1B</i>	211	0.514	1.000	0.857	0.996
<i>BAG4</i>	115	0.528	1.000	0.761	0.988
<i>IL15</i>	372	0.574	1.000	0.528	0.964
<i>MMP14</i>	73	0.604	1.000	0.223	0.963
<i>CCL20</i>	20	0.610	1.000	0.296	0.963
<i>CSF2</i>	12	0.623	1.000	0.477	0.964
<i>TNFRSF1A</i>	42	0.626	1.000	0.938	1.000
<i>TRAF5</i>	162	0.650	1.000	0.536	0.964
<i>CCL2</i>	7	0.718	1.000	0.666	0.988
<i>CREB3L1</i>	191	0.722	1.000	0.332	0.963
<i>DAB2IP</i>	1151	0.724	1.000	0.283	0.963
<i>TNF</i>	10	0.725	1.000	0.918	1.000
<i>CASP3</i>	117	0.734	1.000	0.245	0.963
<i>ITCH</i>	458	0.771	1.000	0.679	0.988

<i>RIPK3</i>	19	0.840	1.000	0.706	0.988
<i>CSF1</i>	74	0.841	1.000	0.946	1.000
<i>CASP10</i>	190	0.866	1.000	0.733	0.988
<i>RPS6KA5</i>	968	0.881	1.000	0.491	0.964
<i>CREB3L2</i>	728	0.882	1.000	0.511	0.964
<i>RPS6KA4</i>	65	0.896	1.000	0.275	0.963
<i>ATF6B</i>	34	0.903	1.000	0.780	0.988
<i>CXCL6</i>	7	0.907	1.000	0.568	0.974
<i>LIF</i>	29	0.913	1.000	0.784	0.988
<i>IL18R1</i>	202	0.935	1.000	0.649	0.988
<i>FAS</i>	154	0.939	1.000	0.533	0.964
<i>MLKL</i>	147	0.940	1.000	0.471	0.964
<i>TRAF3</i>	541	0.975	1.000	0.454	0.964
<i>TRAF1</i>	145	0.992	1.000	0.541	0.964

Abbreviations: TLR = toll-like receptor; NFkB = nuclear factor kappa B; TNF = tumor necrosis factor; EOC = epithelial ovarian cancer; HGSOC = high grade serous ovarian cancer; AACES = African American Cancer Epidemiology Study; OCAC = Ovarian Cancer Association Consortium;

^aAggregate P-value of MAGMA model results. Each model controls for age, and two ancestry principal components.

^bCorrected for multiple testing by the number of genes tested using the Benjamini-Hochberg false discovery rate (FDR).

Supplementary Table ST4.3. Gene associations/BMI interactions within TLR, NFkB, and TNF pathways with invasive EOC risk among White women.

Pathway	Gene	# SNPs	Test Set				Validation Set			
			P_{raw}	P_{BH}	$P_{BMI\ raw}$	$P_{BMI\ FDR}$	P_{raw}	P_{BH}	$P_{BMI\ raw}$	$P_{BMI\ FDR}$
NfkB			0.075		0.856		0.875		0.096	
	<i>CSNK2A1</i>	166	0.008	0.297	0.886	1.000	0.084	0.565	0.035	1.000
	<i>BLNK</i>	253	0.011	0.297	0.988	1.000	0.784	1.000	0.119	1.000
	<i>RIPK1</i>	119	0.012	0.297	0.244	0.871	0.318	0.825	0.886	1.000
	<i>EDA2R</i>	56	0.016	0.334	0.172	0.763	0.792	1.000	0.353	1.000
	<i>ERC1</i>	1966	0.016	0.334	0.795	1.000	0.927	1.000	0.724	1.000
	<i>TAB3</i>	67	0.033	0.477	0.861	1.000	0.402	0.868	0.355	1.000
	<i>CARD10</i>	155	0.042	0.522	0.854	1.000	0.386	0.868	0.826	1.000
	<i>NFKB2</i>	58	0.055	0.553	0.108	0.667	0.992	1.000	0.126	1.000
	<i>BTK</i>	126	0.056	0.553	0.867	1.000	0.231	0.825	0.284	1.000
	<i>CYLD</i>	140	0.070	0.569	0.853	1.000	0.107	0.597	0.767	1.000
	<i>IL1R1</i>	417	0.074	0.569	0.491	1.000	0.088	0.575	0.924	1.000
	<i>CARD11</i>	449	0.077	0.569	0.349	0.903	0.199	0.815	0.254	1.000
	<i>MAP3K14</i>	166	0.077	0.569	0.024	0.397	0.032	0.393	0.604	1.000
	<i>CCL13</i>	61	0.084	0.570	0.582	1.000	0.092	0.586	0.749	1.000
	<i>CXCL12</i>	158	0.096	0.608	0.098	0.667	0.817	1.000	0.442	1.000
	<i>LTBR</i>	38	0.119	0.640	0.384	0.967	0.571	0.952	0.198	1.000
	<i>GADD45B</i>	30	0.141	0.707	0.608	1.000	0.390	0.868	0.458	1.000
	<i>BCL2A1</i>	50	0.169	0.749	0.108	0.667	0.971	1.000	0.679	1.000
	<i>CXCL3</i>	10	0.170	0.749	0.829	1.000	0.884	1.000	0.457	1.000
	<i>BCL2L1</i>	123	0.170	0.749	0.038	0.517	0.878	1.000	0.636	1.000
	<i>EDARADD</i>	241	0.174	0.749	0.720	1.000	0.436	0.907	0.087	1.000
	<i>RELB</i>	73	0.177	0.749	0.633	1.000	0.016	0.335	0.434	1.000
	<i>PLCG2</i>	1060	0.191	0.749	0.973	1.000	0.516	0.952	0.015	1.000
	<i>CSNK2A2</i>	204	0.213	0.760	0.269	0.871	0.872	1.000	0.128	1.000
	<i>VCAM1</i>	28	0.239	0.786	0.750	1.000	0.289	0.825	0.601	1.000
	<i>PARP1</i>	217	0.251	0.786	0.855	1.000	0.002	0.159	0.795	1.000
	<i>BIRC3</i>	40	0.256	0.786	0.338	0.903	0.635	0.962	0.262	1.000

<i>CSNK2B</i>	77	0.265	0.786	0.514	1.000	0.660	0.974	0.575	1.000
<i>PTGS2</i>	116	0.267	0.786	0.587	1.000	0.901	1.000	0.797	1.000
<i>ICAM1</i>	43	0.270	0.786	0.019	0.392	0.806	1.000	0.744	1.000
<i>LAT</i>	33	0.293	0.819	0.635	1.000	0.553	0.952	0.567	1.000
<i>TRADD</i>	21	0.298	0.821	0.969	1.000	0.316	0.825	0.242	1.000
<i>PRKCQ</i>	588	0.301	0.821	0.608	1.000	0.468	0.922	0.695	1.000
<i>TNFRSF13C</i>	61	0.315	0.823	0.669	1.000	0.116	0.597	0.118	1.000
<i>EDA</i>	706	0.342	0.841	0.101	0.667	0.416	0.882	0.208	1.000
<i>CHUK</i>	158	0.342	0.841	0.155	0.754	0.369	0.862	0.992	1.000
<i>TNFSF14</i>	87	0.362	0.841	0.782	1.000	0.763	1.000	0.934	1.000
<i>GADD45G</i>	68	0.409	0.841	0.552	1.000	0.518	0.952	0.577	1.000
<i>CCL21</i>	56	0.413	0.841	0.756	1.000	0.019	0.335	0.043	1.000
<i>ATM</i>	286	0.418	0.841	0.079	0.667	0.632	0.962	0.489	1.000
<i>ZAP70</i>	90	0.426	0.841	0.190	0.770	0.440	0.907	0.252	1.000
<i>PLCG1</i>	85	0.430	0.841	0.336	0.903	0.841	1.000	0.135	1.000
<i>CCL19</i>	57	0.441	0.849	0.938	1.000	0.390	0.868	0.601	1.000
<i>LCK</i>	57	0.456	0.865	0.006	0.392	0.065	0.497	0.855	1.000
<i>PLAU</i>	55	0.462	0.865	0.821	1.000	0.644	0.969	0.794	1.000
<i>SYK</i>	511	0.464	0.865	0.889	1.000	0.130	0.645	0.584	1.000
<i>PRKCB</i>	1205	0.497	0.886	0.791	1.000	0.228	0.825	0.821	1.000
<i>XIAP</i>	113	0.499	0.886	0.770	1.000	0.648	0.969	0.352	1.000
<i>LTB</i>	85	0.512	0.894	0.312	0.903	0.975	1.000	0.827	1.000
<i>NFKB1</i>	301	0.520	0.894	0.143	0.729	0.941	1.000	0.325	1.000
<i>BCL10</i>	123	0.534	0.899	0.650	1.000	0.710	1.000	0.500	1.000
<i>MALT1</i>	292	0.545	0.905	0.563	1.000	0.994	1.000	0.429	1.000
<i>LTA</i>	154	0.563	0.910	0.725	1.000	0.932	1.000	0.945	1.000
<i>TRAF6</i>	95	0.579	0.910	0.904	1.000	0.799	1.000	0.809	1.000
<i>IGH</i>	395	0.582	0.910	0.738	1.000	0.565	0.952	0.335	1.000
<i>TNFSF13B</i>	68	0.591	0.910	0.047	0.561	0.166	0.745	0.651	1.000
<i>BCL2</i>	551	0.601	0.910	0.145	0.729	0.575	0.952	0.648	1.000
<i>TNFRSF11A</i>	338	0.619	0.915	0.444	1.000	0.937	1.000	0.517	1.000
<i>CXCL2</i>	31	0.622	0.915	0.428	1.000	0.794	1.000	0.744	1.000

<i>PIAS4</i>	86	0.688	0.954	0.179	0.763	0.897	1.000	0.957	1.000
<i>BIRC2</i>	90	0.692	0.955	0.518	1.000	0.853	1.000	0.663	1.000
<i>CSNK2A3</i>	22	0.709	0.969	0.313	0.903	0.927	1.000	0.179	1.000
<i>TRIM25</i>	20	0.767	0.985	0.086	0.667	0.268	0.825	0.237	1.000
<i>NFKBIA</i>	81	0.788	0.992	0.399	0.973	0.816	1.000	0.064	1.000
<i>GADD45A</i>	84	0.806	0.997	0.755	1.000	0.525	0.952	0.043	1.000
<i>CD40LG</i>	28	0.827	1.000	0.084	0.667	0.394	0.868	0.722	1.000
<i>CXCL1</i>	72	0.868	1.000	0.640	1.000	0.304	0.825	0.986	1.000
<i>TNFSF11</i>	215	0.900	1.000	0.977	1.000	0.344	0.825	0.386	1.000
<i>RELA</i>	54	0.904	1.000	0.038	0.517	0.354	0.837	0.588	1.000
<i>LYN</i>	508	0.926	1.000	0.318	0.903	0.115	0.597	0.601	1.000
<i>EDAR</i>	171	0.977	1.000	0.215	0.824	0.240	0.825	0.719	1.000
<i>UBE2I</i>	84	0.997	1.000	0.299	0.903	0.322	0.825	0.239	1.000
<i>PIDD1</i>	65	0.999	1.000	0.175	0.763	0.729	1.000	0.130	1.000
<i>CARD14</i>									
TLR		0.537		0.045		0.078		0.328	
<i>CFLAR</i>	200	0.0003	0.052	0.641	1.000	0.167	0.745	0.293	1.000
<i>CASP8</i>	221	0.0005	0.052	0.054	0.618	0.211	0.825	0.405	1.000
<i>IL12B</i>	73	0.005	0.267	0.902	1.000	0.706	1.000	0.048	1.000
<i>MAP3K8</i>	42	0.006	0.267	0.676	1.000	0.910	1.000	0.873	1.000
<i>CD86</i>	206	0.020	0.340	0.252	0.871	0.281	0.825	0.846	1.000
<i>TLR1</i>	161	0.020	0.340	0.448	1.000	0.727	1.000	0.029	1.000
<i>MYD88</i>	35	0.021	0.340	0.980	1.000	0.028	0.385	0.273	1.000
<i>IFNAR1</i>	157	0.039	0.522	0.776	1.000	0.668	0.976	0.477	1.000
<i>AKT3</i>	546	0.044	0.522	0.594	1.000	0.258	0.825	0.639	1.000
<i>TLR6</i>	163	0.052	0.553	0.445	1.000	0.982	1.000	0.575	1.000
<i>CCL5</i>	78	0.058	0.553	0.167	0.763	0.626	0.962	0.578	1.000
<i>TAB1</i>	92	0.068	0.569	0.216	0.824	0.867	1.000	0.800	1.000
<i>IFNAR2</i>	162	0.076	0.569	0.250	0.871	0.539	0.952	0.216	1.000
<i>CD14</i>	65	0.083	0.570	0.093	0.667	0.734	1.000	0.452	1.000
<i>TLR2</i>	105	0.095	0.608	0.351	0.903	0.261	0.825	0.996	1.000
<i>PIK3R3</i>	288	0.106	0.640	0.682	1.000	0.599	0.961	0.483	1.000

MAP2K3	39	0.115	0.640	0.848	1.000	0.448	0.908	0.784	1.000
IL12A	68	0.167	0.749	0.719	1.000	0.243	0.825	0.628	1.000
IFNB1	71	0.175	0.749	0.010	0.392	0.484	0.939	0.900	1.000
PIK3CA	334	0.184	0.749	0.459	1.000	0.992	1.000	0.286	1.000
MAPK3	25	0.190	0.749	0.473	1.000	0.924	1.000	0.149	1.000
AKT1	97	0.192	0.749	0.856	1.000	0.103	0.597	0.139	1.000
IKBKB	138	0.196	0.749	0.017	0.392	0.009	0.335	0.169	1.000
IRF5	113	0.200	0.750	0.751	1.000	0.051	0.449	0.040	1.000
CD80	245	0.216	0.760	0.795	1.000	0.893	1.000	0.446	1.000
MAP2K1	412	0.265	0.786	0.558	1.000	0.004	0.221	0.913	1.000
PIK3CD	217	0.271	0.786	0.393	0.973	0.414	0.882	0.556	1.000
IL1B	52	0.317	0.823	0.257	0.871	0.014	0.335	0.964	1.000
IFNA8	77	0.320	0.823	0.805	1.000	0.597	0.961	0.446	1.000
IRF7	93	0.329	0.836	0.653	1.000	0.840	1.000	0.418	1.000
TIRAP	102	0.345	0.841	0.062	0.645	0.553	0.952	0.445	1.000
MAPK1	335	0.351	0.841	0.010	0.392	0.327	0.825	0.273	1.000
IKBKG	9	0.367	0.841	0.952	1.000	0.022	0.340	0.777	1.000
TLR4	92	0.380	0.841	0.347	0.903	0.255	0.825	0.594	1.000
RAC1	234	0.384	0.841	0.081	0.667	0.578	0.952	0.965	1.000
MAP3K7	291	0.399	0.841	0.730	1.000	0.863	1.000	0.402	1.000
TICAM1	110	0.405	0.841	0.184	0.765	0.175	0.757	0.341	1.000
PIK3R2	98	0.409	0.841	0.942	1.000	0.035	0.393	0.291	1.000
TLR7	9	0.409	0.841	0.020	0.392	0.713	1.000	0.670	1.000
MAPK8	365	0.414	0.841	0.794	1.000	0.013	0.335	0.361	1.000
MAPK13	68	0.421	0.841	0.119	0.675	0.270	0.825	0.749	1.000
IFNA17	133	0.422	0.841	0.817	1.000	0.108	0.597	0.648	1.000
LBP	146	0.427	0.841	0.730	1.000	0.590	0.961	0.851	1.000
TICAM2	90	0.441	0.849	0.124	0.676	0.105	0.597	0.714	1.000
IRF3	32	0.459	0.865	0.415	1.000	0.039	0.393	0.457	1.000
MAP2K7	56	0.490	0.883	0.351	0.903	0.241	0.825	0.134	1.000
IL6	93	0.505	0.890	0.108	0.667	0.672	0.976	0.541	1.000
MAPK9	291	0.523	0.894	0.747	1.000	0.169	0.745	0.671	1.000

LY96	172	0.529	0.897	0.115	0.675	0.280	0.825	0.774	1.000
IFNA21	79	0.546	0.905	0.795	1.000	0.557	0.952	0.438	1.000
TLR8	33	0.549	0.905	0.077	0.667	0.012	0.335	0.513	1.000
TBK1	138	0.570	0.910	0.941	1.000	0.331	0.825	0.568	1.000
IRAK4	123	0.582	0.910	0.951	1.000	0.078	0.542	0.648	1.000
AKT2	164	0.582	0.910	0.803	1.000	0.656	0.974	0.972	1.000
CXCL9	58	0.593	0.910	0.453	1.000	0.679	0.978	0.100	1.000
MAPK14	280	0.599	0.910	0.070	0.667	0.543	0.952	0.616	1.000
CXCL8	44	0.600	0.910	0.059	0.640	0.862	1.000	0.510	1.000
TLR5	117	0.608	0.910	0.655	1.000	0.460	0.915	0.278	1.000
IFNA16	166	0.623	0.915	0.599	1.000	0.064	0.497	0.397	1.000
CD40	102	0.630	0.919	0.903	1.000	0.311	0.825	0.751	1.000
FADD	44	0.654	0.948	0.886	1.000	0.334	0.825	0.861	1.000
IFNA6	62	0.662	0.948	0.130	0.690	0.217	0.825	0.988	1.000
CCL4	9	0.684	0.954	0.606	1.000	0.148	0.705	0.322	1.000
MAP2K6	185	0.711	0.969	0.111	0.667	0.344	0.825	0.734	1.000
CXCL11	175	0.733	0.980	0.785	1.000	0.715	1.000	0.326	1.000
PIK3CB	292	0.737	0.980	0.939	1.000	0.882	1.000	0.355	1.000
CTSK	52	0.737	0.980	0.011	0.392	0.999	1.000	0.165	1.000
TLR3	129	0.738	0.980	0.840	1.000	0.045	0.432	0.939	1.000
MAPK10	1848	0.745	0.981	0.493	1.000	0.792	1.000	0.786	1.000
PIK3R1	301	0.756	0.981	0.329	0.903	0.143	0.697	0.065	1.000
IFNA13	86	0.770	0.985	0.513	1.000	0.246	0.825	0.835	1.000
TLR9	37	0.788	0.992	0.375	0.954	0.931	1.000	0.220	1.000
FOS	44	0.789	0.992	0.699	1.000	0.060	0.496	0.703	1.000
IFNA2	31	0.800	0.995	0.568	1.000	0.448	0.908	0.687	1.000
MAP2K4	216	0.811	0.999	0.774	1.000	0.002	0.159	0.089	1.000
IFNA1	75	0.826	1.000	0.192	0.770	0.530	0.952	0.073	1.000
IFNA10	154	0.835	1.000	0.837	1.000	0.112	0.597	0.326	1.000
CXCL10	101	0.849	1.000	0.828	1.000	0.854	1.000	0.283	1.000
STAT1	170	0.856	1.000	0.022	0.392	0.180	0.765	0.206	1.000
CCL3	6	0.859	1.000	0.160	0.762	0.577	0.952	0.859	1.000

<i>JUN</i>	34	0.867	1.000	0.498	1.000	0.310	0.825	0.643	1.000
<i>IFNA4</i>	126	0.890	1.000	0.571	1.000	0.219	0.825	0.877	1.000
<i>TOLLIP</i>	184	0.897	1.000	0.622	1.000	0.614	0.962	0.141	1.000
<i>IRAK1</i>	15	0.907	1.000	0.087	0.667	0.071	0.506	0.086	1.000
<i>MAP2K2</i>	91	0.914	1.000	0.311	0.903	0.856	1.000	0.835	1.000
<i>SPP1</i>	95	0.938	1.000	0.020	0.392	0.391	0.868	0.854	1.000
<i>IFNA7</i>	149	0.950	1.000	0.839	1.000	0.117	0.597	0.250	1.000
<i>IFNA14</i>	88	0.957	1.000	0.956	1.000	0.456	0.915	0.762	1.000
<i>IFNA5</i>	60	0.960	1.000	0.274	0.871	0.265	0.825	0.872	1.000
<i>IKBKE</i>	111	0.980	1.000	0.741	1.000	0.805	1.000	0.879	1.000
<i>TAB2</i>	0 ^c								
<i>CCL3L1</i>	0 ^c								
<i>CCL3L3</i>	0 ^c								
<i>CCL4L1</i>	0 ^c								
<i>CCL4L2</i>	0 ^c								
<i>MAPK11</i>	0 ^d								
<i>MAPK12</i>	0 ^d								
TNF		0.932		0.225		0.329		0.314	
<i>CASP10</i>	131	0.002	0.141	0.290	0.903	0.280	0.825	0.067	1.000
<i>EDN1</i>	118	0.010	0.297	0.016	0.392	0.069	0.506	0.868	1.000
<i>CCL2</i>	59	0.023	0.345	0.658	1.000	0.039	0.393	0.350	1.000
<i>PGAM5</i>	117	0.046	0.522	0.234	0.865	0.848	1.000	0.636	1.000
<i>CCL20</i>	10	0.063	0.569	0.935	1.000	0.029	0.385	0.752	1.000
<i>BCL3</i>	92	0.085	0.570	0.031	0.473	0.329	0.825	0.445	1.000
<i>ATF4</i>	29	0.099	0.611	0.877	1.000	0.554	0.952	0.582	1.000
<i>JUNB</i>	43	0.113	0.640	0.220	0.828	0.346	0.825	0.481	1.000
<i>TRAF5</i>	184	0.115	0.640	0.536	1.000	0.429	0.901	0.399	1.000
<i>CX3CL1</i>	104	0.120	0.640	0.208	0.823	0.015	0.335	0.519	1.000
<i>MAP3K5</i>	430	0.129	0.669	0.556	1.000	0.498	0.950	0.787	1.000
<i>IRF1</i>	109	0.142	0.707	0.179	0.763	0.471	0.922	0.056	1.000
<i>CSF2</i>	48	0.191	0.749	0.589	1.000	0.038	0.393	0.953	1.000
<i>RIPK3</i>	104	0.195	0.749	0.397	0.973	0.608	0.961	0.608	1.000

<i>CREB3L1</i>	101	0.208	0.760	0.272	0.871	0.550	0.952	0.579	1.000
<i>VEGFC</i>	354	0.211	0.760	0.439	1.000	0.496	0.950	0.818	1.000
<i>RPS6KA4</i>	84	0.225	0.779	0.266	0.871	0.401	0.868	0.192	1.000
<i>CASP3</i>	113	0.231	0.786	0.736	1.000	0.674	0.976	0.539	1.000
<i>CREB3L2</i>	236	0.237	0.786	0.102	0.667	0.048	0.444	0.175	1.000
<i>IL18R1</i>	270	0.241	0.786	0.595	1.000	0.964	1.000	0.865	1.000
<i>CASP7</i>	232	0.258	0.786	0.121	0.675	0.515	0.952	0.834	1.000
<i>TNFRSF1A</i>	40	0.269	0.786	0.246	0.871	0.038	0.393	0.996	1.000
<i>CREB3L4</i>	36	0.284	0.814	0.000	0.071	0.163	0.745	0.385	1.000
<i>ITCH</i>	255	0.288	0.814	0.313	0.903	0.061	0.496	0.378	1.000
<i>MMP9</i>	98	0.315	0.823	0.717	1.000	0.758	1.000	0.857	1.000
<i>CSF1</i>	92	0.316	0.823	0.816	1.000	0.021	0.337	0.237	1.000
<i>ATF6B</i>	76	0.381	0.841	0.867	1.000	0.920	1.000	0.982	1.000
<i>RPS6KA5</i>	521	0.387	0.841	0.102	0.667	0.275	0.825	0.587	1.000
<i>TRAF1</i>	162	0.401	0.841	0.635	1.000	0.997	1.000	0.532	1.000
<i>CREB3</i>	33	0.404	0.841	0.021	0.392	0.627	0.962	0.900	1.000
<i>CXCL5</i>	12	0.406	0.841	0.044	0.558	0.018	0.335	0.340	1.000
<i>DNM1L</i>	361	0.429	0.841	0.896	1.000	0.609	0.961	0.033	1.000
<i>CREB1</i>	169	0.477	0.874	0.542	1.000	0.262	0.825	0.500	1.000
<i>BAG4</i>	83	0.477	0.874	0.438	1.000	0.788	1.000	0.334	1.000
<i>IL15</i>	251	0.484	0.880	0.593	1.000	0.802	1.000	0.041	1.000
<i>MMP3</i>	88	0.516	0.894	0.265	0.871	0.964	1.000	0.865	1.000
<i>TNF</i>	81	0.559	0.910	0.472	1.000	0.977	1.000	0.877	1.000
<i>ATF2</i>	281	0.606	0.910	0.777	1.000	0.630	0.962	0.200	1.000
<i>MLKL</i>	174	0.658	0.948	0.967	1.000	0.567	0.952	0.540	1.000
<i>SOCS3</i>	30	0.675	0.954	0.892	1.000	0.001	0.159	0.133	1.000
<i>CREB5</i>	1704	0.681	0.954	0.465	1.000	0.323	0.825	0.481	1.000
<i>TRAF2</i>	62	0.685	0.954	0.648	1.000	0.226	0.825	0.695	1.000
<i>TNFAIP3</i>	77	0.740	0.980	0.554	1.000	0.192	0.799	0.211	1.000
<i>JAG1</i>	150	0.754	0.981	0.863	1.000	0.346	0.825	0.512	1.000
<i>NOD2</i>	104	0.758	0.981	0.850	1.000	0.316	0.825	0.736	1.000
<i>DAB2IP</i>	563	0.794	0.993	0.180	0.763	0.725	1.000	0.142	1.000

<i>MMP14</i>	72	0.848	1.000	0.329	0.903	0.320	0.825	0.691	1.000
<i>TNFRSF1B</i>	103	0.874	1.000	0.612	1.000	0.389	0.868	0.043	1.000
<i>TRAF3</i>	336	0.894	1.000	0.345	0.903	0.601	0.961	0.220	1.000
<i>CXCL6</i>	56	0.897	1.000	0.003	0.331	0.292	0.825	0.987	1.000
LIF	65	0.903	1.000	0.503	1.000	0.510	0.952	0.550	1.000
<i>CEBPB</i>	41	0.927	1.000	0.147	0.729	0.963	1.000	0.407	1.000
<i>SELE</i>	203	0.951	1.000	0.508	1.000	0.724	1.000	0.304	1.000
<i>FAS</i>	224	0.957	1.000	0.308	0.903	0.103	0.597	0.447	1.000
<i>CREB3L3</i>	27	0.970	1.000	0.618	1.000	0.009	0.335	0.586	1.000

Abbreviations: TLR = toll-like receptor; NFkB = nuclear factor kappa B; TNF = tumor necrosis factor; EOC = epithelial ovarian cancer; HGSOC = high grade serous ovarian cancer; AACES = African American Cancer Epidemiology Study; OCAC = Ovarian Cancer Association Consortium;

^aAggregate P-value of MAGMA model results. Each model controls for age, and two ancestry principal components.

^bCorrected for multiple testing by the number of genes tested using the Benjamini-Hochberg false discovery rate (FDR).

Supplementary Table ST4.4. Gene associations/BMI interactions within TLR, NFkB, and TNF pathways with invasive HGSOC risk among White women.

Pathway	Gene	# SNPs	Test Set				Validation Set			
			P_{raw}	P_{BH}	$P_{BMI\ raw}$	$P_{BMI\ FDR}$	P_{raw}	P_{BH}	$P_{BMI\ raw}$	$P_{BMI\ FDR}$
NfκB			0.345		0.728		0.433		0.942	
	<i>GADD45B</i>	31	0.000	0.069	0.849	1.000	0.693	1.000	0.313	1.000
	<i>MAP3K14</i>	166	0.005	0.223	0.691	1.000	0.276	0.937	0.739	1.000
	<i>IL1R1</i>	417	0.006	0.229	0.113	0.920	0.272	0.937	0.413	1.000
	<i>CARD11</i>	447	0.011	0.349	0.027	0.517	0.955	1.000	0.123	1.000
	<i>TRAF6</i>	95	0.019	0.404	0.793	1.000	0.617	1.000	0.684	1.000
	<i>CSNK2A1</i>	159	0.019	0.404	0.730	1.000	0.193	0.935	0.129	1.000
	<i>TNFSF11</i>	215	0.024	0.413	0.664	1.000	0.605	1.000	0.354	1.000
	<i>CXCL2</i>	31	0.025	0.413	0.293	0.920	0.055	0.745	0.061	1.000
	<i>BCL2L1</i>	123	0.031	0.421	0.397	0.964	0.161	0.900	0.911	1.000
	<i>PARP1</i>	217	0.035	0.421	0.457	0.977	0.016	0.448	0.961	1.000
	<i>CXCL3</i>	10	0.053	0.476	0.417	0.964	0.370	0.937	0.126	1.000
	<i>BIRC3</i>	41	0.057	0.476	0.304	0.920	0.969	1.000	0.695	1.000
	<i>LTBR</i>	38	0.060	0.476	0.817	1.000	0.480	0.959	0.939	1.000
	<i>CXCL12</i>	159	0.077	0.536	0.141	0.920	0.306	0.937	0.361	1.000
	<i>CCL21</i>	56	0.136	0.668	0.571	1.000	0.216	0.937	0.417	1.000
	<i>EDARADD</i>	240	0.151	0.668	0.212	0.920	0.907	1.000	0.107	1.000
	<i>PTGS2</i>	116	0.155	0.668	0.613	1.000	0.904	1.000	0.765	1.000
	<i>TRIM25</i>	21	0.162	0.668	0.642	1.000	0.462	0.957	0.204	1.000
	<i>BIRC2</i>	96	0.162	0.668	0.239	0.920	0.989	1.000	0.324	1.000
	<i>CYLD</i>	140	0.170	0.668	0.705	1.000	0.118	0.900	0.655	1.000
	<i>GADD45G</i>	72	0.171	0.668	0.743	1.000	0.987	1.000	0.561	1.000
	<i>PLCG1</i>	85	0.171	0.668	0.838	1.000	0.126	0.900	0.485	1.000
	<i>BCL2</i>	551	0.178	0.679	0.541	1.000	0.250	0.937	0.850	1.000
	<i>NFKB1</i>	298	0.184	0.689	0.320	0.920	0.463	0.957	0.535	1.000
	<i>CSNK2B</i>	77	0.196	0.711	0.722	1.000	0.360	0.937	0.254	1.000
	<i>LAT</i>	33	0.217	0.713	0.411	0.964	0.952	1.000	0.939	1.000
	<i>CCL13</i>	61	0.220	0.713	0.932	1.000	0.140	0.900	0.921	1.000

<i>TNFRSF13C</i>	61	0.234	0.728	0.854	1.000	0.474	0.959	0.117	1.000
<i>ERC1</i>	1966	0.258	0.728	0.210	0.920	0.157	0.900	0.382	1.000
<i>RIPK1</i>	116	0.273	0.728	0.961	1.000	0.023	0.582	0.659	1.000
<i>EDA2R</i>	55	0.283	0.728	0.312	0.920	0.557	0.983	0.825	1.000
<i>CCL19</i>	57	0.303	0.728	0.493	0.977	0.595	1.000	0.812	1.000
<i>PRKCQ</i>	592	0.315	0.730	0.217	0.920	0.799	1.000	0.614	1.000
<i>TAB3</i>	68	0.329	0.746	0.139	0.920	0.605	1.000	0.752	1.000
<i>BTK</i>	125	0.334	0.749	0.407	0.964	0.136	0.900	0.696	1.000
<i>ATM</i>	286	0.356	0.770	0.293	0.920	0.795	1.000	0.662	1.000
<i>SYK</i>	512	0.365	0.771	0.900	1.000	0.925	1.000	0.291	1.000
<i>NFKB2</i>	58	0.374	0.771	0.777	1.000	0.071	0.745	0.391	1.000
<i>CSNK2A3</i>	22	0.385	0.780	0.287	0.920	0.840	1.000	0.527	1.000
<i>XIAP</i>	118	0.402	0.787	0.573	1.000	0.358	0.937	0.772	1.000
<i>TRADD</i>	21	0.416	0.787	0.325	0.920	0.368	0.937	0.447	1.000
<i>LTA</i>	154	0.422	0.787	0.994	1.000	0.254	0.937	0.605	1.000
<i>EDA</i>	704	0.422	0.787	0.244	0.920	0.786	1.000	0.961	1.000
<i>VCAM1</i>	28	0.424	0.787	0.461	0.977	0.571	0.983	0.863	1.000
<i>BCL2A1</i>	50	0.428	0.787	0.317	0.920	0.292	0.937	0.651	1.000
<i>PLAU</i>	55	0.437	0.787	0.856	1.000	0.316	0.937	0.272	1.000
<i>IGH</i>	392	0.449	0.787	0.240	0.920	0.290	0.937	0.739	1.000
<i>TNFSF13B</i>	68	0.474	0.787	0.128	0.920	0.333	0.937	0.773	1.000
<i>PIDD1</i>	65	0.474	0.787	0.169	0.920	0.216	0.937	0.554	1.000
<i>RELA</i>	54	0.487	0.792	0.395	0.964	0.163	0.900	0.916	1.000
<i>ZAP70</i>	89	0.491	0.792	0.470	0.977	0.061	0.745	0.579	1.000
<i>EDAR</i>	172	0.614	0.919	0.871	1.000	0.917	1.000	0.303	1.000
<i>CARD10</i>	155	0.633	0.934	0.992	1.000	0.390	0.951	0.415	1.000
<i>CHUK</i>	158	0.648	0.934	0.898	1.000	0.464	0.957	0.031	1.000
<i>LTB</i>	85	0.659	0.934	0.993	1.000	0.270	0.937	0.478	1.000
<i>LCK</i>	57	0.671	0.934	0.162	0.920	0.673	1.000	0.909	1.000
<i>ICAM1</i>	41	0.673	0.934	0.023	0.517	0.530	0.970	0.898	1.000
<i>CSNK2A2</i>	205	0.698	0.934	0.940	1.000	0.282	0.937	0.060	1.000
<i>LYN</i>	508	0.708	0.937	0.610	1.000	0.565	0.983	0.745	1.000

<i>PRKCB</i>	1212	0.736	0.958	0.749	1.000	0.820	1.000	0.453	1.000
<i>TNFSF14</i>	87	0.746	0.958	0.932	1.000	0.011	0.448	0.624	1.000
<i>BLNK</i>	254	0.824	0.994	0.339	0.920	0.594	1.000	0.764	1.000
<i>BCL10</i>	123	0.831	0.994	0.437	0.977	0.963	1.000	0.757	1.000
<i>RELB</i>	73	0.856	0.994	0.680	1.000	0.339	0.937	0.520	1.000
<i>UBE2I</i>	84	0.867	0.994	0.206	0.920	0.808	1.000	0.081	1.000
<i>NFKBIA</i>	81	0.912	1.000	0.289	0.920	0.246	0.937	0.170	1.000
<i>PLCG2</i>	1055	0.922	1.000	0.291	0.920	0.666	1.000	0.737	1.000
<i>PIAS4</i>	85	0.933	1.000	0.654	1.000	0.437	0.957	0.710	1.000
<i>CXCL1</i>	71	0.962	1.000	0.639	1.000	0.095	0.900	0.467	1.000
<i>TNFRSF11A</i>	335	0.962	1.000	0.829	1.000	0.685	1.000	0.862	1.000
<i>MALT1</i>	292	0.965	1.000	0.239	0.920	0.811	1.000	0.360	1.000
<i>GADD45A</i>	84	0.988	1.000	0.455	0.977	0.994	1.000	0.081	1.000
<i>CD40LG</i>	28	0.997	1.000	0.298	0.920	0.642	1.000	0.237	1.000
<i>CARD14</i>									
TLR		0.560		0.530		0.822		0.387	
<i>LY96</i>	172	0.001	0.077	0.288	0.920	0.541	0.970	0.070	1.000
<i>TLR1</i>	161	0.012	0.349	0.736	1.000	0.149	0.900	0.004	0.511
<i>TLR6</i>	163	0.019	0.404	0.633	1.000	0.480	0.959	0.026	1.000
<i>PIK3CB</i>	292	0.030	0.421	0.666	1.000	0.570	0.983	0.617	1.000
<i>IL12B</i>	73	0.033	0.421	0.458	0.977	0.228	0.937	0.620	1.000
<i>MYD88</i>	35	0.035	0.421	0.261	0.920	0.715	1.000	0.024	1.000
<i>TICAM2</i>	90	0.043	0.445	0.111	0.920	0.046	0.745	0.292	1.000
<i>PIK3R1</i>	301	0.045	0.445	0.948	1.000	0.456	0.957	0.215	1.000
<i>IRAK4</i>	123	0.074	0.527	0.663	1.000	0.983	1.000	0.854	1.000
<i>CFLAR</i>	200	0.081	0.545	0.322	0.920	0.007	0.448	0.377	1.000
<i>IFNA4</i>	126	0.093	0.611	0.968	1.000	0.583	0.996	0.524	1.000
<i>RAC1</i>	234	0.107	0.668	0.718	1.000	0.444	0.957	0.442	1.000
<i>IFNA13</i>	86	0.111	0.668	0.205	0.920	0.614	1.000	0.576	1.000
<i>IRF3</i>	32	0.121	0.668	0.029	0.517	0.896	1.000	0.714	1.000
<i>IFNA7</i>	149	0.122	0.668	0.365	0.929	0.372	0.937	0.843	1.000
<i>CD14</i>	65	0.128	0.668	0.239	0.920	0.395	0.953	0.664	1.000

<i>IFNAR2</i>	161	0.141	0.668	0.177	0.920	0.132	0.900	0.755	1.000
<i>IFNA6</i>	62	0.149	0.668	0.354	0.928	0.617	1.000	0.303	1.000
<i>IRF5</i>	113	0.152	0.668	0.740	1.000	0.405	0.957	0.869	1.000
<i>IFNA10</i>	154	0.161	0.668	0.293	0.920	0.425	0.957	0.844	1.000
<i>MAP3K8</i>	42	0.164	0.668	0.643	1.000	0.143	0.900	0.004	0.511
<i>TICAM1</i>	110	0.164	0.668	0.024	0.517	0.865	1.000	0.657	1.000
<i>AKT3</i>	546	0.199	0.711	0.361	0.929	0.488	0.959	0.314	1.000
<i>JUN</i>	34	0.212	0.713	0.341	0.920	0.492	0.959	0.837	1.000
<i>IFNA17</i>	133	0.214	0.713	0.259	0.920	0.317	0.937	0.469	1.000
<i>IL1B</i>	54	0.219	0.713	0.538	1.000	0.371	0.937	0.105	1.000
<i>CXCL9</i>	58	0.224	0.713	0.751	1.000	0.770	1.000	0.780	1.000
<i>IRF7</i>	93	0.246	0.728	0.465	0.977	0.064	0.745	0.177	1.000
<i>MAP2K3</i>	39	0.254	0.728	0.892	1.000	0.776	1.000	0.459	1.000
<i>IFNA8</i>	77	0.256	0.728	0.852	1.000	0.999	1.000	0.411	1.000
<i>IFNA21</i>	79	0.267	0.728	0.654	1.000	0.791	1.000	0.699	1.000
<i>IFNA1</i>	75	0.270	0.728	0.978	1.000	0.992	1.000	0.105	1.000
<i>CCL5</i>	78	0.270	0.728	0.492	0.977	0.503	0.960	0.698	1.000
<i>FADD</i>	44	0.288	0.728	0.922	1.000	0.067	0.745	0.900	1.000
<i>IFNA5</i>	60	0.295	0.728	0.598	1.000	0.372	0.937	0.503	1.000
<i>IFNA14</i>	89	0.297	0.728	0.282	0.920	0.406	0.957	0.496	1.000
<i>TAB1</i>	94	0.298	0.728	0.418	0.964	0.383	0.947	0.453	1.000
<i>IFNA16</i>	166	0.303	0.728	0.162	0.920	0.236	0.937	0.671	1.000
<i>AKT1</i>	97	0.305	0.728	0.623	1.000	0.716	1.000	0.938	1.000
<i>TLR4</i>	92	0.313	0.730	0.469	0.977	0.434	0.957	0.437	1.000
<i>TLR2</i>	105	0.319	0.731	0.037	0.558	0.756	1.000	0.140	1.000
<i>IKBKB</i>	138	0.344	0.761	0.788	1.000	0.385	0.947	0.269	1.000
<i>MAP2K7</i>	56	0.348	0.761	0.647	1.000	0.241	0.937	0.665	1.000
<i>MAPK8</i>	366	0.374	0.771	0.206	0.920	0.561	0.983	0.226	1.000
<i>PIK3CA</i>	334	0.375	0.771	0.782	1.000	0.182	0.935	0.894	1.000
<i>TLR8</i>	33	0.377	0.771	0.132	0.920	0.328	0.937	0.785	1.000
<i>IKBKG</i>	9	0.396	0.787	0.835	1.000	0.069	0.745	0.714	1.000
<i>PIK3R2</i>	98	0.445	0.787	0.997	1.000	0.142	0.900	0.839	1.000

<i>IFNB1</i>	71	0.447	0.787	0.493	0.977	0.912	1.000	0.824	1.000
<i>TOLLIP</i>	184	0.447	0.787	0.830	1.000	0.066	0.745	0.607	1.000
<i>TLR5</i>	135	0.448	0.787	0.929	1.000	0.413	0.957	0.774	1.000
<i>PIK3R3</i>	288	0.455	0.787	0.850	1.000	0.732	1.000	0.691	1.000
<i>CASP8</i>	221	0.470	0.787	0.127	0.920	0.016	0.448	0.175	1.000
<i>IFNA2</i>	31	0.488	0.792	0.745	1.000	0.756	1.000	0.431	1.000
<i>TLR3</i>	128	0.498	0.792	0.941	1.000	0.542	0.970	0.171	1.000
<i>MAPK13</i>	68	0.516	0.815	0.495	0.977	0.673	1.000	0.790	1.000
<i>CXCL10</i>	101	0.537	0.837	0.515	1.000	0.689	1.000	0.944	1.000
<i>MAP2K1</i>	412	0.580	0.886	0.149	0.920	0.630	1.000	0.495	1.000
<i>AKT2</i>	164	0.631	0.934	0.649	1.000	0.853	1.000	0.977	1.000
<i>CD80</i>	245	0.637	0.934	0.804	1.000	0.334	0.937	0.341	1.000
<i>CXCL11</i>	175	0.677	0.934	0.421	0.964	0.542	0.970	0.685	1.000
<i>TBK1</i>	137	0.680	0.934	0.982	1.000	0.998	1.000	0.910	1.000
<i>IL12A</i>	68	0.685	0.934	0.935	1.000	0.799	1.000	0.557	1.000
<i>CD40</i>	102	0.689	0.934	0.477	0.977	0.072	0.745	0.488	1.000
<i>CCL3</i>	6	0.690	0.934	0.284	0.920	0.748	1.000	0.114	1.000
<i>IRAK1</i>	14	0.699	0.934	0.027	0.517	0.495	0.959	0.144	1.000
<i>MAPK1</i>	335	0.701	0.934	0.002	0.202	0.511	0.967	0.594	1.000
<i>PIK3CD</i>	218	0.714	0.940	0.543	1.000	0.360	0.937	0.246	1.000
<i>SPP1</i>	95	0.736	0.958	0.480	0.977	0.994	1.000	0.149	1.000
<i>MAPK3</i>	25	0.740	0.958	0.027	0.517	0.812	1.000	0.799	1.000
<i>CD86</i>	205	0.749	0.958	0.149	0.920	0.217	0.937	0.609	1.000
<i>IFNAR1</i>	157	0.791	0.994	0.728	1.000	0.915	1.000	0.887	1.000
<i>TIRAP</i>	102	0.801	0.994	0.316	0.920	0.334	0.937	0.574	1.000
<i>IL6</i>	93	0.809	0.994	0.611	1.000	0.639	1.000	0.057	1.000
<i>LBP</i>	146	0.820	0.994	0.699	1.000	0.791	1.000	0.807	1.000
<i>STAT1</i>	172	0.841	0.994	0.160	0.920	0.712	1.000	0.460	1.000
<i>TLR9</i>	36	0.842	0.994	0.889	1.000	0.809	1.000	0.385	1.000
<i>CXCL8</i>	44	0.845	0.994	0.018	0.517	0.444	0.957	0.863	1.000
<i>MAP2K6</i>	195	0.851	0.994	0.785	1.000	0.345	0.937	0.542	1.000
<i>CCL4</i>	9	0.860	0.994	0.280	0.920	0.788	1.000	0.134	1.000

<i>CTSK</i>	52	0.860	0.994	0.002	0.202	0.717	1.000	0.447	1.000
<i>MAP2K4</i>	215	0.869	0.994	0.882	1.000	0.304	0.937	0.216	1.000
<i>MAPK14</i>	280	0.891	1.000	0.332	0.920	0.863	1.000	0.634	1.000
<i>FOS</i>	44	0.894	1.000	0.896	1.000	0.801	1.000	0.936	1.000
<i>MAPK9</i>	295	0.911	1.000	0.387	0.964	0.835	1.000	0.790	1.000
<i>MAP3K7</i>	292	0.921	1.000	0.751	1.000	0.935	1.000	0.823	1.000
<i>TLR7</i>	9	0.953	1.000	0.267	0.920	0.150	0.900	0.046	1.000
<i>MAP2K2</i>	91	0.957	1.000	0.659	1.000	0.966	1.000	0.872	1.000
<i>IKBKE</i>	109	0.973	1.000	0.602	1.000	0.354	0.937	0.393	1.000
<i>MAPK10</i>	1849	0.977	1.000	0.435	0.977	0.057	0.745	0.066	1.000
<i>TAB2</i>	0 ^c								
<i>CCL3L1</i>	0 ^c								
<i>CCL3L3</i>	0 ^c								
<i>CCL4L1</i>	0 ^c								
<i>CCL4L2</i>	0 ^c								
<i>MAPK11</i>	0 ^d								
<i>MAPK12</i>	0 ^d								
TNF		0.076		0.323		0.876		0.651	
<i>CREB5</i>	1712	0.003	0.196	0.738	1.000	0.098	0.900	0.674	1.000
<i>CREB3</i>	33	0.003	0.196	0.088	0.920	0.203	0.937	0.887	1.000
<i>TNFRSF1A</i>	39	0.022	0.413	0.409	0.964	0.787	1.000	0.693	1.000
<i>TNFRSF1B</i>	103	0.043	0.445	0.762	1.000	0.529	0.970	0.176	1.000
<i>TNFAIP3</i>	77	0.045	0.445	0.155	0.920	0.748	1.000	0.261	1.000
<i>RPS6KA4</i>	85	0.047	0.445	0.070	0.897	0.840	1.000	0.705	1.000
<i>CREB3L1</i>	101	0.058	0.476	0.225	0.920	0.464	0.957	0.959	1.000
<i>CREB1</i>	169	0.059	0.476	0.245	0.920	0.792	1.000	0.495	1.000
<i>CCL2</i>	59	0.063	0.483	0.891	1.000	0.0001	0.016	0.866	1.000
<i>CREB3L2</i>	238	0.070	0.515	0.759	1.000	0.189	0.935	0.245	1.000
<i>BCL3</i>	94	0.120	0.668	0.066	0.897	0.027	0.625	0.524	1.000
<i>EDN1</i>	118	0.125	0.668	0.667	1.000	0.218	0.937	0.146	1.000
<i>MAP3K5</i>	433	0.131	0.668	0.223	0.920	0.427	0.957	0.870	1.000
<i>IL15</i>	251	0.134	0.668	0.445	0.977	0.339	0.937	0.299	1.000

ATF4	29	0.172	0.668	0.400	0.964	0.110	0.900	0.959	1.000
CASP3	116	0.190	0.702	0.280	0.920	0.302	0.937	0.667	1.000
DNM1L	361	0.222	0.713	0.107	0.920	0.773	1.000	0.439	1.000
CASP10	131	0.224	0.713	0.330	0.920	0.430	0.957	0.151	1.000
JUNB	43	0.249	0.728	0.210	0.920	0.342	0.937	0.360	1.000
CREB3L4	36	0.258	0.728	0.185	0.920	0.918	1.000	0.961	1.000
CASP7	232	0.261	0.728	0.357	0.928	0.710	1.000	0.626	1.000
SOCS3	30	0.263	0.728	0.962	1.000	0.315	0.937	0.420	1.000
TRAF2	62	0.300	0.728	0.936	1.000	0.857	1.000	0.401	1.000
IL18R1	270	0.300	0.728	0.809	1.000	0.363	0.937	0.391	1.000
DAB2IP	567	0.303	0.728	0.032	0.524	0.650	1.000	0.440	1.000
ATF6B	76	0.311	0.730	0.870	1.000	0.011	0.448	0.496	1.000
CSF1	89	0.349	0.761	0.334	0.920	0.542	0.970	0.992	1.000
LIF	65	0.368	0.771	0.977	1.000	0.903	1.000	0.340	1.000
CXCL6	56	0.395	0.787	0.003	0.202	0.498	0.959	0.133	1.000
CX3CL1	104	0.404	0.787	0.226	0.920	0.849	1.000	0.643	1.000
MLKL	173	0.409	0.787	0.906	1.000	0.164	0.900	0.388	1.000
ITCH	255	0.430	0.787	0.104	0.920	0.174	0.927	0.540	1.000
TRAF5	184	0.456	0.787	0.699	1.000	0.013	0.448	0.931	1.000
RIPK3	104	0.462	0.787	0.991	1.000	0.075	0.745	0.499	1.000
TRAF1	162	0.466	0.787	0.070	0.897	0.488	0.959	0.697	1.000
SELE	202	0.471	0.787	0.794	1.000	0.523	0.970	0.872	1.000
BAG4	83	0.494	0.792	0.290	0.920	0.007	0.448	0.215	1.000
MMP9	98	0.495	0.792	0.989	1.000	0.074	0.745	0.748	1.000
PGAM5	117	0.525	0.823	0.814	1.000	0.366	0.937	0.404	1.000
ATF2	281	0.546	0.841	0.094	0.920	0.047	0.745	0.470	1.000
TNF	81	0.547	0.841	0.993	1.000	0.165	0.900	0.638	1.000
CXCL5	12	0.588	0.892	0.075	0.905	0.112	0.900	0.778	1.000
JAG1	147	0.607	0.914	0.796	1.000	0.196	0.935	0.650	1.000
IRF1	109	0.658	0.934	0.124	0.920	0.186	0.935	0.316	1.000
CSF2	48	0.670	0.934	0.263	0.920	0.784	1.000	0.239	1.000
FAS	224	0.676	0.934	0.015	0.517	0.321	0.937	0.782	1.000

<i>MMP14</i>	70	0.691	0.934	0.567	1.000	0.798	1.000	0.994	1.000
<i>NOD2</i>	105	0.800	0.994	0.526	1.000	0.809	1.000	0.417	1.000
<i>CCL20</i>	10	0.828	0.994	0.351	0.928	0.770	1.000	0.429	1.000
<i>MMP3</i>	88	0.837	0.994	0.842	1.000	0.420	0.957	0.836	1.000
<i>CEBPB</i>	40	0.849	0.994	0.022	0.517	0.737	1.000	0.701	1.000
<i>VEGFC</i>	354	0.852	0.994	0.881	1.000	0.830	1.000	0.631	1.000
<i>TRAF3</i>	336	0.852	0.994	0.796	1.000	0.966	1.000	0.740	1.000
<i>RPS6KA5</i>	521	0.872	0.994	0.016	0.517	0.809	1.000	0.194	1.000
<i>CREB3L3</i>	27	0.997	1.000	0.680	1.000	0.116	0.900	0.364	1.000

Abbreviations: TLR = toll-like receptor; NFkB = nuclear factor kappa B; TNF = tumor necrosis factor; EOC = epithelial ovarian cancer; HGSOC = high grade serous ovarian cancer; AACES = African American Cancer Epidemiology Study; OCAC = Ovarian Cancer Association Consortium;

^aAggregate P-value of MAGMA model results. Each model controls for age, and two ancestry principal components.

^bCorrected for multiple testing by the number of genes tested using the Benjamini-Hochberg false discovery rate (FDR).

^cNo SNPs mapped to gene after QC filtering.

^dGene chromosomal locations not on raw data file.

Supplementary Table ST5.1. Gene associations/BMI interactions within TLR, NFkB, and TNF pathways with 5-year overall survival among Black women with EOC.

Pathway	Gene	# SNPs	P_{raw}	P_{BH}	$P_{BMI\ raw}$	$P_{BMI\ FDR}$
Nfkb						
	<i>LTA</i>	11	0.026	0.916	0.025	0.604
	<i>BCL2L1</i>	155	0.030	0.916	0.933	0.980
	<i>TNFRSF11A</i>	355	0.032	0.916	0.253	0.918
	<i>LCK</i>	125	0.044	0.916	0.680	0.968
	<i>ZAP70</i>	120	0.046	0.916	0.514	0.933
	<i>PIAS4</i>	214	0.053	0.916	0.583	0.947
	<i>PLAU</i>	22	0.061	0.916	0.284	0.928
	<i>GADD45G</i>	7	0.065	0.916	0.524	0.933
	<i>EDA2R</i>	82	0.073	0.916	0.836	0.973
	<i>EDA</i>	1492	0.087	0.916	0.849	0.973
	<i>CSNK2B</i>	16	0.122	0.916	0.134	0.853
	<i>RELA</i>	41	0.126	0.916	0.001	0.070
	<i>IGH</i>	2142	0.126	0.916	0.548	0.937
	<i>PARP1</i>	240	0.128	0.916	0.767	0.973
	<i>VCAM1</i>	80	0.138	0.916	0.711	0.968
	<i>MAP3K14</i>	208	0.214	1.000	0.604	0.959
	<i>LTBR</i>	87	0.214	1.000	0.590	0.951
	<i>BIRC2</i>	99	0.246	1.000	0.672	0.968
	<i>UBE2I</i>	198	0.257	1.000	0.386	0.928
	<i>TNFSF11</i>	216	0.295	1.000	0.533	0.933
	<i>RELB</i>	193	0.300	1.000	0.193	0.887
	<i>CSNK2A3</i>	12	0.302	1.000	0.527	0.933
	<i>BLNK</i>	487	0.315	1.000	0.642	0.968
	<i>CARD10</i>	197	0.342	1.000	0.826	0.973
	<i>ATM</i>	671	0.344	1.000	0.034	0.604
	<i>BCL2</i>	961	0.347	1.000	0.237	0.891
	<i>PTGS2</i>	34	0.351	1.000	0.747	0.973
	<i>CXCL1</i>	16	0.363	1.000	0.376	0.928
	<i>SYK</i>	662	0.369	1.000	0.949	0.988
	<i>TRAF6</i>	108	0.377	1.000	0.411	0.928
	<i>CXCL12</i>	104	0.413	1.000	0.786	0.973
	<i>CHUK</i>	192	0.423	1.000	0.101	0.794
	<i>PRKCQ</i>	1222	0.427	1.000	0.542	0.933
	<i>CXCL2</i>	4	0.428	1.000	0.489	0.933
	<i>XIAP</i>	254	0.431	1.000	0.829	0.973
	<i>CXCL3</i>	6	0.458	1.000	0.405	0.928
	<i>PRKCB</i>	2384	0.488	1.000	0.050	0.604
	<i>CCL13</i>	7	0.557	1.000	0.213	0.887

<i>NFKB2</i>	26	0.565	1.000	0.421	0.928
<i>CYLD</i>	242	0.571	1.000	0.851	0.973
<i>PLCG2</i>	1937	0.575	1.000	0.770	0.973
<i>TRADD</i>	14	0.579	1.000	0.810	0.973
<i>IL1R1</i>	679	0.595	1.000	0.733	0.971
<i>GADD45B</i>	9	0.596	1.000	0.026	0.604
<i>BCL10</i>	59	0.626	1.000	0.493	0.933
<i>BIRC3</i>	65	0.641	1.000	0.205	0.887
<i>TNFSF14</i>	47	0.654	1.000	0.006	0.343
<i>ICAM1</i>	75	0.681	1.000	0.388	0.928
<i>LAT</i>	16	0.688	1.000	0.360	0.928
<i>TAB3</i>	180	0.705	1.000	0.412	0.928
<i>LYN</i>	857	0.734	1.000	0.094	0.794
<i>EDARADD</i>	710	0.740	1.000	0.360	0.928
<i>LTB</i>	4	0.789	1.000	0.000	0.070
<i>TNFRSF13C</i>	9	0.795	1.000	0.428	0.928
<i>GADD45A</i>	16	0.799	1.000	0.039	0.604
<i>CARD11</i>	1090	0.800	1.000	0.669	0.968
<i>CSNK2A2</i>	166	0.838	1.000	0.686	0.968
<i>CSNK2A1</i>	249	0.851	1.000	0.845	0.973
<i>EDAR</i>	500	0.852	1.000	0.377	0.928
<i>NFKB1</i>	441	0.857	1.000	0.727	0.971
<i>BCL2A1</i>	48	0.866	1.000	0.922	0.980
<i>BTK</i>	152	0.869	1.000	0.580	0.947
<i>ERC1</i>	3618	0.888	1.000	0.466	0.933
<i>TRIM25</i>	80	0.888	1.000	0.086	0.788
<i>PIDD1</i>	82	0.896	1.000	0.902	0.980
<i>CCL19</i>	7	0.910	1.000	0.297	0.928
<i>CCL21</i>	5	0.913	1.000	0.077	0.756
<i>CARD14</i>	271	0.927	1.000	0.056	0.640
<i>MALT1</i>	389	0.948	1.000	0.671	0.968
<i>NFKBIA</i>	18	0.951	1.000	0.560	0.947
<i>CD40LG</i>	34	0.974	1.000	0.210	0.887
<i>PLCG1</i>	87	0.980	1.000	0.329	0.928
<i>RIPK1</i>	368	0.989	1.000	0.125	0.826
<i>TNFSF13B</i>	158	0.994	1.000	0.185	0.882
TLR					
<i>FOS</i>	11	0.009	0.916	0.918	0.980
<i>STAT1</i>	195	0.020	0.916	0.715	0.968
<i>MAP2K4</i>	382	0.032	0.916	0.530	0.933
<i>TAB2</i>	548	0.035	0.916	0.336	0.928
<i>CTSK</i>	22	0.035	0.916	0.928	0.980
<i>IKBKE</i>	163	0.037	0.916	0.893	0.980
<i>TOLLIP</i>	158	0.068	0.916	0.126	0.826

AKT3	1176	0.082	0.916	0.955	0.990
PIK3R2	73	0.082	0.916	0.391	0.928
CXCL11	24	0.089	0.916	0.995	1.000
TICAM1	109	0.099	0.916	0.797	0.973
MAPK9	313	0.121	0.916	0.782	0.973
IRAK4	144	0.124	0.916	0.397	0.928
PIK3CA	326	0.128	0.916	0.787	0.973
IRAK1	25	0.129	0.916	0.337	0.928
CD40	48	0.135	0.916	0.457	0.933
IFNA8	4	0.140	0.916	0.419	0.928
CCL4L1	2	0.146	0.929	0.330	0.928
MAP2K6	609	0.172	0.974	0.874	0.980
CCL4	23	0.173	0.974	0.518	0.933
IKBKB	243	0.174	0.974	0.634	0.968
MAP2K1	542	0.196	1.000	0.032	0.604
MAPK8	598	0.208	1.000	0.851	0.973
MAP3K7	318	0.215	1.000	0.231	0.891
TICAM2	194	0.232	1.000	0.520	0.933
PIK3R3	454	0.269	1.000	0.339	0.928
MYD88	6	0.276	1.000	0.713	0.968
CD86	226	0.279	1.000	0.104	0.794
IRF7	25	0.296	1.000	0.700	0.968
MAPK14	400	0.329	1.000	0.215	0.887
PIK3R1	380	0.346	1.000	0.237	0.891
IL6	29	0.356	1.000	0.243	0.896
TLR9	6	0.374	1.000	0.043	0.604
TBK1	177	0.389	1.000	0.382	0.928
CD14	6	0.390	1.000	0.922	0.980
IL12A	36	0.397	1.000	0.949	0.988
CCL3	16	0.415	1.000	0.217	0.887
LY96	221	0.415	1.000	0.854	0.973
IKBKG	25	0.416	1.000	0.365	0.928
MAPK10	2512	0.469	1.000	0.298	0.928
TLR6	346	0.501	1.000	0.874	0.980
JUN	15	0.524	1.000	0.059	0.640
IFNA13	1	0.528	1.000	0.913	0.980
IFNA4	6	0.541	1.000	0.932	0.980
PIK3CD	323	0.542	1.000	0.143	0.853
IFNAR1	193	0.551	1.000	0.572	0.947
PIK3CB	702	0.566	1.000	0.680	0.968
IFNA5	3	0.567	1.000	0.018	0.604
CASP8	240	0.598	1.000	0.099	0.794
IFNB1	5	0.644	1.000	0.748	0.973
CCL5	23	0.679	1.000	0.402	0.928

<i>TIRAP</i>	61	0.683	1.000	0.595	0.954
<i>IFNA21</i>	6	0.685	1.000	0.209	0.887
<i>IFNA1</i>	8	0.690	1.000	0.160	0.853
<i>MAPK13</i>	46	0.704	1.000	0.367	0.928
<i>IRF3</i>	23	0.709	1.000	0.430	0.928
<i>IL12B</i>	72	0.713	1.000	0.043	0.604
<i>AKT1</i>	167	0.713	1.000	0.858	0.973
<i>TLR8</i>	83	0.730	1.000	0.696	0.968
<i>MAP2K7</i>	61	0.731	1.000	0.916	0.980
<i>MAPK1</i>	513	0.758	1.000	0.533	0.933
<i>LBP</i>	265	0.767	1.000	0.845	0.973
<i>AKT2</i>	154	0.768	1.000	0.764	0.973
<i>MAP2K2</i>	176	0.775	1.000	0.288	0.928
<i>IFNAR2</i>	178	0.781	1.000	0.151	0.853
<i>TLR4</i>	60	0.799	1.000	0.827	0.973
<i>IFNA17</i>	10	0.801	1.000	0.111	0.817
<i>FADD</i>	13	0.806	1.000	0.754	0.973
<i>CD80</i>	217	0.808	1.000	0.162	0.853
<i>MAPK12</i>	58	0.817	1.000	0.032	0.604
<i>IFNA7</i>	2	0.819	1.000	0.267	0.928
<i>IFNA16</i>	12	0.819	1.000	0.714	0.968
<i>CFLAR</i>	228	0.822	1.000	0.825	0.973
<i>TAB1</i>	122	0.853	1.000	0.416	0.928
<i>TLR5</i>	175	0.861	1.000	0.180	0.877
<i>MAP3K8</i>	144	0.863	1.000	0.234	0.891
<i>IFNA6</i>	3	0.863	1.000	0.164	0.853
<i>CXCL8</i>	9	0.864	1.000	0.079	0.756
<i>SPP1</i>	42	0.871	1.000	0.172	0.858
<i>TLR3</i>	98	0.873	1.000	0.893	0.980
<i>RAC1</i>	241	0.881	1.000	0.340	0.928
<i>CCL3L3</i>	1	0.881	1.000	0.154	0.853
<i>TLR1</i>	69	0.885	1.000	0.754	0.973
<i>MAPK3</i>	24	0.886	1.000	0.039	0.604
<i>CXCL10</i>	15	0.919	1.000	0.351	0.928
<i>MAP2K3</i>	185	0.934	1.000	0.456	0.933
<i>MAPK11</i>	28	0.934	1.000	0.274	0.928
<i>IL1B</i>	30	0.945	1.000	0.411	0.928
<i>IFNA2</i>	7	0.946	1.000	0.482	0.933
<i>CXCL9</i>	18	0.951	1.000	0.460	0.933
<i>TLR7</i>	103	0.967	1.000	0.731	0.971
<i>IFNA10</i>	14	0.977	1.000	0.228	0.891
<i>IRF5</i>	62	0.982	1.000	0.802	0.973
<i>TLR2</i>	122	0.998	1.000	0.914	0.980
<i>IFNA14</i>	0°				

	CCL3L1	0°				
	CCL4L2	0°				
TNF						
	LIF	29	0.064	0.916	0.722	0.971
	EDN1	30	0.085	0.916	0.674	0.968
	TRAF3	541	0.132	0.916	0.685	0.968
	MMP9	41	0.175	0.974	0.691	0.968
	CREB3	14	0.176	0.974	0.696	0.968
	CREB3L4	11	0.182	0.974	0.043	0.604
	DNM1L	494	0.183	0.974	0.651	0.968
	TNF	10	0.213	1.000	0.001	0.106
	ATF6B	34	0.290	1.000	0.069	0.715
	TRAF1	145	0.291	1.000	0.621	0.967
	CASP3	117	0.298	1.000	0.094	0.794
	DAB2IP	1151	0.299	1.000	0.123	0.826
	MLKL	147	0.309	1.000	0.653	0.968
	TRAF2	253	0.312	1.000	0.887	0.980
	CREB3L3	105	0.341	1.000	0.817	0.973
	CSF1	74	0.345	1.000	0.009	0.431
	BAG4	115	0.420	1.000	0.621	0.967
	RPS6KA5	968	0.430	1.000	0.348	0.928
	CREB1	227	0.486	1.000	0.512	0.933
	TNFRSF1A	42	0.499	1.000	0.773	0.973
	NOD2	165	0.502	1.000	0.798	0.973
	ITCH	458	0.517	1.000	0.296	0.928
	FAS	154	0.527	1.000	0.437	0.928
	MMP3	46	0.570	1.000	0.353	0.928
	CCL20	20	0.598	1.000	0.674	0.968
	IL18R1	202	0.624	1.000	0.579	0.947
	SELE	81	0.640	1.000	0.047	0.604
	CASP7	276	0.652	1.000	0.329	0.928
	CXCL5	5	0.664	1.000	0.308	0.928
	CASP10	190	0.667	1.000	0.779	0.973
	JAG1	173	0.677	1.000	0.380	0.928
	MMP14	73	0.698	1.000	0.438	0.928
	JUNB	3	0.701	1.000	0.340	0.928
	CREB5	3041	0.705	1.000	0.532	0.933
	VEGFC	572	0.757	1.000	0.503	0.933
	CREB3L1	191	0.762	1.000	0.201	0.887
	BCL3	72	0.763	1.000	0.569	0.947
	RPS6KA4	65	0.789	1.000	0.539	0.933
	IL15	372	0.809	1.000	0.966	0.996
	CREB3L2	728	0.829	1.000	0.522	0.933
	TNFAIP3	48	0.835	1.000	0.168	0.856

<i>TRAF5</i>	162	0.835	1.000	0.408	0.928
<i>CXCL6</i>	7	0.839	1.000	0.715	0.968
<i>CSF2</i>	12	0.843	1.000	0.158	0.853
<i>TNFRSF1B</i>	211	0.887	1.000	0.538	0.933
<i>ATF4</i>	19	0.891	1.000	0.126	0.826
<i>CEBPB</i>	2	0.915	1.000	0.484	0.933
<i>CX3CL1</i>	76	0.917	1.000	0.338	0.928
<i>IRF1</i>	60	0.924	1.000	0.144	0.853
<i>SOCS3</i>	8	0.930	1.000	0.050	0.604
<i>CCL2</i>	7	0.936	1.000	0.525	0.933
<i>MAP3K5</i>	1047	0.937	1.000	0.568	0.947
<i>RIPK3</i>	19	0.956	1.000	0.881	0.980
<i>ATF2</i>	435	0.957	1.000	0.607	0.959
<i>PGAM5</i>	108	0.996	1.000	0.494	0.933

Abbreviations: TLR = toll-like receptor; NFkB = nuclear factor kappa B; TNF = tumor necrosis factor; EOC = epithelial ovarian cancer; HGSOC = high grade serous ovarian cancer; AACES = African American Cancer Epidemiology Study; OCAC = Ovarian Cancer Association Consortium;

^aAggregate P-value of MAGMA model results. Each model controls for age, and two ancestry principal components.

^bCorrected for multiple testing by the number of genes tested using the Benjamini-Hochberg false discovery rate (FDR).

^cNo SNPs mapped to gene after QC filtering.

^dGene chromosomal locations not on raw data file.

Supplementary Table ST5.2. Gene associations/BMI interactions within TLR, NFkB, and TNF pathways with 5-year overall survival among Black women with HGSOc.

Pathway	Gene	# SNPs	P_{raw}	P_{BH}	$P_{BMI\ raw}$	$P_{BMI\ FDR}$
Nfkb						
	<i>LTA</i>	11	0.026	0.916	0.025	0.604
	<i>BCL2L1</i>	155	0.030	0.916	0.933	0.980
	<i>TNFRSF11A</i>	355	0.032	0.916	0.253	0.918
	<i>LCK</i>	125	0.044	0.916	0.680	0.968
	<i>ZAP70</i>	120	0.046	0.916	0.514	0.933
	<i>PIAS4</i>	214	0.053	0.916	0.583	0.947
	<i>PLAU</i>	22	0.061	0.916	0.284	0.928
	<i>GADD45G</i>	7	0.065	0.916	0.524	0.933
	<i>EDA2R</i>	82	0.073	0.916	0.836	0.973
	<i>EDA</i>	1492	0.087	0.916	0.849	0.973
	<i>CSNK2B</i>	16	0.122	0.916	0.134	0.853
	<i>RELA</i>	41	0.126	0.916	0.001	0.070
	<i>IGH</i>	2142	0.126	0.916	0.548	0.937
	<i>PARP1</i>	240	0.128	0.916	0.767	0.973
	<i>VCAM1</i>	80	0.138	0.916	0.711	0.968
	<i>MAP3K14</i>	208	0.214	1.000	0.604	0.959
	<i>LTBR</i>	87	0.214	1.000	0.590	0.951
	<i>BIRC2</i>	99	0.246	1.000	0.672	0.968
	<i>UBE2I</i>	198	0.257	1.000	0.386	0.928
	<i>TNFSF11</i>	216	0.295	1.000	0.533	0.933
	<i>RELB</i>	193	0.300	1.000	0.193	0.887
	<i>CSNK2A3</i>	12	0.302	1.000	0.527	0.933
	<i>BLNK</i>	487	0.315	1.000	0.642	0.968
	<i>CARD10</i>	197	0.342	1.000	0.826	0.973
	<i>ATM</i>	671	0.344	1.000	0.034	0.604
	<i>BCL2</i>	961	0.347	1.000	0.237	0.891

<i>PTGS2</i>	34	0.351	1.000	0.747	0.973
<i>CXCL1</i>	16	0.363	1.000	0.376	0.928
<i>SYK</i>	662	0.369	1.000	0.949	0.988
<i>TRAF6</i>	108	0.377	1.000	0.411	0.928
<i>CXCL12</i>	104	0.413	1.000	0.786	0.973
<i>CHUK</i>	192	0.423	1.000	0.101	0.794
<i>PRKCQ</i>	1222	0.427	1.000	0.542	0.933
<i>CXCL2</i>	4	0.428	1.000	0.489	0.933
<i>XIAP</i>	254	0.431	1.000	0.829	0.973
<i>CXCL3</i>	6	0.458	1.000	0.405	0.928
<i>PRKCB</i>	2384	0.488	1.000	0.050	0.604
<i>CCL13</i>	7	0.557	1.000	0.213	0.887
<i>NFKB2</i>	26	0.565	1.000	0.421	0.928
<i>CYLD</i>	242	0.571	1.000	0.851	0.973
<i>PLCG2</i>	1937	0.575	1.000	0.770	0.973
<i>TRADD</i>	14	0.579	1.000	0.810	0.973
<i>IL1R1</i>	679	0.595	1.000	0.733	0.971
<i>GADD45B</i>	9	0.596	1.000	0.026	0.604
<i>BCL10</i>	59	0.626	1.000	0.493	0.933
<i>BIRC3</i>	65	0.641	1.000	0.205	0.887
<i>TNFSF14</i>	47	0.654	1.000	0.006	0.343
<i>ICAM1</i>	75	0.681	1.000	0.388	0.928
<i>LAT</i>	16	0.688	1.000	0.360	0.928
<i>TAB3</i>	180	0.705	1.000	0.412	0.928
<i>LYN</i>	857	0.734	1.000	0.094	0.794
<i>EDARADD</i>	710	0.740	1.000	0.360	0.928
<i>LTB</i>	4	0.789	1.000	0.000	0.070
<i>TNFRSF13C</i>	9	0.795	1.000	0.428	0.928
<i>GADD45A</i>	16	0.799	1.000	0.039	0.604
<i>CARD11</i>	1090	0.800	1.000	0.669	0.968
<i>CSNK2A2</i>	166	0.838	1.000	0.686	0.968
<i>CSNK2A1</i>	249	0.851	1.000	0.845	0.973

<i>EDAR</i>	500	0.852	1.000	0.377	0.928
<i>NFKB1</i>	441	0.857	1.000	0.727	0.971
<i>BCL2A1</i>	48	0.866	1.000	0.922	0.980
<i>BTK</i>	152	0.869	1.000	0.580	0.947
<i>ERC1</i>	3618	0.888	1.000	0.466	0.933
<i>TRIM25</i>	80	0.888	1.000	0.086	0.788
<i>PIDD1</i>	82	0.896	1.000	0.902	0.980
<i>CCL19</i>	7	0.910	1.000	0.297	0.928
<i>CCL21</i>	5	0.913	1.000	0.077	0.756
<i>CARD14</i>	271	0.927	1.000	0.056	0.640
<i>MALT1</i>	389	0.948	1.000	0.671	0.968
<i>NFKBIA</i>	18	0.951	1.000	0.560	0.947
<i>CD40LG</i>	34	0.974	1.000	0.210	0.887
<i>PLCG1</i>	87	0.980	1.000	0.329	0.928
<i>RIPK1</i>	368	0.989	1.000	0.125	0.826
<i>TNFSF13B</i>	158	0.994	1.000	0.185	0.882
TLR					
<i>FOS</i>	11	0.009	0.916	0.918	0.980
<i>STAT1</i>	195	0.020	0.916	0.715	0.968
<i>MAP2K4</i>	382	0.032	0.916	0.530	0.933
<i>TAB2</i>	548	0.035	0.916	0.336	0.928
<i>CTSK</i>	22	0.035	0.916	0.928	0.980
<i>IKBKE</i>	163	0.037	0.916	0.893	0.980
<i>TOLLIP</i>	158	0.068	0.916	0.126	0.826
<i>AKT3</i>	1176	0.082	0.916	0.955	0.990
<i>PIK3R2</i>	73	0.082	0.916	0.391	0.928
<i>CXCL11</i>	24	0.089	0.916	0.995	1.000
<i>TICAM1</i>	109	0.099	0.916	0.797	0.973
<i>MAPK9</i>	313	0.121	0.916	0.782	0.973
<i>IRAK4</i>	144	0.124	0.916	0.397	0.928
<i>PIK3CA</i>	326	0.128	0.916	0.787	0.973
<i>IRAK1</i>	25	0.129	0.916	0.337	0.928

<i>CD40</i>	48	0.135	0.916	0.457	0.933
<i>IFNA8</i>	4	0.140	0.916	0.419	0.928
<i>CCL4L1</i>	2	0.146	0.929	0.330	0.928
<i>MAP2K6</i>	609	0.172	0.974	0.874	0.980
<i>CCL4</i>	23	0.173	0.974	0.518	0.933
<i>IKBKB</i>	243	0.174	0.974	0.634	0.968
<i>MAP2K1</i>	542	0.196	1.000	0.032	0.604
<i>MAPK8</i>	598	0.208	1.000	0.851	0.973
<i>MAP3K7</i>	318	0.215	1.000	0.231	0.891
<i>TICAM2</i>	194	0.232	1.000	0.520	0.933
<i>PIK3R3</i>	454	0.269	1.000	0.339	0.928
<i>MYD88</i>	6	0.276	1.000	0.713	0.968
<i>CD86</i>	226	0.279	1.000	0.104	0.794
<i>IRF7</i>	25	0.296	1.000	0.700	0.968
<i>MAPK14</i>	400	0.329	1.000	0.215	0.887
<i>PIK3R1</i>	380	0.346	1.000	0.237	0.891
<i>IL6</i>	29	0.356	1.000	0.243	0.896
<i>TLR9</i>	6	0.374	1.000	0.043	0.604
<i>TBK1</i>	177	0.389	1.000	0.382	0.928
<i>CD14</i>	6	0.390	1.000	0.922	0.980
<i>IL12A</i>	36	0.397	1.000	0.949	0.988
<i>CCL3</i>	16	0.415	1.000	0.217	0.887
<i>LY96</i>	221	0.415	1.000	0.854	0.973
<i>IKBKG</i>	25	0.416	1.000	0.365	0.928
<i>MAPK10</i>	2512	0.469	1.000	0.298	0.928
<i>TLR6</i>	346	0.501	1.000	0.874	0.980
<i>JUN</i>	15	0.524	1.000	0.059	0.640
<i>IFNA13</i>	1	0.528	1.000	0.913	0.980
<i>IFNA4</i>	6	0.541	1.000	0.932	0.980
<i>PIK3CD</i>	323	0.542	1.000	0.143	0.853
<i>IFNAR1</i>	193	0.551	1.000	0.572	0.947
<i>PIK3CB</i>	702	0.566	1.000	0.680	0.968

<i>IFNA5</i>	3	0.567	1.000	0.018	0.604
<i>CASP8</i>	240	0.598	1.000	0.099	0.794
<i>IFNB1</i>	5	0.644	1.000	0.748	0.973
<i>CCL5</i>	23	0.679	1.000	0.402	0.928
<i>TIRAP</i>	61	0.683	1.000	0.595	0.954
<i>IFNA21</i>	6	0.685	1.000	0.209	0.887
<i>IFNA1</i>	8	0.690	1.000	0.160	0.853
<i>MAPK13</i>	46	0.704	1.000	0.367	0.928
<i>IRF3</i>	23	0.709	1.000	0.430	0.928
<i>IL12B</i>	72	0.713	1.000	0.043	0.604
<i>AKT1</i>	167	0.713	1.000	0.858	0.973
<i>TLR8</i>	83	0.730	1.000	0.696	0.968
<i>MAP2K7</i>	61	0.731	1.000	0.916	0.980
<i>MAPK1</i>	513	0.758	1.000	0.533	0.933
<i>LBP</i>	265	0.767	1.000	0.845	0.973
<i>AKT2</i>	154	0.768	1.000	0.764	0.973
<i>MAP2K2</i>	176	0.775	1.000	0.288	0.928
<i>IFNAR2</i>	178	0.781	1.000	0.151	0.853
<i>TLR4</i>	60	0.799	1.000	0.827	0.973
<i>IFNA17</i>	10	0.801	1.000	0.111	0.817
<i>FADD</i>	13	0.806	1.000	0.754	0.973
<i>CD80</i>	217	0.808	1.000	0.162	0.853
<i>MAPK12</i>	58	0.817	1.000	0.032	0.604
<i>IFNA7</i>	2	0.819	1.000	0.267	0.928
<i>IFNA16</i>	12	0.819	1.000	0.714	0.968
<i>CFLAR</i>	228	0.822	1.000	0.825	0.973
<i>TAB1</i>	122	0.853	1.000	0.416	0.928
<i>TLR5</i>	175	0.861	1.000	0.180	0.877
<i>MAP3K8</i>	144	0.863	1.000	0.234	0.891
<i>IFNA6</i>	3	0.863	1.000	0.164	0.853
<i>CXCL8</i>	9	0.864	1.000	0.079	0.756
<i>SPP1</i>	42	0.871	1.000	0.172	0.858

<i>TLR3</i>	98	0.873	1.000	0.893	0.980
<i>RAC1</i>	241	0.881	1.000	0.340	0.928
<i>CCL3L3</i>	1	0.881	1.000	0.154	0.853
<i>TLR1</i>	69	0.885	1.000	0.754	0.973
<i>MAPK3</i>	24	0.886	1.000	0.039	0.604
<i>CXCL10</i>	15	0.919	1.000	0.351	0.928
<i>MAP2K3</i>	185	0.934	1.000	0.456	0.933
<i>MAPK11</i>	28	0.934	1.000	0.274	0.928
<i>IL1B</i>	30	0.945	1.000	0.411	0.928
<i>IFNA2</i>	7	0.946	1.000	0.482	0.933
<i>CXCL9</i>	18	0.951	1.000	0.460	0.933
<i>TLR7</i>	103	0.967	1.000	0.731	0.971
<i>IFNA10</i>	14	0.977	1.000	0.228	0.891
<i>IRF5</i>	62	0.982	1.000	0.802	0.973
<i>TLR2</i>	122	0.998	1.000	0.914	0.980
<i>IFNA14</i>	0				
<i>CCL3L1</i>					
<i>CCL4L2</i>					
TNF					
<i>LIF</i>	29	0.064	0.916	0.722	0.971
<i>EDN1</i>	30	0.085	0.916	0.674	0.968
<i>TRAF3</i>	541	0.132	0.916	0.685	0.968
<i>MMP9</i>	41	0.175	0.974	0.691	0.968
<i>CREB3</i>	14	0.176	0.974	0.696	0.968
<i>CREB3L4</i>	11	0.182	0.974	0.043	0.604
<i>DNM1L</i>	494	0.183	0.974	0.651	0.968
<i>TNF</i>	10	0.213	1.000	0.001	0.106
<i>ATF6B</i>	34	0.290	1.000	0.069	0.715
<i>TRAF1</i>	145	0.291	1.000	0.621	0.967
<i>CASP3</i>	117	0.298	1.000	0.094	0.794
<i>DAB2IP</i>	1151	0.299	1.000	0.123	0.826
<i>MLKL</i>	147	0.309	1.000	0.653	0.968

<i>TRAF2</i>	253	0.312	1.000	0.887	0.980
<i>CREB3L3</i>	105	0.341	1.000	0.817	0.973
<i>CSF1</i>	74	0.345	1.000	0.009	0.431
<i>BAG4</i>	115	0.420	1.000	0.621	0.967
<i>RPS6KA5</i>	968	0.430	1.000	0.348	0.928
<i>CREB1</i>	227	0.486	1.000	0.512	0.933
<i>TNFRSF1A</i>	42	0.499	1.000	0.773	0.973
<i>NOD2</i>	165	0.502	1.000	0.798	0.973
<i>ITCH</i>	458	0.517	1.000	0.296	0.928
<i>FAS</i>	154	0.527	1.000	0.437	0.928
<i>MMP3</i>	46	0.570	1.000	0.353	0.928
<i>CCL20</i>	20	0.598	1.000	0.674	0.968
<i>IL18R1</i>	202	0.624	1.000	0.579	0.947
<i>SELE</i>	81	0.640	1.000	0.047	0.604
<i>CASP7</i>	276	0.652	1.000	0.329	0.928
<i>CXCL5</i>	5	0.664	1.000	0.308	0.928
<i>CASP10</i>	190	0.667	1.000	0.779	0.973
<i>JAG1</i>	173	0.677	1.000	0.380	0.928
<i>MMP14</i>	73	0.698	1.000	0.438	0.928
<i>JUNB</i>	3	0.701	1.000	0.340	0.928
<i>CREB5</i>	3041	0.705	1.000	0.532	0.933
<i>VEGFC</i>	572	0.757	1.000	0.503	0.933
<i>CREB3L1</i>	191	0.762	1.000	0.201	0.887
<i>BCL3</i>	72	0.763	1.000	0.569	0.947
<i>RPS6KA4</i>	65	0.789	1.000	0.539	0.933
<i>IL15</i>	372	0.809	1.000	0.966	0.996
<i>CREB3L2</i>	728	0.829	1.000	0.522	0.933
<i>TNFAIP3</i>	48	0.835	1.000	0.168	0.856
<i>TRAF5</i>	162	0.835	1.000	0.408	0.928
<i>CXCL6</i>	7	0.839	1.000	0.715	0.968
<i>CSF2</i>	12	0.843	1.000	0.158	0.853
<i>TNFRSF1B</i>	211	0.887	1.000	0.538	0.933

<i>ATF4</i>	19	0.891	1.000	0.126	0.826
<i>CEBPB</i>	2	0.915	1.000	0.484	0.933
<i>CX3CL1</i>	76	0.917	1.000	0.338	0.928
<i>IRF1</i>	60	0.924	1.000	0.144	0.853
<i>SOCS3</i>	8	0.930	1.000	0.050	0.604
<i>CCL2</i>	7	0.936	1.000	0.525	0.933
<i>MAP3K5</i>	1047	0.937	1.000	0.568	0.947
<i>RIPK3</i>	19	0.956	1.000	0.881	0.980
<i>ATF2</i>	435	0.957	1.000	0.607	0.959
<i>PGAM5</i>	108	0.996	1.000	0.494	0.933

Abbreviations: TLR = toll-like receptor; NFkB = nuclear factor kappa B; TNF = tumor necrosis factor; EOC = epithelial ovarian cancer; HGSOC = high grade serous ovarian cancer; AACES = African American Cancer Epidemiology Study; OCAC = Ovarian Cancer Association Consortium;

^aAggregate P-value of MAGMA model results. Each model controls for age, and two ancestry principal components.

^bCorrected for multiple testing by the number of genes tested using the Benjamini-Hochberg false discovery rate (FDR).

^cNo SNPs mapped to gene after QC filtering.

Supplementary Table ST5.3. Gene associations/BMI interactions within TLR, NFkB, and TNF pathways with EOC 5-year survival among White women.^a

Pathway	Gene	# SNPs	Test set				Validation set			
			P_{raw}	P_{BH}	$P_{BMI\ raw}$	$P_{BMI\ FDR}$	P_{raw}	P_{BH}	$P_{BMI\ raw}$	$P_{BMI\ FDR}$
NFKB			0.236		0.190		0.523		0.925	
	<i>PTGS2</i>	115	0.002	0.414	0.762	0.982	0.827	0.932	0.156	0.982
	<i>CXCL12</i>	158	0.017	0.535	0.997	1.000	0.753	0.910	0.385	0.982
	<i>TAB3</i>	66	0.020	0.535	0.217	0.982	0.975	0.993	0.980	0.999
	<i>GADD45B</i>	30	0.029	0.535	0.330	0.982	0.100	0.778	0.178	0.982
	<i>SYK</i>	512	0.030	0.535	0.696	0.982	0.128	0.778	0.100	0.982
	<i>VCAM1</i>	30	0.041	0.535	0.474	0.982	0.270	0.787	0.142	0.982
	<i>PLCG1</i>	86	0.047	0.535	0.959	0.987	0.269	0.787	0.828	0.982
	<i>ICAM1</i>	43	0.078	0.670	0.198	0.982	0.072	0.778	0.429	0.982
	<i>NFKBIA</i>	84	0.080	0.670	0.368	0.982	0.787	0.918	0.359	0.982
	<i>TRADD</i>	21	0.113	0.855	0.456	0.982	0.904	0.966	0.590	0.982
	<i>BLNK</i>	252	0.114	0.855	0.205	0.982	0.831	0.932	0.606	0.982
	<i>CCL13</i>	61	0.153	0.889	0.590	0.982	0.221	0.787	0.652	0.982
	<i>TNFRSF11A</i>	335	0.159	0.889	0.715	0.982	0.928	0.980	0.769	0.982
	<i>CYLD</i>	140	0.160	0.889	0.929	0.983	0.431	0.833	0.670	0.982
	<i>CCL19</i>	57	0.169	0.889	0.991	1.000	0.631	0.905	0.339	0.982
	<i>PRKCQ</i>	590	0.177	0.889	0.363	0.982	0.394	0.813	0.928	0.982
	<i>BIRC3</i>	41	0.177	0.889	0.909	0.982	0.848	0.933	0.359	0.982
	<i>LTB</i>	85	0.183	0.889	0.535	0.982	0.225	0.787	0.587	0.982
	<i>CARD10</i>	155	0.218	0.889	0.149	0.982	0.484	0.842	0.753	0.982
	<i>LTA</i>	154	0.252	0.889	0.631	0.982	0.457	0.836	0.661	0.982
	<i>CCL21</i>	56	0.255	0.889	0.834	0.982	0.910	0.968	0.307	0.982
	<i>PLCG2</i>	1063	0.263	0.889	0.819	0.982	0.442	0.833	0.406	0.982
	<i>LTBR</i>	38	0.270	0.889	0.221	0.982	0.147	0.787	0.405	0.982
	<i>CXCL1</i>	72	0.273	0.889	0.257	0.982	0.414	0.820	0.197	0.982
	<i>CSNK2A3</i>	22	0.289	0.889	0.879	0.982	0.755	0.910	0.892	0.982

<i>IGH</i>	405	0.294	0.889	0.248	0.982	0.050	0.778	0.692	0.982
<i>EDA2R</i>	56	0.315	0.889	0.344	0.982	0.729	0.910	0.750	0.982
<i>BCL2L1</i>	123	0.335	0.889	0.508	0.982	0.206	0.787	0.208	0.982
<i>CSNK2B</i>	77	0.343	0.889	0.672	0.982	0.208	0.787	0.420	0.982
<i>XIAP</i>	112	0.346	0.889	0.369	0.982	0.181	0.787	0.822	0.982
<i>NFKB1</i>	303	0.355	0.889	0.969	0.987	0.650	0.910	0.581	0.982
<i>ATM</i>	286	0.356	0.889	0.559	0.982	0.114	0.778	0.506	0.982
<i>RELA</i>	54	0.369	0.889	0.274	0.982	0.308	0.787	0.888	0.982
<i>EDARADD</i>	241	0.404	0.889	0.189	0.982	0.503	0.842	0.520	0.982
<i>LCK</i>	56	0.405	0.889	0.608	0.982	0.453	0.836	0.099	0.982
<i>TRIM25</i>	23	0.439	0.889	0.116	0.982	0.757	0.910	0.390	0.982
<i>NFKB2</i>	58	0.442	0.889	0.080	0.982	0.335	0.787	0.051	0.982
<i>EDAR</i>	171	0.451	0.889	0.063	0.982	0.076	0.778	0.540	0.982
<i>PLAU</i>	55	0.463	0.889	0.463	0.982	0.796	0.918	0.558	0.982
<i>RIPK1</i>	125	0.481	0.889	0.828	0.982	0.974	0.993	0.058	0.982
<i>LAT</i>	33	0.515	0.904	0.274	0.982	0.160	0.787	0.999	0.999
<i>CSNK2A2</i>	208	0.524	0.904	0.700	0.982	0.278	0.787	0.655	0.982
<i>CSNK2A1</i>	167	0.537	0.904	0.149	0.982	0.032	0.778	0.458	0.982
<i>BIRC2</i>	90	0.547	0.907	1.000	1.000	0.168	0.787	0.753	0.982
<i>BTK</i>	126	0.558	0.915	0.733	0.982	0.086	0.778	0.591	0.982
<i>TNFSF13B</i>	67	0.567	0.917	0.735	0.982	0.059	0.778	0.606	0.982
<i>PIAS4</i>	85	0.576	0.917	0.367	0.982	0.563	0.862	0.695	0.982
<i>GADD45G</i>	73	0.597	0.917	0.959	0.987	0.101	0.778	0.581	0.982
<i>BCL10</i>	123	0.604	0.917	0.403	0.982	0.732	0.910	0.202	0.982
<i>IL1R1</i>	417	0.643	0.917	0.799	0.982	0.714	0.910	0.916	0.982
<i>TRAF6</i>	95	0.670	0.917	0.181	0.982	0.990	0.995	0.974	0.999
<i>TNFSF14</i>	89	0.679	0.919	0.254	0.982	0.367	0.801	0.124	0.982
<i>TNFSF11</i>	213	0.717	0.936	0.061	0.982	0.567	0.862	0.272	0.982
<i>CD40LG</i>	28	0.722	0.936	0.855	0.982	0.739	0.910	0.990	0.999
<i>LYN</i>	508	0.729	0.936	0.795	0.982	0.211	0.787	0.200	0.982
<i>CXCL3</i>	10	0.734	0.936	0.208	0.982	0.302	0.787	0.232	0.982
<i>PARP1</i>	217	0.775	0.953	0.512	0.982	0.522	0.842	0.787	0.982

<i>TNFRSF13C</i>	61	0.795	0.953	0.339	0.982	0.653	0.910	0.415	0.982
<i>CXCL2</i>	30	0.799	0.953	0.318	0.982	0.077	0.778	0.307	0.982
<i>UBE2I</i>	94	0.813	0.953	0.855	0.982	0.473	0.838	0.169	0.982
<i>CHUK</i>	158	0.826	0.953	0.334	0.982	0.377	0.803	0.777	0.982
<i>MALT1</i>	292	0.828	0.953	0.552	0.982	0.025	0.778	0.821	0.982
<i>ERC1</i>	1966	0.886	0.973	0.277	0.982	0.226	0.787	0.262	0.982
<i>RELB</i>	73	0.897	0.973	0.592	0.982	0.771	0.913	0.284	0.982
<i>MAP3K14</i>	166	0.907	0.973	0.409	0.982	0.064	0.778	0.960	0.999
<i>EDA</i>	711	0.922	0.973	0.276	0.982	0.413	0.820	0.738	0.982
<i>BCL2</i>	556	0.925	0.973	0.802	0.982	0.720	0.910	0.121	0.982
<i>GADD45A</i>	84	0.925	0.973	0.906	0.982	0.565	0.862	0.252	0.982
<i>ZAP70</i>	90	0.926	0.973	0.136	0.982	0.496	0.842	0.517	0.982
<i>CARD11</i>	451	0.952	0.976	0.121	0.982	0.703	0.910	0.593	0.982
<i>BCL2A1</i>	50	0.964	0.981	0.607	0.982	0.734	0.910	0.689	0.982
<i>PIDD1</i>	65	0.973	0.981	0.061	0.982	0.395	0.813	0.809	0.982
<i>PRKCB</i>	1214	0.981	0.981	0.361	0.982	0.332	0.787	0.598	0.982
<i>CARD14</i>	0 ^c								
TLR		0.241		0.647		0.098		0.185	
<i>CTSK</i>	52	0.010	0.535	0.550	0.982	0.662	0.910	0.835	0.982
<i>TAB1</i>	94	0.011	0.535	0.568	0.982	0.769	0.913	0.119	0.982
<i>TLR9</i>	37	0.024	0.535	0.969	0.987	0.023	0.778	0.448	0.982
<i>IL6</i>	94	0.029	0.535	0.159	0.982	0.013	0.762	0.327	0.982
<i>PIK3CA</i>	335	0.030	0.535	0.717	0.982	0.576	0.866	0.465	0.982
<i>TLR8</i>	33	0.039	0.535	0.906	0.982	0.197	0.787	0.243	0.982
<i>IFNAR2</i>	164	0.045	0.535	0.739	0.982	0.375	0.803	0.109	0.982
<i>IRAK4</i>	123	0.045	0.535	0.889	0.982	0.086	0.778	0.195	0.982
<i>CD86</i>	206	0.067	0.660	0.733	0.982	0.014	0.762	0.072	0.982
<i>MAP2K3</i>	39	0.073	0.667	0.366	0.982	0.830	0.932	0.512	0.982
<i>MAP3K8</i>	44	0.101	0.819	0.950	0.987	0.464	0.837	0.396	0.982
<i>PIK3CD</i>	220	0.159	0.889	0.683	0.982	0.364	0.801	0.625	0.982
<i>MAP3K7</i>	291	0.168	0.889	0.748	0.982	0.306	0.787	0.417	0.982
<i>SPP1</i>	95	0.183	0.889	0.401	0.982	0.002	0.525	0.737	0.982

<i>MAPK13</i>	68	0.202	0.889	0.835	0.982	0.708	0.910	0.902	0.982
<i>IFNAR1</i>	157	0.205	0.889	0.534	0.982	0.222	0.787	0.304	0.982
<i>MAP2K6</i>	197	0.205	0.889	0.456	0.982	0.246	0.787	0.261	0.982
<i>MAPK8</i>	366	0.205	0.889	0.801	0.982	0.177	0.787	0.441	0.982
<i>CCL5</i>	78	0.224	0.889	0.331	0.982	0.805	0.919	0.217	0.982
<i>AKT3</i>	543	0.248	0.889	0.463	0.982	0.700	0.910	0.941	0.987
<i>PIK3R2</i>	98	0.270	0.889	0.495	0.982	0.132	0.778	0.584	0.982
<i>IKBKB</i>	138	0.279	0.889	0.776	0.982	0.109	0.778	0.908	0.982
<i>IKBKE</i>	109	0.286	0.889	0.325	0.982	0.674	0.910	0.155	0.982
<i>TOLLIP</i>	184	0.306	0.889	0.402	0.982	0.536	0.856	0.765	0.982
<i>IRAK1</i>	19	0.336	0.889	0.034	0.982	0.308	0.787	0.296	0.982
<i>CXCL10</i>	101	0.374	0.889	0.338	0.982	0.121	0.778	0.197	0.982
<i>IFNA1</i>	75	0.392	0.889	0.045	0.982	0.748	0.910	0.893	0.982
<i>PIK3R1</i>	301	0.399	0.889	0.568	0.982	0.107	0.778	0.782	0.982
<i>AKT2</i>	164	0.404	0.889	0.542	0.982	0.336	0.787	0.999	0.999
<i>IFNA13</i>	86	0.405	0.889	0.472	0.982	0.185	0.787	0.893	0.982
<i>FOS</i>	44	0.410	0.889	0.659	0.982	0.190	0.787	0.136	0.982
<i>PIK3CB</i>	288	0.410	0.889	0.987	1.000	0.696	0.910	0.773	0.982
<i>TBK1</i>	137	0.412	0.889	0.329	0.982	0.337	0.787	0.214	0.982
<i>CD40</i>	102	0.412	0.889	0.017	0.982	0.263	0.787	0.979	0.999
<i>IFNA2</i>	31	0.421	0.889	0.828	0.982	0.239	0.787	0.824	0.982
<i>TLR1</i>	161	0.431	0.889	0.572	0.982	0.550	0.862	0.797	0.982
<i>MAPK9</i>	294	0.434	0.889	0.327	0.982	0.638	0.910	0.171	0.982
<i>TICAM1</i>	110	0.444	0.889	0.094	0.982	0.022	0.778	0.320	0.982
<i>TIRAP</i>	102	0.448	0.889	0.304	0.982	0.392	0.813	0.274	0.982
<i>MAPK3</i>	26	0.450	0.889	0.441	0.982	0.516	0.842	0.665	0.982
<i>TLR2</i>	105	0.453	0.889	0.351	0.982	0.608	0.901	0.680	0.982
<i>CFLAR</i>	200	0.456	0.889	0.573	0.982	0.834	0.932	0.470	0.982
<i>IFNA7</i>	149	0.459	0.889	0.893	0.982	0.213	0.787	0.862	0.982
<i>CXCL9</i>	58	0.467	0.889	0.291	0.982	0.117	0.778	0.244	0.982
<i>FADD</i>	42	0.467	0.889	0.070	0.982	0.283	0.787	0.575	0.982
<i>IFNA4</i>	126	0.473	0.889	0.808	0.982	0.119	0.778	0.777	0.982

<i>IL12A</i>	68	0.475	0.889	0.335	0.982	0.961	0.993	0.535	0.982
<i>STAT1</i>	172	0.479	0.889	0.950	0.987	0.778	0.915	0.982	0.999
<i>TLR7</i>	9	0.489	0.895	0.912	0.982	0.439	0.833	0.413	0.982
<i>IFNA21</i>	79	0.493	0.896	0.804	0.982	0.180	0.787	0.692	0.982
<i>CASP8</i>	221	0.509	0.904	0.729	0.982	0.724	0.910	0.703	0.982
<i>IFNA8</i>	77	0.536	0.904	0.488	0.982	0.267	0.787	0.509	0.982
<i>MAP2K4</i>	218	0.539	0.904	0.526	0.982	0.781	0.915	0.989	0.999
<i>TLR3</i>	129	0.539	0.904	0.415	0.982	0.965	0.993	0.152	0.982
<i>IFNA10</i>	154	0.572	0.917	0.825	0.982	0.301	0.787	0.847	0.982
<i>MAPK14</i>	280	0.589	0.917	0.154	0.982	0.878	0.952	0.803	0.982
<i>IRF5</i>	113	0.617	0.917	0.444	0.982	0.444	0.833	0.552	0.982
<i>AKT1</i>	96	0.625	0.917	0.772	0.982	0.496	0.842	0.820	0.982
<i>TLR5</i>	134	0.636	0.917	0.080	0.982	0.127	0.778	0.497	0.982
<i>MAP2K7</i>	59	0.643	0.917	0.571	0.982	0.538	0.856	0.156	0.982
<i>IFNA14</i>	89	0.645	0.917	0.923	0.982	0.265	0.787	0.963	0.999
<i>MAP2K1</i>	412	0.649	0.917	0.870	0.982	0.235	0.787	0.150	0.982
<i>CXCL8</i>	49	0.653	0.917	0.264	0.982	0.447	0.833	0.871	0.982
<i>CD80</i>	243	0.660	0.917	0.175	0.982	0.249	0.787	0.152	0.982
<i>IFNA17</i>	133	0.666	0.917	0.885	0.982	0.240	0.787	0.753	0.982
<i>IFNA6</i>	62	0.709	0.936	0.691	0.982	0.417	0.820	0.858	0.982
<i>CCL3</i>	6	0.714	0.936	0.772	0.982	0.622	0.903	0.882	0.982
<i>IFNA16</i>	166	0.719	0.936	0.805	0.982	0.335	0.787	0.744	0.982
<i>IKBKG</i>	12	0.728	0.936	0.190	0.982	0.714	0.910	0.733	0.982
<i>CXCL11</i>	175	0.732	0.936	0.355	0.982	0.070	0.778	0.152	0.982
<i>IL12B</i>	73	0.733	0.936	0.266	0.982	0.742	0.910	0.293	0.982
<i>TICAM2</i>	90	0.746	0.944	0.918	0.982	0.488	0.842	0.043	0.982
<i>JUN</i>	34	0.773	0.953	0.650	0.982	0.754	0.910	0.279	0.982
<i>MYD88</i>	36	0.792	0.953	0.191	0.982	0.131	0.778	0.214	0.982
<i>LBP</i>	147	0.801	0.953	0.705	0.982	0.595	0.888	0.571	0.982
<i>MAP2K2</i>	91	0.812	0.953	0.669	0.982	0.970	0.993	0.757	0.982
<i>IRF3</i>	32	0.822	0.953	0.705	0.982	0.508	0.842	0.903	0.982
<i>MAPK10</i>	1853	0.837	0.953	0.241	0.982	0.047	0.778	0.770	0.982

<i>RAC1</i>	232	0.839	0.953	0.913	0.982	0.437	0.833	0.284	0.982
<i>LY96</i>	175	0.839	0.953	0.063	0.982	0.285	0.787	0.771	0.982
<i>IL1B</i>	52	0.847	0.957	0.829	0.982	0.557	0.862	0.087	0.982
<i>PIK3R3</i>	288	0.896	0.973	0.021	0.982	0.897	0.963	0.171	0.982
<i>IRF7</i>	93	0.919	0.973	0.039	0.982	0.188	0.787	0.427	0.982
<i>CD14</i>	65	0.925	0.973	0.096	0.982	0.971	0.993	0.710	0.982
<i>MAPK1</i>	335	0.925	0.973	0.556	0.982	0.619	0.903	0.315	0.982
<i>IFNB1</i>	71	0.931	0.973	0.853	0.982	0.564	0.862	0.668	0.982
<i>TLR6</i>	163	0.940	0.973	0.203	0.982	0.842	0.932	0.825	0.982
<i>CCL4</i>	9	0.942	0.973	0.788	0.982	0.931	0.980	0.942	0.987
<i>TLR4</i>	92	0.954	0.976	0.399	0.982	0.073	0.778	0.767	0.982
<i>IFNA5</i>	60	0.981	0.981	0.730	0.982	0.273	0.787	0.824	0.982
<i>TAB2</i>	0 ^c								
<i>CCL3L1</i>	0 ^c								
<i>CCL3L3</i>	0 ^c								
<i>CCL4L1</i>	0 ^c								
<i>CCL4L2</i>	0 ^c								
<i>MAPK11</i>	0 ^d								
<i>MAPK12</i>	0 ^d								
TNF		0.050		0.260		0.135		0.493	
<i>CREB3L4</i>	30	0.011	0.535	0.924	0.982	0.625	0.903	0.683	0.982
<i>CSF1</i>	240	0.036	0.535	0.870	0.982	0.346	0.789	0.468	0.982
<i>SELE</i>	88	0.045	0.535	0.849	0.982	0.660	0.910	0.860	0.982
<i>TNFRSF1B</i>	76	0.046	0.535	0.838	0.982	0.130	0.778	0.015	0.982
<i>TRAF5</i>	361	0.052	0.570	0.401	0.982	0.470	0.838	0.309	0.982
<i>ATF2</i>	62	0.060	0.627	0.944	0.987	0.518	0.842	0.790	0.982
<i>CASP10</i>	57	0.071	0.667	0.193	0.982	0.351	0.789	0.192	0.982
<i>CCL20</i>	81	0.142	0.889	0.555	0.982	0.329	0.787	0.498	0.982
<i>CREB1</i>	98	0.147	0.889	0.204	0.982	0.981	0.994	0.249	0.982
<i>IL18R1</i>	43	0.149	0.889	0.813	0.982	0.327	0.787	0.737	0.982
<i>CASP3</i>	39	0.158	0.889	0.170	0.982	0.218	0.787	0.677	0.982
<i>CXCL5</i>	116	0.186	0.889	0.876	0.982	0.089	0.778	0.835	0.982

<i>CXCL6</i>	104	0.201	0.889	0.185	0.982	0.412	0.820	0.075	0.982
<i>IL15</i>	225	0.208	0.889	0.951	0.987	0.178	0.787	0.133	0.982
<i>VEGFC</i>	33	0.265	0.889	0.608	0.982	0.624	0.903	0.241	0.982
<i>CSF2</i>	203	0.265	0.889	0.116	0.982	0.351	0.789	0.270	0.982
<i>IRF1</i>	104	0.282	0.889	0.510	0.982	0.696	0.910	0.715	0.982
<i>ATF6B</i>	100	0.292	0.889	0.670	0.982	0.194	0.787	0.492	0.982
<i>EDN1</i>	59	0.294	0.889	0.654	0.982	0.236	0.787	0.641	0.982
<i>MAP3K5</i>	119	0.307	0.889	0.618	0.982	0.668	0.910	0.337	0.982
<i>TNF</i>	1707	0.308	0.889	0.048	0.982	0.759	0.910	0.158	0.982
<i>TNFAIP3</i>	38	0.323	0.889	0.063	0.982	0.657	0.910	0.696	0.982
<i>CREB3L2</i>	270	0.329	0.889	0.897	0.982	0.689	0.910	0.439	0.982
<i>CREB5</i>	20	0.382	0.889	0.786	0.982	0.888	0.959	0.896	0.982
<i>BAG4</i>	168	0.386	0.889	0.407	0.982	0.101	0.778	0.813	0.982
<i>CREB3</i>	336	0.423	0.889	0.576	0.982	0.284	0.787	0.896	0.982
<i>DAB2IP</i>	104	0.446	0.889	0.905	0.982	0.460	0.836	0.543	0.982
<i>TRAF1</i>	88	0.457	0.889	0.276	0.982	0.324	0.787	0.645	0.982
<i>TRAF2</i>	28	0.457	0.889	0.360	0.982	0.995	0.995	0.731	0.982
<i>CASP7</i>	65	0.469	0.889	0.474	0.982	0.245	0.787	0.383	0.982
<i>FAS</i>	16	0.517	0.904	0.225	0.982	0.963	0.993	0.534	0.982
<i>CREB3L1</i>	72	0.531	0.904	0.455	0.982	0.321	0.787	0.023	0.982
<i>MMP3</i>	232	0.538	0.904	0.732	0.982	0.231	0.787	0.659	0.982
<i>RPS6KA4</i>	102	0.549	0.907	0.038	0.982	0.411	0.820	0.607	0.982
<i>DNM1L</i>	87	0.576	0.917	0.742	0.982	0.496	0.842	0.678	0.982
<i>PGAM5</i>	142	0.583	0.917	0.388	0.982	0.796	0.918	0.920	0.982
<i>TNFRSF1A</i>	255	0.591	0.917	0.794	0.982	0.339	0.787	0.897	0.982
<i>MMP14</i>	281	0.596	0.917	0.679	0.982	0.285	0.787	0.590	0.982
<i>RIPK3</i>	118	0.614	0.917	0.638	0.982	0.013	0.762	0.040	0.982
<i>RPS6KA5</i>	109	0.625	0.917	0.699	0.982	0.872	0.950	0.594	0.982
<i>TRAF3</i>	36	0.652	0.917	0.731	0.982	0.092	0.778	0.924	0.982
<i>CX3CL1</i>	353	0.662	0.917	0.296	0.982	0.854	0.936	0.470	0.982
<i>MLKL</i>	91	0.668	0.917	0.093	0.982	0.990	0.995	0.691	0.982
<i>NOD2</i>	162	0.673	0.917	0.521	0.982	0.841	0.932	0.208	0.982

<i>CCL2</i>	251	0.749	0.944	0.249	0.982	0.228	0.787	0.857	0.982
<i>SOCS3</i>	83	0.790	0.953	0.341	0.982	0.805	0.919	0.483	0.982
<i>BCL3</i>	48	0.797	0.953	0.174	0.982	0.511	0.842	0.915	0.982
<i>CREB3L3</i>	564	0.806	0.953	0.107	0.982	0.128	0.778	0.606	0.982
<i>JUNB</i>	521	0.806	0.953	0.911	0.982	0.380	0.803	0.400	0.982
<i>CEBPB</i>	175	0.831	0.953	0.619	0.982	0.697	0.910	0.007	0.982
<i>ITCH</i>	131	0.857	0.963	0.515	0.982	0.570	0.862	0.430	0.982
<i>JAG1</i>	73	0.899	0.973	0.581	0.982	0.359	0.798	0.357	0.982
<i>MMP9</i>	10	0.909	0.973	0.748	0.982	0.051	0.778	0.580	0.982
<i>ATF4</i>	184	0.939	0.973	0.597	0.982	0.336	0.787	0.632	0.982
<i>LIF</i>	435	0.973	0.981	0.761	0.982	0.517	0.842	0.489	0.982

Abbreviations: TLR = toll-like receptor; NFkB = nuclear factor kappa B; TNF = tumor necrosis factor; EOC = epithelial ovarian cancer; HGSOC = high grade serous ovarian cancer; AACES = African American Cancer Epidemiology Study; OCAC = Ovarian Cancer Association Consortium;

^aAggregate P-value of MAGMA model results. Each model controls for age, and two ancestry principal components.

^bCorrected for multiple testing by the number of genes tested using the Benjamini-Hochberg false discovery rate (FDR).

^cNo SNPs mapped to gene after QC filtering.

^dGene chromosomal locations not on raw data file.

Supplementary Table 5.4. Gene associations/BMI interactions within TLR, NfκB, and TNF pathways with HGSOc 5-year survival among White women.^a

Pathway	Gene	# SNPs	Test set				Validation set			
			P_{raw}	P_{BH}	$P_{BMI\ raw}$	$P_{BMI\ FDR}$	P_{raw}	P_{BH}	$P_{BMI\ raw}$	$P_{BMI\ FDR}$
NfκB			0.236		0.775		0.523		0.925	
	<i>PTGS2</i>	115	0.016	0.755	0.573	1.000	0.555	0.956	0.007	0.811
	<i>VCAM1</i>	29	0.025	0.755	0.074	1.000	0.012	0.628	0.020	0.820
	<i>PLCG2</i>	1052	0.026	0.755	0.887	1.000	0.197	0.916	0.914	1.000
	<i>GADD45B</i>	30	0.038	0.755	0.508	1.000	0.164	0.852	0.293	1.000
	<i>NFKBIA</i>	83	0.082	0.878	0.734	1.000	0.862	1.000	0.046	0.968
	<i>BIRC3</i>	41	0.096	0.878	0.678	1.000	0.499	0.956	0.309	1.000
	<i>BLNK</i>	251	0.098	0.878	0.156	1.000	0.899	1.000	0.639	1.000
	<i>CYLD</i>	140	0.107	0.878	0.902	1.000	0.021	0.628	0.791	1.000
	<i>CXCL12</i>	158	0.120	0.878	0.653	1.000	0.661	0.956	0.220	1.000
	<i>PARP1</i>	217	0.135	0.878	0.694	1.000	0.152	0.852	0.558	1.000
	<i>PLCG1</i>	85	0.154	0.878	0.855	1.000	0.572	0.956	0.396	1.000
	<i>EDA</i>	707	0.158	0.878	0.498	1.000	0.394	0.956	0.837	1.000
	<i>BCL2L1</i>	123	0.173	0.878	0.992	1.000	0.392	0.956	0.471	1.000
	<i>TRADD</i>	21	0.185	0.878	0.914	1.000	0.475	0.956	0.801	1.000
	<i>CCL13</i>	61	0.208	0.895	0.782	1.000	0.642	0.956	0.440	1.000
	<i>ICAM1</i>	44	0.211	0.895	0.342	1.000	0.366	0.956	0.920	1.000
	<i>TNFRSF11A</i>	336	0.222	0.895	0.077	1.000	0.755	0.978	0.611	1.000
	<i>TAB3</i>	67	0.223	0.895	0.385	1.000	0.928	1.000	0.996	1.000
	<i>SYK</i>	512	0.257	0.895	0.088	1.000	0.265	0.951	0.262	1.000
	<i>ATM</i>	286	0.302	0.895	0.342	1.000	0.156	0.852	0.876	1.000
	<i>LTBR</i>	38	0.307	0.895	0.415	1.000	0.240	0.951	0.898	1.000
	<i>CSNK2A3</i>	22	0.360	0.895	0.729	1.000	0.895	1.000	0.845	1.000
	<i>GADD45G</i>	69	0.361	0.895	0.979	1.000	0.251	0.951	0.787	1.000
	<i>CHUK</i>	158	0.374	0.895	0.812	1.000	0.083	0.676	0.288	1.000
	<i>BIRC2</i>	90	0.377	0.895	0.661	1.000	0.039	0.637	0.864	1.000
	<i>CARD10</i>	155	0.378	0.895	0.156	1.000	0.311	0.951	0.763	1.000
	<i>IGH</i>	398	0.378	0.895	0.614	1.000	0.218	0.951	0.424	1.000

<i>LTB</i>	85	0.382	0.895	0.715	1.000	0.438	0.956	0.556	1.000
<i>BTK</i>	126	0.404	0.895	0.402	1.000	0.162	0.852	0.634	1.000
<i>CSNK2A1</i>	163	0.404	0.895	0.785	1.000	0.167	0.852	0.492	1.000
<i>LTA</i>	154	0.418	0.895	0.678	1.000	0.656	0.956	0.675	1.000
<i>XIAP</i>	111	0.424	0.895	0.683	1.000	0.684	0.967	0.860	1.000
<i>PRKCQ</i>	578	0.426	0.895	0.698	1.000	0.548	0.956	0.979	1.000
<i>CSNK2B</i>	77	0.448	0.895	0.724	1.000	0.316	0.953	0.849	1.000
<i>LYN</i>	507	0.483	0.895	0.802	1.000	0.556	0.956	0.105	0.997
<i>LCK</i>	55	0.494	0.895	0.589	1.000	0.293	0.951	0.185	1.000
<i>CCL19</i>	58	0.521	0.901	0.845	1.000	0.163	0.852	0.435	1.000
<i>CCL21</i>	56	0.537	0.901	0.764	1.000	0.149	0.852	0.106	0.997
<i>ZAP70</i>	89	0.548	0.909	0.622	1.000	0.409	0.956	0.575	1.000
<i>EDA2R</i>	56	0.570	0.909	0.580	1.000	0.912	1.000	0.420	1.000
<i>CD40LG</i>	28	0.581	0.909	0.950	1.000	0.773	0.978	0.864	1.000
<i>PIDD1</i>	65	0.584	0.909	0.532	1.000	0.306	0.951	0.625	1.000
<i>CXCL1</i>	72	0.588	0.909	0.546	1.000	0.153	0.852	0.198	1.000
<i>LAT</i>	33	0.592	0.909	0.982	1.000	0.733	0.978	0.707	1.000
<i>EDAR</i>	171	0.594	0.909	0.329	1.000	0.026	0.628	0.316	1.000
<i>TNFSF14</i>	87	0.596	0.909	0.518	1.000	0.512	0.956	0.096	0.997
<i>BCL10</i>	123	0.648	0.947	0.131	1.000	0.581	0.956	0.029	0.820
<i>EDARADD</i>	237	0.695	0.949	0.800	1.000	0.799	0.992	0.933	1.000
<i>MALT1</i>	291	0.699	0.949	0.705	1.000	0.010	0.628	0.948	1.000
<i>NFKB1</i>	302	0.700	0.949	0.746	1.000	0.829	1.000	0.390	1.000
<i>PIAS4</i>	86	0.729	0.949	0.576	1.000	0.286	0.951	0.693	1.000
<i>PRKCB</i>	1211	0.739	0.949	0.184	1.000	0.916	1.000	0.840	1.000
<i>TRIM25</i>	22	0.740	0.949	0.503	1.000	0.788	0.992	0.176	1.000
<i>RIPK1</i>	124	0.752	0.959	0.801	1.000	0.599	0.956	0.077	0.997
<i>TRAF6</i>	95	0.770	0.971	0.142	1.000	0.988	1.000	0.957	1.000
<i>UBE2I</i>	85	0.783	0.974	0.945	1.000	0.588	0.956	0.502	1.000
<i>TNFSF11</i>	208	0.795	0.974	0.031	1.000	0.478	0.956	0.127	1.000
<i>TNFSF13B</i>	66	0.800	0.974	0.612	1.000	0.900	1.000	0.936	1.000
<i>IL1R1</i>	417	0.834	0.974	0.937	1.000	0.092	0.676	0.922	1.000

<i>RELA</i>	54	0.838	0.974	0.643	1.000	0.548	0.956	0.991	1.000
<i>BCL2A1</i>	50	0.843	0.974	0.398	1.000	0.717	0.977	0.662	1.000
<i>NFKB2</i>	58	0.868	0.974	0.040	1.000	0.667	0.956	0.066	0.997
<i>RELB</i>	73	0.879	0.974	0.565	1.000	0.446	0.956	0.573	1.000
<i>PLAU</i>	55	0.880	0.974	0.108	1.000	0.881	1.000	0.538	1.000
<i>BCL2</i>	557	0.882	0.974	0.331	1.000	0.984	1.000	0.658	1.000
<i>TNFRSF13C</i>	61	0.882	0.974	0.539	1.000	0.700	0.967	0.771	1.000
<i>CXCL3</i>	10	0.900	0.975	0.063	1.000	0.393	0.956	0.273	1.000
<i>GADD45A</i>	84	0.953	0.989	0.622	1.000	0.837	1.000	0.899	1.000
<i>ERC1</i>	1966	0.973	0.995	0.813	1.000	0.423	0.956	0.266	1.000
<i>CARD11</i>	446	0.984	0.995	0.481	1.000	0.131	0.852	0.765	1.000
<i>CXCL2</i>	31	0.985	0.995	0.349	1.000	0.089	0.676	0.175	1.000
<i>CSNK2A2</i>	204	0.986	0.995	0.590	1.000	0.121	0.836	0.278	1.000
<i>MAP3K14</i>	166	0.997	0.997	0.046	1.000	0.027	0.628	0.671	1.000
<i>CARD14</i>	0 ^b								
TLR		0.241		0.655		0.098		0.185	
<i>TAB1</i>	86	0.018	0.755	0.740	1.000	0.501	0.956	0.173	1.000
<i>TLR9</i>	37	0.026	0.755	0.860	1.000	0.491	0.956	0.359	1.000
<i>PIK3CA</i>	335	0.028	0.755	0.907	1.000	0.362	0.956	0.701	1.000
<i>TLR8</i>	33	0.036	0.755	0.947	1.000	0.532	0.956	0.836	1.000
<i>AKT3</i>	541	0.038	0.755	0.812	1.000	0.474	0.956	0.559	1.000
<i>CTSK</i>	52	0.055	0.878	0.252	1.000	0.700	0.967	0.648	1.000
<i>IFNAR2</i>	163	0.058	0.878	0.812	1.000	0.248	0.951	0.025	0.820
<i>MAP2K6</i>	195	0.090	0.878	0.099	1.000	0.067	0.676	0.570	1.000
<i>STAT1</i>	172	0.103	0.878	0.981	1.000	0.652	0.956	0.868	1.000
<i>CASP8</i>	221	0.126	0.878	0.100	1.000	0.503	0.956	0.483	1.000
<i>IKBKB</i>	138	0.131	0.878	0.591	1.000	0.701	0.967	0.921	1.000
<i>TICAM2</i>	92	0.135	0.878	0.826	1.000	0.668	0.956	0.407	1.000
<i>IFNA2</i>	31	0.143	0.878	0.283	1.000	0.199	0.916	0.450	1.000
<i>MAPK13</i>	68	0.150	0.878	0.409	1.000	0.387	0.956	0.757	1.000
<i>MAP2K3</i>	38	0.150	0.878	0.473	1.000	0.332	0.956	0.777	1.000
<i>MAP3K8</i>	44	0.150	0.878	0.851	1.000	0.021	0.628	0.810	1.000

IL6	94	0.153	0.878	0.257	1.000	0.014	0.628	0.862	1.000
MAP3K7	291	0.154	0.878	0.885	1.000	0.079	0.676	0.448	1.000
IRAK4	123	0.167	0.878	0.775	1.000	0.334	0.956	0.306	1.000
IL12B	74	0.178	0.878	0.037	1.000	0.886	1.000	0.239	1.000
MAP2K7	58	0.178	0.878	0.724	1.000	0.967	1.000	0.354	1.000
IFNA6	62	0.180	0.878	0.156	1.000	0.459	0.956	0.353	1.000
CD86	206	0.184	0.878	0.443	1.000	0.092	0.676	0.240	1.000
JUN	34	0.216	0.895	0.617	1.000	0.771	0.978	0.632	1.000
PIK3CD	219	0.225	0.895	0.856	1.000	0.308	0.951	0.867	1.000
PIK3CB	288	0.235	0.895	0.998	1.000	0.772	0.978	0.954	1.000
TOLLIP	184	0.237	0.895	0.187	1.000	0.944	1.000	0.742	1.000
TICAM1	110	0.241	0.895	0.162	1.000	0.033	0.628	0.333	1.000
IKBKG	12	0.263	0.895	0.479	1.000	0.716	0.977	0.242	1.000
MAPK9	294	0.272	0.895	0.115	1.000	0.434	0.956	0.265	1.000
IFNA7	149	0.289	0.895	0.976	1.000	0.352	0.956	0.219	1.000
MAPK8	366	0.310	0.895	0.875	1.000	0.240	0.951	0.405	1.000
IFNA10	155	0.310	0.895	0.656	1.000	0.426	0.956	0.167	1.000
FADD	43	0.345	0.895	0.487	1.000	0.068	0.676	0.093	0.997
IFNA21	79	0.370	0.895	0.833	1.000	0.303	0.951	0.532	1.000
IFNA1	75	0.376	0.895	0.255	1.000	0.390	0.956	0.457	1.000
TLR7	9	0.377	0.895	0.281	1.000	0.660	0.956	0.774	1.000
IRF5	113	0.381	0.895	0.084	1.000	0.237	0.951	0.553	1.000
CFLAR	200	0.413	0.895	0.058	1.000	0.663	0.956	0.278	1.000
MAP2K4	218	0.417	0.895	0.698	1.000	0.859	1.000	0.931	1.000
IL12A	68	0.418	0.895	0.612	1.000	0.948	1.000	0.285	1.000
AKT2	163	0.420	0.895	0.328	1.000	0.306	0.951	0.774	1.000
TBK1	138	0.433	0.895	0.818	1.000	0.443	0.956	0.253	1.000
IFNA4	126	0.437	0.895	0.745	1.000	0.110	0.785	0.632	1.000
IRAK1	18	0.438	0.895	0.074	1.000	0.463	0.956	0.339	1.000
CCL5	78	0.447	0.895	0.593	1.000	0.992	1.000	0.041	0.944
IKBKE	108	0.468	0.895	0.866	1.000	0.629	0.956	0.041	0.944
MAP2K1	412	0.480	0.895	0.886	1.000	0.396	0.956	0.012	0.818

<i>CCL3</i>	6	0.481	0.895	0.585	1.000	0.443	0.956	0.444	1.000
<i>TLR1</i>	161	0.486	0.895	0.464	1.000	0.870	1.000	0.505	1.000
<i>CD40</i>	102	0.491	0.895	0.167	1.000	0.520	0.956	0.998	1.000
<i>MAPK14</i>	280	0.494	0.895	0.047	1.000	0.978	1.000	0.706	1.000
<i>CD14</i>	65	0.496	0.895	0.568	1.000	0.645	0.956	0.625	1.000
<i>IRF7</i>	93	0.497	0.895	0.137	1.000	0.042	0.648	0.196	1.000
<i>AKT1</i>	96	0.502	0.897	0.954	1.000	0.734	0.978	0.751	1.000
<i>IFNAR1</i>	157	0.512	0.901	0.845	1.000	0.602	0.956	0.102	0.997
<i>SPP1</i>	95	0.519	0.901	0.823	1.000	0.004	0.628	0.758	1.000
<i>CXCL8</i>	50	0.521	0.901	0.524	1.000	0.730	0.978	0.089	0.997
<i>CXCL10</i>	101	0.571	0.909	0.499	1.000	0.534	0.956	0.236	1.000
<i>IFNA8</i>	77	0.572	0.909	0.291	1.000	0.073	0.676	0.240	1.000
<i>MYD88</i>	36	0.577	0.909	0.212	1.000	0.200	0.916	0.185	1.000
<i>IFNB1</i>	71	0.612	0.920	0.947	1.000	0.456	0.956	0.226	1.000
<i>CXCL9</i>	58	0.633	0.946	0.318	1.000	0.611	0.956	0.248	1.000
<i>FOS</i>	48	0.646	0.947	0.728	1.000	0.079	0.676	0.251	1.000
<i>TLR4</i>	92	0.660	0.947	0.273	1.000	0.071	0.676	0.562	1.000
<i>PIK3R2</i>	98	0.663	0.947	0.411	1.000	0.803	0.992	0.778	1.000
<i>IFNA13</i>	85	0.689	0.949	0.523	1.000	0.334	0.956	0.324	1.000
<i>CD80</i>	245	0.716	0.949	0.352	1.000	0.813	0.996	0.076	0.997
<i>IFNA16</i>	167	0.722	0.949	0.692	1.000	0.505	0.956	0.101	0.997
<i>TIRAP</i>	102	0.723	0.949	0.478	1.000	0.132	0.852	0.785	1.000
<i>TLR5</i>	138	0.731	0.949	0.216	1.000	0.258	0.951	0.583	1.000
<i>MAPK3</i>	26	0.735	0.949	0.753	1.000	0.141	0.852	0.713	1.000
<i>RAC1</i>	232	0.757	0.959	0.990	1.000	0.239	0.951	0.419	1.000
<i>LY96</i>	172	0.778	0.974	0.349	1.000	0.032	0.628	0.654	1.000
<i>MAPK1</i>	336	0.817	0.974	0.234	1.000	0.854	1.000	0.299	1.000
<i>PIK3R1</i>	301	0.819	0.974	0.621	1.000	0.291	0.951	0.707	1.000
<i>IFNA17</i>	133	0.823	0.974	0.879	1.000	0.619	0.956	0.265	1.000
<i>IRF3</i>	32	0.824	0.974	0.975	1.000	0.483	0.956	0.770	1.000
<i>TLR3</i>	128	0.859	0.974	0.255	1.000	0.805	0.992	0.390	1.000
<i>TLR6</i>	163	0.860	0.974	0.195	1.000	0.765	0.978	0.728	1.000

<i>TLR2</i>	105	0.873	0.974	0.032	1.000	0.865	1.000	0.660	1.000
<i>CXCL11</i>	175	0.883	0.974	0.668	1.000	0.491	0.956	0.176	1.000
<i>MAP2K2</i>	91	0.886	0.974	0.638	1.000	0.879	1.000	0.837	1.000
<i>IFNA14</i>	89	0.900	0.975	0.722	1.000	0.578	0.956	0.239	1.000
<i>PIK3R3</i>	288	0.908	0.975	0.076	1.000	0.693	0.967	0.187	1.000
<i>CCL4</i>	9	0.913	0.975	0.726	1.000	0.793	0.992	0.377	1.000
<i>LBP</i>	146	0.921	0.975	0.763	1.000	0.993	1.000	0.333	1.000
<i>IL1B</i>	52	0.922	0.975	0.639	1.000	0.548	0.956	0.240	1.000
<i>MAPK10</i>	1854	0.943	0.985	0.125	1.000	0.737	0.978	0.702	1.000
<i>IFNA5</i>	60	0.944	0.985	0.412	1.000	0.196	0.916	0.330	1.000
<i>TAB2</i>	0 ^c								
<i>CCL3L1</i>	0 ^c								
<i>CCL3L3</i>	0 ^c								
<i>CCL4L1</i>	0 ^c								
<i>CCL4L2</i>	0 ^c								
<i>MAPK11</i>	0 ^d								
<i>MAPK12</i>	0 ^d								
TNF		0.050		0.157		0.135		0.493	
<i>MMP3</i>	88	0.003	0.755	0.740	1.000	0.622	0.956	0.963	1.000
<i>CX3CL1</i>	104	0.033	0.755	0.306	1.000	0.228	0.951	0.014	0.818
<i>CREB3L1</i>	100	0.047	0.859	0.923	1.000	0.277	0.951	0.779	1.000
<i>BAG4</i>	83	0.096	0.878	0.325	1.000	0.629	0.956	0.842	1.000
<i>TNFRSF1A</i>	37	0.104	0.878	0.312	1.000	0.008	0.628	0.775	1.000
<i>CEBPB</i>	40	0.112	0.878	0.056	1.000	0.620	0.956	0.856	1.000
<i>TRAF1</i>	162	0.175	0.878	0.606	1.000	0.516	0.956	0.712	1.000
<i>IL18R1</i>	270	0.182	0.878	0.394	1.000	0.257	0.951	0.686	1.000
<i>CXCL6</i>	40	0.183	0.878	0.653	1.000	0.286	0.951	0.547	1.000
<i>EDN1</i>	119	0.218	0.895	0.250	1.000	0.762	0.978	0.369	1.000
<i>TRAF2</i>	64	0.239	0.895	0.789	1.000	0.274	0.951	0.428	1.000
<i>SOCS3</i>	30	0.244	0.895	0.929	1.000	0.570	0.956	0.233	1.000
<i>CREB3L3</i>	28	0.253	0.895	0.563	1.000	0.995	1.000	0.963	1.000
<i>SELE</i>	202	0.264	0.895	0.070	1.000	0.337	0.956	0.507	1.000

<i>ATF6B</i>	76	0.285	0.895	0.992	1.000	0.531	0.956	0.000	0.041
<i>CREB3L2</i>	241	0.289	0.895	0.505	1.000	0.364	0.956	0.631	1.000
<i>TNFRSF1B</i>	102	0.297	0.895	0.187	1.000	0.629	0.956	0.066	0.997
<i>TNF</i>	81	0.318	0.895	0.731	1.000	0.645	0.956	0.646	1.000
<i>JAG1</i>	142	0.320	0.895	0.705	1.000	0.622	0.956	0.831	1.000
<i>NOD2</i>	104	0.322	0.895	0.966	1.000	0.063	0.676	0.744	1.000
<i>FAS</i>	226	0.373	0.895	0.612	1.000	0.688	0.967	0.621	1.000
<i>MLKL</i>	175	0.384	0.895	0.616	1.000	0.620	0.956	0.069	0.997
<i>VEGFC</i>	351	0.392	0.895	0.265	1.000	0.745	0.978	0.672	1.000
<i>CSF1</i>	86	0.416	0.895	0.635	1.000	0.606	0.956	0.909	1.000
<i>RPS6KA4</i>	89	0.439	0.895	0.660	1.000	0.213	0.951	0.975	1.000
<i>IL15</i>	251	0.441	0.895	0.630	1.000	0.501	0.956	0.876	1.000
<i>CASP3</i>	117	0.446	0.895	0.504	1.000	0.088	0.676	0.974	1.000
<i>DNM1L</i>	361	0.446	0.895	0.109	1.000	0.880	1.000	0.716	1.000
<i>CREB5</i>	1701	0.451	0.895	0.470	1.000	0.402	0.956	0.185	1.000
<i>DAB2IP</i>	564	0.479	0.895	0.021	1.000	0.175	0.871	0.850	1.000
<i>MMP9</i>	98	0.485	0.895	0.849	1.000	0.755	0.978	0.159	1.000
<i>PGAM5</i>	118	0.525	0.901	0.105	1.000	0.029	0.628	0.222	1.000
<i>CCL20</i>	10	0.533	0.901	0.897	1.000	0.036	0.628	0.808	1.000
<i>JUNB</i>	43	0.534	0.901	0.824	1.000	0.086	0.676	0.698	1.000
<i>CSF2</i>	48	0.555	0.909	0.405	1.000	0.884	1.000	0.313	1.000
<i>CCL2</i>	59	0.563	0.909	0.551	1.000	0.583	0.956	0.318	1.000
<i>ATF2</i>	281	0.602	0.911	0.886	1.000	0.091	0.676	0.074	0.997
<i>CREB1</i>	165	0.662	0.947	0.187	1.000	0.456	0.956	0.695	1.000
<i>CREB3</i>	33	0.662	0.947	0.234	1.000	0.637	0.956	0.427	1.000
<i>RPS6KA5</i>	521	0.665	0.947	0.457	1.000	0.155	0.852	0.749	1.000
<i>CXCL5</i>	16	0.669	0.948	0.417	1.000	0.506	0.956	0.238	1.000
<i>CASP10</i>	131	0.680	0.949	0.050	1.000	0.353	0.956	0.254	1.000
<i>CASP7</i>	232	0.703	0.949	0.717	1.000	0.286	0.951	0.625	1.000
<i>MMP14</i>	71	0.725	0.949	0.557	1.000	0.501	0.956	0.109	0.997
<i>RIPK3</i>	104	0.735	0.949	0.718	1.000	0.557	0.956	0.404	1.000
<i>MAP3K5</i>	437	0.802	0.974	0.660	1.000	0.773	0.978	0.375	1.000

<i>TRAF3</i>	336	0.829	0.974	0.405	1.000	0.902	1.000	0.518	1.000
<i>IRF1</i>	109	0.854	0.974	0.761	1.000	0.973	1.000	0.385	1.000
<i>TNFAIP3</i>	72	0.865	0.974	0.965	1.000	0.652	0.956	0.631	1.000
<i>ATF4</i>	20	0.889	0.974	0.252	1.000	0.310	0.951	0.941	1.000
<i>LIF</i>	65	0.919	0.975	0.928	1.000	0.896	1.000	0.025	0.820
<i>ITCH</i>	255	0.926	0.975	0.703	1.000	0.066	0.676	0.858	1.000
<i>TRAF5</i>	184	0.970	0.995	0.661	1.000	0.450	0.956	0.528	1.000
<i>CREB3L4</i>	36	0.984	0.995	0.738	1.000	0.088	0.676	0.996	1.000
<i>BCL3</i>	91	0.995	0.997	0.207	1.000	0.840	1.000	0.432	1.000

Abbreviations: TLR = toll-like receptor; NFkB = nuclear factor kappa B; TNF = tumor necrosis factor; EOC = epithelial ovarian cancer; HGSOC = high grade serous ovarian cancer; AACES = African American Cancer Epidemiology Study; OCAC = Ovarian Cancer Association Consortium;

^aAggregate P-value of MAGMA model results. Each model controls for age, and two ancestry principal components.

^bCorrected for multiple testing by the number of genes tested using the Benjamini-Hochberg false discovery rate (FDR).

^cNo SNPs mapped to gene after QC filtering.

^dGene chromosomal locations not on raw data file.

Supplementary Table ST6.1. RNASeq meta data.

main_metadata_table

ID	ran_in_pipeline	ClusterK2_kmeans	ClusterK3_kmeans	ClusterK4_kmeans	ClusterK2_NMF	ClusterK3_NMF	ClusterK4_NMF	ClusterK4_kmeans_TCGA_names	suid	external_HGSCsubtype_estimate	failed_seq	resequenced	under35M	low_start	version	REMOVE_WHITE	REMOVE_NEGADJ	REMOVE_LOW_EXPRESSION
18341X1	NA	NA	NA	NA	NA	NA	NA	NA	41580	C4.DIF	NA	NA	NA	NA	pilot	TRUE	NA	NA
18341X10	TRUE	1	1	1	1	2	2	Mesenchymal	45369	C4.DIF	NA	NA	NA	NA	pilot	NA	NA	NA
18341X11	NA	NA	NA	NA	NA	NA	NA	NA	46327	C1.MES	NA	NA	NA	NA	pilot	TRUE	NA	NA
18341X12	TRUE	2	2	2	2	2	2	Proliferative	47261	C5.PRO	NA	NA	NA	NA	pilot	NA	NA	NA
18341X13	TRUE	1	2	2	2	2	4	Proliferative	47791	C4.DIF	NA	NA	NA	NA	pilot	NA	NA	NA
18341X14	TRUE	2	3	3	2	3	3	Immunoreactive	47916	C4.DIF	NA	NA	NA	NA	pilot	NA	NA	NA
18341X15	TRUE	1	1	1	1	2	2	Mesenchymal	48002	C1.MES	NA	NA	NA	NA	pilot	NA	NA	NA
18341X17	TRUE	2	3	3	2	3	3	Immunoreactive	46782	C2.IMM	NA	NA	NA	NA	pilot	NA	NA	NA
18341X18	NA	NA	NA	NA	NA	NA	NA	NA	48123	C1.MES	NA	NA	NA	NA	pilot	TRUE	NA	NA
18341X19	NA	NA	NA	NA	NA	NA	NA	NA	45327	C2.IMM	NA	NA	NA	NA	pilot	TRUE	NA	NA
18341X2	NA	NA	NA	NA	NA	NA	NA	NA	41764	C4.DIF	NA	NA	NA	NA	pilot	TRUE	NA	NA
18341X20	NA	NA	NA	NA	NA	NA	NA	NA	47289	C5.PRO	NA	NA	NA	NA	pilot	TRUE	NA	NA
18341X21	NA	NA	NA	NA	NA	NA	NA	NA	48557	C5.PRO	NA	NA	NA	NA	pilot	TRUE	NA	NA
18341X22	TRUE	2	3	3	2	3	3	Immunoreactive	41736	C2.IMM	NA	NA	NA	NA	pilot	NA	NA	NA
18341X23	TRUE	1	1	1	2	3	3	Mesenchymal	42282	C1.MES	NA	NA	NA	NA	pilot	NA	NA	NA

Full tables available at:

https://github.com/greenelab/hgsc_characterization/blob/master/reference_data/main_AA_meta_data_table.tsv

https://github.com/greenelab/hgsc_characterization/blob/master/reference_data/main_white_me_tadata_table.tsv

Supplementary Table ST6.2. DEGs for HGSOc 5- year survival (no vs yes) among Black and White HGSOc cases.								
	Black women			White women				
	Mean	Log fold change ^a (95% CI)	<i>P</i>	<i>P</i> _{FDR} ^b	Mean	Log fold change ^a (95% CI)	<i>P</i>	<i>P</i> _{FDR} ^b
CXCL1	358	-0.2 (-0.5, 0.1)	0.454	0.853	362	-1.1 (-1.4, -0.9)	0.00003	0.003
CSF2	3	0.2 (-0.4, 0.9)	0.729	0.956	3	-2.2 (-2.7, -1.7)	0.00002	0.003
CXCL6	32	0.6 (0.2, 1)	0.132	0.637	29	-1.3 (-1.6, -1)	0.0001	0.006
BLNK	438	0.1 (-0.1, 0.2)	0.621	0.932	395	-0.5 (-0.7, -0.4)	0.0001	0.006
LTB	30	-0.4 (-0.8, 0.1)	0.381	0.822	32	-1.3 (-1.7, -1)	0.0002	0.009
TLR8	125	-0.3 (-0.5, -0.1)	0.092	0.637	98	-0.5 (-0.7, -0.4)	0.0004	0.016
LBP	18	-0.2 (-1.2, 0.8)	0.862	0.968	25	1.8 (1.2, 2.3)	0.002	0.066
CCL21	85	0.5 (0.2, 0.9)	0.128	0.637	76	0.9 (0.6, 1.2)	0.003	0.076
CTSK	1388	0.3 (0.1, 0.4)	0.057	0.637	921	0.4 (0.2, 0.5)	0.003	0.076
MAPK13	1132	-0.1 (-0.3, 0)	0.233	0.689	1221	-0.3 (-0.4, -0.2)	0.003	0.076
IL12A	112	-0.4 (-0.6, -0.1)	0.125	0.637	118	-0.6 (-0.8, -0.4)	0.005	0.099
CX3CL1	245	0.3 (0.1, 0.5)	0.070	0.637	290	-0.4 (-0.6, -0.3)	0.006	0.113
EDARADD	189	-0.6 (-0.9, -0.4)	0.013	0.407	161	0.5 (0.3, 0.8)	0.011	0.191
BCL2A1	123	-0.2 (-0.4, 0)	0.226	0.686	81	-0.4 (-0.6, -0.2)	0.017	0.267
CREB3	969	-0.1 (-0.2, 0)	0.189	0.655	1180	-0.2 (-0.3, -0.1)	0.021	0.304
CXCL12	1127	0.3 (0.1, 0.5)	0.082	0.637	976	0.3 (0.2, 0.5)	0.027	0.308
CARD11	1154	0.1 (-0.1, 0.3)	0.506	0.888	1185	0.4 (0.2, 0.5)	0.028	0.308
AKT3	1120	0.1 (-0.1, 0.3)	0.545	0.904	845	0.4 (0.2, 0.6)	0.028	0.308
TRAF5	2145	0 (-0.2, 0.1)	0.693	0.956	2093	-0.3 (-0.4, -0.1)	0.024	0.308
TNFSF11	14	0 (-0.4, 0.4)	0.978	0.999	12	0.9 (0.5, 1.4)	0.026	0.308
CD40LG	22	-0.4 (-0.7, -0.2)	0.101	0.637	14	-0.5 (-0.7, -0.3)	0.034	0.345
CXCL8	427	-0.4 (-0.6, -0.1)	0.135	0.637	286	-0.5 (-0.7, -0.2)	0.040	0.345
PLCG1	9728	0.1 (0, 0.2)	0.164	0.642	10004	0.2 (0.1, 0.3)	0.039	0.345
IFNA2	2	-1.6 (-3, -0.3)	0.223	0.686	2	1.6 (0.8, 2.3)	0.043	0.345
NOD2	481	-0.1 (-0.2, 0.1)	0.665	0.956	529	-0.3 (-0.4, -0.1)	0.035	0.345
CREB3L3	2	0 (-0.8, 0.8)	0.988	0.999	3	-1.3 (-2, -0.7)	0.037	0.345
NFKB2	3119	0 (-0.1, 0.1)	0.961	0.999	3868	-0.2 (-0.2, -0.1)	0.042	0.345

SELE	30	0.9 (0.6, 1.2)	0.002	0.132	22	0.6 (0.3, 0.9)	0.053	0.356
MMP14	5287	0.2 (0.1, 0.3)	0.074	0.637	4188	0.2 (0.1, 0.3)	0.051	0.356
VCAM1	856	0.2 (0, 0.3)	0.205	0.671	763	-0.3 (-0.4, -0.1)	0.051	0.356
MAPK1	2840	0.1 (0, 0.2)	0.502	0.888	2361	-0.2 (-0.3, -0.1)	0.050	0.356
CXCL2	134	-0.1 (-0.3, 0.2)	0.780	0.956	223	-0.5 (-0.7, -0.2)	0.047	0.356
RAC1	3319	0 (0, 0.1)	0.659	0.956	2550	0.2 (0.1, 0.2)	0.055	0.361
CARD14	167	0.5 (0.3, 0.7)	0.022	0.407	282	-0.3 (-0.5, -0.2)	0.057	0.364
TNFSF13B	209	-0.2 (-0.4, -0.1)	0.168	0.642	193	-0.2 (-0.4, -0.1)	0.065	0.401
CCL5	698	-0.2 (-0.4, -0.1)	0.114	0.637	714	-0.2 (-0.3, -0.1)	0.073	0.440
CXCL9	379	-0.8 (-1.1, -0.6)	0.002	0.124	385	-0.4 (-0.7, -0.2)	0.078	0.444
MLKL	330	-0.1 (-0.2, 0.1)	0.576	0.909	354	-0.2 (-0.3, -0.1)	0.076	0.444
MMP9	1221	-0.2 (-0.5, 0)	0.387	0.822	905	-0.4 (-0.6, -0.2)	0.082	0.455
GADD45B	608	0.2 (0.1, 0.4)	0.133	0.637	713	0.2 (0.1, 0.4)	0.088	0.457
CREB3L1	1279	0.2 (0, 0.4)	0.254	0.713	1311	0.3 (0.1, 0.4)	0.088	0.457
IRAK1	4574	0 (-0.1, 0.2)	0.724	0.956	5566	-0.2 (-0.3, -0.1)	0.087	0.457
EDA	189	0.3 (0.1, 0.5)	0.109	0.637	225	0.3 (0.1, 0.5)	0.094	0.460
CXCL3	70	-0.5 (-0.7, -0.2)	0.056	0.637	83	-0.4 (-0.6, -0.1)	0.093	0.460
MAP2K1	1388	0 (-0.1, 0.1)	0.860	0.968	1341	-0.1 (-0.2, 0)	0.095	0.460
VEGFC	422	0.2 (0, 0.4)	0.249	0.710	366	-0.3 (-0.4, -0.1)	0.100	0.466
MAPK14	1547	-0.1 (-0.2, 0)	0.363	0.811	1282	-0.1 (-0.2, -0.1)	0.101	0.466
BTK	301	-0.2 (-0.3, -0.1)	0.137	0.637	306	-0.2 (-0.3, -0.1)	0.106	0.471
MAP2K2	3643	-0.1 (-0.2, 0)	0.604	0.925	3827	-0.1 (-0.2, 0)	0.106	0.471
CCL13	16	-1.8 (-2.2, -1.3)	0.00002	0.005	15	-0.6 (-1, -0.2)	0.109	0.471
PLAU	1413	0.4 (0.2, 0.5)	0.028	0.470	1291	0.2 (0.1, 0.3)	0.113	0.471
RELB	1174	0.1 (-0.1, 0.2)	0.687	0.956	1248	-0.2 (-0.3, -0.1)	0.111	0.471
TRAF3	1519	-0.1 (-0.2, 0)	0.340	0.787	1411	-0.1 (-0.2, 0)	0.118	0.483
LAT	381	-0.1 (-0.3, 0)	0.326	0.763	523	-0.2 (-0.3, -0.1)	0.124	0.497
BCL10	914	-0.2 (-0.3, -0.1)	0.056	0.637	838	-0.1 (-0.2, 0)	0.135	0.516
TNF	79	-0.5 (-0.8, -0.2)	0.108	0.637	87	-0.4 (-0.6, -0.1)	0.142	0.516
ITCH	7029	-0.1 (-0.1, 0)	0.403	0.822	6604	0.1 (0, 0.2)	0.143	0.516
CXCL5	33	-0.3 (-0.7, 0.1)	0.410	0.822	40	-0.6 (-1, -0.2)	0.143	0.516

BIRC3	2106	-0.1 (-0.3, 0.1)	0.724	0.956	2486	-0.3 (-0.4, -0.1)	0.132	0.516
TRAF1	447	0 (-0.2, 0.1)	0.755	0.956	507	0.2 (0, 0.3)	0.141	0.516
JUNB	3168	0.3 (0.1, 0.5)	0.064	0.637	4242	0.2 (0.1, 0.3)	0.150	0.532
CSNK2A3	64	0.3 (0, 0.5)	0.315	0.752	48	-0.3 (-0.5, -0.1)	0.160	0.535
TRADD	224	-0.1 (-0.3, 0)	0.427	0.831	250	-0.2 (-0.3, 0)	0.157	0.535
GADD45A	485	0 (-0.2, 0.1)	0.713	0.956	541	-0.2 (-0.3, 0)	0.160	0.535
CASP7	701	0 (-0.1, 0.1)	0.891	0.972	646	-0.1 (-0.2, 0)	0.160	0.535
LYN	1536	-0.1 (-0.2, 0)	0.363	0.811	1438	-0.1 (-0.2, 0)	0.166	0.547
TNFRSF1A	5894	-0.1 (-0.2, 0)	0.311	0.752	6120	0.1 (0, 0.2)	0.174	0.564
TLR7	280	-0.1 (-0.3, 0)	0.306	0.752	224	0.1 (0, 0.3)	0.180	0.575
CCL19	27	0.6 (0.3, 1)	0.042	0.637	25	0.4 (0.1, 0.8)	0.192	0.605
IFNAR1	3595	-0.2 (-0.3, -0.1)	0.102	0.637	2709	0.1 (0, 0.2)	0.201	0.605
MALT1	2874	0.1 (0, 0.2)	0.382	0.822	2159	-0.1 (-0.2, 0)	0.195	0.605
TIRAP	281	0 (-0.1, 0.1)	0.998	0.999	334	-0.1 (-0.2, 0)	0.198	0.605
CFLAR	4891	-0.1 (-0.1, 0)	0.315	0.752	5695	-0.1 (-0.2, 0)	0.208	0.610
TLR4	1143	0 (-0.2, 0.1)	0.779	0.956	884	0.1 (0, 0.2)	0.207	0.610
CXCL11	201	-0.5 (-0.8, -0.2)	0.101	0.637	171	-0.3 (-0.6, -0.1)	0.215	0.623
AKT2	6983	0.1 (0, 0.2)	0.247	0.710	7273	0.1 (0, 0.2)	0.255	0.628
PIDD1	539	-0.2 (-0.3, 0)	0.312	0.752	866	0.1 (0, 0.2)	0.231	0.628
CASP10	638	-0.1 (-0.2, 0)	0.359	0.811	710	-0.1 (-0.3, 0)	0.239	0.628
CSNK2A2	2259	0.1 (0, 0.1)	0.508	0.888	2306	-0.1 (-0.2, 0)	0.233	0.628
TRIM25	3568	-0.1 (-0.1, 0)	0.493	0.888	3812	-0.1 (-0.2, 0)	0.254	0.628
IFNB1	2	0.3 (-0.2, 0.8)	0.562	0.909	1	-0.6 (-1.1, -0.1)	0.237	0.628
TICAM2	10	0.2 (-0.2, 0.6)	0.596	0.919	5	0.5 (0.1, 0.9)	0.233	0.628
CARD10	939	-0.1 (-0.2, 0.1)	0.619	0.932	1160	-0.2 (-0.3, 0)	0.244	0.628
UBE2I	3720	0 (-0.1, 0.1)	0.801	0.968	3072	-0.1 (-0.2, 0)	0.252	0.628
CCL20	127	-0.1 (-0.4, 0.3)	0.835	0.968	148	-0.4 (-0.7, -0.1)	0.226	0.628
RIPK1	1588	0 (-0.1, 0.1)	0.851	0.968	1689	-0.1 (-0.2, 0)	0.253	0.628
CREB3L2	1847	0 (-0.1, 0.1)	0.815	0.968	2141	-0.1 (-0.2, 0)	0.237	0.628
CEBPB	3421	0 (-0.1, 0.1)	0.985	0.999	5088	-0.1 (-0.2, 0)	0.242	0.628
CXCL10	839	-0.6 (-0.8, -0.3)	0.020	0.407	756	-0.2 (-0.4, 0)	0.269	0.641

PIK3R3	917	-0.1 (-0.2, 0.1)	0.684	0.956	743	-0.1 (-0.3, 0)	0.266	0.641
IFNA21	0	1.1 (-2, 4.2)	0.724	0.956	2	3.5 (0.4, 6.7)	0.265	0.641
MMP3	31	0.1 (-1.2, 1.4)	0.946	0.990	24	-0.6 (-1.2, 0)	0.284	0.669
IL1R1	5195	0 (-0.1, 0.2)	0.871	0.968	4266	0.1 (0, 0.2)	0.289	0.674
CSNK2B	3	1.2 (-0.2, 2.7)	0.396	0.822	2	-1.6 (-3.1, -0.1)	0.294	0.678
LTBR	3988	0 (-0.1, 0.1)	0.739	0.956	5052	0.1 (0, 0.2)	0.300	0.686
LY96	140	-0.1 (-0.2, 0.1)	0.690	0.956	73	0.1 (0, 0.3)	0.309	0.699
CD80	68	0 (-0.2, 0.2)	0.992	0.999	75	-0.2 (-0.3, 0)	0.317	0.710
RPS6KA5	826	0 (-0.1, 0.1)	0.827	0.968	791	-0.1 (-0.2, 0)	0.327	0.723
RELA	4709	0.1 (0.1, 0.2)	0.075	0.637	4538	-0.1 (-0.1, 0)	0.337	0.726
NFKBIA	6278	0.2 (0, 0.3)	0.182	0.653	6887	-0.1 (-0.2, 0)	0.333	0.726
IKBKB	3996	0 (-0.1, 0.1)	0.745	0.956	4738	0.1 (0, 0.2)	0.338	0.726
TAB3	2896	-0.1 (-0.2, 0)	0.265	0.726	2661	-0.1 (-0.2, 0)	0.354	0.741
SOCS3	1088	0.2 (0, 0.4)	0.283	0.738	1738	-0.1 (-0.3, 0)	0.354	0.741
RPS6KA4	1032	0 (-0.1, 0.1)	0.905	0.972	1332	0.1 (0, 0.2)	0.355	0.741
PIK3CA	5849	-0.1 (-0.2, -0.1)	0.125	0.637	4864	0.1 (0, 0.2)	0.383	0.750
MAPK10	473	0.2 (0.1, 0.4)	0.158	0.642	456	-0.1 (-0.3, 0)	0.382	0.750
IFNA13	5	-1.5 (-2.7, -0.4)	0.167	0.642	2	0.7 (-0.1, 1.5)	0.368	0.750
EDN1	272	-0.2 (-0.4, 0)	0.218	0.686	319	-0.2 (-0.3, 0)	0.375	0.750
TBK1	2863	-0.1 (-0.2, 0)	0.407	0.822	2186	-0.1 (-0.2, 0)	0.370	0.750
GADD45G	94	-0.2 (-0.4, 0.1)	0.491	0.888	103	-0.2 (-0.3, 0)	0.374	0.750
TNFRSF13C	53	0 (-0.2, 0.2)	0.860	0.968	61	0.1 (0, 0.3)	0.382	0.750
BCL2	227	0.1 (-0.1, 0.3)	0.518	0.892	176	0.1 (0, 0.3)	0.398	0.762
NFKB1	2224	0 (0, 0.1)	0.669	0.956	2240	0.1 (0, 0.1)	0.395	0.762
ATF2	5713	0 (-0.1, 0.1)	0.910	0.972	5197	-0.1 (-0.1, 0)	0.401	0.762
LCK	137	-0.1 (-0.3, 0.1)	0.579	0.909	143	-0.1 (-0.3, 0)	0.417	0.786
PIK3R2	3378	0.1 (0, 0.2)	0.415	0.822	4530	0.1 (0, 0.2)	0.441	0.808
DAB2IP	4088	0.1 (0, 0.2)	0.419	0.823	5308	0.1 (0, 0.2)	0.435	0.808
TNFAIP3	3734	-0.1 (-0.2, 0)	0.439	0.833	4393	-0.1 (-0.2, 0)	0.437	0.808
MAP3K8	1456	-0.1 (-0.2, 0)	0.546	0.904	1795	-0.1 (-0.2, 0)	0.443	0.808
STAT1	16431	-0.2 (-0.3, -0.1)	0.058	0.637	15719	-0.1 (-0.2, 0)	0.454	0.814

TLR1	602	-0.1 (-0.2, 0)	0.229	0.686	498	-0.1 (-0.2, 0)	0.451	0.814
BCL3	2820	0.1 (0, 0.3)	0.365	0.811	3473	-0.1 (-0.2, 0)	0.476	0.815
IL12B	4	-0.3 (-0.8, 0.2)	0.513	0.890	3	0.3 (-0.1, 0.8)	0.471	0.815
RIPK3	283	0 (-0.1, 0.2)	0.780	0.956	381	0.1 (0, 0.2)	0.472	0.815
MAPK12	299	0 (-0.2, 0.1)	0.775	0.956	333	0.1 (0, 0.2)	0.476	0.815
TLR3	950	0 (-0.1, 0.2)	0.868	0.968	837	0.1 (0, 0.2)	0.477	0.815
CCL4	87	-0.1 (-0.3, 0.2)	0.829	0.968	71	0.2 (-0.1, 0.4)	0.465	0.815
CCL2	1416	0 (-0.1, 0.2)	0.823	0.968	1058	-0.1 (-0.2, 0)	0.483	0.819
FOS	11158	0.4 (0.2, 0.6)	0.022	0.407	14841	0.1 (-0.1, 0.3)	0.549	0.822
TRAF2	1359	-0.2 (-0.3, -0.1)	0.048	0.637	1806	-0.1 (-0.2, 0)	0.517	0.822
JUN	7169	0.2 (0.1, 0.3)	0.116	0.637	8752	-0.1 (-0.2, 0)	0.510	0.822
CHUK	1605	-0.1 (-0.2, 0)	0.145	0.637	1109	-0.1 (-0.1, 0)	0.540	0.822
PIK3CD	1445	-0.1 (-0.3, 0)	0.272	0.727	1656	-0.1 (-0.1, 0)	0.549	0.822
MAP2K7	1044	-0.1 (-0.2, 0)	0.292	0.752	1120	-0.1 (-0.2, 0)	0.513	0.822
PIAS4	911	0.1 (0, 0.2)	0.383	0.822	1102	-0.1 (-0.1, 0)	0.511	0.822
EDAR	71	-0.3 (-0.6, 0.1)	0.414	0.822	75	0.2 (-0.1, 0.5)	0.546	0.822
AKT1	8755	0.1 (0, 0.2)	0.398	0.822	8850	0 (-0.1, 0)	0.523	0.822
ICAM1	2389	-0.1 (-0.3, 0.1)	0.479	0.880	2369	-0.1 (-0.2, 0.1)	0.527	0.822
CYLD	2661	-0.1 (-0.1, 0)	0.498	0.888	2416	0 (-0.1, 0)	0.509	0.822
PGAM5	910	0.1 (0, 0.2)	0.535	0.904	1014	-0.1 (-0.1, 0)	0.541	0.822
TNFRSF1B	489	0.1 (-0.1, 0.2)	0.562	0.909	604	-0.1 (-0.2, 0)	0.524	0.822
TLR6	309	0.1 (-0.1, 0.2)	0.568	0.909	251	-0.1 (-0.2, 0)	0.537	0.822
PIK3CB	4550	0 (-0.1, 0.1)	0.872	0.968	3903	-0.1 (-0.1, 0)	0.506	0.822
MAPK8	1453	0 (-0.1, 0.1)	0.911	0.972	1098	-0.1 (-0.1, 0)	0.496	0.822
FADD	721	0 (-0.1, 0.1)	0.908	0.972	660	0 (-0.1, 0)	0.515	0.822
TLR9	70	-0.2 (-1.3, 0.8)	0.822	0.968	69	0.2 (-0.2, 0.6)	0.554	0.824
ZAP70	201	-0.1 (-0.3, 0.1)	0.649	0.956	246	-0.1 (-0.2, 0.1)	0.562	0.829
MAPK11	110	0.4 (0.2, 0.5)	0.060	0.637	131	0.1 (-0.1, 0.2)	0.573	0.833
ATF6B	4104	-0.3 (-0.4, -0.1)	0.068	0.637	3445	-0.1 (-0.3, 0.1)	0.576	0.833
TLR2	739	-0.1 (-0.2, 0)	0.224	0.686	716	-0.1 (-0.2, 0)	0.572	0.833
CASP8	1484	-0.2 (-0.3, -0.1)	0.015	0.407	1421	0 (-0.1, 0)	0.594	0.847

MAP3K7	3579	0 (-0.1, 0)	0.542	0.904	3136	0 (0, 0.1)	0.593	0.847
CREB3L4	828	0 (-0.1, 0.1)	0.834	0.968	874	0.1 (0, 0.1)	0.604	0.857
IRF3	2329	-0.2 (-0.3, 0)	0.173	0.642	2797	0 (0, 0.1)	0.635	0.862
PIK3R1	5051	0.2 (0.1, 0.3)	0.160	0.642	4313	-0.1 (-0.2, 0.1)	0.635	0.862
TOLLIP	517	0.1 (0, 0.2)	0.431	0.833	574	0 (-0.1, 0)	0.628	0.862
MAPK3	2910	0.1 (0, 0.2)	0.436	0.833	2816	0 (-0.1, 0)	0.622	0.862
SPP1	11058	-0.1 (-0.2, 0.1)	0.723	0.956	8657	-0.1 (-0.2, 0.1)	0.635	0.862
ATF4	4463	0 (-0.1, 0.1)	0.772	0.956	5985	0 (-0.1, 0)	0.630	0.862
IKBKE	1403	0 (-0.1, 0.1)	0.876	0.968	1583	-0.1 (-0.2, 0.1)	0.623	0.862
TICAM1	925	-0.2 (-0.3, -0.1)	0.140	0.637	1031	0 (-0.1, 0.1)	0.663	0.876
IFNA5	1	1.4 (0.4, 2.4)	0.162	0.642	1	-0.3 (-1, 0.4)	0.659	0.876
CD14	644	0 (-0.1, 0.2)	0.722	0.956	635	0 (-0.2, 0.1)	0.662	0.876
BCL2L1	2416	0 (-0.1, 0.1)	0.765	0.956	2129	0 (-0.1, 0)	0.666	0.876
LTA	4	0.1 (-1.8, 1.9)	0.974	0.999	7	0.4 (-0.5, 1.4)	0.656	0.876
TRAF6	1019	-0.1 (-0.2, 0)	0.197	0.663	956	0 (-0.1, 0)	0.679	0.888
IFNA8	2	0 (-3.1, 3.2)	0.991	0.999	0	-1.3 (-4.4, 1.9)	0.687	0.893
JAG1	4935	0.4 (0.2, 0.5)	0.009	0.407	4451	0 (-0.1, 0.2)	0.696	0.896
MAPK9	1685	-0.1 (-0.2, 0)	0.119	0.637	1382	0 (-0.1, 0.1)	0.699	0.896
IRF5	257	0.1 (0, 0.3)	0.472	0.874	347	0 (-0.2, 0.1)	0.706	0.896
FAS	2295	0 (-0.1, 0.1)	0.999	0.999	1765	0 (-0.1, 0.2)	0.702	0.896
DNM1L	7247	-0.2 (-0.3, -0.1)	0.016	0.407	5932	0 (-0.1, 0.1)	0.776	0.920
MAP2K6	678	-0.2 (-0.4, -0.1)	0.143	0.637	521	0 (-0.1, 0.2)	0.745	0.920
IRF1	2204	-0.2 (-0.3, -0.1)	0.142	0.637	2727	0 (-0.1, 0.1)	0.769	0.920
IFNAR2	1075	-0.2 (-0.3, 0)	0.146	0.637	857	0 (-0.1, 0.1)	0.759	0.920
CCL3L1	36	0.6 (0.2, 1.1)	0.173	0.642	14	-0.2 (-1, 0.5)	0.768	0.920
TAB2	17354	-0.1 (-0.2, 0)	0.185	0.653	13306	0 (-0.1, 0.1)	0.770	0.920
TNFRSF11A	109	0.2 (0.1, 0.4)	0.185	0.653	125	0 (-0.1, 0.2)	0.752	0.920
TNFSF14	47	-0.3 (-0.6, -0.1)	0.206	0.671	92	0.1 (-0.2, 0.3)	0.754	0.920
XIAP	9666	-0.1 (-0.2, 0)	0.214	0.686	6847	0 (-0.1, 0.1)	0.737	0.920
LIF	751	-0.2 (-0.4, 0)	0.391	0.822	950	0.1 (-0.1, 0.2)	0.745	0.920
PARP1	10820	0 (-0.1, 0)	0.625	0.932	9814	0 (-0.1, 0.1)	0.775	0.920

IFNA1	1	-0.6 (-2.7, 1.4)	0.761	0.956	1	-0.4 (-1.8, 0.9)	0.752	0.920
TLR5	896	0.2 (0, 0.3)	0.250	0.710	813	0 (-0.2, 0.1)	0.801	0.940
CREB1	1922	0 (-0.1, 0)	0.612	0.930	1798	0 (0, 0.1)	0.801	0.940
TAB1	779	0.3 (0.1, 0.4)	0.021	0.407	942	0 (-0.1, 0.1)	0.808	0.942
EDA2R	49	-0.4 (-0.6, -0.1)	0.123	0.637	35	0 (-0.2, 0.2)	0.820	0.945
CSNK2A1	5836	-0.1 (-0.2, 0)	0.172	0.642	4793	0 (-0.1, 0.1)	0.823	0.945
CD40	516	0 (-0.2, 0.1)	0.880	0.968	654	0 (-0.1, 0.1)	0.818	0.945
BIRC2	2794	0.1 (0, 0.2)	0.581	0.909	2601	0 (-0.1, 0.1)	0.845	0.960
SYK	2973	0 (-0.1, 0.2)	0.747	0.956	2627	0 (-0.1, 0.1)	0.845	0.960
IL6	134	0 (-0.3, 0.2)	0.915	0.972	152	0 (-0.3, 0.2)	0.854	0.966
IKBKG	529	0 (-0.1, 0.2)	0.848	0.968	726	0 (-0.1, 0.1)	0.862	0.969
CREB5	1113	0.6 (0.4, 0.7)	0.0002	0.018	1210	0 (-0.1, 0.2)	0.885	0.976
CASP3	594	-0.2 (-0.3, 0)	0.138	0.637	401	0 (-0.1, 0.1)	0.893	0.976
PLCG2	4337	0.1 (0, 0.3)	0.271	0.727	5083	0 (-0.1, 0.1)	0.891	0.976
PRKCQ	1134	-0.2 (-0.3, 0)	0.304	0.752	1047	0 (-0.2, 0.1)	0.895	0.976
IFNA16	0	0.6 (-2.5, 3.7)	0.851	0.968	0	0.4 (-2.7, 3.6)	0.886	0.976
IRF7	128	0.2 (-2.1, 2.5)	0.933	0.982	205	-0.1 (-0.6, 0.5)	0.884	0.976
IFNA6	1	0.7 (-1.7, 3.2)	0.757	0.956	0	0.2 (-1.4, 1.8)	0.903	0.977
MAP2K3	1489	0 (-0.1, 0.1)	0.837	0.968	1747	0 (-0.1, 0.1)	0.905	0.977
BAG4	2383	0.2 (0.1, 0.3)	0.072	0.637	2383	0 (-0.1, 0.1)	0.916	0.984
CD86	184	-0.2 (-0.4, -0.1)	0.091	0.637	161	0 (-0.1, 0.1)	0.929	0.988
IL1B	243	0.1 (-0.1, 0.3)	0.466	0.869	261	0 (-0.1, 0.2)	0.929	0.988
CSF1	1000	0.1 (0, 0.3)	0.325	0.763	1217	0 (-0.1, 0.1)	0.940	0.990
ERC1	9795	0.1 (0, 0.2)	0.529	0.904	11550	0 (-0.1, 0.1)	0.939	0.990
IRAK4	681	0 (-0.2, 0.1)	0.673	0.956	572	0 (-0.1, 0.1)	0.945	0.991
IL15	121	-0.2 (-0.4, -0.1)	0.193	0.658	123	0 (-0.2, 0.2)	0.957	0.994
MYD88	1030	0 (-0.1, 0.1)	0.712	0.956	887	0 (-0.1, 0.1)	0.957	0.994
MAP2K4	876	-0.1 (-0.2, 0)	0.585	0.909	701	0 (-0.1, 0.1)	0.963	0.995
MAP3K5	2762	0 (-0.1, 0.1)	0.702	0.956	2465	0 (-0.1, 0.1)	0.970	0.998
IL18R1	186	-0.2 (-0.4, 0)	0.261	0.725	149	0 (-0.2, 0.2)	0.986	0.999
ATM	17847	-0.1 (-0.2, 0)	0.281	0.738	15600	0 (-0.1, 0.1)	0.995	0.999

PRKCB	355	0.2 (0, 0.3)	0.296	0.752	348	0 (-0.1, 0.1)	0.999	0.999
MAP3K14	1278	0.1 (0, 0.2)	0.575	0.909	1419	0 (-0.1, 0.1)	0.985	0.999
CCL3	108	-0.1 (-0.3, 0.1)	0.763	0.956	105	0 (-0.2, 0.2)	0.994	0.999
PTGS2	400	-0.1 (-0.3, 0.2)	0.810	0.968	367	0 (-0.2, 0.2)	0.979	0.999
IFNA4	0	1.7 (-1.4, 4.9)	0.581	0.909	0	0.1 (-3, 3.3)	0.969	1.00
IFNA14	0	0.9 (-2.2, 4)	0.774	0.956	0	0.3 (-2.9, 3.4)	0.933	1.00
IFNA17	0	-0.3 (-3.5, 2.8)	0.912	0.972	0	0 (-3.2, 3.1)	0.994	1.00
IFNA7	0	0.3 (-2.9, 3.4)	0.932	0.982	0	0.4 (-2.8, 3.5)	0.912	1.00
IFNA10	0	0.1 (-3, 3.2)	0.976	0.999	0	-0.8 (-4, 2.4)	0.801	1.00

Abbreviations: TLR = toll-like receptor; NFkB = nuclear factor kappa B; TNF = tumor necrosis factor; EOC = epithelial ovarian cancer; HGSOC = high grade serous ovarian cancer; AACES = African American Cancer Epidemiology Study; OCAC = Ovarian Cancer Association Consortium;

^aAdjusted for age, tumor purity, and two ancestry principal components.

^bCorrected for the number of genes tested using the Benjamini-Hochberg false discovery rate (FDR).

Supplementary Table ST6.3. Cox proportional hazard models to assess high/low RNA expression in association with 5-year Survival (no/yes) in TLR, NFKB, TNF genes among Black and White HGSOC cases.

Gene	Black cases		White cases	
	HR (95% CI) ^a	p	HR (95% CI) ^a	p
<i>BLNK</i>	1.02 (0.74, 1.41)	0.899	0.63 (0.48, 0.83)	0.001
<i>CD80</i>	1.02 (0.73, 1.41)	0.921	0.64 (0.48, 0.84)	0.001
<i>MLKL</i>	1 (0.72, 1.38)	0.997	0.64 (0.49, 0.84)	0.002
<i>NOD2</i>	0.89 (0.64, 1.23)	0.473	0.69 (0.52, 0.9)	0.007
<i>CXCL9</i>	0.67 (0.48, 0.93)	0.017	0.68 (0.51, 0.9)	0.007
<i>TICAM1</i>	1.23 (0.89, 1.71)	0.213	0.7 (0.53, 0.92)	0.010
<i>CXCL6</i>	0.98 (0.71, 1.36)	0.908	0.7 (0.53, 0.92)	0.012
<i>CX3CL1</i>	1.1 (0.8, 1.52)	0.565	0.71 (0.54, 0.93)	0.014
<i>MAPK13</i>	0.95 (0.69, 1.31)	0.745	0.72 (0.55, 0.94)	0.018
<i>FADD</i>	0.98 (0.71, 1.35)	0.909	0.72 (0.54, 0.95)	0.018
<i>PIK3R2</i>	1.18 (0.85, 1.65)	0.324	1.37 (1.04, 1.8)	0.024
<i>MAP3K7</i>	0.74 (0.54, 1.03)	0.071	1.32 (1.01, 1.73)	0.043
<i>LYN</i>	0.85 (0.61, 1.19)	0.356	0.75 (0.57, 0.99)	0.044
<i>TNFSF13B</i>	0.84 (0.6, 1.17)	0.294	0.76 (0.58, 1)	0.047
<i>TAB2</i>	0.77 (0.56, 1.07)	0.119	1.32 (1, 1.75)	0.047
<i>CCL21</i>	1 (0.72, 1.38)	0.996	1.32 (1, 1.74)	0.047
<i>MAP2K1</i>	0.95 (0.69, 1.31)	0.760	0.76 (0.58, 1)	0.049
<i>TRADD</i>	1 (0.73, 1.38)	0.976	0.76 (0.58, 1)	0.051
<i>IL6</i>	1.05 (0.76, 1.45)	0.751	0.77 (0.58, 1.01)	0.058
<i>ICAM1</i>	1.02 (0.74, 1.41)	0.907	0.77 (0.59, 1.01)	0.060
<i>CASP7</i>	0.84 (0.61, 1.15)	0.276	0.77 (0.59, 1.01)	0.060
<i>TNFAIP3</i>	1 (0.72, 1.38)	0.977	0.77 (0.59, 1.01)	0.061
<i>CREB5</i>	1.89 (1.36, 2.62)	0.000	1.29 (0.99, 1.7)	0.063
<i>CTSK</i>	1.1 (0.8, 1.52)	0.563	1.29 (0.99, 1.7)	0.063
<i>ZAP70</i>	1.05 (0.76, 1.45)	0.779	0.78 (0.59, 1.02)	0.072
<i>CXCL10</i>	0.72 (0.52, 1)	0.047	0.78 (0.59, 1.03)	0.079

<i>IRAK1</i>	1.31 (0.94, 1.82)	0.113	0.78 (0.59, 1.03)	0.082
<i>TICAM2</i>	1.22 (0.88, 1.68)	0.233	1.28 (0.97, 1.69)	0.084
<i>PIK3R3</i>	1.03 (0.75, 1.43)	0.852	0.79 (0.6, 1.03)	0.084
<i>TLR8</i>	0.8 (0.58, 1.11)	0.184	0.78 (0.59, 1.03)	0.084
<i>ITCH</i>	0.83 (0.6, 1.16)	0.277	1.27 (0.97, 1.67)	0.088
<i>CXCL11</i>	0.67 (0.49, 0.93)	0.017	0.79 (0.6, 1.04)	0.090
<i>RELB</i>	1.46 (1.05, 2.04)	0.026	0.79 (0.6, 1.04)	0.090
<i>CREB3L1</i>	1.21 (0.87, 1.67)	0.254	1.26 (0.96, 1.66)	0.090
<i>CARD14</i>	1.49 (1.06, 2.08)	0.021	0.79 (0.6, 1.04)	0.097
<i>PIDD1</i>	0.89 (0.65, 1.23)	0.474	1.26 (0.96, 1.65)	0.100
<i>MAPK14</i>	0.92 (0.67, 1.27)	0.633	0.8 (0.61, 1.05)	0.111
<i>CXCL1</i>	0.76 (0.54, 1.05)	0.097	0.8 (0.61, 1.05)	0.113
<i>CARD10</i>	0.75 (0.54, 1.04)	0.084	0.81 (0.62, 1.05)	0.115
<i>TLR3</i>	1.08 (0.78, 1.5)	0.640	1.24 (0.94, 1.63)	0.123
<i>MAPK9</i>	0.79 (0.57, 1.1)	0.161	1.24 (0.94, 1.62)	0.123
<i>CCL13</i>	0.74 (0.53, 1.02)	0.068	0.8 (0.61, 1.06)	0.124
<i>XIAP</i>	0.9 (0.65, 1.24)	0.515	0.81 (0.61, 1.07)	0.130
<i>CCL5</i>	0.95 (0.69, 1.31)	0.752	0.81 (0.62, 1.07)	0.138
<i>AKT3</i>	1.22 (0.89, 1.69)	0.215	1.23 (0.94, 1.61)	0.140
<i>TNFRSF1A</i>	1.11 (0.81, 1.53)	0.513	1.22 (0.93, 1.6)	0.148
<i>LCK</i>	1.13 (0.82, 1.56)	0.455	0.82 (0.62, 1.07)	0.148
<i>TNFSF11</i>	0.94 (0.68, 1.3)	0.716	1.22 (0.93, 1.6)	0.149
<i>BCL2A1</i>	0.86 (0.62, 1.18)	0.346	0.82 (0.62, 1.08)	0.155
<i>BCL10</i>	0.66 (0.48, 0.93)	0.016	0.82 (0.63, 1.08)	0.161
<i>RIPK3</i>	1.24 (0.9, 1.72)	0.195	0.83 (0.63, 1.09)	0.181
<i>IRF1</i>	0.99 (0.71, 1.36)	0.936	0.83 (0.63, 1.09)	0.181
<i>CCL2</i>	0.86 (0.62, 1.19)	0.352	0.83 (0.63, 1.09)	0.183
<i>GADD45A</i>	1 (0.72, 1.38)	0.988	0.83 (0.64, 1.09)	0.191
<i>RIPK1</i>	0.92 (0.67, 1.27)	0.606	0.84 (0.64, 1.1)	0.204
<i>GADD45G</i>	0.99 (0.72, 1.36)	0.926	0.84 (0.64, 1.1)	0.210
<i>TRAF3</i>	0.88 (0.63, 1.23)	0.454	0.84 (0.64, 1.11)	0.221
<i>TNF</i>	0.84 (0.61, 1.16)	0.290	0.84 (0.64, 1.11)	0.223

<i>IFNAR2</i>	0.82 (0.59, 1.13)	0.222	1.18 (0.9, 1.55)	0.228
<i>IKBKB</i>	1.3 (0.94, 1.8)	0.111	1.18 (0.9, 1.56)	0.237
<i>PIK3CB</i>	1.04 (0.76, 1.43)	0.810	1.18 (0.9, 1.55)	0.240
<i>TNFRSF11A</i>	1.44 (1.04, 2.01)	0.029	0.85 (0.65, 1.12)	0.240
<i>CCL19</i>	1.16 (0.83, 1.61)	0.380	0.85 (0.64, 1.12)	0.240
<i>CARD11</i>	1.32 (0.95, 1.84)	0.095	1.17 (0.9, 1.54)	0.244
<i>STAT1</i>	0.8 (0.58, 1.1)	0.167	0.85 (0.64, 1.12)	0.244
<i>TLR9</i>	1.06 (0.77, 1.46)	0.725	1.18 (0.89, 1.55)	0.250
<i>BCL3</i>	0.93 (0.67, 1.3)	0.669	0.85 (0.65, 1.12)	0.261
<i>LIF</i>	0.88 (0.63, 1.21)	0.433	1.17 (0.89, 1.54)	0.263
<i>ERC1</i>	0.99 (0.72, 1.37)	0.973	1.17 (0.89, 1.53)	0.269
<i>PIK3R1</i>	1.06 (0.77, 1.46)	0.731	1.17 (0.89, 1.54)	0.269
<i>MYD88</i>	1.33 (0.96, 1.86)	0.086	0.86 (0.65, 1.13)	0.273
<i>NFKB2</i>	1.13 (0.82, 1.57)	0.462	0.86 (0.66, 1.13)	0.278
<i>PRKCQ</i>	0.96 (0.69, 1.33)	0.796	1.16 (0.88, 1.51)	0.288
<i>CD40</i>	0.98 (0.71, 1.35)	0.894	0.86 (0.66, 1.13)	0.295
<i>CXCL3</i>	0.7 (0.51, 0.97)	0.033	0.86 (0.66, 1.14)	0.297
<i>NFKBIA</i>	1.13 (0.81, 1.58)	0.471	0.87 (0.66, 1.14)	0.302
<i>BIRC2</i>	1.07 (0.78, 1.48)	0.675	1.15 (0.88, 1.51)	0.304
<i>MAPK1</i>	0.97 (0.7, 1.34)	0.864	0.87 (0.66, 1.14)	0.307
<i>LTB</i>	0.86 (0.62, 1.18)	0.347	1.15 (0.88, 1.5)	0.309
<i>CCL3</i>	0.98 (0.71, 1.35)	0.885	0.87 (0.66, 1.14)	0.310
<i>IL12A</i>	0.79 (0.57, 1.09)	0.143	0.87 (0.65, 1.14)	0.312
<i>BCL2</i>	1.02 (0.74, 1.41)	0.908	1.15 (0.87, 1.52)	0.320
<i>TNFSF14</i>	0.9 (0.64, 1.25)	0.514	0.87 (0.66, 1.14)	0.323
<i>RPS6KA4</i>	1.01 (0.73, 1.4)	0.961	0.87 (0.66, 1.15)	0.326
<i>RELA</i>	1.16 (0.82, 1.64)	0.414	0.88 (0.67, 1.15)	0.339
<i>CREB1</i>	0.91 (0.66, 1.26)	0.562	1.14 (0.87, 1.5)	0.343
<i>ATF6B</i>	0.88 (0.64, 1.21)	0.424	1.14 (0.87, 1.49)	0.348
<i>CSF1</i>	1.32 (0.95, 1.82)	0.096	0.88 (0.67, 1.16)	0.354
<i>PLCG1</i>	1.08 (0.78, 1.51)	0.635	1.13 (0.86, 1.49)	0.371
<i>MAP2K7</i>	0.91 (0.66, 1.27)	0.583	0.88 (0.67, 1.16)	0.378

<i>CFLAR</i>	0.89 (0.64, 1.23)	0.481	0.89 (0.68, 1.16)	0.378
<i>PRKCB</i>	1.06 (0.76, 1.48)	0.714	0.89 (0.67, 1.17)	0.391
<i>PLCG2</i>	1.24 (0.9, 1.71)	0.186	0.89 (0.67, 1.17)	0.397
<i>PLAU</i>	1.49 (1.08, 2.06)	0.015	1.12 (0.86, 1.47)	0.398
<i>CXCL8</i>	0.57 (0.41, 0.79)	0.001	0.89 (0.68, 1.17)	0.400
<i>IKBKE</i>	1.01 (0.72, 1.41)	0.963	0.89 (0.68, 1.17)	0.400
<i>CEBPB</i>	0.88 (0.64, 1.22)	0.454	0.89 (0.68, 1.17)	0.407
<i>JUN</i>	1.33 (0.96, 1.84)	0.090	1.12 (0.85, 1.47)	0.411
<i>BAG4</i>	0.98 (0.71, 1.35)	0.904	0.9 (0.68, 1.17)	0.419
<i>IKBKG</i>	0.82 (0.59, 1.14)	0.239	1.12 (0.85, 1.46)	0.421
<i>LTBR</i>	0.81 (0.58, 1.12)	0.196	0.89 (0.68, 1.18)	0.423
<i>CD40LG</i>	1.05 (0.75, 1.46)	0.781	0.9 (0.68, 1.19)	0.442
<i>TRAF5</i>	1.16 (0.84, 1.6)	0.379	1.11 (0.85, 1.46)	0.443
<i>TRAF2</i>	0.82 (0.59, 1.13)	0.228	0.9 (0.68, 1.19)	0.457
<i>PARP1</i>	0.81 (0.58, 1.12)	0.197	0.9 (0.69, 1.18)	0.464
<i>CD86</i>	0.77 (0.55, 1.08)	0.127	0.9 (0.69, 1.19)	0.464
<i>IL15</i>	1.06 (0.77, 1.47)	0.705	1.1 (0.84, 1.45)	0.472
<i>CREB3</i>	0.84 (0.61, 1.16)	0.293	0.91 (0.69, 1.19)	0.473
<i>CXCL5</i>	0.86 (0.63, 1.19)	0.376	0.91 (0.69, 1.19)	0.477
<i>FOS</i>	1.24 (0.89, 1.71)	0.203	1.1 (0.84, 1.45)	0.478
<i>RPS6KA5</i>	0.98 (0.71, 1.37)	0.927	0.91 (0.69, 1.19)	0.483
<i>FAS</i>	0.81 (0.59, 1.12)	0.208	1.1 (0.84, 1.45)	0.489
<i>VEGFC</i>	1.24 (0.9, 1.71)	0.179	1.1 (0.84, 1.44)	0.493
<i>TOLLIP</i>	1.21 (0.88, 1.67)	0.244	1.1 (0.84, 1.45)	0.493
<i>TNFRSF1B</i>	1.13 (0.82, 1.56)	0.454	0.91 (0.69, 1.19)	0.494
<i>IRAK4</i>	0.87 (0.63, 1.21)	0.417	0.91 (0.69, 1.2)	0.500
<i>ATF2</i>	0.98 (0.71, 1.35)	0.910	1.1 (0.83, 1.44)	0.504
<i>CYLD</i>	0.81 (0.59, 1.11)	0.191	0.91 (0.7, 1.2)	0.509
<i>DNM1L</i>	0.81 (0.58, 1.12)	0.195	1.09 (0.83, 1.44)	0.513
<i>EDN1</i>	0.93 (0.67, 1.28)	0.653	0.92 (0.7, 1.2)	0.518
<i>TLR1</i>	0.86 (0.62, 1.19)	0.364	1.1 (0.83, 1.44)	0.519
<i>IL18R1</i>	0.98 (0.71, 1.35)	0.896	1.09 (0.84, 1.43)	0.520

<i>TLR6</i>	1.18 (0.86, 1.64)	0.304	0.91 (0.7, 1.2)	0.521
<i>MAPK10</i>	1.16 (0.84, 1.6)	0.374	1.09 (0.83, 1.43)	0.525
<i>TRIM25</i>	0.99 (0.71, 1.36)	0.928	1.09 (0.83, 1.44)	0.526
<i>CASP3</i>	0.81 (0.58, 1.12)	0.203	0.92 (0.7, 1.2)	0.537
<i>SELE</i>	1.09 (0.79, 1.5)	0.598	1.09 (0.83, 1.43)	0.538
<i>TLR5</i>	1.28 (0.93, 1.77)	0.129	0.92 (0.7, 1.2)	0.542
<i>MAPK11</i>	1.28 (0.93, 1.77)	0.128	0.92 (0.7, 1.21)	0.559
<i>CSNK2A3</i>	1.12 (0.81, 1.54)	0.493	0.92 (0.71, 1.21)	0.563
<i>EDARADD</i>	1.01 (0.73, 1.4)	0.940	1.08 (0.83, 1.42)	0.571
<i>BTK</i>	1 (0.72, 1.38)	0.987	0.93 (0.7, 1.22)	0.579
<i>DAB2IP</i>	0.97 (0.7, 1.34)	0.845	1.08 (0.82, 1.42)	0.582
<i>CD14</i>	1.08 (0.79, 1.49)	0.624	0.93 (0.7, 1.22)	0.583
<i>PIAS4</i>	1.26 (0.92, 1.74)	0.155	0.93 (0.7, 1.22)	0.589
<i>EDA</i>	1.02 (0.74, 1.41)	0.886	0.93 (0.71, 1.22)	0.590
<i>MMP9</i>	0.83 (0.6, 1.14)	0.250	0.93 (0.71, 1.22)	0.594
<i>CSNK2A1</i>	1.04 (0.75, 1.45)	0.808	1.08 (0.82, 1.41)	0.596
<i>JUNB</i>	0.98 (0.71, 1.35)	0.886	1.08 (0.82, 1.42)	0.601
<i>PTGS2</i>	1.12 (0.81, 1.54)	0.494	0.93 (0.71, 1.22)	0.606
<i>CHUK</i>	0.89 (0.64, 1.25)	0.504	1.07 (0.82, 1.41)	0.612
<i>CXCL2</i>	0.79 (0.57, 1.1)	0.170	0.93 (0.71, 1.22)	0.623
<i>VCAM1</i>	1.16 (0.84, 1.61)	0.353	1.07 (0.82, 1.4)	0.623
<i>GADD45B</i>	0.96 (0.69, 1.34)	0.823	1.07 (0.81, 1.4)	0.639
<i>UBE2I</i>	1.42 (1.03, 1.97)	0.033	0.94 (0.72, 1.23)	0.640
<i>PIK3CD</i>	1.1 (0.8, 1.51)	0.569	0.94 (0.71, 1.24)	0.648
<i>IRF5</i>	1.26 (0.91, 1.74)	0.160	0.94 (0.71, 1.23)	0.649
<i>CXCL12</i>	1.14 (0.82, 1.57)	0.437	1.06 (0.81, 1.4)	0.650
<i>TBK1</i>	0.94 (0.68, 1.3)	0.693	0.94 (0.72, 1.24)	0.663
<i>TAB1</i>	1.23 (0.89, 1.69)	0.216	0.94 (0.72, 1.24)	0.671
<i>EDAR</i>	1.07 (0.77, 1.5)	0.690	1.06 (0.81, 1.39)	0.678
<i>MAP2K4</i>	0.98 (0.71, 1.36)	0.903	1.06 (0.81, 1.38)	0.680
<i>IL1B</i>	1.07 (0.77, 1.49)	0.684	1.06 (0.81, 1.39)	0.680
<i>MAP2K6</i>	0.88 (0.64, 1.22)	0.452	1.06 (0.81, 1.39)	0.685

<i>CREB3L4</i>	0.9 (0.65, 1.25)	0.515	1.05 (0.81, 1.38)	0.699
<i>MAP3K5</i>	1.05 (0.76, 1.46)	0.757	0.95 (0.73, 1.24)	0.709
<i>IFNAR1</i>	0.88 (0.64, 1.22)	0.450	1.05 (0.8, 1.38)	0.716
<i>LAT</i>	0.98 (0.71, 1.36)	0.923	0.95 (0.73, 1.25)	0.718
<i>ATM</i>	0.92 (0.66, 1.29)	0.637	0.95 (0.73, 1.25)	0.727
<i>MAPK12</i>	0.86 (0.63, 1.19)	0.378	0.95 (0.72, 1.25)	0.732
<i>TLR7</i>	1.05 (0.75, 1.45)	0.792	1.05 (0.8, 1.37)	0.739
<i>CREB3L2</i>	1.03 (0.75, 1.43)	0.846	0.96 (0.73, 1.26)	0.745
<i>CASP8</i>	0.92 (0.66, 1.28)	0.610	0.96 (0.73, 1.26)	0.746
<i>MAP3K8</i>	1.04 (0.75, 1.44)	0.807	0.96 (0.73, 1.26)	0.765
<i>CCL4</i>	1 (0.72, 1.38)	1.000	0.96 (0.73, 1.26)	0.780
<i>MAPK8</i>	0.98 (0.71, 1.37)	0.926	1.04 (0.79, 1.36)	0.783
<i>MAPK3</i>	1.17 (0.84, 1.63)	0.341	1.04 (0.79, 1.36)	0.783
<i>EDA2R</i>	0.98 (0.71, 1.35)	0.912	1.04 (0.79, 1.36)	0.793
<i>TRAF6</i>	0.92 (0.66, 1.28)	0.624	0.96 (0.74, 1.26)	0.796
<i>IL1R1</i>	1.12 (0.81, 1.54)	0.493	1.03 (0.79, 1.36)	0.806
<i>SYK</i>	1.01 (0.74, 1.39)	0.938	1.03 (0.79, 1.36)	0.813
<i>TNFRSF13C</i>	0.84 (0.61, 1.16)	0.292	1.03 (0.79, 1.36)	0.814
<i>BIRC3</i>	0.94 (0.67, 1.32)	0.735	0.97 (0.74, 1.27)	0.828
<i>AKT1</i>	1.09 (0.79, 1.51)	0.604	0.97 (0.74, 1.28)	0.838
<i>TLR4</i>	0.79 (0.57, 1.1)	0.159	1.03 (0.78, 1.35)	0.841
<i>JAG1</i>	1.36 (0.98, 1.88)	0.069	0.97 (0.74, 1.27)	0.842
<i>NFKB1</i>	1.34 (0.96, 1.86)	0.084	1.03 (0.78, 1.35)	0.842
<i>MAP2K3</i>	1.14 (0.82, 1.59)	0.421	0.97 (0.74, 1.29)	0.855
<i>TIRAP</i>	1.02 (0.74, 1.41)	0.920	1.02 (0.78, 1.34)	0.859
<i>ATF4</i>	0.83 (0.59, 1.15)	0.260	0.98 (0.75, 1.28)	0.862
<i>MAP2K2</i>	1.21 (0.87, 1.66)	0.252	0.98 (0.75, 1.28)	0.868
<i>TLR2</i>	0.92 (0.67, 1.27)	0.627	1.02 (0.78, 1.34)	0.870
<i>MALT1</i>	0.72 (0.53, 1)	0.050	0.98 (0.74, 1.3)	0.880
<i>CSNK2A2</i>	0.89 (0.65, 1.23)	0.485	1.02 (0.78, 1.33)	0.890
<i>LY96</i>	0.88 (0.63, 1.22)	0.435	1.02 (0.77, 1.33)	0.905
<i>CASP10</i>	1.32 (0.95, 1.83)	0.098	1.02 (0.77, 1.34)	0.908

<i>SPP1</i>	0.85 (0.61, 1.17)	0.315	0.98 (0.75, 1.29)	0.912
<i>TAB3</i>	0.8 (0.58, 1.1)	0.174	1.01 (0.77, 1.33)	0.918
<i>SOCS3</i>	1.04 (0.75, 1.44)	0.826	0.99 (0.74, 1.31)	0.922
<i>BCL2L1</i>	1.07 (0.77, 1.49)	0.690	0.99 (0.75, 1.3)	0.936
<i>MMP14</i>	1.07 (0.77, 1.48)	0.698	1.01 (0.77, 1.33)	0.939
<i>MAP3K14</i>	1.06 (0.76, 1.46)	0.741	1.01 (0.77, 1.32)	0.946
<i>PGAM5</i>	1 (0.72, 1.39)	0.991	0.99 (0.76, 1.3)	0.949
<i>CCL20</i>	0.89 (0.64, 1.23)	0.478	1.01 (0.76, 1.33)	0.962
<i>AKT2</i>	1.07 (0.77, 1.48)	0.692	1.01 (0.77, 1.32)	0.966
<i>TRAF1</i>	0.97 (0.71, 1.34)	0.860	1 (0.77, 1.31)	0.984
<i>RAC1</i>	0.83 (0.6, 1.15)	0.262	1 (0.76, 1.31)	0.995
<i>IRF3</i>	1.11 (0.8, 1.53)	0.542	1 (0.76, 1.31)	0.996
<i>PIK3CA</i>	0.83 (0.6, 1.15)	0.263	1 (0.76, 1.32)	1.000
<i>LBP</i>	0.78 (0.56, 1.07)	0.128	0 (0, 0)	
<i>CCL3L1</i>	1.24 (0.9, 1.73)	0.194	0 (0, 0)	

Abbreviations: TLR = toll-like receptor; NFkB = nuclear factor kappa B; TNF = tumor necrosis factor; EOC = epithelial ovarian cancer; HGSOC = high grade serous ovarian cancer; AACES = African American Cancer Epidemiology Study; OCAC = Ovarian Cancer Association Consortium;
^aAdjusted for age, stage at diagnosis, and two ancestry principal components.

Supplementary Table ST6.4. DEGs for stage at diagnosis (late vs early) among Black and White HGSOc cases.								
Gene	Mean	Log fold change ^a (95% CI)	Black Cases		White Cases			
			<i>P</i>	<i>P</i> _{FDR} ^b	Mean	Log fold change ^a (95% CI)	<i>P</i>	<i>P</i> _{FDR} ^b
BLNK	438	-1 (-1.2, -0.9)	0.0000000004	0.000000008	367	-1.33 (-1.6, -1.1)	0.000002	0.0005
CEBPB	3421	0.7 (0.5, 0.8)	0.000001	0.0001	921.4	0.84 (0.7, 1)	0.000008	0.001
PIK3R1	5051	-0.6 (-0.7, -0.4)	0.00003	0.002	4451.4	-0.66 (-0.8, -0.5)	0.00008	0.006
PIK3CD	1445	0.6 (0.4, 0.7)	0.00003	0.002	521.4	-0.68 (-0.9, -0.5)	0.00034	0.012
TLR4	1143	-0.5 (-0.7, -0.4)	0.00005	0.002	1031.3	-0.5 (-0.6, -0.4)	0.00034	0.012
MMP14	5287	0.5 (0.4, 0.6)	0.0002	0.005	384.5	-1.26 (-1.6, -0.9)	0.00026	0.012
JUN	7169	0.5 (0.4, 0.6)	0.0005	0.015	4188.2	0.52 (0.4, 0.7)	0.001	0.029
ICAM1	2389	0.7 (0.5, 0.8)	0.0007	0.016	8751.5	0.53 (0.4, 0.7)	0.001	0.029
MAPK10	473	-0.7 (-0.9, -0.5)	0.0007	0.016	98.1	-0.71 (-0.9, -0.5)	0.001	0.029
TRAF6	1019	-0.3 (-0.4, -0.2)	0.001	0.022	653.7	-0.53 (-0.7, -0.4)	0.002	0.040
SOCS3	1088	0.6 (0.4, 0.8)	0.001	0.023	1438	-0.39 (-0.5, -0.3)	0.004	0.055
FAS	2295	-0.4 (-0.6, -0.3)	0.001	0.023	529.4	-0.53 (-0.7, -0.3)	0.004	0.055
XIAP	9666	-0.4 (-0.5, -0.3)	0.002	0.023	365.6	0.65 (0.4, 0.9)	0.003	0.055
CARD14	167	0.8 (0.5, 1)	0.002	0.023	245.8	-0.52 (-0.7, -0.3)	0.004	0.055
CFLAR	4891	-0.2 (-0.3, -0.1)	0.002	0.031	290.4	-0.66 (-0.9, -0.4)	0.004	0.055
CD40	516	0.5 (0.3, 0.6)	0.004	0.046	249.5	-0.48 (-0.6, -0.3)	0.003	0.055
PIK3R2	3378	0.3 (0.2, 0.5)	0.004	0.046	2485.5	-0.73 (-1, -0.5)	0.004	0.055
LBP	18	1.6 (1, 2.1)	0.004	0.046	2627	0.49 (0.3, 0.7)	0.005	0.061
PARP1	10820	0.3 (0.2, 0.4)	0.004	0.046	14840.8	0.65 (0.4, 0.9)	0.006	0.067
CSNK2B	3	4.6 (3, 6.2)	0.004	0.046	1160.3	-0.52 (-0.7, -0.3)	0.008	0.091
EDARADD	189	0.8 (0.5, 1)	0.005	0.048	726.4	-0.44 (-0.6, -0.3)	0.009	0.092
MAPK3	2910	0.3 (0.2, 0.4)	0.006	0.053	142.9	-0.56 (-0.8, -0.3)	0.010	0.098
JUNB	3168	0.5 (0.3, 0.7)	0.007	0.061	260.7	0.57 (0.3, 0.8)	0.013	0.126
DAB2IP	4088	0.3 (0.2, 0.4)	0.007	0.062	11.6	1.5 (0.9, 2.1)	0.014	0.128
TRAF5	2145	-0.3 (-0.5, -0.2)	0.008	0.064	883.7	-0.33 (-0.5, -0.2)	0.018	0.134
CXCL12	1127	0.5 (0.3, 0.7)	0.009	0.070	756	-0.71 (-1, -0.4)	0.018	0.134
CASP8	1484	-0.3 (-0.3, -0.2)	0.009	0.071	353.8	-0.34 (-0.5, -0.2)	0.016	0.134

CREB3	969	0.3 (0.2, 0.4)	0.010	0.075	152.2	0.78 (0.5,1.1)	0.016	0.134
PLAU	1413	0.5 (0.3, 0.7)	0.010	0.075	13.8	-0.81 (-1.1,-0.5)	0.017	0.134
FOS	11158	0.5 (0.3, 0.7)	0.012	0.083	836.7	-0.43 (-0.6,-0.2)	0.018	0.134
ATM	17847	-0.3 (-0.4, -0.2)	0.013	0.085	176.1	-0.51 (-0.7,-0.3)	0.021	0.140
CASP10	638	-0.3 (-0.5, -0.2)	0.016	0.099	5082.5	-0.38 (-0.6,-0.2)	0.021	0.140
LYN	1536	-0.3 (-0.4, -0.2)	0.016	0.099	24.4	2.01 (1.1,2.9)	0.020	0.140
ATF4	4463	-0.2 (-0.3, -0.1)	0.018	0.108	8657.2	-0.5 (-0.7,-0.3)	0.024	0.147
MAP2K6	678	-0.4 (-0.6, -0.2)	0.018	0.109	224.4	-0.35 (-0.5,-0.2)	0.024	0.147
LIF	751	0.5 (0.3, 0.7)	0.022	0.124	170.9	-0.79 (-1.2,-0.4)	0.028	0.160
RPS6KA4	1032	0.3 (0.2, 0.4)	0.022	0.124	14.9	-1.24 (-1.8,-0.7)	0.028	0.160
CASP3	594	-0.3 (-0.4, -0.1)	0.023	0.124	540.6	0.36 (0.2,0.5)	0.028	0.160
CSF1	1000	0.4 (0.2, 0.5)	0.023	0.124	347.3	-0.36 (-0.5,-0.2)	0.036	0.201
IFNB1	2	1.3 (0.7, 1.9)	0.024	0.125	1795.1	0.26 (0.1,0.4)	0.040	0.209
LY96	140	-0.4 (-0.6, -0.2)	0.025	0.130	0.9	-3.97 (-5.9,-2)	0.039	0.209
BCL2L1	2416	0.2 (0.1, 0.4)	0.026	0.130	394.6	-0.41 (-0.6,-0.2)	0.045	0.227
CTSK	1388	0.3 (0.2, 0.5)	0.028	0.134	3135.9	0.22 (0.1,0.3)	0.045	0.227
CHUK	1605	-0.2 (-0.3, -0.1)	0.031	0.146	1221.4	-0.32 (-0.5,-0.2)	0.046	0.227
TOLLIP	517	0.3 (0.1, 0.4)	0.038	0.171	161.2	0.62 (0.3,0.9)	0.048	0.230
TNFSF11	14	-0.9 (-1.4, -0.5)	0.037	0.171	1108.7	0.25 (0.1,0.4)	0.051	0.241
IRF5	257	0.4 (0.2, 0.5)	0.042	0.171	523.3	-0.28 (-0.4,-0.1)	0.055	0.254
AKT1	8755	0.2 (0.1, 0.3)	0.041	0.171	955.7	0.22 (0.1,0.3)	0.067	0.279
EDA	189	0.4 (0.2, 0.6)	0.040	0.171	4529.8	-0.24 (-0.4,-0.1)	0.066	0.279
CCL19	27	0.7 (0.4, 1.1)	0.042	0.171	975.7	0.38 (0.2,0.6)	0.062	0.279
MAP3K5	2762	-0.2 (-0.3, -0.1)	0.039	0.171	763	0.39 (0.2,0.6)	0.064	0.279
IKBKE	1403	0.3 (0.1, 0.4)	0.045	0.182	1098.1	0.22 (0.1,0.3)	0.064	0.279
IKBKG	529	0.3 (0.2, 0.5)	0.046	0.182	1746.5	-0.22 (-0.3,-0.1)	0.074	0.285
AKT3	1120	-0.4 (-0.6, -0.2)	0.049	0.191	5196.9	0.2 (0.1,0.3)	0.072	0.285
CSF2	3	1.4 (0.7, 2.2)	0.061	0.233	92.3	-0.57 (-0.9,-0.3)	0.072	0.285
RELB	1174	0.3 (0.1, 0.4)	0.065	0.237	4793.4	0.18 (0.1,0.3)	0.075	0.285
CXCL5	33	-0.8 (-1.3, -0.4)	0.065	0.237	4863.8	0.21 (0.1,0.3)	0.074	0.285
TLR6	309	-0.2 (-0.4, -0.1)	0.066	0.237	844.9	0.44 (0.2,0.7)	0.078	0.285

TNFRSF1A	5894	0.2 (0.1, 0.3)	0.067	0.237	4265.6	-0.3 (-0.5,-0.1)	0.077	0.285
MAP2K2	3643	0.2 (0.1, 0.3)	0.068	0.237	1382.2	0.23 (0.1,0.4)	0.079	0.285
MAP2K3	1489	0.2 (0.1, 0.3)	0.070	0.241	950.1	-0.44 (-0.7,-0.2)	0.084	0.298
TNFRSF13C	53	0.4 (0.2, 0.6)	0.075	0.252	362	-0.67 (-1.1,-0.3)	0.090	0.314
TLR1	602	-0.2 (-0.3, -0.1)	0.078	0.260	125.2	-0.35 (-0.6,-0.1)	0.093	0.320
TIRAP	281	-0.2 (-0.3, -0.1)	0.084	0.274	4312.6	0.27 (0.1,0.4)	0.098	0.330
NFKBIA	6278	0.2 (0.1, 0.4)	0.088	0.281	3867.8	-0.18 (-0.3,-0.1)	0.100	0.330
LTBR	3988	0.2 (0.1, 0.3)	0.090	0.282	2727	-0.26 (-0.4,-0.1)	0.100	0.330
BCL2	227	-0.4 (-0.6, -0.1)	0.091	0.282	1421	-0.2 (-0.3,-0.1)	0.105	0.340
TICAM2	10	-0.7 (-1.1, -0.3)	0.099	0.305	3811.7	-0.2 (-0.3,-0.1)	0.107	0.341
RPS6KA5	826	-0.2 (-0.3, -0.1)	0.113	0.331	25.4	-1.33 (-2.2,-0.5)	0.111	0.344
CCL2	1416	-0.3 (-0.5, -0.1)	0.111	0.331	333.1	-0.26 (-0.4,-0.1)	0.111	0.344
RELA	4709	0.1 (0, 0.2)	0.112	0.331	75.7	0.72 (0.3,1.2)	0.114	0.347
CYLD	2661	-0.1 (-0.2, 0)	0.118	0.342	348.2	-0.33 (-0.5,-0.1)	0.122	0.367
BAG4	2383	0.2 (0.1, 0.3)	0.126	0.360	5051.5	-0.18 (-0.3,-0.1)	0.126	0.374
IRAK4	681	-0.2 (-0.3, -0.1)	0.132	0.374	1290.7	0.29 (0.1,0.5)	0.131	0.376
IFNAR1	3595	-0.2 (-0.3, -0.1)	0.137	0.381	3903	0.2 (0.1,0.3)	0.130	0.376
NOD2	481	-0.2 (-0.4, -0.1)	0.146	0.402	1310.8	0.35 (0.1,0.6)	0.132	0.376
EDA2R	49	-0.4 (-0.7, -0.1)	0.151	0.410	225.3	-0.36 (-0.6,-0.1)	0.144	0.397
CREB3L2	1847	-0.1 (-0.2, 0)	0.157	0.421	5566	-0.22 (-0.4,-0.1)	0.142	0.397
MAP3K14	1278	0.2 (0, 0.3)	0.181	0.443	102.8	-0.39 (-0.7,-0.1)	0.144	0.397
PRKCQ	1134	-0.2 (-0.4, -0.1)	0.187	0.443	21.7	0.6 (0.2,1)	0.157	0.420
MAP2K7	1044	0.2 (0, 0.3)	0.185	0.443	6603.5	0.13 (0,0.2)	0.156	0.420
CD86	184	-0.2 (-0.4, 0)	0.185	0.443	715.6	-0.23 (-0.4,-0.1)	0.161	0.427
IL1R1	5195	-0.2 (-0.3, 0)	0.187	0.443	2368.6	0.28 (0.1,0.5)	0.165	0.432
IL18R1	186	-0.3 (-0.4, -0.1)	0.174	0.443	2185.5	0.17 (0,0.3)	0.171	0.442
PLCG1	9728	0.2 (0, 0.3)	0.186	0.443	857.3	0.18 (0,0.3)	0.174	0.445
CXCL6	32	0.6 (0.2, 1)	0.178	0.443	75	-0.56 (-1,-0.1)	0.177	0.446
BCL2A1	123	-0.3 (-0.5, -0.1)	0.173	0.443	75	-0.3 (-0.5,-0.1)	0.180	0.449
FADD	721	-0.2 (-0.3, 0)	0.171	0.443	790.7	0.16 (0,0.3)	0.188	0.462
CXCL10	839	-0.4 (-0.6, -0.1)	0.189	0.443	13306.3	0.15 (0,0.3)	0.189	0.462

PIK3CB	4550	-0.1 (-0.2, 0)	0.196	0.445	333.7	-0.2 (-0.4,0)	0.197	0.476
IRF3	2329	0.2 (0, 0.3)	0.195	0.445	812.5	-0.25 (-0.5,0)	0.221	0.526
TLR2	739	-0.1 (-0.3, 0)	0.196	0.445	5694.6	-0.12 (-0.2,0)	0.242	0.540
CXCL11	201	-0.4 (-0.7, -0.1)	0.198	0.445	15600.4	0.14 (0,0.3)	0.255	0.540
PTGS2	400	-0.3 (-0.5, -0.1)	0.222	0.484	3827.2	-0.13 (-0.2,0)	0.250	0.540
GADD45B	608	0.2 (0, 0.4)	0.221	0.484	498.2	-0.2 (-0.4,0)	0.244	0.540
PIK3R3	917	-0.2 (-0.3, 0)	0.222	0.484	2383.1	0.16 (0,0.3)	0.241	0.540
EDAR	71	-0.5 (-0.9, -0.1)	0.227	0.487	2796.5	0.13 (0,0.2)	0.256	0.540
IRAK1	4574	0.2 (0, 0.3)	0.228	0.487	712.8	0.23 (0,0.4)	0.255	0.540
TNFSF13B	209	0.2 (0, 0.4)	0.239	0.505	192.8	-0.21 (-0.4,0)	0.240	0.540
CSNK2A3	64	0.3 (0, 0.6)	0.244	0.510	305.7	-0.17 (-0.3,0)	0.256	0.540
TAB3	2896	-0.1 (-0.2, 0)	0.255	0.528	222.7	0.39 (0.1,0.7)	0.247	0.540
PGAM5	910	0.1 (0, 0.3)	0.262	0.536	645.9	-0.17 (-0.3,0)	0.241	0.540
RAC1	3319	-0.1 (-0.2, 0)	0.269	0.546	204.6	-0.93 (-1.7,-0.1)	0.248	0.540
NFKB2	3119	0.1 (0, 0.2)	0.272	0.546	11550.3	-0.16 (-0.3,0)	0.269	0.561
UBE2I	3720	0.1 (0, 0.2)	0.281	0.559	3.1	-0.69 (-1.3,-0.1)	0.278	0.575
MAP2K4	876	-0.1 (-0.2, 0)	0.284	0.559	1765.4	-0.17 (-0.3,0)	0.294	0.596
TBK1	2863	-0.1 (-0.2, 0)	0.286	0.559	1058.2	0.17 (0,0.3)	0.292	0.596
BIRC2	2794	-0.1 (-0.2, 0)	0.303	0.581	104.9	0.24 (0,0.5)	0.298	0.598
BCL10	914	-0.1 (-0.2, 0)	0.302	0.581	2240.3	-0.1 (-0.2,0)	0.302	0.602
IL15	121	-0.2 (-0.4, 0)	0.306	0.581	1.4	-0.71 (-1.4,0)	0.307	0.604
IL1B	243	0.2 (0, 0.4)	0.337	0.625	286.2	0.34 (0,0.7)	0.309	0.604
TICAM1	925	-0.1 (-0.2, 0)	0.338	0.625	1689.4	-0.11 (-0.2,0)	0.318	0.615
CCL3	108	0.2 (0, 0.4)	0.332	0.625	1102.1	-0.13 (-0.3,0)	0.320	0.615
LTB	30	-0.4 (-0.9, 0)	0.343	0.628	4737.7	-0.11 (-0.2,0)	0.324	0.618
VCAM1	856	0.2 (0, 0.3)	0.347	0.631	574.1	-0.12 (-0.2,0)	0.339	0.619
CD80	68	-0.2 (-0.4, 0)	0.354	0.631	2.9	0.76 (0,1.6)	0.338	0.619
RIPK1	1588	0.1 (0, 0.2)	0.356	0.631	1185.1	-0.22 (-0.5,0)	0.339	0.619
PIDD1	539	0.2 (0, 0.3)	0.356	0.631	117.7	0.29 (0,0.6)	0.338	0.619
BTK	301	-0.1 (-0.3, 0)	0.360	0.633	887	-0.13 (-0.3,0)	0.339	0.619
CCL5	698	-0.1 (-0.3, 0)	0.366	0.638	1582.6	-0.14 (-0.3,0)	0.352	0.637

VEGFC	422	0.2 (0, 0.3)	0.372	0.643	5.1	-0.51 (-1.1,0)	0.360	0.646
SYK	2973	0.1 (0, 0.3)	0.381	0.653	2416.3	-0.09 (-0.2,0)	0.372	0.658
RIPK3	283	-0.2 (-0.4, 0)	0.385	0.654	2.1	-0.99 (-2.1,0.1)	0.373	0.658
SELE	30	0.3 (-0.1, 0.6)	0.401	0.672	713.6	-0.13 (-0.3,0)	0.406	0.710
AKT2	6983	0.1 (0, 0.2)	0.408	0.672	2709	0.1 (0,0.2)	0.414	0.718
MAP3K7	3579	0.1 (0, 0.2)	0.411	0.672	9813.9	0.09 (0,0.2)	0.431	0.725
MLKL	330	-0.1 (-0.2, 0)	0.403	0.672	1119.7	-0.11 (-0.3,0)	0.432	0.725
CCL3L1	36	0.4 (-0.1, 1)	0.412	0.672	635.3	-0.12 (-0.3,0)	0.434	0.725
CD14	644	0.1 (0, 0.3)	0.416	0.674	5931.6	0.11 (0,0.2)	0.431	0.725
TNFRSF1B	489	0.1 (0, 0.2)	0.439	0.695	3472.8	0.14 (0,0.3)	0.428	0.725
MAPK14	1547	-0.1 (-0.2, 0)	0.437	0.695	6847.2	0.09 (0,0.2)	0.443	0.729
IL12B	4	0.4 (-0.1, 1)	0.437	0.695	122.7	-0.19 (-0.4,0.1)	0.447	0.729
MAPK8	1453	-0.1 (-0.2, 0)	0.450	0.707	904.6	-0.23 (-0.5,0.1)	0.449	0.729
NFKB1	2224	-0.1 (-0.1, 0)	0.458	0.715	7	-1.07 (-2.5,0.3)	0.450	0.729
IKBKB	3996	0.1 (0, 0.2)	0.466	0.717	1209.8	-0.15 (-0.4,0.1)	0.457	0.735
SPP1	11058	0.1 (0, 0.3)	0.467	0.717	0.2	-1.64 (-3.9,0.6)	0.470	0.750
CXCL2	134	0.2 (-0.1, 0.5)	0.474	0.722	47.7	0.23 (-0.1,0.6)	0.475	0.752
ATF2	5713	0.1 (0, 0.1)	0.493	0.741	4537.9	0.06 (0,0.2)	0.485	0.763
CARD11	1154	0.1 (-0.1, 0.3)	0.490	0.741	1216.9	-0.12 (-0.3,0.1)	0.500	0.764
ZAP70	201	0.1 (-0.1, 0.3)	0.497	0.742	149.1	-0.16 (-0.4,0.1)	0.489	0.764
CX3CL1	245	0.1 (-0.1, 0.3)	0.531	0.745	742.9	-0.13 (-0.3,0.1)	0.496	0.764
TRIM25	3568	0.1 (0, 0.2)	0.522	0.745	1.6	3.09 (-1.5,7.6)	0.498	0.764
TNFSF14	47	0.2 (-0.1, 0.5)	0.504	0.745	1.9	-0.73 (-1.8,0.4)	0.506	0.767
GADD45G	94	0.2 (-0.1, 0.4)	0.528	0.745	2549.7	-0.08 (-0.2,0)	0.511	0.770
IL6	134	0.2 (-0.1, 0.5)	0.508	0.745	572.4	0.08 (0,0.2)	0.520	0.778
CXCL3	70	-0.2 (-0.5, 0.1)	0.529	0.745	1282.1	-0.07 (-0.2,0)	0.535	0.793
IL12A	112	0.2 (-0.1, 0.5)	0.511	0.745	3445.2	0.17 (-0.1,0.5)	0.537	0.793
CXCL8	427	-0.2 (-0.4, 0.1)	0.528	0.745	2816.2	0.06 (0,0.2)	0.560	0.797
CCL4	87	0.2 (-0.1, 0.5)	0.515	0.745	4241.5	-0.11 (-0.3,0.1)	0.562	0.797
MALT1	2874	-0.1 (-0.2, 0)	0.535	0.745	710.3	0.1 (-0.1,0.3)	0.544	0.797
TRAF2	1359	0.1 (-0.1, 0.2)	0.565	0.783	659.5	-0.06 (-0.2,0)	0.554	0.797

MAP3K8	1456	0.1 (-0.1, 0.2)	0.571	0.786	7272.5	0.08 (-0.1,0.2)	0.556	0.797
MAPK11	110	0.1 (-0.1, 0.3)	0.583	0.797	70.6	0.18 (-0.1,0.5)	0.558	0.797
ATF6B	4104	0.1 (-0.1, 0.2)	0.598	0.811	603.6	-0.08 (-0.2,0.1)	0.589	0.821
TRADD	224	-0.1 (-0.3, 0.1)	0.606	0.817	2159.3	0.07 (-0.1,0.2)	0.589	0.821
BIRC3	2106	-0.1 (-0.3, 0.1)	0.624	0.825	1806.1	0.07 (-0.1,0.2)	0.590	0.821
CSNK2A2	2259	0 (0, 0.1)	0.617	0.825	5088.3	-0.08 (-0.2,0.1)	0.610	0.828
PIAS4	911	0.1 (-0.1, 0.2)	0.622	0.825	1655.9	0.06 (-0.1,0.2)	0.611	0.828
MAPK13	1132	-0.1 (-0.2, 0.1)	0.628	0.825	5985.4	0.06 (-0.1,0.2)	0.616	0.828
DNM1L	7247	0 (-0.1, 0.1)	0.648	0.833	80.9	-0.13 (-0.4,0.1)	0.602	0.828
JAG1	4935	-0.1 (-0.2, 0.1)	0.646	0.833	1013.7	-0.07 (-0.2,0.1)	0.619	0.828
STAT1	16431	0.1 (-0.1, 0.2)	0.648	0.833	82.5	-0.16 (-0.5,0.2)	0.622	0.828
CREB5	1113	-0.1 (-0.3, 0.1)	0.650	0.833	1797.7	0.05 (0,0.1)	0.615	0.828
TAB2	17354	0 (-0.1, 0.1)	0.665	0.843	24.5	0.23 (-0.2,0.7)	0.631	0.836
ITCH	7029	0 (-0.1, 0)	0.666	0.843	160.8	-0.08 (-0.2,0.1)	0.651	0.847
TLR8	125	-0.1 (-0.3, 0.1)	0.679	0.849	10004.1	0.07 (-0.1,0.2)	0.655	0.847
CCL20	127	0.2 (-0.2, 0.5)	0.675	0.849	319.1	0.11 (-0.1,0.4)	0.656	0.847
MYD88	1030	0 (-0.1, 0.2)	0.685	0.852	69	0.24 (-0.3,0.8)	0.654	0.847
TAB1	779	0 (-0.1, 0.2)	0.696	0.861	942.3	-0.05 (-0.2,0.1)	0.687	0.877
TRAF1	447	0.1 (-0.1, 0.2)	0.708	0.871	1341.1	0.04 (-0.1,0.2)	0.687	0.877
CD40LG	22	-0.1 (-0.4, 0.2)	0.719	0.878	401.3	-0.05 (-0.2,0.1)	0.696	0.883
TNF	79	0.1 (-0.2, 0.5)	0.741	0.900	1046.8	-0.08 (-0.3,0.1)	0.700	0.883
PLCG2	4337	0 (-0.1, 0.2)	0.745	0.900	34.6	0.11 (-0.2,0.4)	0.709	0.890
TRAF3	1519	0 (-0.1, 0.1)	0.753	0.904	455.7	0.07 (-0.1,0.3)	0.730	0.891
MAPK1	2840	0 (-0.1, 0.1)	0.767	0.914	1737.8	0.07 (-0.1,0.3)	0.745	0.891
CARD10	939	0.1 (-0.1, 0.2)	0.770	0.914	281.8	-0.09 (-0.4,0.2)	0.723	0.891
EDN1	272	-0.1 (-0.3, 0.2)	0.790	0.919	1.9	0.67 (-1.5,2.9)	0.760	0.891
MMP9	1221	-0.1 (-0.3, 0.2)	0.795	0.919	2093.1	-0.06 (-0.2,0.1)	0.725	0.891
MMP3	31	0.4 (-1, 1.8)	0.790	0.919	2129.1	-0.04 (-0.2,0.1)	0.728	0.891
CASP7	701	0 (-0.1, 0.1)	0.794	0.919	8850.2	-0.04 (-0.1,0.1)	0.747	0.891
LCK	137	-0.1 (-0.3, 0.2)	0.798	0.919	6887	0.04 (-0.1,0.2)	0.744	0.891
TLR9	70	0.3 (-0.9, 1.5)	0.800	0.919	2661.1	0.04 (-0.1,0.2)	0.752	0.891

TNFAIP3	3734	0 (-0.1, 0.2)	0.815	0.925	3071.8	0.03 (-0.1,0.1)	0.758	0.891
CCL13	16	0.1 (-0.4, 0.6)	0.813	0.925	130.5	-0.06 (-0.3,0.1)	0.747	0.891
MAPK9	1685	0 (-0.1, 0.1)	0.845	0.928	2.6	0.32 (-0.6,1.2)	0.733	0.891
BCL3	2820	0 (-0.1, 0.2)	0.840	0.928	701	-0.04 (-0.2,0.1)	0.766	0.894
ERC1	9795	0 (-0.1, 0.1)	0.825	0.928	0.4	1.23 (-3.1,5.6)	0.777	0.902
CSNK2A1	5836	0 (-0.1, 0.1)	0.851	0.928	837.9	-0.03 (-0.2,0.1)	0.794	0.913
GADD45A	485	0 (-0.1, 0.2)	0.858	0.928	866	-0.04 (-0.2,0.1)	0.801	0.913
CCL21	85	-0.1 (-0.4, 0.3)	0.869	0.928	13.5	0.28 (-0.8,1.3)	0.796	0.913
CREB3L1	1279	0 (-0.2, 0.2)	0.874	0.928	2361	0.03 (-0.1,0.2)	0.803	0.913
IFNAR2	1075	0 (-0.1, 0.1)	0.832	0.928	250.7	-0.04 (-0.2,0.1)	0.808	0.914
CXCL1	358	-0.1 (-0.4, 0.2)	0.854	0.928	1179.7	-0.02 (-0.1,0.1)	0.837	0.922
TLR3	950	0 (-0.2, 0.1)	0.861	0.928	2465.2	-0.03 (-0.2,0.1)	0.825	0.922
PRKCB	355	0 (-0.2, 0.2)	0.874	0.928	380.7	0.04 (-0.2,0.2)	0.823	0.922
LAT	381	0 (-0.1, 0.2)	0.857	0.928	2306.4	-0.03 (-0.1,0.1)	0.835	0.922
IFNA13	5	-0.2 (-1.5, 1)	0.850	0.928	0.9	0.2 (-0.8,1.2)	0.832	0.922
LTA	4	-0.3 (-2.4, 1.7)	0.880	0.929	15718.6	0.03 (-0.1,0.2)	0.844	0.925
MAP2K1	1388	0 (-0.1, 0.1)	0.909	0.955	40.2	0.1 (-0.5,0.7)	0.856	0.933
PIK3CA	5849	0 (-0.1, 0.1)	0.930	0.972	6120.3	0.02 (-0.1,0.1)	0.874	0.939
CREB1	1922	0 (-0.1, 0.1)	0.935	0.972	147.9	-0.07 (-0.5,0.4)	0.871	0.939
IRF1	2204	0 (-0.2, 0.1)	0.952	0.977	0.2	0.77 (-3.8,5.3)	0.866	0.939
CREB3L4	828	0 (-0.1, 0.1)	0.954	0.977	1332.4	-0.02 (-0.2,0.1)	0.884	0.945
TLR5	896	0 (-0.2, 0.2)	0.953	0.977	28.6	-0.06 (-0.6,0.4)	0.904	0.957
TLR7	280	0 (-0.2, 0.1)	0.962	0.980	2601.1	0.01 (-0.1,0.1)	0.904	0.957
IRF7	128	-0.1 (-2.7, 2.5)	0.967	0.982	5308	-0.01 (-0.1,0.1)	0.929	0.959
TNFRSF11A	109	0 (-0.2, 0.2)	0.973	0.983	1247.5	-0.01 (-0.2,0.1)	0.933	0.959
MAPK12	299	0 (-0.2, 0.2)	0.979	0.984	2141.3	-0.01 (-0.1,0.1)	0.935	0.959
CXCL9	379	0 (-0.3, 0.3)	0.985	0.985	1419.4	0.01 (-0.1,0.1)	0.937	0.959
CREB3L3	2	-0.2 (-1.1, 0.7)	0.855	1.00	1411.2	0.01 (-0.1,0.1)	0.918	0.959
IFNA6	1	1 (-1.6, 3.6)	0.710	1.00	4393.1	0.02 (-0.1,0.2)	0.918	0.959
IFNA8	2	0.1 (-3.4, 3.6)	0.978	1.00	874.1	-0.01 (-0.2,0.1)	0.920	0.959
IFNA21	0	0.7 (-2.8, 4.2)	0.846	1.00	73.3	-0.01 (-0.2,0.2)	0.970	0.983

IFNA5	1	0.7 (-0.4, 1.8)	0.511	1.00	61	-0.01 (-0.2,0.2)	0.967	0.983
IFNA16	0	-0.3 (-3.8, 3.2)	0.936	1.00	32.1	0.01 (-0.5,0.5)	0.983	0.983
IFNA10	0	0.1 (-3.3, 3.6)	0.969	1.00	507.3	0.01 (-0.1,0.2)	0.974	0.983
IFNA2	2	0 (-1.5, 1.5)	0.983	1.00	86.9	0.01 (-0.4,0.4)	0.981	0.983
IFNA1	1	0.8 (-1.4, 3.1)	0.712	1.00	0.1	0.22 (-4.3,4.8)	0.962	1.00
IFNA7	0	0.3 (-3.2, 3.8)	0.927	1.00	0.1	0.46 (-4.1,5)	0.919	1.00
IFNA14	0	0.8 (-2.6, 4.3)	0.810	1.00	0.1	0.07 (-4.5,4.6)	0.988	1.00
IFNA17	0	0.7 (-2.8, 4.1)	0.849	1.00	0	0.02 (-4.5,4.6)	0.996	1.00
IFNA4	0	1.6 (-1.9, 5.1)	0.648	1.00	0.1	0.35 (-4.2,4.9)	0.939	1.00

Abbreviations: TLR = toll-like receptor; NFkB = nuclear factor kappa B; TNF = tumor necrosis factor; EOC = epithelial ovarian cancer; HGSOC = high grade serous ovarian cancer; AACES = African American Cancer Epidemiology Study; OCAC = Ovarian Cancer Association Consortium;

^aAdjusted for age, tumor purity and two ancestry principal components.

^bCorrected for the number of genes tested using the Benjamini-Hochberg false discovery rate (FDR).

Supplementary Table ST6.5. Logistic Regression assessing high/low RNA expression in association with stage at diagnosis (late/early) in TLR, NFkB, and TNF genes among Black and White HGSOE cases.

	Black		White	
	OR (95% CI) ^a	<i>P</i>	OR (95% CI) ^a	<i>P</i>
CTSK	1.73 (0.89, 3.36)	0.104	4.52 (1.76, 11.6)	0.002
MMP14	2.12 (1.09, 4.13)	0.027	4.07 (1.63, 10.16)	0.003
CD40LG	0.84 (0.43, 1.62)	0.598	0.27 (0.11, 0.67)	0.004
CD40	1.97 (1.02, 3.83)	0.045	0.27 (0.11, 0.67)	0.004
IL6	1.56 (0.81, 2.99)	0.183	3.58 (1.47, 8.73)	0.005
CCL13	0.84 (0.44, 1.6)	0.588	0.28 (0.11, 0.69)	0.005
BCL2	0.72 (0.37, 1.38)	0.322	0.28 (0.12, 0.69)	0.006
CASP8	0.73 (0.37, 1.41)	0.342	0.31 (0.13, 0.73)	0.008
MLKL	1.39 (0.72, 2.69)	0.326	0.33 (0.14, 0.79)	0.012
TLR8	0.91 (0.47, 1.74)	0.768	0.34 (0.14, 0.8)	0.013
TNFSF11	1.24 (0.65, 2.37)	0.520	2.93 (1.24, 6.92)	0.014
PIK3R1	0.6 (0.31, 1.16)	0.126	2.93 (1.24, 6.92)	0.014
ZAP70	1.22 (0.63, 2.35)	0.552	0.34 (0.14, 0.81)	0.015
BIRC3	0.76 (0.39, 1.47)	0.414	0.37 (0.16, 0.86)	0.021
TLR3	0.81 (0.42, 1.54)	0.518	0.38 (0.16, 0.87)	0.023
CXCL10	1.14 (0.59, 2.19)	0.693	0.39 (0.17, 0.91)	0.029
TLR4	0.53 (0.27, 1.03)	0.061	0.4 (0.17, 0.92)	0.030
JUN	2.36 (1.19, 4.65)	0.014	2.51 (1.09, 5.81)	0.031
GADD45G	1.04 (0.54, 2)	0.905	0.4 (0.17, 0.93)	0.032
FOS	1.7 (0.88, 3.28)	0.115	2.48 (1.08, 5.72)	0.033
MAP2K7	1.99 (1.02, 3.86)	0.043	0.41 (0.18, 0.94)	0.034
SYK	1.12 (0.59, 2.16)	0.726	2.45 (1.06, 5.65)	0.035
GADD45A	1.46 (0.76, 2.82)	0.255	2.4 (1.04, 5.52)	0.039
PRKCB	0.94 (0.48, 1.82)	0.852	0.41 (0.18, 0.96)	0.040
PLCG2	0.87 (0.46, 1.67)	0.684	0.42 (0.18, 0.97)	0.042
MAPK13	1.02 (0.53, 1.94)	0.962	0.45 (0.2, 1.02)	0.057
NOD2	0.82 (0.43, 1.57)	0.547	0.46 (0.2, 1.04)	0.061
IKBKE	1.31 (0.68, 2.52)	0.425	0.46 (0.2, 1.04)	0.063
CX3CL1	1.12 (0.58, 2.14)	0.742	0.46 (0.2, 1.04)	0.063
SOCS3	2.56 (1.29, 5.07)	0.007	2.17 (0.95, 4.95)	0.066
TIRAP	0.82 (0.43, 1.58)	0.557	0.47 (0.21, 1.06)	0.069
ATF2	1.22 (0.64, 2.35)	0.543	2.13 (0.94, 4.83)	0.069
MAPK1	0.6 (0.31, 1.15)	0.125	0.47 (0.21, 1.07)	0.071
EDARADD	2.36 (1.2, 4.65)	0.013	2.11 (0.93, 4.78)	0.072
MAP3K7	0.94 (0.49, 1.82)	0.864	2.1 (0.93, 4.73)	0.074

IRF5	1.38 (0.72, 2.64)	0.335	0.48 (0.21, 1.08)	0.075
IKBKG	1.58 (0.82, 3.05)	0.176	0.48 (0.21, 1.08)	0.075
VEGFC	1.12 (0.59, 2.15)	0.725	2.06 (0.91, 4.64)	0.082
LTBR	1.72 (0.89, 3.32)	0.109	0.49 (0.22, 1.1)	0.082
AKT3	0.98 (0.52, 1.88)	0.960	2.06 (0.91, 4.63)	0.082
CD80	0.82 (0.43, 1.56)	0.538	0.48 (0.21, 1.1)	0.083
MAP2K3	1.43 (0.73, 2.8)	0.293	0.49 (0.22, 1.1)	0.084
IL1R1	0.56 (0.29, 1.09)	0.088	0.49 (0.22, 1.1)	0.084
LCK	1.03 (0.54, 1.96)	0.939	0.49 (0.22, 1.11)	0.087
CREB3L2	1 (0.52, 1.92)	0.989	0.49 (0.22, 1.11)	0.089
CXCL9	1.25 (0.65, 2.4)	0.497	0.49 (0.22, 1.12)	0.092
CCL19	1.59 (0.81, 3.09)	0.175	0.5 (0.22, 1.13)	0.095
TRAF6	0.29 (0.14, 0.59)	0.001	1.97 (0.87, 4.47)	0.103
CCL20	0.93 (0.48, 1.79)	0.833	0.51 (0.23, 1.16)	0.110
MYD88	1.37 (0.7, 2.67)	0.359	0.53 (0.24, 1.19)	0.124
ITCH	0.42 (0.21, 0.85)	0.015	1.85 (0.83, 4.15)	0.135
RIPK1	1.29 (0.67, 2.47)	0.444	0.54 (0.24, 1.22)	0.139
TRIM25	1.01 (0.53, 1.94)	0.971	0.55 (0.24, 1.22)	0.141
MAPK10	0.49 (0.25, 0.96)	0.039	1.83 (0.82, 4.09)	0.143
IL15	0.72 (0.38, 1.38)	0.325	0.55 (0.25, 1.23)	0.144
CXCL12	1.71 (0.88, 3.3)	0.112	1.83 (0.81, 4.1)	0.145
TNFSF13B	1.15 (0.59, 2.23)	0.678	0.55 (0.25, 1.23)	0.146
CASP7	1.14 (0.6, 2.19)	0.682	0.55 (0.25, 1.23)	0.147
CFLAR	0.51 (0.26, 1)	0.051	0.56 (0.25, 1.23)	0.148
CCL21	1.12 (0.59, 2.13)	0.734	1.81 (0.81, 4.08)	0.150
FADD	0.9 (0.47, 1.73)	0.759	0.56 (0.25, 1.24)	0.151
CASP3	0.67 (0.35, 1.28)	0.225	0.56 (0.25, 1.24)	0.151
JUNB	1.12 (0.59, 2.14)	0.729	1.81 (0.8, 4.08)	0.152
PLAU	1.55 (0.81, 2.97)	0.188	1.79 (0.8, 4.01)	0.159
TICAM2	0.58 (0.3, 1.12)	0.105	0.56 (0.25, 1.26)	0.162
BLNK	0.41 (0.21, 0.81)	0.010	0.57 (0.26, 1.27)	0.168
CARD10	1.38 (0.72, 2.63)	0.336	0.58 (0.26, 1.27)	0.173
ATF6B	0.85 (0.44, 1.63)	0.616	1.74 (0.78, 3.86)	0.173
TBK1	0.47 (0.24, 0.91)	0.025	1.74 (0.78, 3.88)	0.174
TNFRSF1A	1.75 (0.91, 3.38)	0.094	0.57 (0.26, 1.28)	0.175
GADD45B	1.7 (0.87, 3.31)	0.122	1.75 (0.78, 3.97)	0.178
CEBPB	3.1 (1.55, 6.22)	0.001	0.58 (0.26, 1.28)	0.178
MMP9	0.92 (0.48, 1.76)	0.810	0.58 (0.26, 1.29)	0.182
VCAM1	1.41 (0.74, 2.71)	0.301	1.71 (0.77, 3.81)	0.190
TOLLIP	2.13 (1.1, 4.16)	0.026	0.59 (0.26, 1.31)	0.194
IL12A	1.58 (0.82, 3.04)	0.172	1.67 (0.74, 3.78)	0.216
TAB3	0.72 (0.38, 1.39)	0.331	1.64 (0.72, 3.72)	0.236
IRAK1	2.54 (1.28, 5.04)	0.008	0.62 (0.28, 1.38)	0.240

TICAM1	0.81 (0.41, 1.59)	0.540	0.62 (0.28, 1.39)	0.247
FAS	0.52 (0.27, 1.01)	0.052	0.63 (0.28, 1.39)	0.253
XIAP	0.46 (0.24, 0.9)	0.024	0.63 (0.28, 1.4)	0.255
TLR1	0.74 (0.39, 1.43)	0.378	0.64 (0.29, 1.41)	0.264
LYN	0.41 (0.21, 0.83)	0.013	0.64 (0.29, 1.41)	0.267
IKBKB	1.28 (0.67, 2.46)	0.451	0.65 (0.29, 1.43)	0.279
TLR2	0.74 (0.38, 1.42)	0.361	0.65 (0.29, 1.43)	0.282
TRADD	1.03 (0.54, 1.96)	0.937	0.65 (0.29, 1.44)	0.288
CREB3	1.92 (0.99, 3.72)	0.054	0.66 (0.3, 1.44)	0.294
BIRC2	0.58 (0.3, 1.12)	0.106	0.66 (0.3, 1.44)	0.295
CXCL11	1.58 (0.82, 3.05)	0.176	0.66 (0.3, 1.45)	0.297
PRKCQ	0.98 (0.51, 1.88)	0.940	0.66 (0.3, 1.45)	0.299
CREB5	1 (0.52, 1.9)	0.991	1.52 (0.69, 3.34)	0.300
BCL2A1	0.82 (0.43, 1.57)	0.554	0.66 (0.3, 1.46)	0.307
BTK	1.26 (0.66, 2.42)	0.487	0.66 (0.3, 1.46)	0.310
TAB2	0.64 (0.33, 1.23)	0.177	1.51 (0.68, 3.34)	0.312
MALT1	0.73 (0.38, 1.4)	0.342	1.5 (0.68, 3.3)	0.316
CXCL5	0.73 (0.38, 1.4)	0.351	0.67 (0.3, 1.48)	0.317
EDA2R	0.7 (0.36, 1.34)	0.277	1.49 (0.67, 3.28)	0.326
MAPK12	0.74 (0.39, 1.43)	0.370	0.67 (0.3, 1.49)	0.327
LAT	0.99 (0.52, 1.9)	0.988	0.68 (0.31, 1.48)	0.327
RELA	1.51 (0.77, 2.96)	0.226	1.48 (0.67, 3.28)	0.328
STAT1	0.8 (0.42, 1.52)	0.490	0.67 (0.31, 1.49)	0.329
CXCL2	1.44 (0.75, 2.78)	0.275	1.48 (0.67, 3.26)	0.334
CREB3L1	1.2 (0.63, 2.3)	0.584	1.46 (0.66, 3.23)	0.345
PIAS4	1.01 (0.53, 1.92)	0.980	0.68 (0.31, 1.52)	0.351
CHUK	0.99 (0.51, 1.93)	0.984	1.45 (0.66, 3.2)	0.352
CSNK2A1	1.09 (0.57, 2.09)	0.787	1.45 (0.66, 3.19)	0.356
CREB3L4	1.34 (0.69, 2.57)	0.385	0.69 (0.31, 1.52)	0.358
PIK3CA	1.38 (0.72, 2.64)	0.336	1.45 (0.66, 3.19)	0.358
CARD11	0.73 (0.37, 1.41)	0.343	1.45 (0.65, 3.21)	0.361
CCL5	1.24 (0.64, 2.39)	0.518	0.69 (0.31, 1.53)	0.365
CSNK2A3	0.92 (0.48, 1.75)	0.794	1.44 (0.65, 3.16)	0.367
MAPK9	1.25 (0.65, 2.4)	0.502	1.44 (0.65, 3.18)	0.369
BCL3	1.33 (0.68, 2.6)	0.399	1.42 (0.64, 3.14)	0.392
BCL10	1.05 (0.54, 2.04)	0.886	0.73 (0.33, 1.61)	0.434
CSF1	2.04 (1.05, 3.99)	0.036	0.74 (0.34, 1.64)	0.461
TNFSF14	2.68 (1.34, 5.37)	0.005	0.74 (0.34, 1.64)	0.462
CYLD	0.78 (0.41, 1.5)	0.462	0.74 (0.34, 1.64)	0.464
IRF1	1.42 (0.74, 2.73)	0.293	0.75 (0.34, 1.64)	0.469
IRAK4	0.57 (0.3, 1.1)	0.095	0.75 (0.34, 1.65)	0.474
ATM	0.37 (0.18, 0.73)	0.004	0.75 (0.34, 1.65)	0.480
EDN1	1.31 (0.68, 2.51)	0.423	0.75 (0.34, 1.66)	0.482

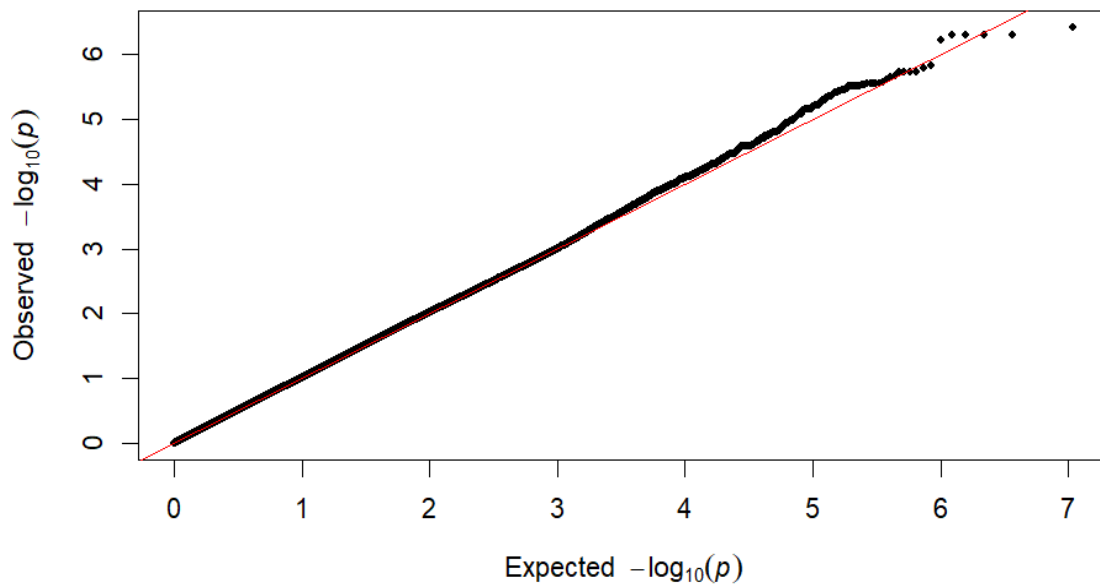
NFKBIA	2.65 (1.33, 5.3)	0.006	0.76 (0.34, 1.67)	0.491
RPS6KA4	1.29 (0.67, 2.5)	0.445	0.76 (0.35, 1.67)	0.496
CCL2	0.48 (0.24, 0.93)	0.030	0.76 (0.35, 1.67)	0.497
AKT2	1.24 (0.65, 2.37)	0.515	1.31 (0.6, 2.86)	0.505
RPS6KA5	0.59 (0.3, 1.14)	0.114	0.77 (0.35, 1.68)	0.505
CREB1	1.42 (0.74, 2.73)	0.297	1.3 (0.59, 2.85)	0.513
NFKB1	0.67 (0.35, 1.31)	0.242	0.78 (0.36, 1.7)	0.527
ATF4	0.28 (0.14, 0.57)	0.000	0.78 (0.36, 1.7)	0.530
CCL3	1.54 (0.8, 2.97)	0.192	1.29 (0.58, 2.84)	0.532
TLR7	1.13 (0.59, 2.16)	0.717	0.78 (0.36, 1.7)	0.535
JAG1	0.73 (0.38, 1.4)	0.337	0.78 (0.36, 1.7)	0.537
UBE2I	1.66 (0.86, 3.21)	0.132	1.28 (0.58, 2.8)	0.538
PIK3R2	3.52 (1.73, 7.16)	0.001	1.27 (0.58, 2.78)	0.545
BAG4	0.99 (0.52, 1.89)	0.980	0.79 (0.36, 1.72)	0.550
MAP3K5	0.63 (0.33, 1.22)	0.172	0.8 (0.36, 1.74)	0.566
RAC1	0.91 (0.48, 1.74)	0.781	0.79 (0.36, 1.75)	0.567
NFKB2	1.29 (0.67, 2.47)	0.451	0.8 (0.37, 1.74)	0.568
IL1B	1.3 (0.68, 2.51)	0.431	1.25 (0.57, 2.72)	0.577
LIF	1.77 (0.92, 3.43)	0.089	1.25 (0.57, 2.74)	0.578
MAP2K4	0.43 (0.22, 0.85)	0.016	0.8 (0.37, 1.75)	0.581
MAP3K8	0.9 (0.47, 1.72)	0.755	1.24 (0.57, 2.71)	0.586
PARP1	2.74 (1.38, 5.46)	0.004	0.81 (0.37, 1.76)	0.589
TRAF1	1.14 (0.6, 2.18)	0.687	1.24 (0.57, 2.7)	0.590
TAB1	0.9 (0.47, 1.72)	0.760	0.81 (0.37, 1.78)	0.598
ERC1	0.78 (0.41, 1.49)	0.452	0.81 (0.37, 1.78)	0.599
SPP1	1.63 (0.84, 3.14)	0.148	1.22 (0.55, 2.7)	0.617
PIK3CB	0.88 (0.46, 1.69)	0.706	1.21 (0.55, 2.67)	0.632
CARD14	1.78 (0.91, 3.47)	0.091	0.86 (0.39, 1.89)	0.703
PLCG1	1.74 (0.89, 3.4)	0.108	1.16 (0.53, 2.58)	0.707
IFNAR1	0.73 (0.38, 1.39)	0.336	0.86 (0.39, 1.89)	0.707
TLR5	1 (0.52, 1.9)	0.988	0.87 (0.39, 1.9)	0.719
RIPK3	0.92 (0.48, 1.76)	0.800	0.88 (0.4, 1.92)	0.744
PTGS2	0.92 (0.48, 1.76)	0.798	1.13 (0.52, 2.49)	0.753
TNFRSF11A	1.59 (0.82, 3.09)	0.168	0.88 (0.4, 1.93)	0.754
PIK3CD	1.94 (1, 3.76)	0.051	1.13 (0.51, 2.48)	0.760
TNFRSF13C	1.9 (0.98, 3.69)	0.058	1.13 (0.51, 2.47)	0.765
MAP2K6	0.69 (0.36, 1.33)	0.270	1.12 (0.51, 2.45)	0.778
LTB	1.12 (0.59, 2.14)	0.729	0.9 (0.41, 1.95)	0.785
SELE	1.1 (0.57, 2.1)	0.778	1.11 (0.51, 2.43)	0.787
MAPK14	0.7 (0.37, 1.36)	0.295	0.9 (0.41, 1.96)	0.788
MAP3K14	1.4 (0.73, 2.68)	0.309	0.9 (0.41, 1.96)	0.789
MAP2K1	1.4 (0.73, 2.68)	0.312	0.9 (0.41, 1.96)	0.792
PIDD1	1.22 (0.64, 2.33)	0.548	1.11 (0.51, 2.42)	0.801

PGAM5	1.95 (1.01, 3.8)	0.048	1.1 (0.51, 2.42)	0.803
EDA	1.25 (0.66, 2.4)	0.494	0.91 (0.42, 1.97)	0.805
CD14	1.4 (0.73, 2.69)	0.306	1.1 (0.5, 2.39)	0.813
TNF	1.37 (0.72, 2.63)	0.337	0.91 (0.42, 1.99)	0.817
MAPK3	2.56 (1.28, 5.11)	0.008	0.91 (0.42, 1.98)	0.817
IRF3	1.27 (0.66, 2.45)	0.474	0.92 (0.42, 1.99)	0.823
CCL4	1.75 (0.9, 3.38)	0.096	1.09 (0.5, 2.38)	0.823
CXCL3	0.93 (0.48, 1.78)	0.823	0.92 (0.42, 2)	0.825
MAPK8	0.97 (0.5, 1.87)	0.922	1.09 (0.5, 2.37)	0.825
DNM1L	0.69 (0.36, 1.33)	0.263	1.09 (0.5, 2.38)	0.825
TNFRSF1B	1.02 (0.54, 1.95)	0.944	1.09 (0.5, 2.37)	0.827
CXCL1	0.85 (0.44, 1.64)	0.629	0.92 (0.42, 2.01)	0.834
TRAF5	0.65 (0.34, 1.25)	0.195	0.92 (0.42, 2)	0.836
MAPK11	0.82 (0.43, 1.56)	0.543	0.92 (0.42, 2.03)	0.837
IFNAR2	1.02 (0.53, 1.94)	0.963	0.92 (0.43, 2.01)	0.841
CD86	0.81 (0.43, 1.56)	0.532	1.07 (0.49, 2.33)	0.857
LY96	0.72 (0.37, 1.38)	0.322	0.93 (0.43, 2.03)	0.861
RELB	2.08 (1.06, 4.1)	0.033	0.93 (0.43, 2.04)	0.866
ICAM1	1.8 (0.93, 3.5)	0.082	1.07 (0.49, 2.33)	0.866
MAP2K2	1.51 (0.78, 2.91)	0.221	1.07 (0.49, 2.32)	0.869
TNFAIP3	1.78 (0.92, 3.44)	0.088	1.06 (0.49, 2.32)	0.878
IL18R1	0.73 (0.38, 1.4)	0.343	1.06 (0.49, 2.31)	0.881
CXCL6	1.3 (0.68, 2.5)	0.426	1.06 (0.48, 2.32)	0.883
DAB2IP	3.65 (1.78, 7.49)	0.000	1.06 (0.48, 2.31)	0.890
TLR9	1.12 (0.59, 2.14)	0.725	0.95 (0.43, 2.08)	0.898
CXCL8	0.82 (0.43, 1.57)	0.549	1.05 (0.48, 2.29)	0.906
AKT1	1.32 (0.68, 2.55)	0.411	1.05 (0.48, 2.28)	0.907
BCL2L1	3.26 (1.61, 6.6)	0.001	0.96 (0.44, 2.1)	0.917
CSNK2A2	0.64 (0.33, 1.23)	0.180	1.04 (0.47, 2.27)	0.926
TLR6	0.47 (0.24, 0.91)	0.026	1.04 (0.48, 2.26)	0.928
PIK3R3	0.59 (0.31, 1.15)	0.121	1.03 (0.47, 2.25)	0.942
TRAF2	1.38 (0.71, 2.65)	0.340	1.02 (0.46, 2.23)	0.967
EDAR	0.81 (0.42, 1.58)	0.536	1.01 (0.46, 2.22)	0.975
TRAF3	0.84 (0.44, 1.62)	0.606	1 (0.45, 2.21)	0.997
LBP	1.35 (0.71, 2.59)	0.363	0 (0, 0)	
CCL3L1	1.26 (0.65, 2.45)	0.485	0 (0, 0)	

Abbreviations: TLR = toll-like receptor; NFkB = nuclear factor kappa B; TNF = tumor necrosis factor; EOC = epithelial ovarian cancer; HGSOC = high grade serous ovarian cancer; AACES = African American Cancer Epidemiology Study; OCAC = Ovarian Cancer Association Consortium;

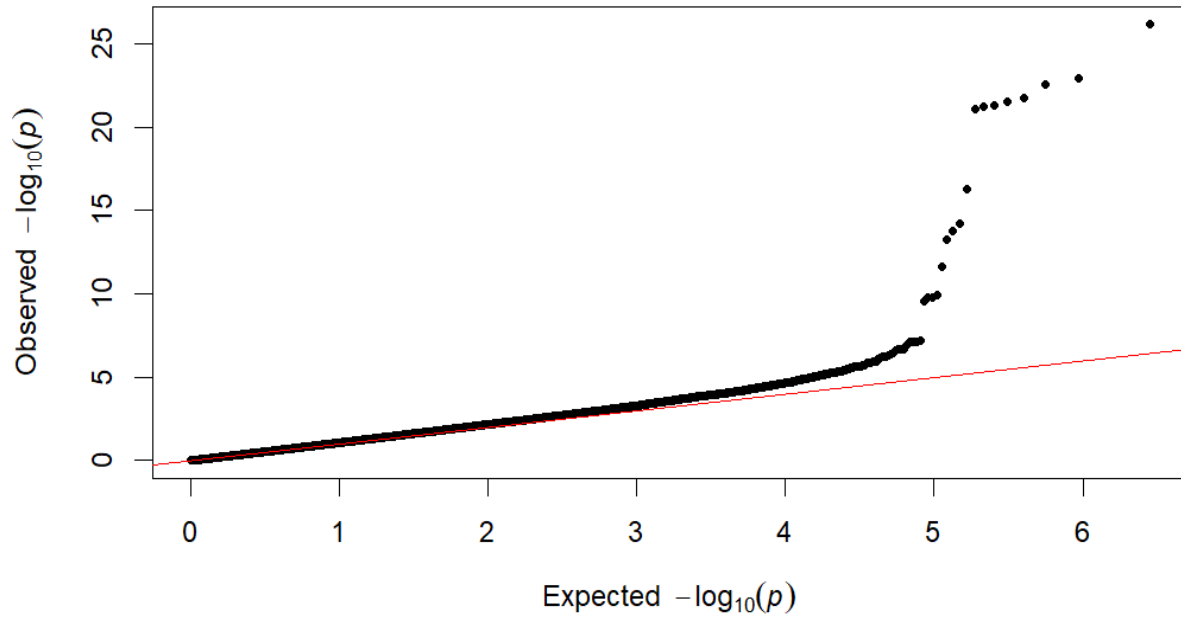
^aAdjusted for age and two ancestry principal components.

Supplementary Figure SF1. Genome-wide association QxQ plot assessing inflation due to population admixture among Black women.

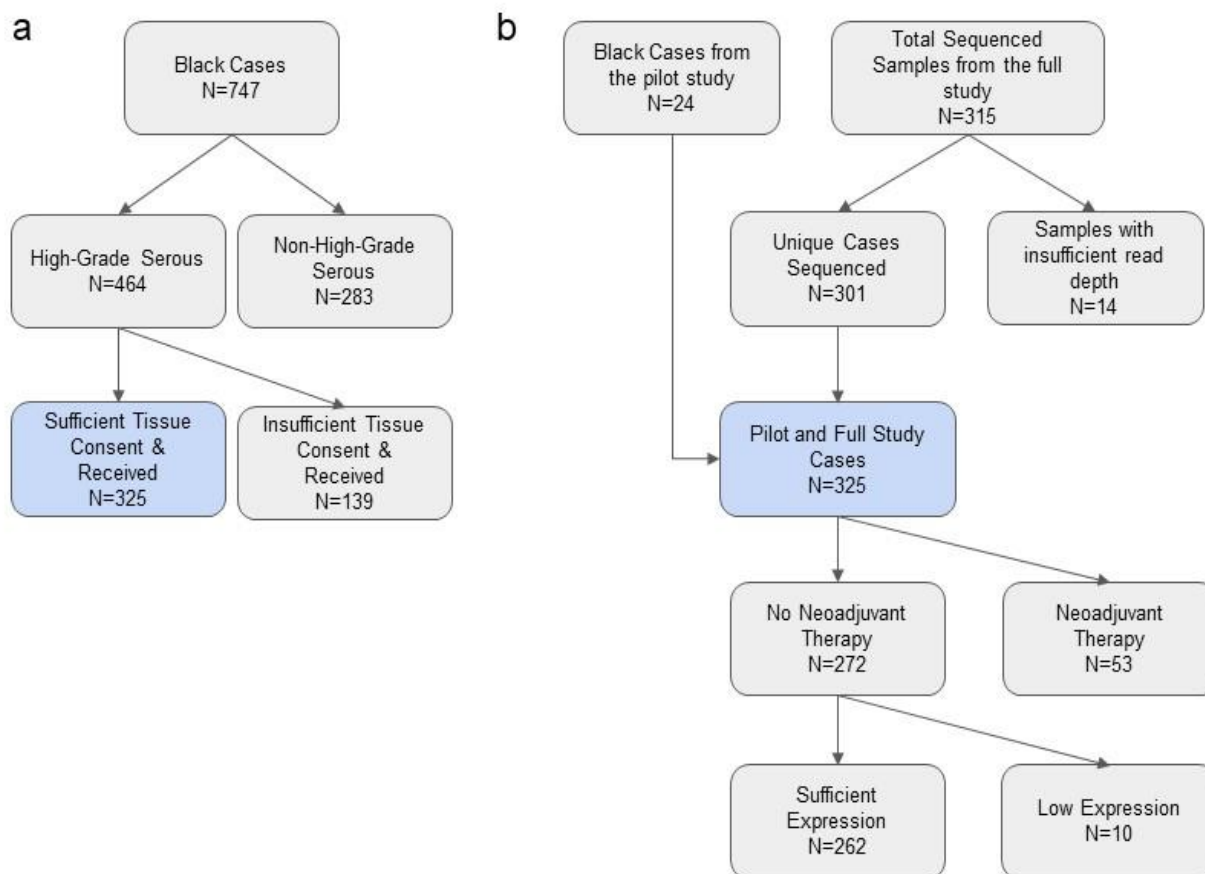


$\Lambda = 1.02$

Supplementary Figure SF2. Genome-wide association QxQ plot assessing inflation due to population admixture among White women.

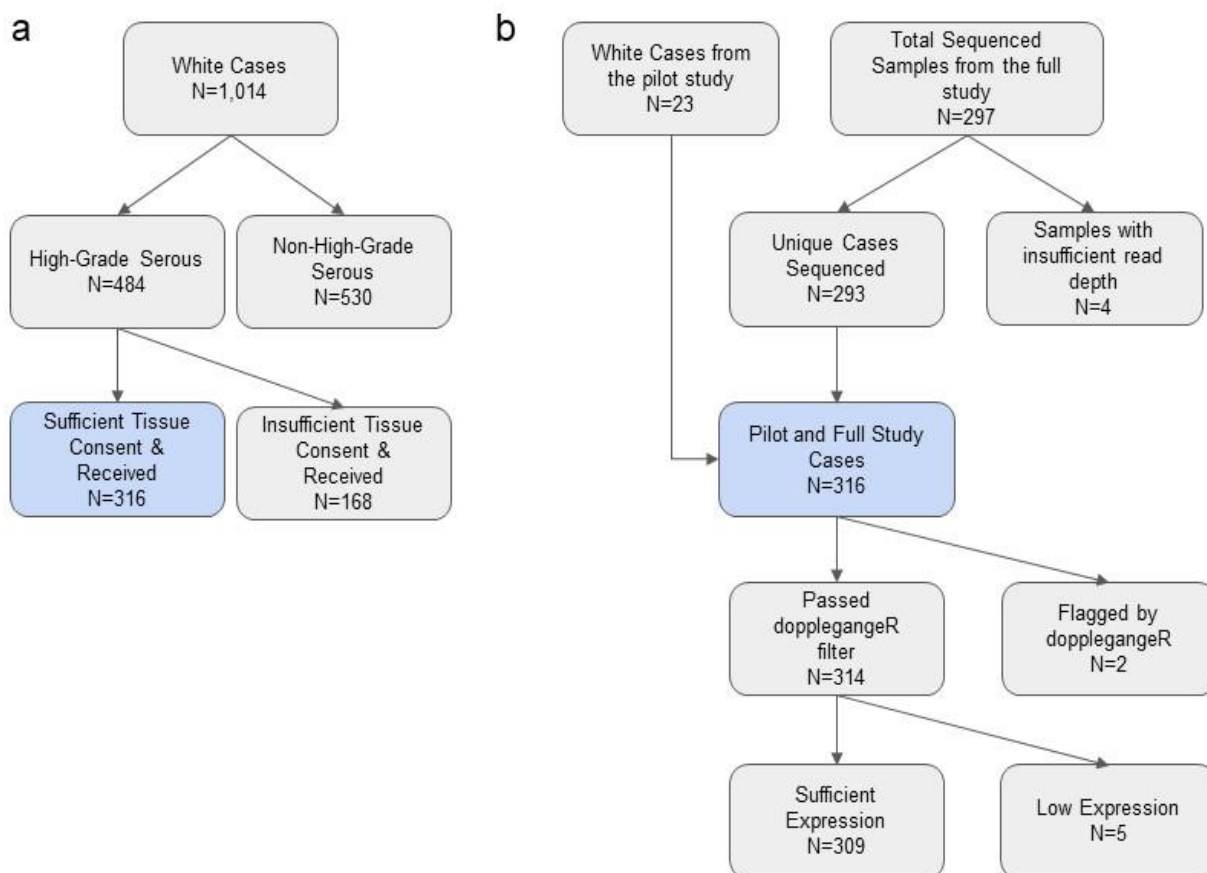


Supplementary Figure SF6.1.



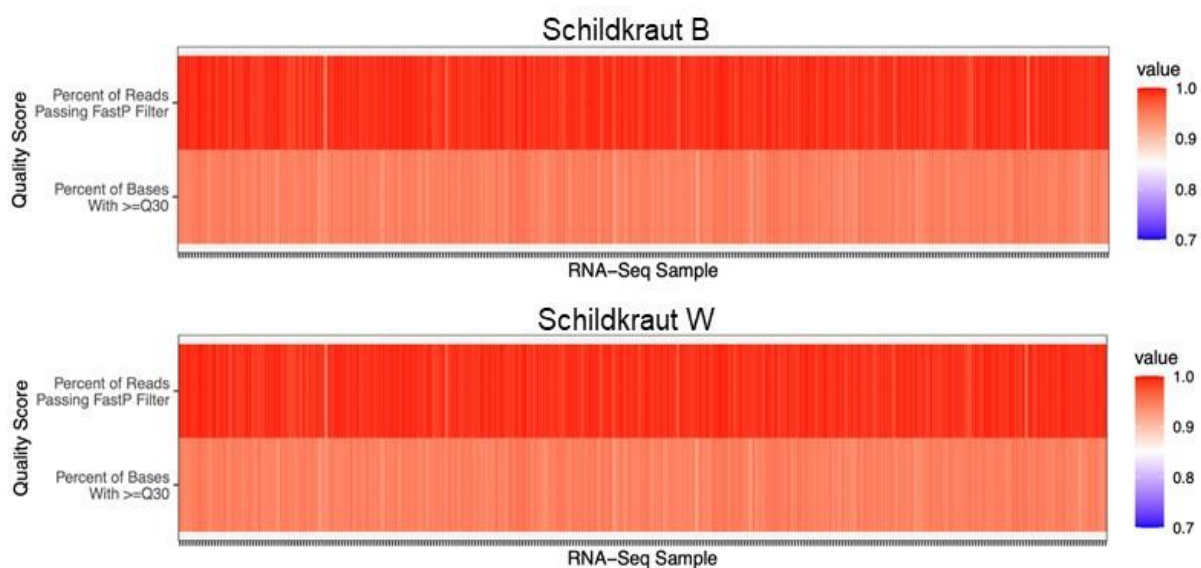
Supplemental Figure 1. Panels a and b depict the case selection process for Black study participants before (a) and after (b) sequencing. Blue rectangles indicate the cases that are the same in panels a and b, and are included in **Supplemental Table 3**. All cases listed as “samples with insufficient read depth” were successfully resequenced with sufficient read depth so, while 14 samples were excluded, no participants were excluded between “Total Sequenced Samples from the full study” and “Unique Cases Sequenced.”

Supplementary Figure SF6.2.



Supplemental Figure 2. Panels a and b depict the case selection process for White study participants before **(a)** and after **(b)** sequencing. Blue rectangles indicate the cases that are the same in panels a and b, and are included in **Supplemental Table 4**. All cases listed as "samples with insufficient read depth" were successfully resequenced with sufficient read depth so, while 4 samples were excluded, no participants were excluded between "Total Sequenced Samples from the full study" and "Unique Cases Sequenced."

Supplementary Figure SF6.3



Supplemental Figure 3. This figure depicts the percentage of reads that passed the FastP filtering (top), and the percentage of bases that had a quality score ≥ 30 in the SchildkrautB and SchildkrautW datasets. Each column is an RNA-seq sample and its coloring is based upon its quality score for each metric. For SchildkrautB the sample with the minimum percent of reads passing the FastP filter was 89.8%, and the sample with the minimum percentage of bases with a quality score ≥ 30 was 83.3%. For SchildkrautW the sample with the minimum percent of reads passing the FastP filter was 92.4% and the sample with the minimum percentage of bases with a quality score ≥ 30 was 88.2%.